AD_____

Award Number: W81XWH-11-1-0792

TITLE: Portable Body Temperature Conditioner

PRINCIPAL INVESTIGATOR: Timothy D. Browder, MD

CONTRACTING ORGANIZATION : University of Nevada
Reno Reno, NV
89557-0001

REPORT DATE: DECEMBER 2014

TYPE OF REPORT: Final Report

PREPARED FOR: U.S. Army Medical Research and Materiel Command
Fort Detrick, Maryland 21702-5012

DISTRIBUTION STATEMENT:

☒ Approved for public release; distribution unlimited

REPORT DOCUMENTATION PAGE

Form Approved
OMB No. 0704-0188

1. REPORT DATE: DECEMBER 2014	**2. REPORT TYPE** Final Report	**3. DATES COVERED** *(From – To)* 19 Sep 2011 – 18 Sep 2014

4. TITLE AND SUBTITLE

Portable Body Temperature Conditioner

5a. CONTRACT NUMBER
W81XWH-11-1-0792

5b. GRANT NUMBER

5c. PROGRAM ELEMENT NUMBER

6. AUTHOR(S)
Browder, Timothy, D., MD
Kuhls, Deborah, A., MD
Fildes, John, MD, FACS, FCCM
EMAIL: sjwilliams@medicine.nevada.edu

5d. PROJECT NUMBER

5e. TASK NUMBER

5f. WORK UNIT NUMBER

7. PERFORMING ORGANIZATION NAME(S) AND ADDRESS(ES)

UNIVERSITY OF NEVADA, RENO
204 ROSS HALL MS 325
RENO NV 89557-0001

8. PERFORMING ORGANIZATION REPORT NUMBER

9. SPONSORING / MONITORING AGENCY NAME(S) AND ADDRESS(ES)
U.S. Army Medical Research and Materiel Command
Fort Detrick, Maryland 21702-5012

10. SPONSOR/MONITOR'S ACRONYM(S)

11. SPONSOR/MONITOR'S REPORT NUMBER(S)

12. DISTRIBUTION / AVAILABILITY STATEMENT
Approved for Public Release; Distribution Unlimited

13. SUPPLEMENTARY NOTES

14. ABSTRACT Many patients become hypothermic after severe injury due to environmental exposure during transport. These patients also have decreased thermoregulation due to blood loss. Normal core body temperature is defined as 37^{o}C and core body temperature below 35^{o}C and above 40^{o}C is defined as hypothermia and hyperthermia respectively. Studies have shown much better outcomes for patients with either trauma or hypothermia compared to patients with both trauma and hypothermia. Additionally, studies have shown that decreasing the hyperthermic patient's core body temperature rapidly to 38^{o}C lowers the incidence of complications and the risk of death. Currently, one of the most effective treatments for dysthermic patients involves the use of active convective/conductive heating/cooling devices. However, current devices require heavy or bulky equipment not suitable for military applications. Rocky Research and University of Nevada School of Medicine (UNSOM) have developed a novel Portable Body Temperature Conditioner (PBTC). This portable device is designed to promote normothermic conditions in injured or ill patients under typical conditions encountered in the field and during medical evacuation when access to electrical power is not available. The heating/cooling system has been designed to maximize efficiency allowing for a reduction in component and battery weight. Patient simulation testing was performed to evaluate thermal load and efficacy of PBTC with the use of a thermal manikin. Quality system regulation (QSR) and several design phase documents were started that are required for future FDA 510(k) submission of this medical device. The PBTC prototype allows thermal management therapy to be delivered to patients in a previously unattainable manner.

15. SUBJECT TERMS
Hypothermia, Circulating Water-blanket, Trauma, Hyperthermia, Military, Thermal Manikin

16. SECURITY CLASSIFICATION OF:			**17. LIMITATION OF ABSTRACT**	**18. NUMBER OF PAGES**	**19a. NAME OF RESPONSIBLE PERSON**
a. REPORT	**b. ABSTRACT**	**c. THIS PAGE**			USAMRMC
U	U	U	UU	163	**19b. TELEPHONE NUMBER** *(include area code)*

Table of Contents

INTRODUCTION:

Defensive medical installations require efficient and reliable environmental control systems for wounded and injured soldiers. Particularly, the maintenance of body temperature needs to be consistent and reliable with portable capabilities. The combination of critical injuries, environmental exposure and resuscitation efforts following trauma frequently result in body temperature derangement. Normal cellular physiology works optimally at 37°C. Human beings are homeothermic and require a narrow core body temperature range to maintain normal homeostasis. Currently, the most effective treatments for hyper-hypothermia patients involve active convective heating/cooling devices[1-8]. However, these methods require heavy or bulky equipment and are not practical for military applications in the field. Rocky Research and University of Nevada School of Medicine (UNSOM) have developed a novel Portable Body Temperature Conditioner (PBTC). This portable device is designed to promote normothermic conditions in injured or ill patients under typical conditions encountered in the field and during medical evacuation when access to electrical power is not available. The purpose of this project was to design, build, and test a PBTC. Additionally, upon completion of the prototype for the portable body temperature conditioner, patient simulation testing was performed to measure the heating/cooling capacity of the device. A thermal manikin was purchased to simulate various conditions as part of the patient simulation testing. Quality system regulation (QSR) and several design phase documents were started that will be required for future FDA 510(k) submission of this medical device. The innovative PBTC design is distinctly unique from comparable products in two ways; it offers both heating and cooling in a single compact package, and it can operate on either AC or DC electrical power. Both factors contribute significantly to the portability and adaptability of the appliance, allowing thermal management therapy to be delivered to patients in a previously unattainable manner.

KEYWORDS:

Hypothermia, Hyperthermia, Circulating Water-blanket, Trauma, Military, Thermal Manikin

OVERALL PROJECT SUMMARY:

Summary of Work

The PBTC was designed to promote normothermic conditions in injured or ill patients under typical conditions encountered in the field and during medical evacuation when access to electrical power is not available. The body warmer consists of two elements: the heating/cooling module and water circulating blanket or wrap. The blanket/wrap system consists of a heat exchanger with circulation passages, insulation and a contact surface to allow intimate contact with the patient's body. The heating/cooling module comprises a high efficiency vapor compression cooling/heat pump with an advanced variable speed drive and innovative refrigerant

flow control for optimal performance and maximum energy efficiency. The heat/cooling module of the body warmer is designed to allow controlled heating or cooling of a patient in an efficient manner in order to minimize battery weight. The battery pack utilized consists of high energy density polymer Li-Ion battery cells, optimizing operating time of the appliance while minimizing weight. The high efficiency variable speed vapor compression system has a DC driven inverter that minimizes battery power consumption, and accommodates either AC or DC operation of the device.

The vapor compression makes use of Rocky Research's unique thermal expansion valve (TXV). This TXV is an enabling device that allows variable speed operation of the vapor compression system over a wide range of capacities without damage to the compressor. It also offers extremely precise control of superheat, thereby optimizing the operation of the evaporator and condenser components for high efficiency cycle operation. This control system modulates the vapor compression system operation to allow temperature ramp rates in accordance with the user input. The user friendly interface allows operation using intuitive instructions and outputs patient temperature in conjunction with other critical information related to operation of the device.

The PBTC was developed utilizing a system breadboard designed to accommodate the interchangeability of crucial components for testing. The hermetically sealed vapor compression system was the primary design focus of the breadboard. Essential component selection was based on breadboard testing results, and a fully functional appliance was subsequently designed and developed. Extensive analysis was implemented to optimize component selection based on size and performance characteristics, allowing for the final prototype components to be identified and selected. The principal devices evaluated on the breadboard include compressors, pumps, heat exchangers, thermal expansion valves (TXV), fans, battery packs, power supplies, chargers, and fittings. The largest emphasis was directed towards compressor selection in an effort to optimize weight, size and performance characteristics. Testing analysis was initially performed using an open loop system with a water bath simulating the load. The breadboard was then evaluated utilizing a closed loop system, as well as a thermal manikin replicating a patient load on the system.

Utilizing the breadboard design, Rocky Research focused time on evaluating the performance of the PBTC on Newton, the thermal manikin. A significant effort was spent learning how to utilize the thermal manikin, along with its corresponding ThermDac software. Efforts then focused developing methods for effectively exploiting the manikin to gauge system capabilities and facilitate final prototype development. Several system modifications were implemented based on discoveries found during functional and performance assessments, founded on testing results with and without the thermal manikin. Testing methods were established for properly quantifying the effective cooling capacity of the PBTC. The procedure consisted of monitoring the additional heat flux of each zone required to maintain a constant surface temperature. By

multiplying the additional heat flux of each zone with its corresponding area and summing the products, the total effective cooling capacity on the manikin was ascertained.

Based on testing results the TXV orifices on both the heating and cooling sides were modified to better modulate refrigerant flow into the evaporator at an optimal proportion to the evaporation rate of the refrigerant in the evaporator. A concern in regards to the control board utilized to drive the compressor was identified and a solution addressed. A heat sink has been designed and developed to mitigate concerns of overheating. Furthermore, Underwriters Laboratories (UL) approved boards were acquired from the manufacturer of the compressor that have been developed to resolve this known outstanding issue. Cooling and heating performance test matrices were established and implemented to evaluate the cooling and heating capacities under different ambient and operating conditions. A water reservoir was also sized and integrated into the PBTC breadboard for seamlessly filling the blanket and plumbing of the system upon startup while purging entrained air. The same water volume sized for breadboard was assimilated into the final case design.

As system breadboard testing evolved, a prominent emphasis was directed towards evaluating performance and design enhancements required to maintain mechanical integrity over long-term operation of the PBTC. A high energy density battery pack was identified to ensure efficient operational longevity of the system; even under de-rating conditions. Vibration dampers have been integrated into the design of the PBTC at the suction and discharge lines of the compressor to mitigate concerns of mechanical failure, an observed malfunction during bench top performance testing of the appliance breadboard. TXV bulb saddles were added to the system to improve the surface area contact between the evaporator outlet refrigeration plumbing and the TXV bulb, thus reducing thermal gradients between the two locations. The enhancement allowed for tighter control and modulation of refrigerant mass flow rate, resulting in improved performance of the system. Thermistor saddles were additionally constructed to ensure accurate temperature readings and fast response time for the control scheme. The heat sink designed and implemented for temperature management of the compressor control board continued to be evaluated for effectiveness and long term operation of the compressor. An actuator valve was identified, sized, and retrofit in order to automate the process of switching between heating and cooling modes. Temperature probes were also identified, acquired, and assimilated into the system design for monitoring circulating water and patient body temperature.

During breadboard testing the effectiveness of the air coil was found to be insufficient. An alternative coil of larger surface area was installed on the breadboard for testing and analysis to determine selection of the coil utilized in the final prototype. To accommodate the bigger air coil a larger fan was also required. The TXV bulb charge was adjusted to address the increased refrigerant side pressure drop through the bigger air coil. Capacity evaluations of the larger micro-channel air heat exchanger were implemented in both heating and cooling modes. A

thinner fan of larger face surface area was selected and tested in conjunction with the new air coil. The plumbing of the system was reconfigured and tubing sizes were modified to ensure air is fully purged from the system. The combination of smaller tubing sizes and faster required fluid velocity resulted in the selection of a new pump capable of producing higher volumetric flow rates. The water reservoir integral to the case was adjusted to accommodate the additional volume of fluid in the system when all of the air is fully purged. The air inlet ports to the case have been moved directly in front of the fan in an effort to reduce pressure drop. Additionally, the open volume of the air passage was also increased to minimize pressure drop. An extensive test matrix for both heating and cooling modes at different operating temperatures and compressor speeds was then evaluated.

Investigations into reducing system weight and improving functional performance over the entire range of operating conditions of the prototype were also implemented. An alternate plate heat exchanger of smaller mass was acquired and tested. Furthermore, a tube in tube heat exchanger designed by Rocky Research was analyzed as a feasible method for reducing system weight. For both heat exchangers it was ultimately deemed that the loss in heat transfer effectiveness was not substantiated by the small reduction in system weight. A method for improving system heating capacity at low ambient conditions when the heat pump cycle capacity is reduced was developed to improve PBTC versatility. The design consists of a copper heat exchanger utilized in conjunction with electrical resistance heaters. PCB modifications to accommodate electrical resistance heaters, as well as a high pressure safety switch as an additional failsafe were implemented.

Once functional and performance testing of the breadboard was complete Rocky Research's attention was directed towards optimal control development, case finalization, and user interface design. A control logic diagram was constructed to identify the operating modes of the appliance. Furthermore, the boolean logic expressions were defined for each operating mode based on the decision tree hierarchy of the logic diagram. Safeties and system defaults were also identified and integrated into the control logic design. A keypad design was then developed based on the user inputs require to guide the handler through properly selecting an operating mode. An LCD display optimal for the case design was also acquired for the system. The case design and keypad were refined in an iterative process to best accommodate system enhancements designed to improve overall performance. Stability analysis has been implemented on the case to gauge how easily the appliance can be overturned. Removable feet have been designed for the case of the PBTC to evaluate the optimal balance between case stability and transportability of the appliance. Control safeties have been specified for the different operating modes of the device. They include high temperature safeties, a high pressure safety, low temperature safeties, and a patient temperature feedback safety.

Rocky Research completed the development and implementation of a compact dedicated control printable circuit board (PCB) for the management and control of the PBTC. The controller incorporates a mixture of analog and digital circuits to achieve optimal control of the system. Along with the controller hardware, the control firmware was also developed and refined based on prototype testing. The control firmware incorporates several algorithms intended to optimize the delivery of thermal energy while also minimizing power consumption. Ultimately, the approach provides the system with maximized endurance when operated on the internal battery.

Once breadboard testing was complete, the PBTC case was acquired and installation of all system components was implemented to create a final fully functional prototype. The prototype was wired and each electrical component evaluated for proper functionality. The prominent emphasis was then directed towards development of the control logic for each of the specified operating modes. A diagnostic control mode was constructed to evaluate performance of the cooling and heating cycles at user specified compressor speeds. The assembled prototype was then tested in both heating and cooling cycles and the manual, auto, and gradient operating modes were further developed and refined. The proportional-integral-derivative (PID) control constants were defined for all three modes, and evaluated for responsiveness and temperature maintenance accuracy under different operating conditions with various load sources. The robustness of each algorithm was analyzed by varying operating parameters and ensuring that the control scheme responded appropriately and as expected.

Required prototype modifications were documented and implemented during the assembly of the first prototype. Enhancements identified were minimal, and primarily target towards improving the durability and ruggedness of the PBTC. A bracket was designed, fabricated, and installed to support the filter/dryer during system operation. Shock rubber was installed on the compressor, pump, battery pack, TXV's, and heat exchangers in order to enhance system resistance to shock and vibration. An aluminum plate was added to the quick connect fittings to eliminate the potential for damage during field operation. The TXV's were also relocated so that spring force adjustments could be easily made once installed in the case. The case design was slightly modified to accommodate these changes as well as facilitate the ability to mold the water reservoir and two halves of the case instead of 3D printing them. The refined case design was then ordered and acquired.

Task 1: Design of the System

Breadboard design was initiated by identifying fundamental components of the vapor compression system and installing them on a fabricated template designed to replicate the briefcase profile of the PBTC case. Initially installed components consisted of a compressor, liquid-side plate heat exchanger, air-side micro channel heat exchanger, fan, two TXV's, two check valves, and a reversing valve to cycle between heating and cooling modes. The breadboard was implemented such that components could be easily interchanged to accommodate the

installation and testing of different system components during prototype development. This was accomplished utilizing easily breakable Swagelok fittings in in lieu of the hard soldered joints formed to create a hermetically sealed system in the final prototype. A fully functional data acquisition system (DAQ) was installed on the breadboard so that critical operating parameters could be monitored. Figure 1 demonstrates the isolated breadboard while Figure 2 depicts the breadboard along with the corresponding DAQ for quantifying performance characteristics with different system components installed.

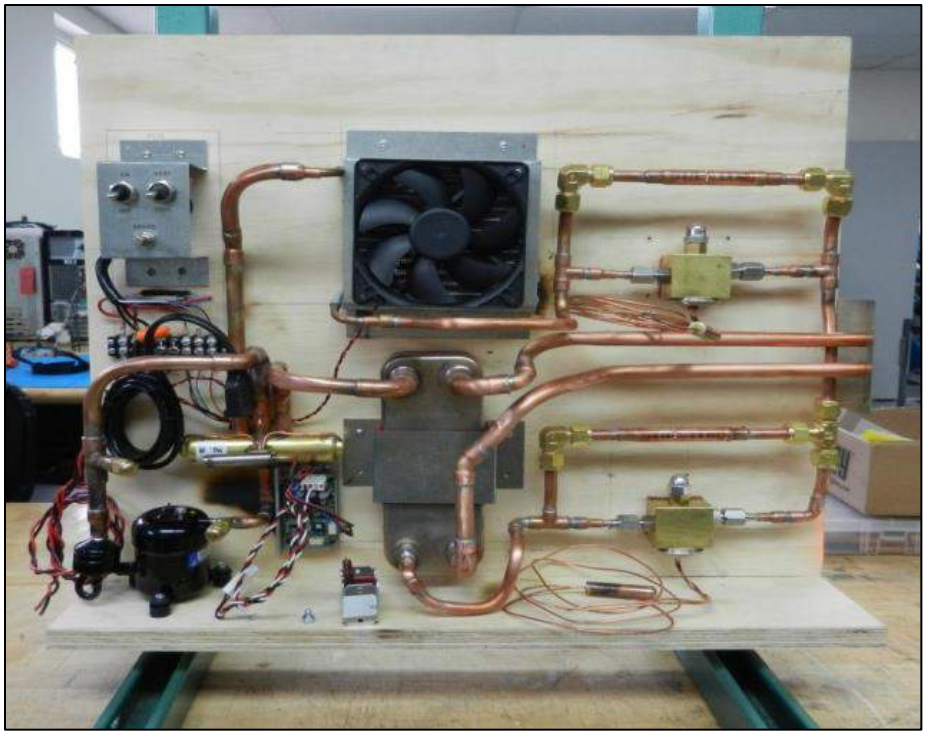

Figure 1. Fabricated initial bench-top design

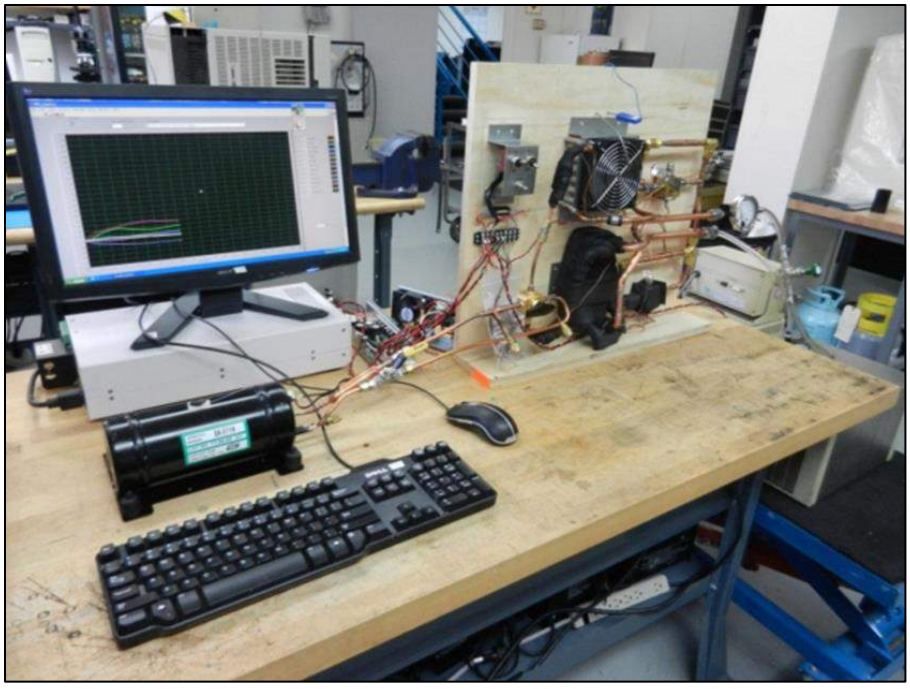

Figure 2. Fabricated initial bench-top prototype with DAQ

Task 2: Breadboard Testing

Component selection, specifically compressor determination, was a primary focus of breadboard testing. Complete test matrices have been constructed and evaluated for each of the compressors under consideration. The test matrices are extensive because each compressor was analyzed at varying compressor speeds under different heating and cooling conditions. Table 1 is a preliminary physical and performance comparison of the compressors analyzed based on manufacturer specified data. Tables 2, 3, and 4 depict the test matrices for the Aspen, Danfoss, and Sawafuji compressors, initially under consideration for utilization in the PBTC based on Rocky Research's in-house performance evaluations. Cooling modes were tested for bath temperatures of 20 ℃, 10 ℃, and 5 ℃ while heating performance was evaluated with bath temperatures of 42 ℃ and 40 ℃. Voltage was maintained constant for each test at 25.2v. The coefficient of performance (COP) was calculated for each compressor under each heating and cooling assessment to evaluate overall compressor performance. The performance of each compressor was then compared and contrasted in terms of capacity, efficiency, and system implementation feasibility while considering size and weight parameters.

Table 1: Compressor Preliminary Comparison

	Engel rotary compressor	**Hitachi reciprocating compressor**	**Aspen rotary compressor**
Physical Specifications			
Height (mm)	166	195	78
Length/diameter (mm)	85	204	56
Width (mm)	-	13 mm	-
Displacement (cc)	2.3	2.0	1.4
Weight (kg)	2.8	4.3	0.6
Performance with refrigerant R134a			
Pressure ratio	2.1 – 3.2	1.9 – 3.0	2.0 – 3.5
Speed (rpm)	2000	2000	2000 – 6000
Volumetric efficiency (%)	57.0 – 79.3	58.1 – 73.0	73.2 – 90.5
Overall isentropic efficiency (%)	40.6 – 59.5	43.2 – 56.5	44.1 – 70.3
Cooling capacity (W)	130.1 – 256.4	152.2 – 208.8	85 – 797
System COP	3.0 – 5.7	2.6 – 3.7	0.4 – 9.1

Table 2: Complete Test matrix for Aspen Compressor

	Aspen Compressor Test Matrix			.2 A compressor cooling fan						
		1180 - PBTC		.4 A condensor fan and H2O pump combined						
Control Voltage:	2.13									
	RPM (3000)									
		H_2O Out (°C)	**ΔT H_2O (°C)**	**V (V)**	**I (A)**	**ṁ (kg/s)**	**Cp (kJ/kg*C)**	**P (W)**	**Q (W)**	**COP**
Bath Temperature (20°C)	26June12 C7	15	5	25.2	5.2	0.016	4.18	131.0	329.8	**2.5**
Bath Temperature (10°C)	27June12 C4	6.5	3.5	25.2	4.0	0.016	4.19	100.8	231.4	**2.3**
Bath Temperature (5°C)	27June12 C8	3.5	1.5	25.2	3.8	0.016	4.20	95.8	99.4	**1.0**
Bath Temperature (42°C)	27June12 H1	45.0	3.0	25.2	4.9	0.016	4.18	123.5	197.7	**1.6**
Bath Temperature (40°C)	28June12 H5	43.0	3.0	25.2	4.7	0.016	4.18	118.4	197.7	**1.7**
Control Voltage:	2.8									
	RPM (4000)									
		H_2O Out (°C)	**ΔT H_2O (°C)**	**V (V)**	**I (A)**	**ṁ (kg/s)**	**Cp (kJ/kg*C)**	**P (W)**	**Q (W)**	**COP**
Bath Temperature (20°C)	26June12 C8	14	6	25.2	6.1	0.016	4.18	153.7	395.7	**2.6**
Bath Temperature (10°C)	27June12 C5	6	4	25.2	4.8	0.016	4.19	121.0	264.4	**2.2**
Bath Temperature (5°C)	27June12 C9	3	2	25.2	4.6	0.016	4.20	115.9	132.6	**1.1**
Bath Temperature (42°C)	27June12 H2	45.0	3.0	25.2	5.4	0.016	4.18	136.1	197.7	**1.5**
Bath Temperature (40°C)	28June12 H6	43.0	3.0	25.2	5.1	0.016	4.18	128.5	197.7	**1.5**
Control Voltage:	3.54									
	RPM (5000)									
		H_2O Out (°C)	**ΔT H_2O (°C)**	**V (V)**	**I (A)**	**ṁ (kg/s)**	**Cp (kJ/kg*C)**	**P (W)**	**Q (W)**	**COP**
Bath Temperature (20°C)	27June12 C2	14	6	25.2	6.8	0.016	4.18	171.4	395.7	**2.3**
Bath Temperature (10°C)	27June12 C6	6	4	25.2	5.7	0.016	4.19	143.6	264.4	**1.8**
Bath Temperature (5°C)	27June12 C10	2	3	25.2	5.5	0.016	4.20	138.6	198.9	**1.4**
Bath Temperature (42°C)	27June12 H3	45.0	3.0	25.2	5.6	0.016	4.18	141.1	197.7	**1.4**
Bath Temperature (40°C)	28June12 H7	43.5	3.5	25.2	5.6	0.016	4.18	141.1	230.6	**1.6**
Control Voltage:	4.1									
	RPM (6000)									
		H_2O Out (°C)	**ΔT H_2O (°C)**	**V (V)**	**I (A)**	**ṁ (kg/s)**	**Cp (kJ/kg*C)**	**P (W)**	**Q (W)**	**COP**
Bath Temperature (20°C)	27June12 C3	14	6.0	25.2	8.0	0.016	4.18	201.6	395.7	**2.0**
Bath Temperature (10°C)	27June12 C7	5.5	4.5	25.2	7.7	0.016	4.19	194.0	297.5	**1.5**
Bath Temperature (5°C)	27June12 C11	2	3	25.2	6.1	0.016	4.20	153.7	198.9	**1.3**
Bath Temperature (42°C)	28June12 H4	46.0	4.0	25.2	6.5	0.016	4.18	163.8	263.6	**1.6**
Bath Temperature (40°C)	28June12 H8	44.0	4.0	25.2	6.2	0.016	4.18	156.2	263.6	**1.7**

Table 3: Complete Test matrix for Danfoss Compressor

	Danfoss Compressor Test Matrix			.2 A compressor cooling fan						
		1180 - PBTC		.4 A condensor fan and H2O pump combined						
Control Resistance: Ohms	0									
	RPM (2000)									
		H_2O Out (°C)	**ΔT H_2O (°C)**	**V (V)**	**I (A)**	**ṁ (kg/s)**	**Cp (kJ/kg*C)**	**P (W)**	**Q (W)**	**COP**
Bath Temperature (20°C)	02July12_C1	17	3	25.2	2.3	0.016	4.18	58.0	197.9	**3.4**
Bath Temperature (10°C)	02July12_C5	8	2.0	25.2	2.2	0.016	4.19	55.4	132.2	**2.4**
Bath Temperature (5°C)	02July12_C9	4	1	25.2	2.1	0.016	4.20	52.9	66.3	**1.3**
Bath Temperature (42°C)	03July12_H1	43.0	1.0	25.2	2.6	0.016	4.18	65.5	65.9	**1.0**
Bath Temperature (40°C)	03July12_H5	41.5	1.5	25.2	2.5	0.016	4.18	63.0	98.8	**1.6**
Control Resistance: Ohms	277									
	RPM (2500)									
		H_2O Out (°C)	**ΔT H_2O (°C)**	**V (V)**	**I (A)**	**ṁ (kg/s)**	**Cp (kJ/kg*C)**	**P (W)**	**Q (W)**	**COP**
Bath Temperature (20°C)	02July12_C2	17	3	25.2	2.9	0.016	4.18	73.1	197.9	**2.7**
Bath Temperature (10°C)	02July12_C6	7.5	2.5	25.2	2.7	0.016	4.19	68.0	165.3	**2.4**
Bath Temperature (5°C)	02July12_C10	3.5	1.5	25.2	2.6	0.016	4.20	65.5	99.4	**1.5**
Bath Temperature (42°C)	03July12_H2	43.0	1.0	25.2	3.1	0.016	4.18	78.1	65.9	**0.8**
Bath Temperature (40°C)	03July12_H6	42.0	2.0	25.2	3.0	0.016	4.18	75.6	131.8	**1.7**
Control Resistance: Ohms	692									
	RPM (3000)									
		H_2O Out (°C)	**ΔT H_2O (°C)**	**V (V)**	**I (A)**	**ṁ (kg/s)**	**Cp (kJ/kg*C)**	**P (W)**	**Q (W)**	**COP**
Bath Temperature (20°C)	02July12_C3	17	3	25.2	3.5	0.016	4.18	88.2	197.9	**2.2**
Bath Temperature (10°C)	02July12_C7	7	3	25.2	3.3	0.016	4.19	83.2	198.3	**2.4**
Bath Temperature (5°C)	02July12_C11	3.5	1.5	25.2	3.1	0.016	4.20	78.1	99.4	**1.3**
Bath Temperature (42°C)	03July12_H3	43.0	1.0	25.2	3.8	0.016	4.18	95.8	65.9	**0.7**
Bath Temperature (40°C)	03July12_H7	42.5	2.5	25.2	3.7	0.016	4.18	93.2	164.7	**1.8**
Control Resistance: Ohms	1523									
	RPM (3500)									
		H_2O Out (°C)	**ΔT H_2O (°C)**	**V (V)**	**I (A)**	**ṁ (kg/s)**	**Cp (kJ/kg*C)**	**P (W)**	**Q (W)**	**COP**
Bath Temperature (20°C)	02July12_C4	16.5	3.5	25.2	4.2	0.016	4.18	105.8	230.8	**2.2**
Bath Temperature (10°C)	02July12_C8	7	3	25.2	3.9	0.016	4.19	98.3	198.3	**2.0**
Bath Temperature (5°C)	03July12_C12	3	2	25.2	3.8	0.016	4.20	95.8	132.6	**1.4**
Bath Temperature (42°C)	03July12_H4	44.0	2.0	25.2	4.3	0.016	4.18	108.4	131.8	**1.2**
Bath Temperature (40°C)	03July12_H8	43.0	3.0	25.2	4.4	0.016	4.18	110.9	197.7	**1.8**

Table 4: Complete Test matrix for Sawafuji Compressor

	Sawafuji Compressor Test Matrix			.2 A compressor cooling fan						
		1180 - PBTC		.4 A condensor fan and H2O pump combined						
		Cooling Mode								
		H_2O Out (°C)	**$\Delta T\ H_2O$ (°C)**	**V (V)**	**I (A)**	**$\dot{m}$ (kg/s)**	**Cp (kJ/kg*C)**	**P (W)**	**Q (W)**	**COP**
Bath Temperature (20°C)	09July2012_C3	19	1	25.2	2.2	0.016	4.18	55.4	66.0	**1.2**
Bath Temperature (10°C)	09July2012_C1	9.5	0.5	25.2	2.1	0.016	4.19	52.9	33.1	**0.6**
Bath Temperature (5°C)	09July2012_C2	4.8	0.2	25.2	2.0	0.016	4.20	50.4	13.3	**0.3**
		Heating Mode								
		H_2O Out (°C)	**$\Delta T\ H_2O$ (°C)**	**V (V)**	**I (A)**	**$\dot{m}$ (kg/s)**	**Cp (kJ/kg*C)**	**P (W)**	**Q (W)**	**COP**
Bath Temperature (42°C)	10July2012_H2	41.5	0.5	25.2	2.3	0.016	4.18	58.0	33.0	**0.6**
Bath Temperature (40°C)	10July2012_H1	39.5	0.5	25.2	2.3	0.016	4.18	58.0	32.9	**0.6**
	* No Heating									
	*No Heating									

Upon completion of the compressor test matrices several observations were realized. The Sawafuji swing motor compressor did not allow for the variance of motor speed. Resultantly, the compressor demonstrated poor efficiency performance as depicted by the COP in table 4, particularly for the heating mode tests. Consequently, the Sawafuji compressor was immediately eliminated as a viable option for prototype and final product fabrication.

Contrasting the Aspen compressor with the Danfoss compressor it was observed that the COP of each was comparable. Depending on motor speed, the general trend was that the Aspen performed slightly superior in terms of heating effectiveness and the Danfoss slightly better in terms of cooling efficiency. Identification of the most suitable compressor for continuing with system prototyping was subsequently determined by the size and weight of all required components. The Aspen compressor has an approximate volume of $14.8in^3$ and weighs approximately 1.32lb. The Danfoss compressor measures approximately $221.2in^3$ and weighs approximately 10.03lb. Although the Aspen compressor is much smaller in size and weight than the Danfoss it also draws more current. Subsequently, a larger battery pack is required for similar operational length conditions. Therefore, in order to properly analyze size and weight comparisons between the two, system battery sizing and evaluation was implemented.

Polymer Li-Ion batteries with high energy density were designated for battery pack selection and analysis. Battery packs with polymer Li-Ion cells of 3.7v and varying nominal capacities were evaluated. Since 7 cells were required for both the Aspen and Danfoss compressors, cell size and weight was only varied by the capacity required for each compressor. It was found that little weight and size, in comparison to the compressors themselves, was eliminated by employing a battery pack with the less capacity required to power the Danfoss compressor for the same period

of time as the Aspen compressor. Therefore, overall system component size and weight was drastically smaller with utilization of the Aspen compressor in comparison to the Danfoss compressor. With similar performance characteristics, the Aspen compressor was selected for utilization in progressing forward with the portable body temperature conditioner prototype.

The battery selected for the breadboard and prototype is a 25.9v and 12.6Ah (326.34Wh) Li-Ion polymer battery pack. The dimensions of the pack are 7.1" (181mm) x 3.0" (77mm) x 3.3" (85mm) and the pack weighs 3.5lb (1585g). The pack was tested on the breadboard in both heating and cooling modes with the Aspen compressor operating at maximum speed. Some Li-ion polymer batteries demonstrate a de-rating at lower operating temperatures (60% at -20 °C). With the 12.6Ah even if the battery pack is de-rated to 60% at -20 °C, it is still within the acceptable operating parameters for the Aspen compressor functioning at maximum speed. For the heating test the battery was placed in a freezer at -20 °C in order to emulate any de-rating effects. The result of both the cooling and heating test are presented in Figures 3 and 4, respectively.

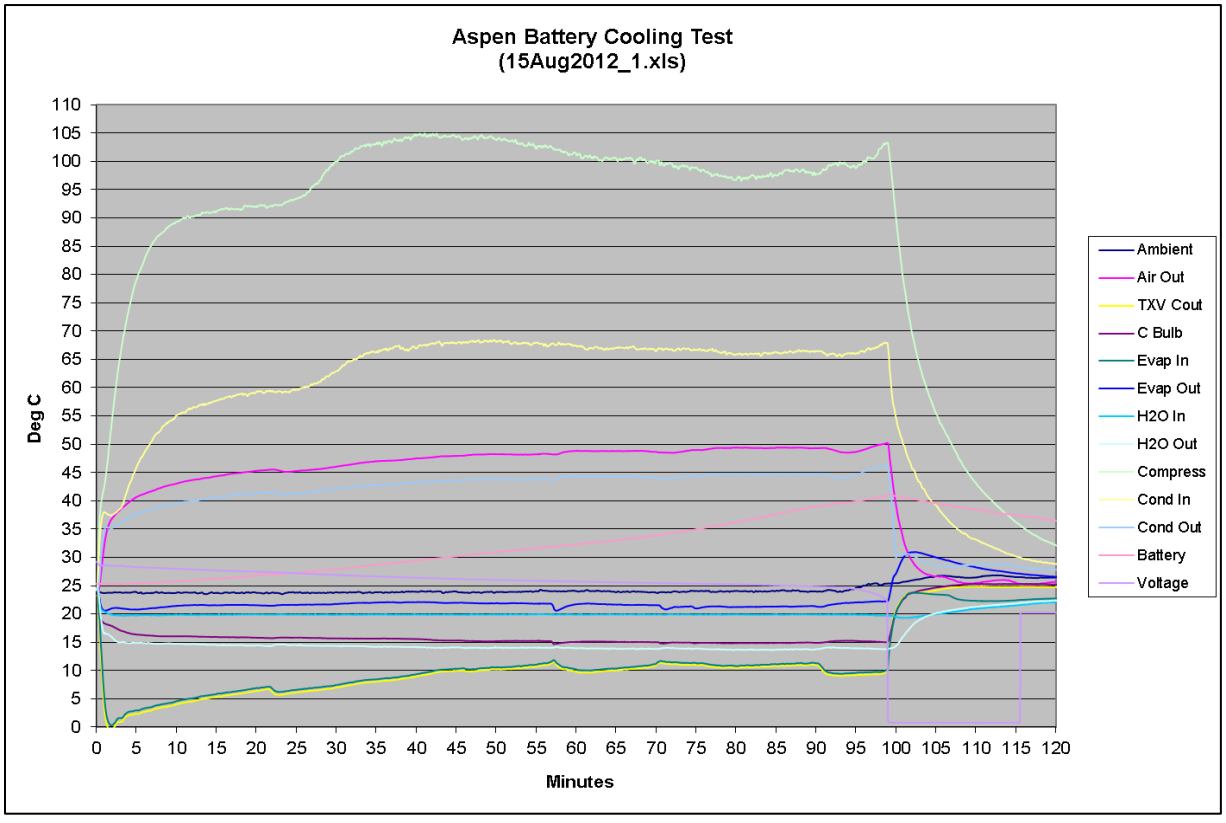

Figure 3. Battery pack cooling test with Aspen compressor

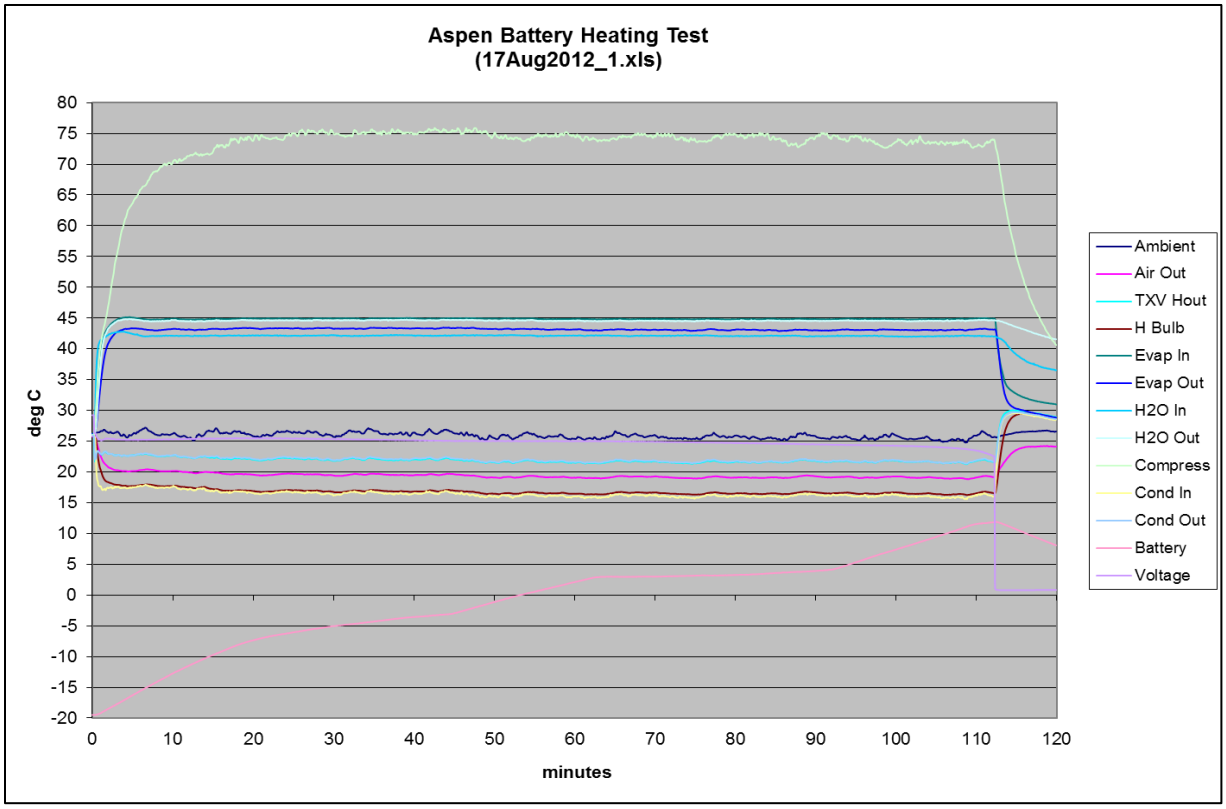

Figure 4. Battery pack heating test with Aspen compressor

As can be observed, the battery pack was able to adequately supply power to all of the breadboard components for 100 minutes in cooling mode and 110 minutes in heating mode. Consequently, the battery pack was verified as a sufficient selection for progressing forward with the portable body temperature conditioner prototype. A battery charger and power supply were also identified based on the battery pack selected. The smart charger has a standard charging rate of 6.0A, capable of recharging the entire battery pack in approximately 3.15 hours. The power supply is a high efficiency, low profile, component with full digital control and high peak loading capability. Both components were initially tested on the breadboard. The charger and power supply are packaged separately from the portable body temperature conditioner unit as a detachable external component. Such an approach allows for the unit to retain its minimal characteristics in terms of weight and size. Figure 5 presents a drawing of the prototype unit at the initial design phase along with the packaged external power supply and charger. The dimensions have been specified on the drawing in inches.

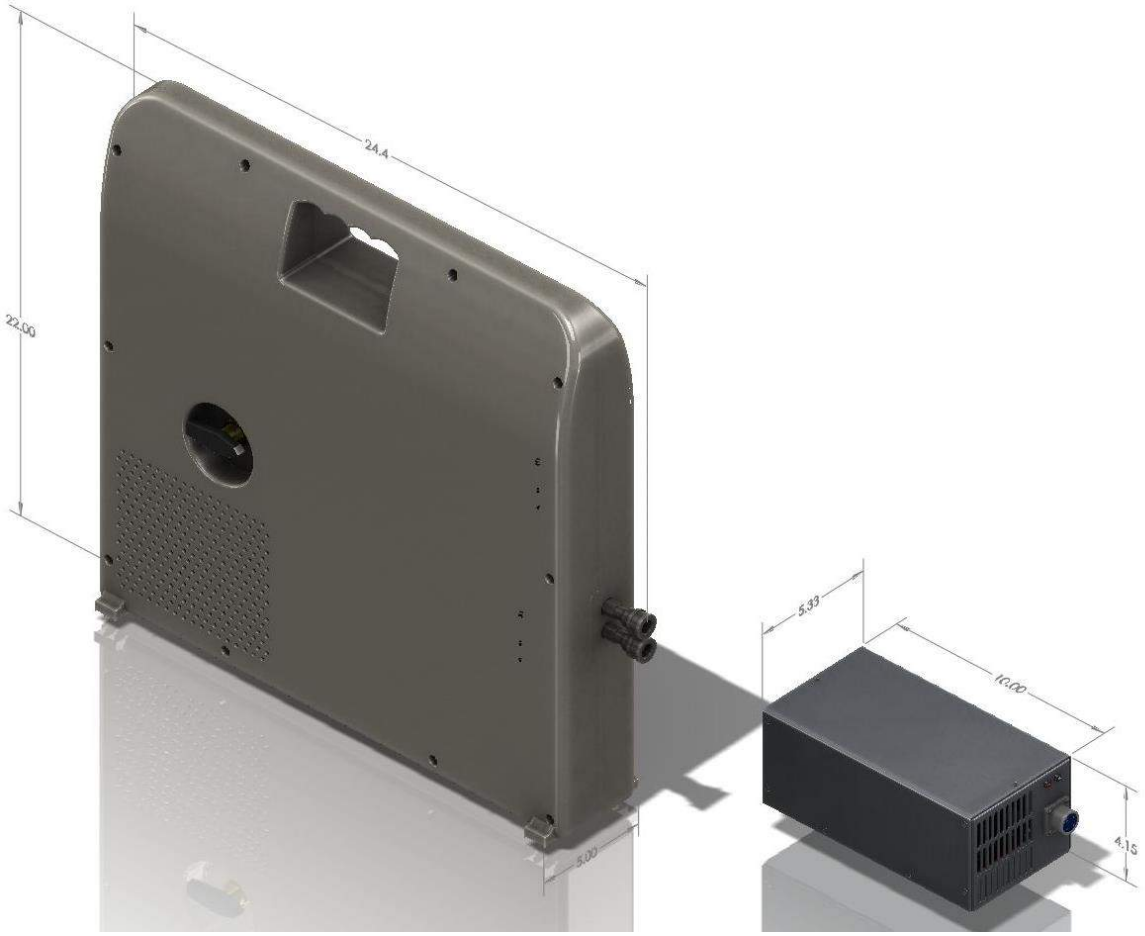

Figure 5. Prototype initial design with externally packaged power supply and charger unit

Two pumps were initially investigated for utilization in the PBTC unit. After testing, a 24v centrifugal pump with dimensions of 3.75" L x 3" W x 3" H and a maximum flow rate of 1.1gpm was selected for initial prototype development. The other pump under consideration was a small micro pump with 0.57" D x 2.5" L. Although the micro pump was optimal in terms of size, after extensive testing it was concluded that the pump did not provide adequate capability in maintaining flow rates. Furthermore, the micro pump was relatively noisy and raised concerns in terms of reliability. Open loop testing of the selected centrifugal pump through the entire system loop, including hyper-hypothermia blanket, revealed the pump was able to maintain a flow rate of approximately 0.5gpm with 1ft of pressure head.

The hyper-hypothermia blanket utilized for system performance design, development, and analysis is a Cincinnati Sub-Zero adult sized Maxi-Therm® blanket measuring 60" L x 24" W. The hose configuration developed to operate in conjunction with the blanket was also assimilated into the system design. Proper quick connect hydraulic couplings have been acquired and fitted to the plumbing of the breadboard unit to allow connection of the PBTC to the blanket via the 9′ connection hose. Flow has been analyzed through the blanket and weight measurements of full

and empty blankets, as well as connection hoses, were taken in order to quantify water content. It was found that at ambient conditions (25 °C) the blanket and hose contain approximately 15.6L (95in^3) of water during operation, a crucial quantification in designing for system filling procedures, and the water reservoir volume integrated into the PBTC.

Task 3: Prototype Fabrication and Testing.

3a. Functional Testing

Functional testing was accomplished in an iterative process along with performance testing in order to enhance the capacity, robustness, mechanical integrity, and operational longevity of the PBTC. For the purpose of demonstrating the development process of the appliance system enhancements are reported in the order that they were implemented. All enhancements, modifications, and alterations required additional functional testing before performance testing could ensue.

Functional testing of all system components was first manifested while cycling the unit in a cooling mode with the adult sized heat transfer blanket laid on the thermal manikin, Newton. Ambient temperatures were controlled at approximately 20°C by implementing the test configuration in an environmental chamber. The Aspen compressor was maintained at a control voltage of 4.1 V, equating to a speed of 6,000rpm. Such a speed is the maximum analyzed for the individual performance component testing of the compressor, and was therefore deemed appropriate for initial functional analysis while operating the PBTC on the thermal manikin. Figure 6, depicts the initial functional and performance testing configuration of the PBTC in the environmental chamber utilizing the thermal manikin.

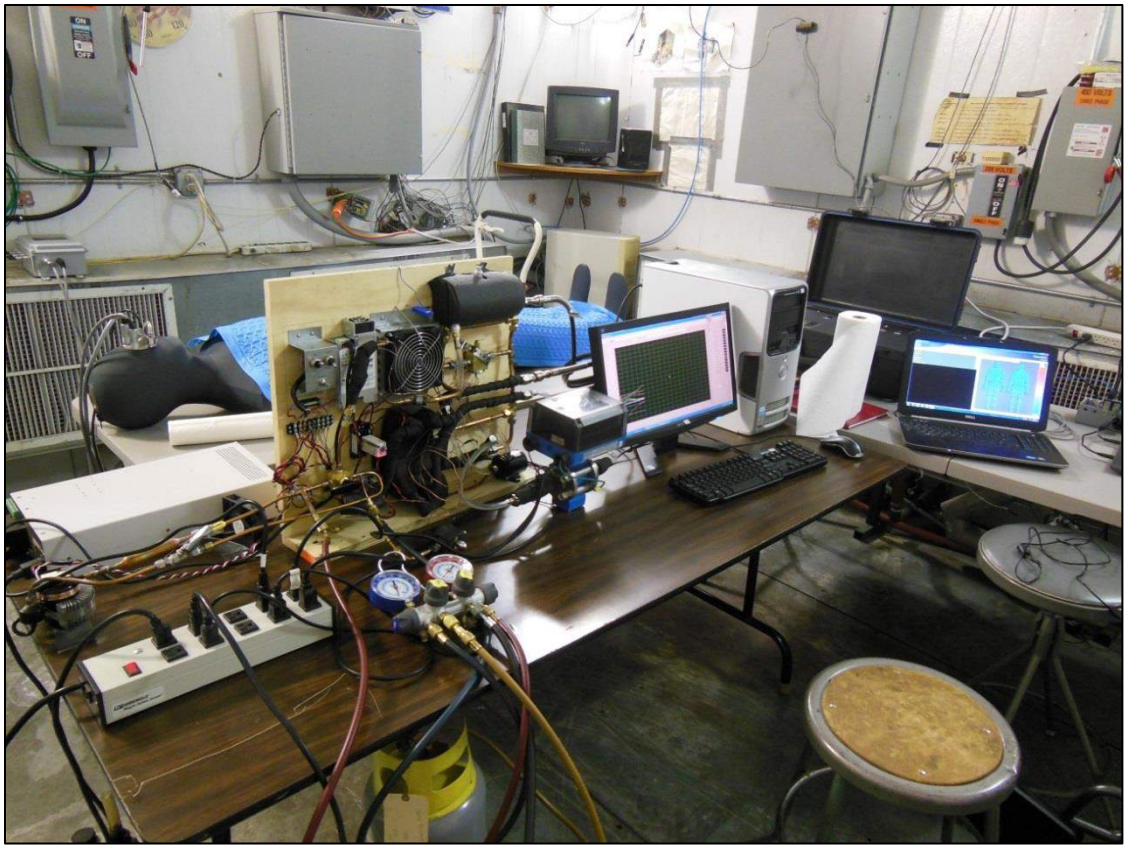

Figure 6. Initial functional & performance testing configuration

While operating the PBTC breadboard for extended periods of time on the thermal manikin the compressor was found to consistently approach overheating conditions. The practical operating temperature limit for the Aspen compressor is 135°C before damage can occur. Functional testing of the unit revealed that the compressor was uncomfortably close to that sensible limit. Since for breadboard functional testing the prototype was not enclosed in a casing, concerns of overheating the compressor required being addressed before final design implementation. The following performance plot, Figure 7, depicts the PBTC component temperatures as a function of time while testing the unit on the thermal manikin. The heat generation load from the manikin was that necessary to maintain a surface temperature of 35°C. The compressor, operating at a maximum speed of 6,000rpm, is the top curve represented in blue.

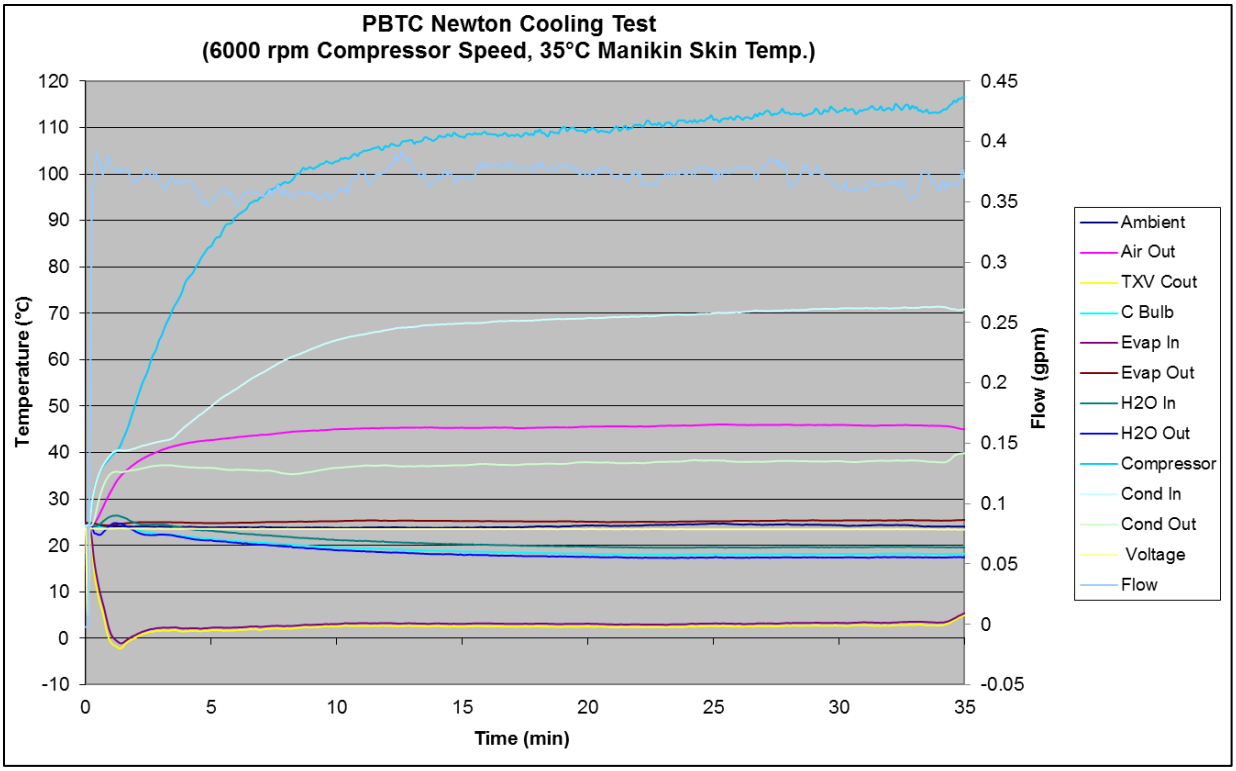

Figure 7. PBTC functional testing operating temperature characteristics

As can be observed, compressor temperatures exceeded 110 °C within 25 minutes of operation under the presented operating conditions. At such a temperature the performance of the compressor began to degrade, and the cooling capacity of the unit was limited to less than maximum capacity. The overheating quandary was resolved by adding a small 40mm fan to accommodate airflow over the compressor and more effectively dissipate heat. Additionally, the case design was modified and the compressor located such that inlet airflow is drawn across the compressor, assisting in heat rejection.

Breadboard analysis revealed that the maximum operating pressure differential (MOPD) was not consistently enough to cycle between the heating and cooling cycles as desired. Resultantly, a 4-way valve was utilized to replace the reversing valve as a more effective and reliable way to switch between the heating and cooling cycles. The conceptual case and system design was then updated to reflect those current enhancements. Figure 8 presents a new layout of the prototype at the developmental stage in which the 4-way valve was added to the system.

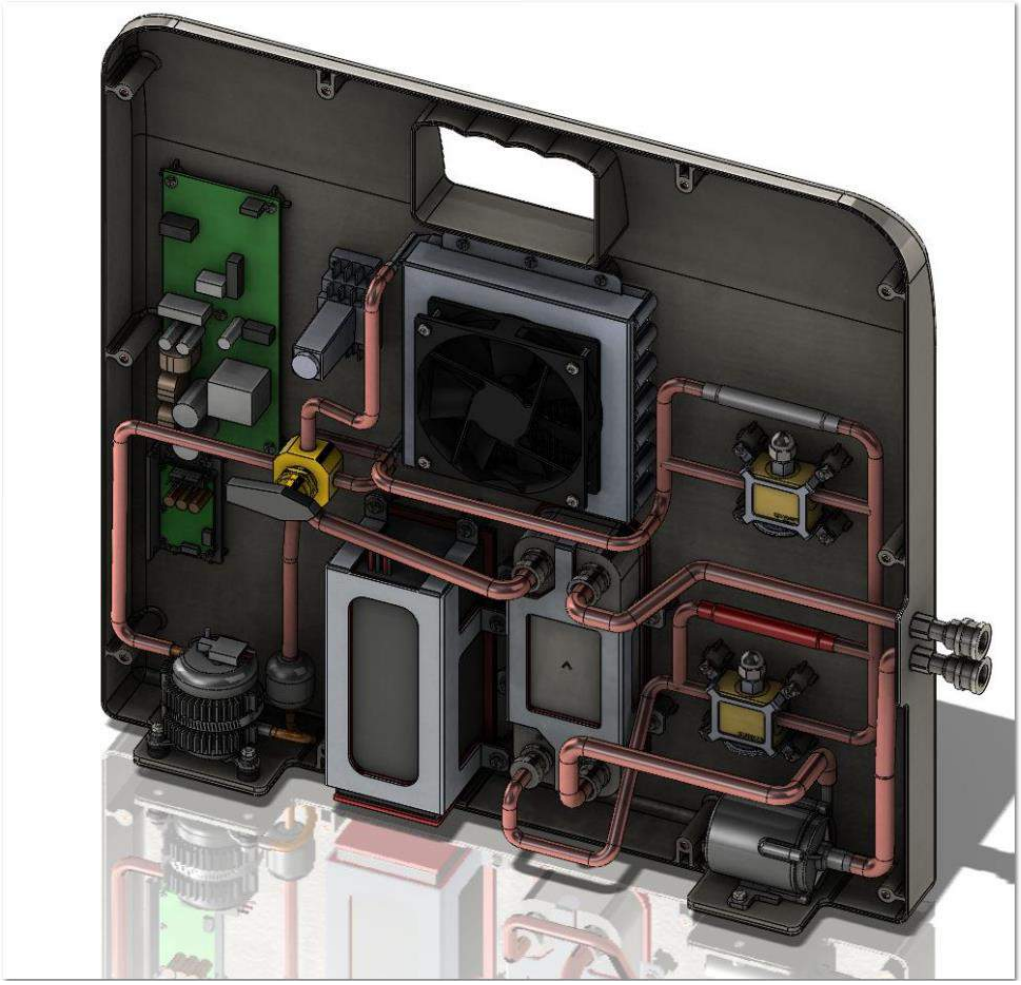

Figure 8. PBTC at developmental stage of adding 4-way valve

Functional testing of the pump on the breadboard prototype was also investigated before performance testing of the appliance was initiated. The fluid volumetric flow rate vs. pump voltage was analyzed over the entire operating range of the pump. First, the pump was configured in-line with a bath in order to circulate water through the PBTC unit as well as the blanket. The blanket was oriented horizontally, on a flat lab bench at a similar height as the pump, in order to eliminate the restriction of flow and the effects of pressure head. A voltage of 24 V was then applied to the pump and decreased in 0.5 V increments every minute until the pump shut off. The testing approach allowed for a generalized curve of signal voltage vs. flow rate to be developed for the system in a typical operating configuration. The results from the test are presented in Figure 9.

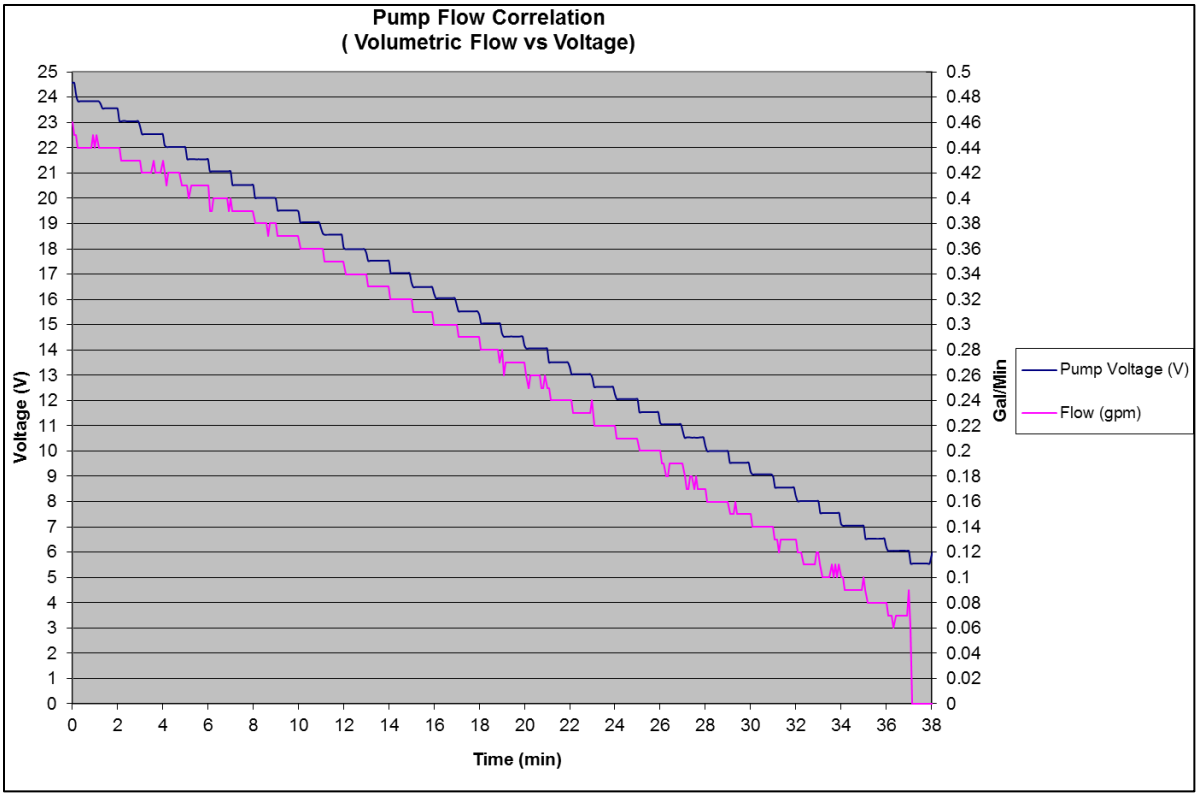

Figure 9. Pump voltage & volumetric flow comparison

As can be observed from the figure, the pump was able to maintain a volumetric flow rate of approximately 0.5 gpm at 24 V for the specified testing conditions. Furthermore, the pump voltage was reducible to 5.5 V before shutting down entirely. At this voltage a flow rate of 0.07 gpm was achieved. Flow analysis was then analyzed while operating the PBTC on the thermal manikin. It was immediately observed that the flow rate of 0.5 gpm was not attainable due to thermal blanket pressure drop. Depending on how the blanket was positioned on the manikin, flow rates ranged from 0.28 gpm to 0.4 gpm. The process of forming the blanket to fit the contour of the manikin in order to allow for decent surface contact explains the additional flow restriction, and subsequent pressure drop. Consequently, the blanket was not entirely flat as in the case of the bench top testing. The loss of volumetric flow rate is not detrimental to system design as long as similar heating and cooling capacities can be obtained, and all air can be purged from the system. With the breadboard prototypes components operating as a cohesive functional unit, performance testing was initiated so that system optimization could be completed.

3b. Performance Testing

Initial performance testing was also implemented utilizing the thermal manikin. Cooling capacity was first investigated utilizing a circulating bath in conjunction with the CSZ adult size Maxi-Therm® blanket. Bath temperatures were set to 30°C, 15°C, and 10°C respectively. In order to develop a testing procedure for quantifying the effective cooling capacity of the blanket,

the additional heat input required by the manikin in maintaining a surface temperate at 35°C was monitored. The testing process was to first set a constant skin temperature for the manikin at 35°C in the environmental chamber held close to 20°C. The heat flux from each zone required to maintain the 35°C surface temperature was allowed to come to steady-state. Once equilibrium was achieved the Maxi-Therm® blanket was then placed over the thermal manikin and the zone heat fluxes were again allowed to achieve steady-state conditions. The blanket was centered on top of the manikin to allow good contact with the chest, hip, and leg regions. The blanket was not forced to make ideal contact with the manikin, nor was it insulated by an additional garment to mitigate heat transfer with the ambient environment. The motivation was to simulate performance of a user just placing the blanket on the patient and operating the unit. The bath was then turned on and allowed to circulate at approximately 0.5 gpm through the blanket at the specified temperature while the spike in individual zone heat flux was monitored until steady-state conditions were obtained. By multiplying the surface area of each zone by the additional heat flux, the cooling capacity of the blanket on the individual zones was calculated. Presented in Figure 10 is the additional heat input required by the manikin for each individual zone with an input temperature of 15°C from the bath.

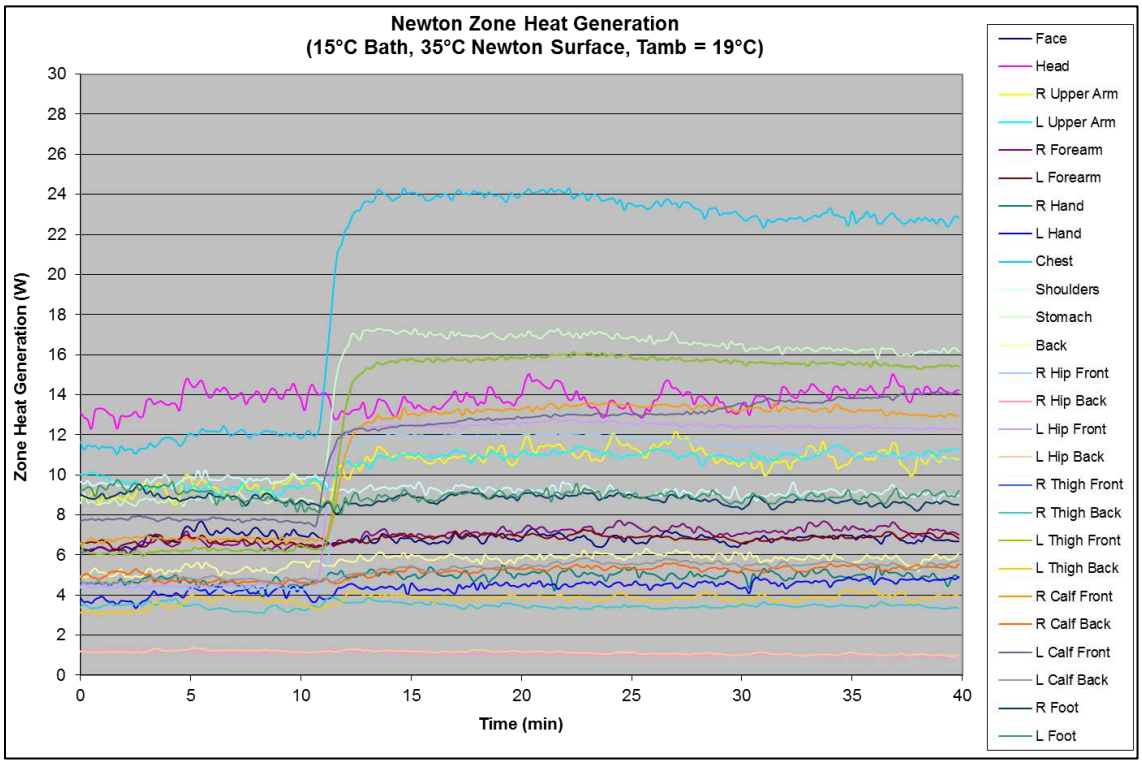

Figure 10. Individual zone heat generation rate (15°C bath)

The plot depicts which zones are most substantially impacted by the placement of the blanket. As can be observed, there is a significant increase in heat input from the chest, stomach, hip, and leg zones. Expectantly, there is no cooling provided by the blanket on the head, feet, hands, or

back regions. In order to quantify the overall effective cooling capacity on the manikin the sum of the increase in each zone heat input was compiled. The heat removal rate, as measured by the total additional power required from each zone of the manikin, was analyzed against the heat transfer rate into the water of the blanket. Presented in the following figure are the results for the 15°C bath.

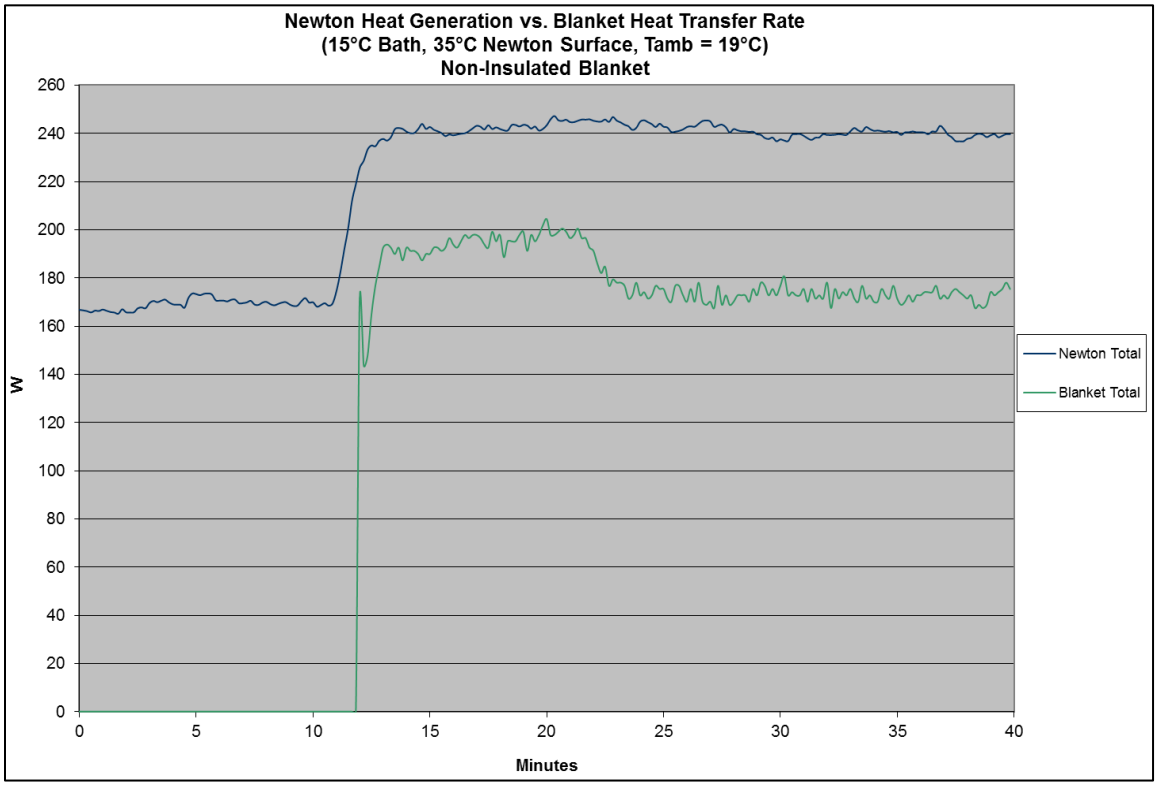

Figure 11. Accumulated increased heat generation & heat transfer rate (15°C bath)

As can be ascertained from the figure, a total increased heat generation rate of approximately 80 W is required for the manikin to maintain a surface temperature of 35°C for the given testing conditions. Consequently, from an energy balance analysis, the blanket is providing an effective cooling capacity of approximately 80 W. A total of approximately 160 W is being input into the water based on the mass flow rate and temperature change as the water circulates through the blanket. The water was at a temperature of about 15.5°C by the time it entered the blanket from the bath and in the range of 17°C by the time it had completely traversed through the blanket. In Figure 12 the accumulated results are also presented for the 10°C blanket inlet temperature, as provided by the bath.

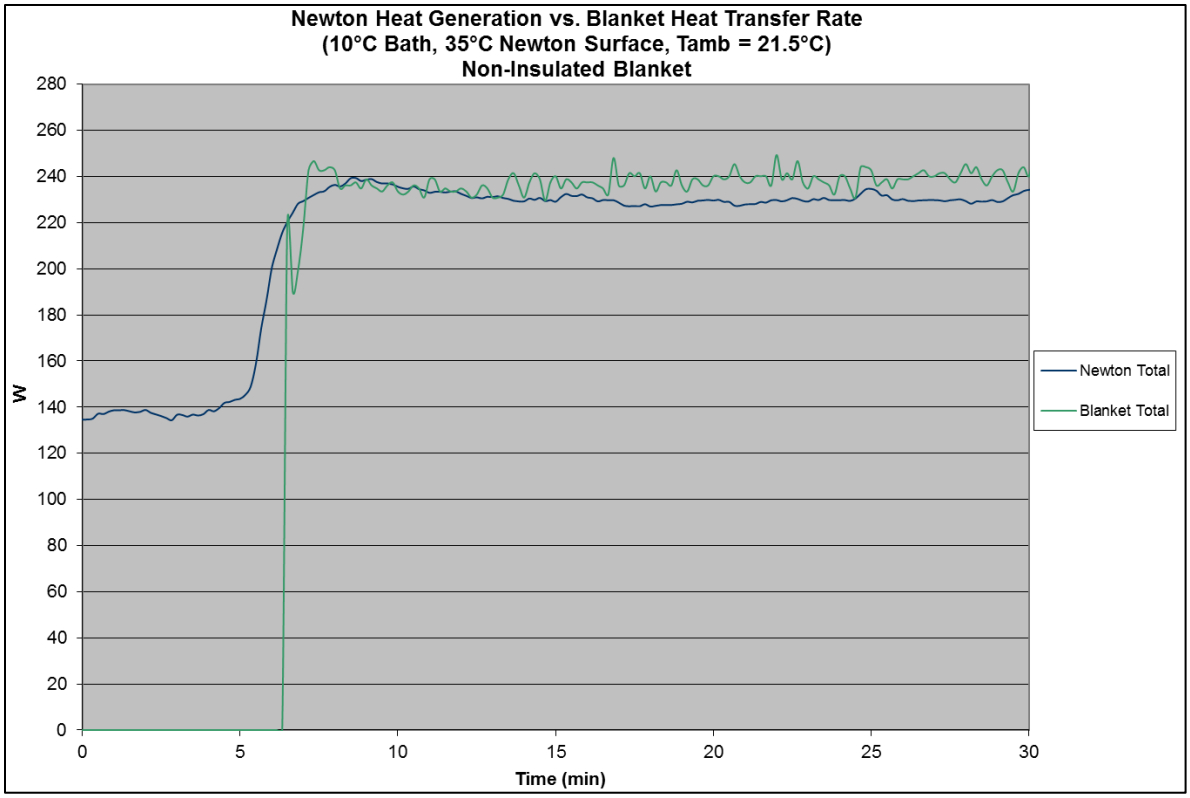

Figure 12. Accumulated increased heat generation & heat transfer rate (10°C bath)

The plot depicts an increased heat generation rate of approximately 100 W for the 10°C bath temperature. Therefore, the effective cooling capacity of the blanket for the specified testing conditions is in the range of 100 W. In analyzing the heat transfer rate into the blanket, based on the mass flow rate and increased water temperature, nearly 240 W is present. From an energy balance, the higher heat input rate is a result of the slightly higher ambient temperature as well as the significantly larger temperature gradient between the water and the ambient air. Consequently, there is a substantial heat input from the ambient to the water justifying the significantly higher heat input rate to the water than the additional rate being lost from the manikin. The manifestation is depicted above in Figure 12.

With a general understanding of the available effective cooling capacity performance of the Maxi-Therm® blanket operating at different conditions on the thermal manikin, performance testing was redirected towards the PBTC. A similar procedure was implemented for system cooling capacity analysis as with the circulating bath configuration. Initially, the manikin surface temperature was set be maintained at 35°C in the environmental chamber held at approximately 20°C. The heat flux from each zone required to maintain that 35°C temperature was monitored at steady-state conditions. Once equilibrium was achieved the Maxi-Therm® blanket was then placed over the thermal manikin and the zone heat fluxes were again allowed to achieve equilibrium. Yet again, the blanket was not insulated. The PBTC was then turned on

and allowed to circulate water at the maximum capacity of the pump, approximately 0.32 gpm. The increase in each zone heat flux was then monitored until steady-state conditions were obtained. The heat input rate and cooling capacity were then analyzed in comparison to the bath results.

In analyzing the data it was immediately realized that the performance was poor in comparison to initial testing of the compressor with a bath simulating the load instead of the manikin. The problem was identified as an issue with the TXV limiting adequate refrigerant flow into the evaporator. Upon further investigations it was thought the issue may be traced back to swelling of the seals, due to compatibility problems with the refrigerant, restricting the flow path through the valve. The seals initially utilized are comprised of ethylene propylene rubber (EPR) and the refrigerant is R134a. The seals were replaced with neoprene and the bulb of the TXV was recharged and installed on the PBTC unit. The refrigerant charge was also re-adjusted on the prototype in order to optimize superheat in the evaporator and subcooling in the condenser. Although system performance improved, it was still significantly less than anticipated based on initial performance testing of the compressor. Instead of the nearly 200 W at a 5°C inlet temperature only 100 W was attained, a nearly 50% degradation in performance.

A manual regulating valve was replaced in lieu of the TXV in order to manually control the flow coefficient (C_V) through the valve and further pin-point the problem. The orifice size of the valve was adjusted to optimize performance of the system and the unit was allowed to stabilize. The process was implemented without a load from the manikin in order to quantify the cooling capacity of the PBTC in relation to the inlet water temperature into the unit. The results are transient since the cooling capacity varies as a function of inlet temperature. The volumetric flow rate was maintained constant at approximately 0.32 gpm. A graphical depiction of the results is presented in figure 13.

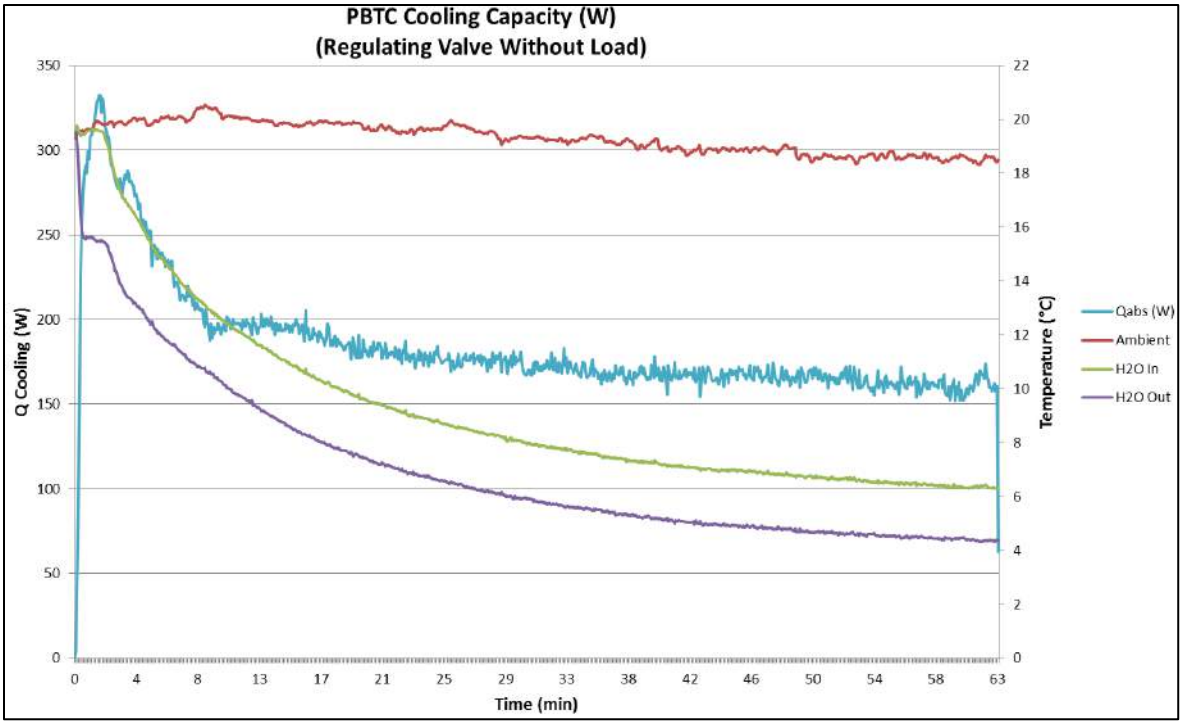

Figure 13. PBTC performance curve with regulating valve

The results demonstrate that even at an inlet water temperature of 6°C the PBTC with the regulating valve is able to maintain well above 150 W of cooling based strictly on the heat transfer rate from the water. That is not to say that all 150 W would be effective on the manikin, as was the case demonstrated in Figures 11 and 12 based on the total increased heat flux required to maintain a surface temperature of 35°C.

Based on the orifice size of the regulating valve, and corresponding flow coefficient, the TXV was adapted and optimized to implement similar performance. The regulating valve was then replaced with a TXV of the correct orifice diameter. The adaptation allows for refrigerant flow into the evaporator at an optimal proportion to the evaporation rate of the refrigerant in the evaporator. As a result, better superheat is obtained in the evaporator and sub-cooling in the condenser, improving overall system performance. The impact of adjusting the TXV orifice has been compared against the cooling capacity obtained from manually tuning the regulating valve. The comparison was implemented without a load from Newton to better assess PBTC system behavior. Presented in Figure 14 is the performance plot for the cooling test with the adjusted TXV orifice at a 20°C ambient temperature.

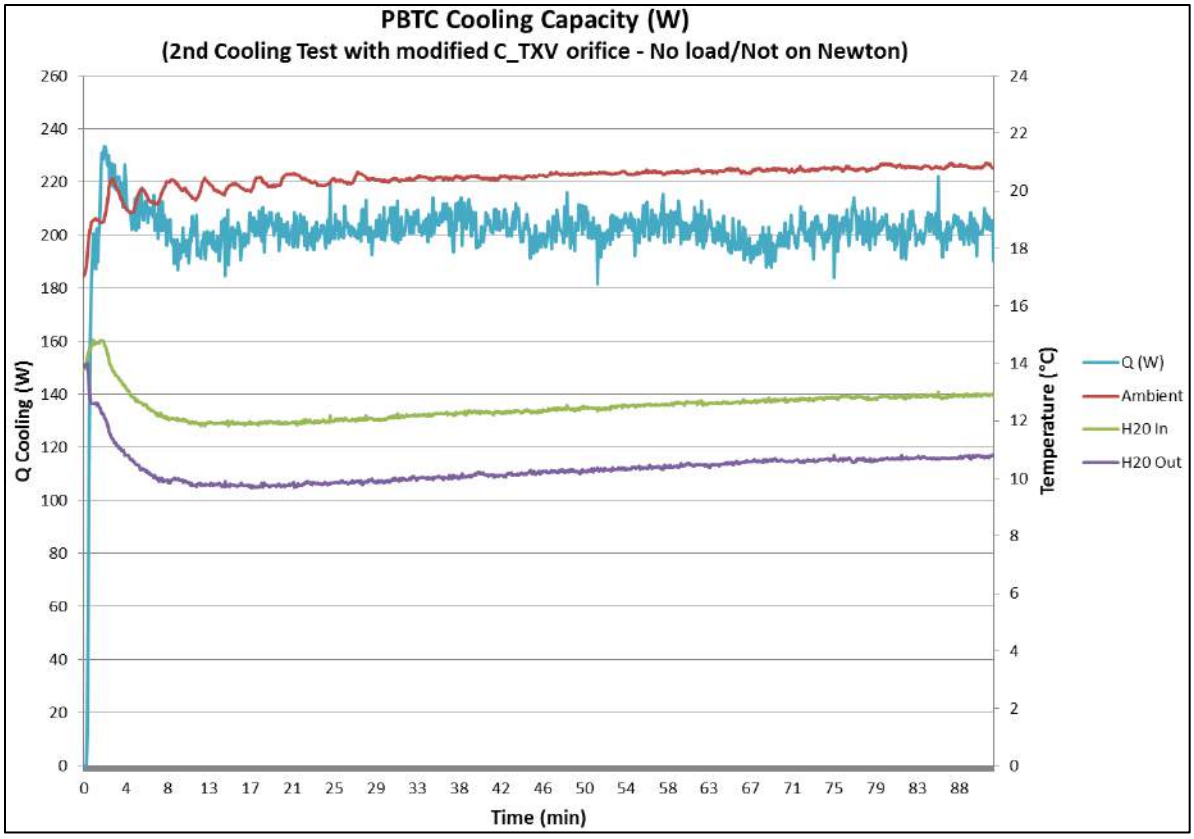

Figure 14. Modified TXV orifice cooling performance plot

As presented in the figure, the PBTC was able to maintain a cooling capacity of 200 W under steady-state conditions, a significant improvement over the 160 W steady-state capacity obtainable with the regulating valve. Adjusting refrigerant charge and spring force of the TXV, optimized superheat in the evaporator was obtained. The TXV was adjusted to obtain approximately 8°C superheat in the evaporator. A comprehensive testing matrix was then executed with a thermal load provided by Newton, the thermal manikin.

Cooling tests were implemented for varying ambient and operating conditions, while maintaining the surface temperature of Newton, the thermal manikin, at 35°C. The increased heat flux required to maintain the 35°C surface temperature was monitored while operating the PBTC along with the cooling capacity of the unit. The tests were performed for compressor speeds of 4,000rpm, 5,000rpm, and 6,000rpm each at ambient temperatures of 10°C, 20°C, 30°C, and 35°C. The tests were limited to the range of operating ambient temperatures because below 10°C the water would approach freezing conditions and above 35°C the heat flux from the manikin was not required to maintain the desired surface temperatures. Consequently, the impact of the blanket on the manikin could not be quantified. All tests were implemented as dry tests, implying no simulated perspiring from the thermal manikin. Through testing, it was demonstrated that the PBTC was able to maintain a cooling capacity in the range of 285 W to

425 W depending on testing conditions. With concerns of running the compressor for extended periods of time at the high 6,000rpm speed, risks of overheating and mechanical vibration failure lend to the requirement of being capable to achieve good heating and cooling capacities at lower compressor speeds. Resultantly, the cooling capacity performance plot for the 35°C ambient, 5,000rpm compressor speed is presented in figure 15.

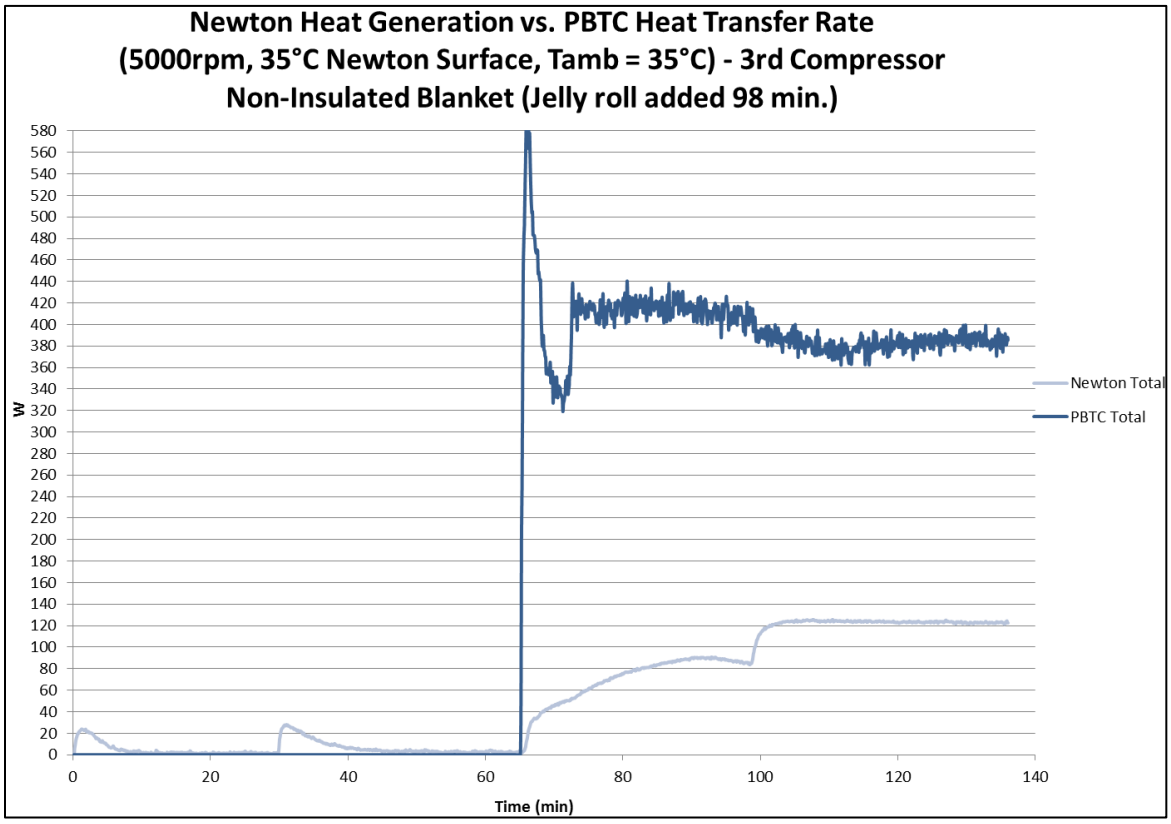

Figure 15. PBTC cooling capacity evaluation

As depicted in Figure 15, the PBTC was able to maintain approximately 420 W of cooling while operating under the specified conditions. At the 98 minute mark a large Gelli-Roll® blanket was placed on top of the Maxi-Therm® blanket to increase skin surface contact with Newton. The plot presents an additional 40 W of cooling provided to Newton by increasing the surface contact utilizing the Gelli-Roll® blanket. It is important to recognize that Rocky Research's design efforts were strictly directed towards maximizing the cooling and heating capacities of the PBTC, not the blanket design or placement and insulation of the blanket. The tests with the blanket on the manikin were strictly to demonstrate the significance of these parameters on the realizable effectiveness to the patient. As with all thermal management products utilizing conductive heat transfer, it is up to the caregiver to ensure proper contact between the patient and blanket is achieved so that optimal and adequate therapy can be provided.

A specific instance of operating the compressor at the maximum speed of 6,000rpm for an extended period of time, exceeding 3 hours, resulted in mechanical failure of the compressor. It was observed that vibrations from the higher threshold of the compressor speed appeared to have caused the structural failure at the interface between the compressor and the discharge line. In order to alleviate the possibility of a similar occurrence within an operating prototype, vibration dampers were integrated into the design on both the suction and discharge lines of the compressor. The vibration dampers consist of flexible refrigeration hose, and their effectiveness has been evaluated over long term operation of the PBTC. The flexible hoses preserve the mechanical integrity of the compressor.

Operating the PBTC at high compressor speeds and at elevated ambient temperatures resulted in compressor damage. A fan had previously been sized, installed, tested, and verified to prevent the compressor from overheating. Furthermore, it was found that the compressor was always well below the practical operating temperature limit of 135°C when experiencing the problem. Upon further examination, it was determined that the control board driving the compressor was the component overheating and causing the compressor to stop. The heat sink provided for the board with the compressor was not capable of effectively dissipating enough heat for the drive to maintain consistent functionality. To alleviate this problem, Rocky Research designed, built, and tested a new finned heat sink capable of dissipating enough heat to prevent the problem from occurring over long-term operation of the PBTC. Furthermore, an additional fan was incorporated into the design to allow for direct air circulation over the finned heat exchanger facilitating forced convective heat transfer.

Rocky Research contacted the design team of the Aspen compressor to express a concern with overheating of the control board utilized to drive the compressor. Upon doing so it was found that a new UL approved control board has been developed by Aspen to address the issue of the control board overheating. The UL approved board has a finned heat exchanger very similar in design to the one implemented by Rocky Research. Rocky Research acquired the UL approved boards for evaluation and integrated them into the system design. Figure 16 portrays the performance of the PBTC without the Rocky Research implemented heat sink on the compressor control board while Figure 17 portrays the same test with the heat exchanger intact. Both tests were implemented at the higher end capacity of the compressor in terms of speed, 6000rpm.

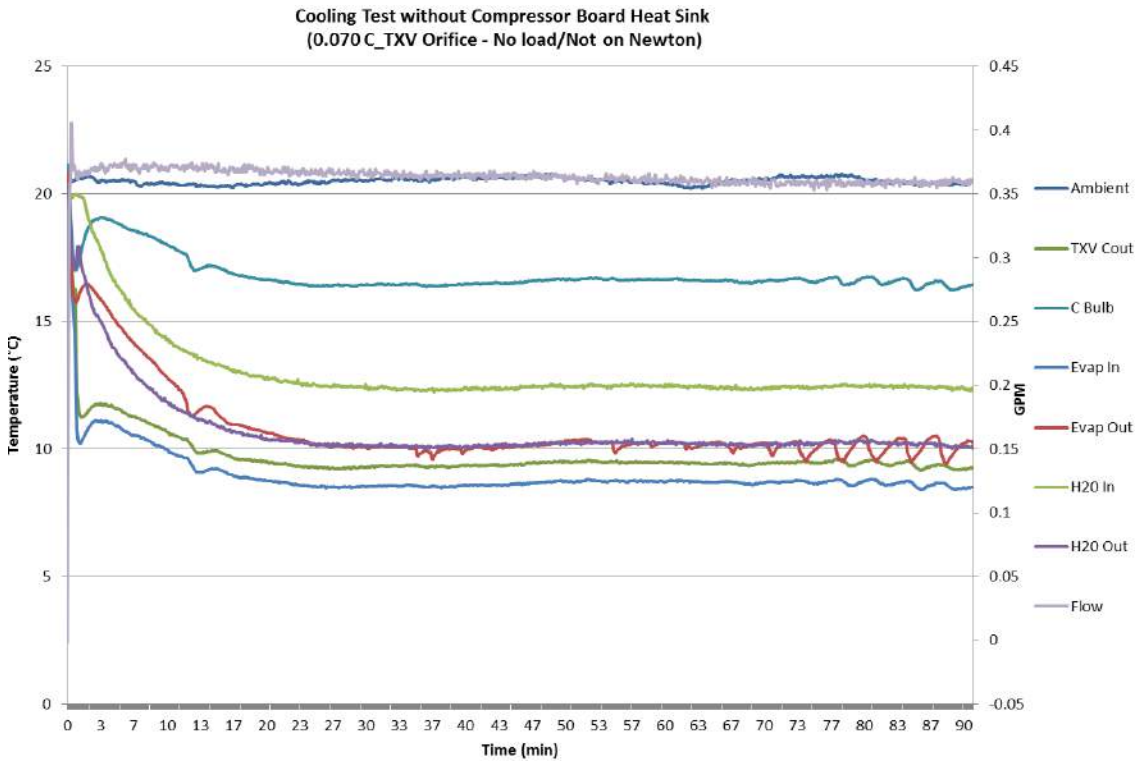

Figure 16. Performance without compressor board heat sink

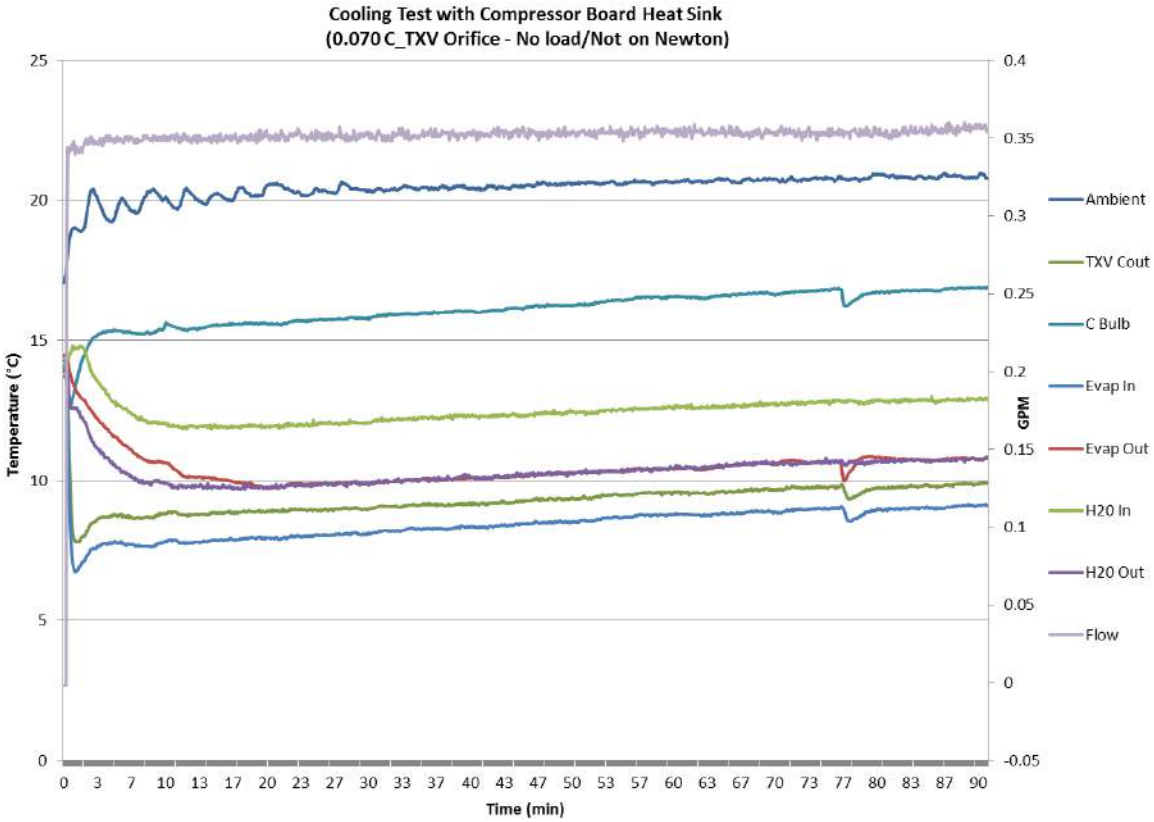

Figure 17. Performance with compressor board heat sink

In analyzing the data depicted in Figure 16, around the 70 minute mark, instability in the evaporator outlet temperature is observed. The fluctuation directly corresponds to the compressor cycling on and off as the compressor board began to overheat. Figure 17 shows the same testing conditions with the heat sink for the board installed as implemented by Rocky Research. The system ran considerably more stable, and is able to maintain long-term operational performance of the compressor with the heat sink intact and direct forced convection air flow available. The PBTC has operated at ambient temperatures of 50°C and compressor speeds of 6000rpm for several hours during performance testing without experiencing a single compressor board failure since the heat sink and additional fan have been installed.

A reservoir for filling the blanket was then integrated into the design of the case of the PBTC along with the proper plumbing to circulate water from the pump and to the blanket. The reservoir is designed to accommodate enough water to fill a large CSZ adult size Maxi-Therm® blanket along with the connection hoses and plumbing of the PBTC. A graphical depiction of the reservoir, along with all other described design component enhancements at that development state of the prototype is presented in Figure 18. Figure 18 also portrays the additional compressor control board heat exchanger along with the fan, compressor vibration dampers and how they are each integrated into the system.

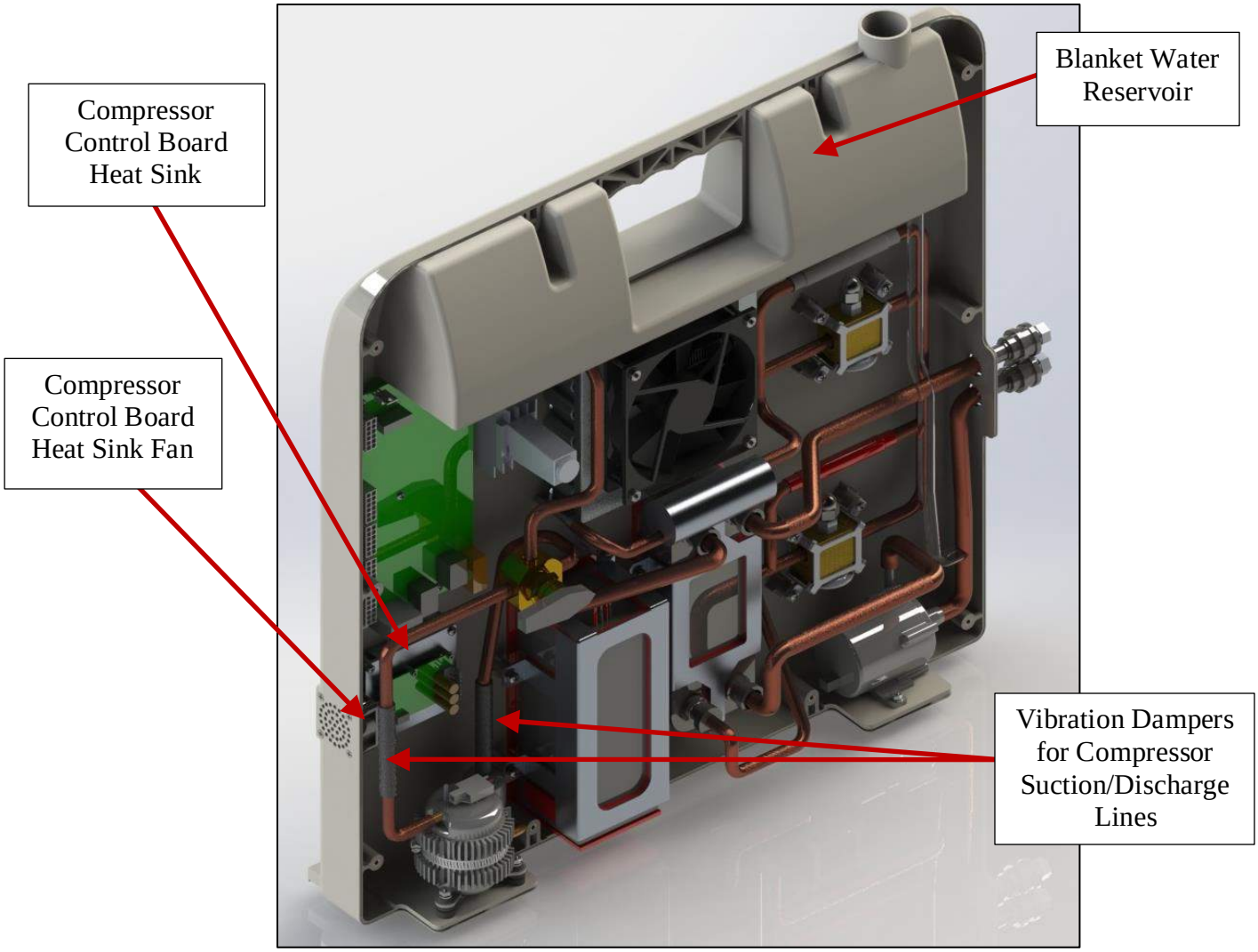

Figure 18. PBTC system component design enhancements

With a comprehensive evaluation of impactful cooling capacities, testing was direct towards the heating cycle performance of the PBTC. Similar to the cooling performance evaluations, heating tests were initially implemented at compressor speeds of 4,000rpm, 5,000rpm, and 6,000rpm with ambient conditions of 10°C, 20°C, 30°C, and 35°C. Since Newton is not capable of providing a cooling load, which is a necessity to perform the heating analysis in the same manner as the cooling tests, the testing procedure varied for evaluating the heating capacity effectiveness on the manikin. Initial testing consisted of first placing the Maxi-Therm® blanket on top of the thermal manikin. The blanket was not forced to make ideal contact with the manikin, nor was it insulated by an additional garment to mitigate heat transfer with the ambient environment. The ambient temperature in the environmental chamber was set, and the manikin was calibrated to allow the manikin zone heat fluxes to achieve a surface temperature of 35°C. Once the chamber and manikin reached steady-state conditions, a new test was run forcing the manikin heat flux to 0 W/m^2 while simultaneously starting the PBTC. Consequently, it is significant to recognize that

the manikin does not provide a load during the heat pump evaluation of the PBTC utilizing this procedure on the manikin. The heat input into the water was then documented along with the temperature profiles of the water in and out of the blanket. Furthermore, the surface temperatures of each zone and the average surface temperature of Newton were recorded. The individual Newton surface temperatures are presented in Figure 19. Similar to the cooling tests, the compressor speed for the plots presented was set to 5,000rpm at an ambient temperature of 35°C.

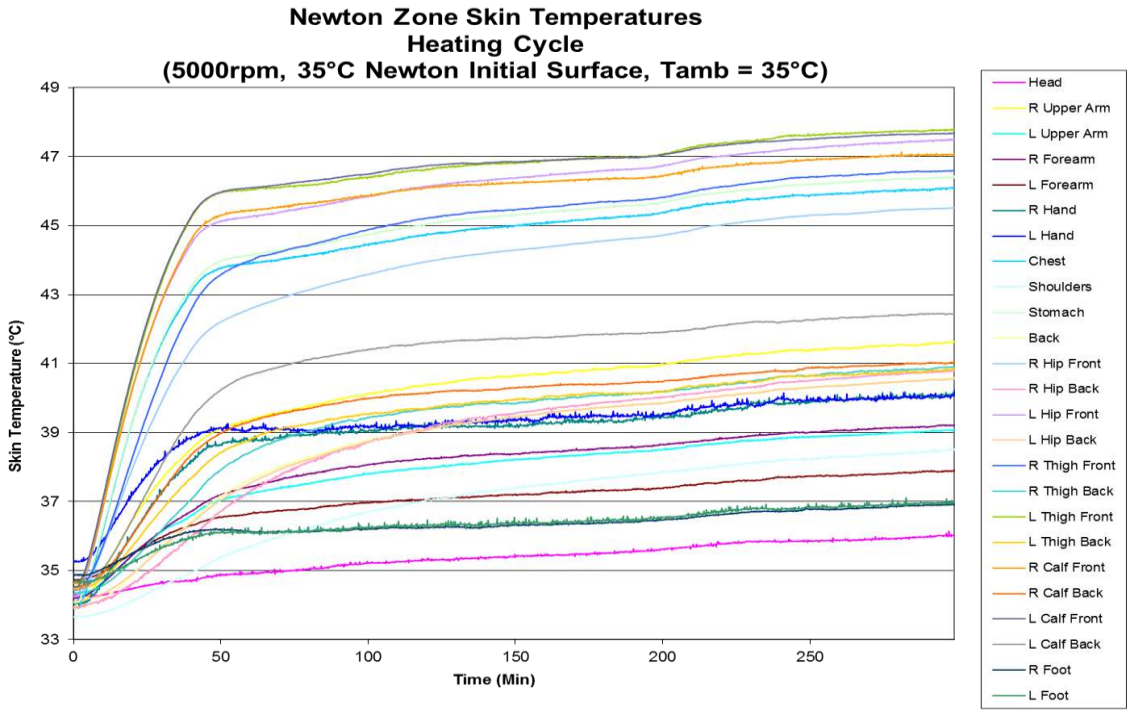

Figure 19. Newton heating test skin temperatures

Analogous to the cooling evaluations, the plot demonstrates good contact with the hips, thighs and chest. The PBTC was capable of increasing the surface temperature of several Newton zones to well above 42°C within 30 minutes, a 7°C increase in temperature. Heating surface temperatures much hotter initiates the risk of skin damage to the patient. The figure also establishes that after about 4 hours of continuous operation the PBTC was proficient in bringing the surface temperature of highly impacted zones up to 48°C. Zones not in contact with the blanket show a much slower increase in surface temperature, and the impact is primarily due to lateral heat transfer from the affected areas. The average Newton surface temperature is plotted against the heat transfer rate provided by the PBTC to the blanket water in Figure 20.

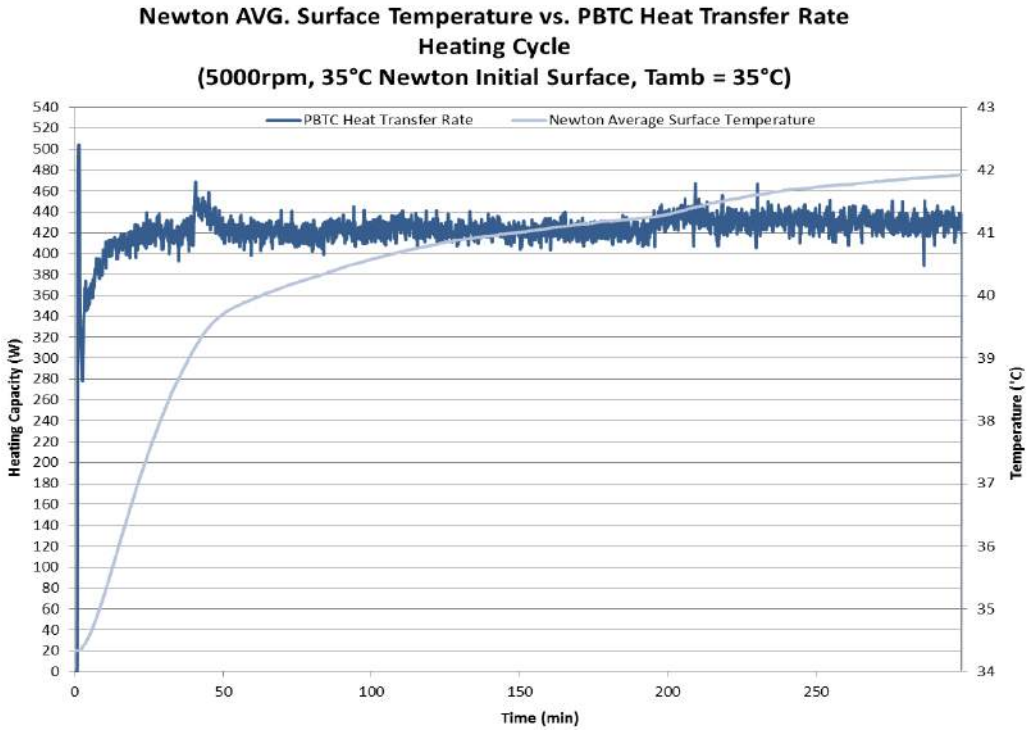

Figure 20. Heating performance & average Newton surface temperature

As can be ascertained from the figure, the majority of the PBTC heating impact on the manikin for the demonstrated testing conditions occurs within the first 45 minutes. There is, however, still a significant influence on Newton after that time frame. The average temperature is lower than many of the surface temperatures presented in Figure 19 due to the fact that the blanket is not in contact with several manikin zones, specifically the entire backside of Newton. Steady-state capacity reflects 430 W of heating for the presented evaluation. Similar to the cooling capacity, the heating capacity of the PBTC has been demonstrated to be within the targeted performance capabilities of the unit on the breadboard.

An actuator valve was integrated into the system design in order to automate the process of switching from heating to cooling modes and vice-versa. The actuator allows system operators to seamlessly transition between operating modes with the selection of a button instead of manually having to turn the 4-way valve. The actuator is a GM part initially designed and utilized in the automotive industry. In the design of the PBTC it has been retrofit and mounted to the existing 4-way valve utilizing a custom bracket. The actuator requires an input voltage of 12 V and a varying signal voltage is then utilized to control the position of the valve for cooling and heating modes. The valve has been oriented on the mounting bracket such that a signal voltage of 0 V corresponds to the heating mode and 8.66 V corresponds to the cooling mode. The actuator has been extensively evaluated to ensure it supplies sufficient torque and is capable of transitioning the system between heating and cooling modes effectively. Presented in Figure 21 is a depiction of the actuator mounted to the 4-way valve on the breadboard. Figure 22

portrays how the actuator is integrated into the case of the PBTC along with its relative positioning in comparison to other system components.

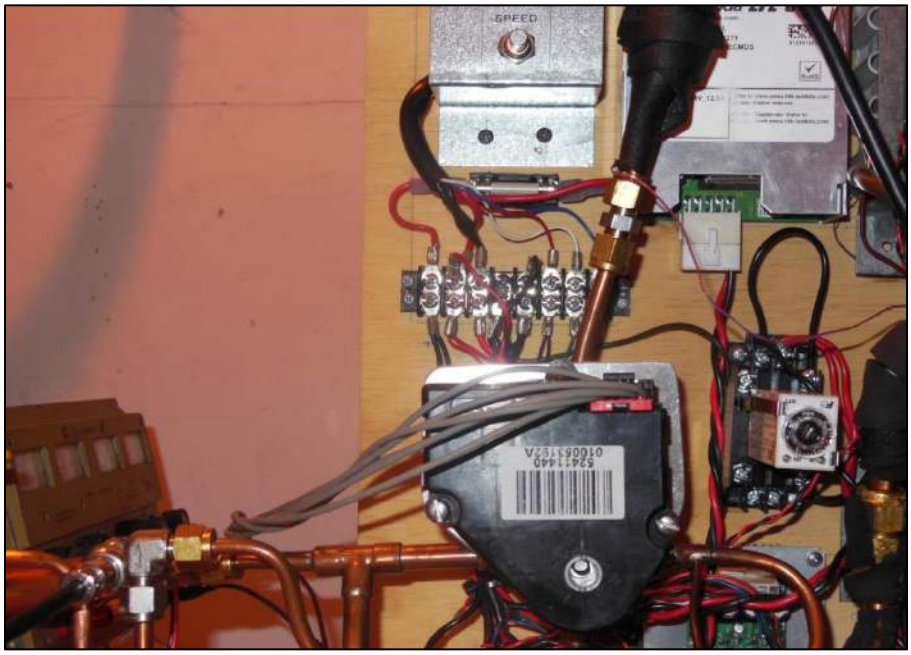

Figure 21. Actuator valve for PBTC installed on system breadboard

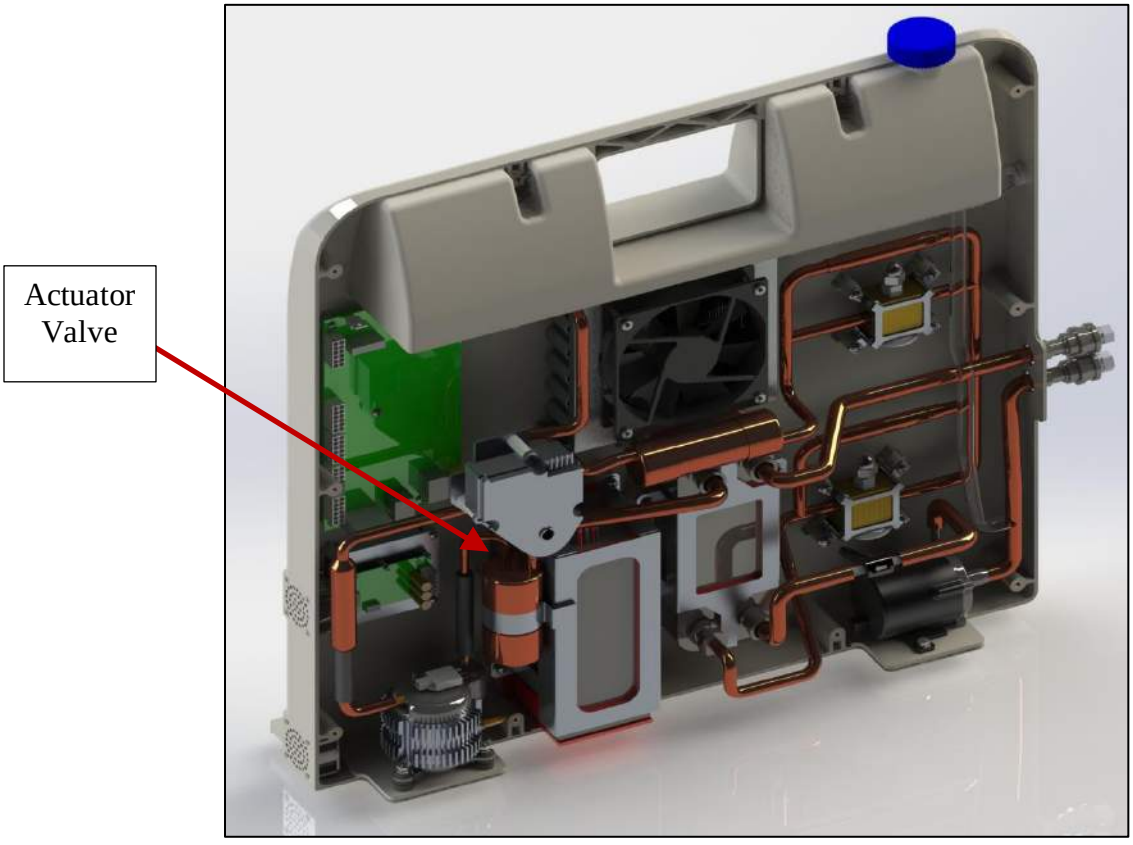

Figure 22. PBTC prototype layout with actuator added

The effectiveness of the originally selected air coil heat exchanger was found to be less than optimal in both heating and cooling modes. A larger air coil was selected to be analyzed as a replacement to increase heat exchanger effectiveness. The larger replacement coil has been deemed as an appropriate alternative to improving system capacity. The newly selected coil is a micro-channel condenser similar to the original coil but of larger surface area. The larger coil has a face surface area of 40.9 in^2 in comparison to the original 26.3 in^2. The bigger coil weighs in at 1.1 lbs, whereas the smaller coil weighed approximately 0.7 lbs. The additional weight of the larger coil is justified by the increased capacity and elimination of the required refrigerant reservoir. The increased refrigerant volume of the larger air coil reduces the discrepancy between the plate heat exchanger in terms of refrigerant storage capacity. It was found that with the larger air coil the refrigerant reservoir was no longer required. Consequently, the larger air coil allows for overall system weight to be reduced while increasing both the heating and cooling capabilities of the appliance. A new fan was sized, acquired, and tested to better accommodate the larger air coil. The increased surface area of the fan allows for the entire face of the air coil to be utilized. The fan is of dimensions 6.77 in X 5.9 in X 1 in and is rated for a maximum air flow of 250 CFM. The relatively thin fan allows the larger air coil and fan to fit inside the case without modifying the case geometry. Therefore, the coil and fan alterations are essentially seamless to the end user.

Upon initial testing of the larger coil it was found that the refrigerant side pressure drop was significantly higher, resulting in a restriction of refrigerant flow and subsequently depleted system performance. In the heating cycle, nearly 22°C superheat was being observed out of the evaporator. The TXV bulb charge was consequently adjusted to reduce superheat by 10°C and increase refrigerant mass flow. The system was then recharged and the performance re-evaluated. Presented in Figure 23 is representation of the system performance with the new coil and adjusted bulb charge. Heating capacity is plotted along with the high and low side operating pressures at an ambient temperature of 30°C and a compressor speed of 5000rpm.

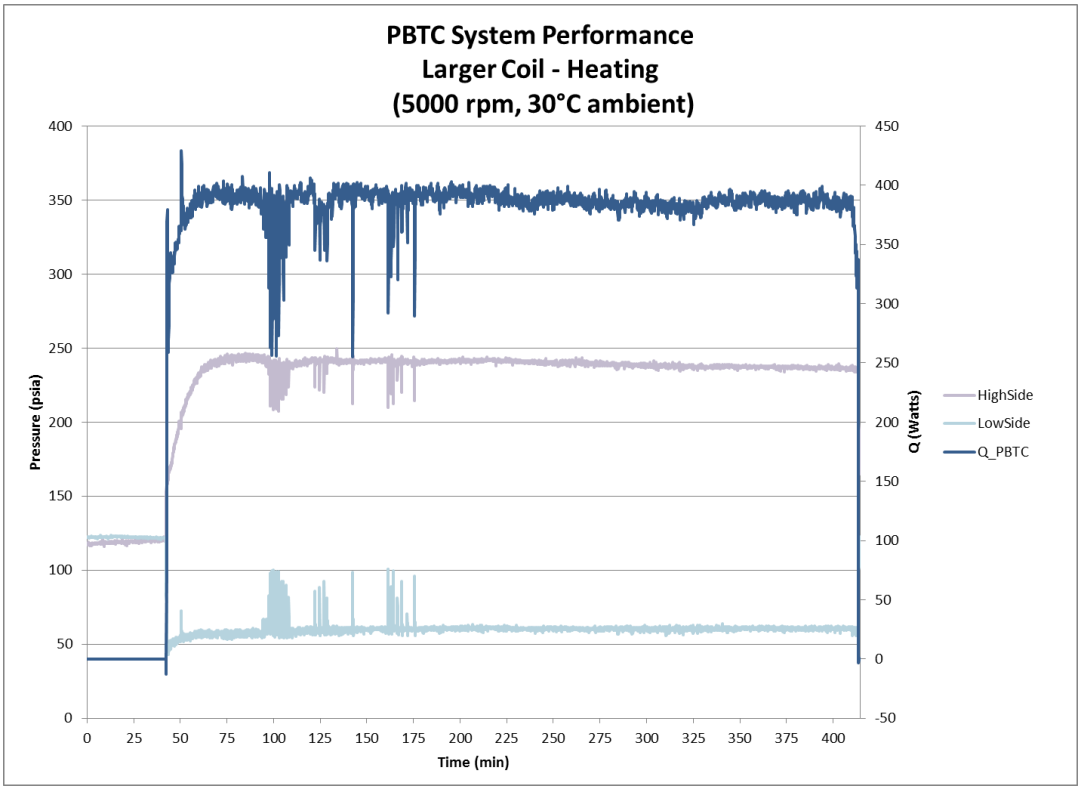

Figure 23. PBTC performance with larger air coil

As represented in Figure 23, approximately 400W of heating capacity was demonstrated with the larger coil for the specified operating conditions. The plot also portrays fluctuations in system low side pressure along with a corresponding instability in compressor performance. Such behavior is indicative of liquid slugging or flooding of the compressor. Tuning of the spring force on the TXV was not allowing for better control of system superheat by adjusting refrigerant mass flow rate. Closer analysis revealed that surface contact of the TXV bulb to the evaporator outlet refrigeration line had poor thermal contact resulting in a large temperature gradient. As a result the TXV was not accurately modulating refrigerant flow, and either large superheat or flooding of the compressor was occurring. Presented in Figure 24 is a performance plot portraying the discrepancy between the evaporator outlet temperature and the sensible temperature of the TXV bulb.

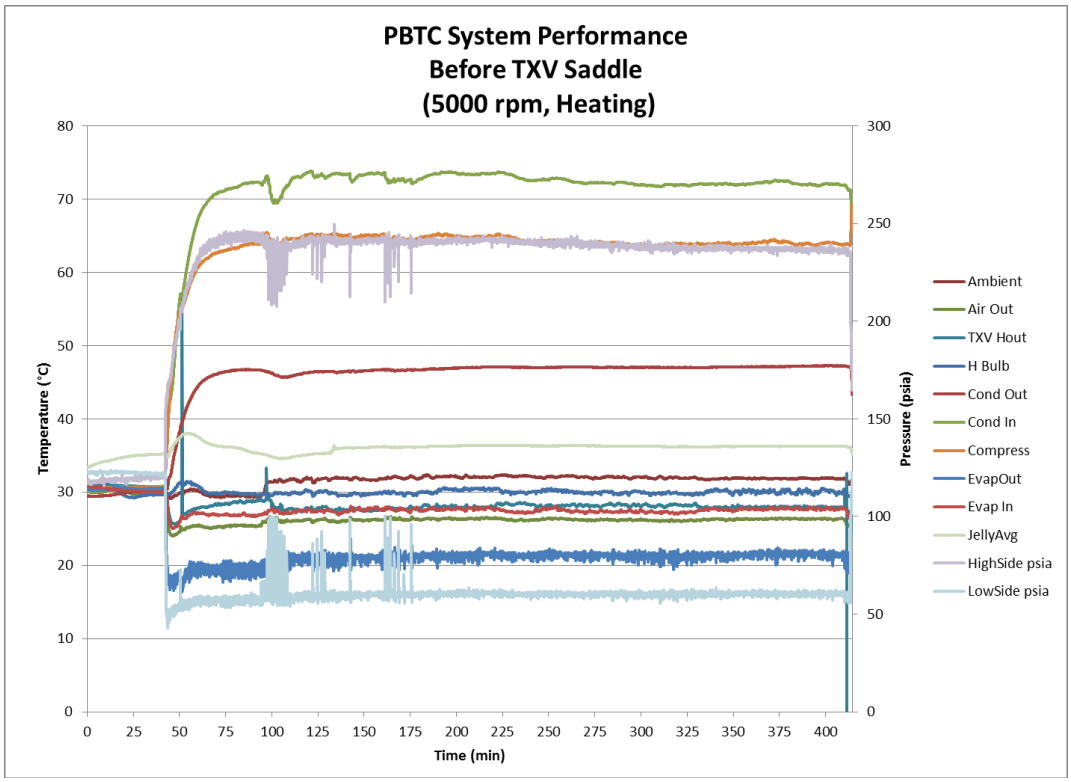

Figure 24. PBTC testing without TXV bulb saddle installed

Figure 24 demonstrates that the steady-state evaporator outlet temperature is approximately 20°C. Conversely, the steady-state TXV bulb temperature was around 30°C. In order for the TXV to function as designed the two temperatures should be similar. To remedy the problem, and reduce the thermal gradient between the evaporator outlet and TXV bulb temperatures, a saddle was installed. The function of the saddle is to provide a larger contact surface area in order to facilitate heat transfer. Figure 25 demonstrates the surface contact between the TXV bulb and refrigeration line with and without the saddle installed. On the left the saddle in non-existent while on the right the saddle is present.

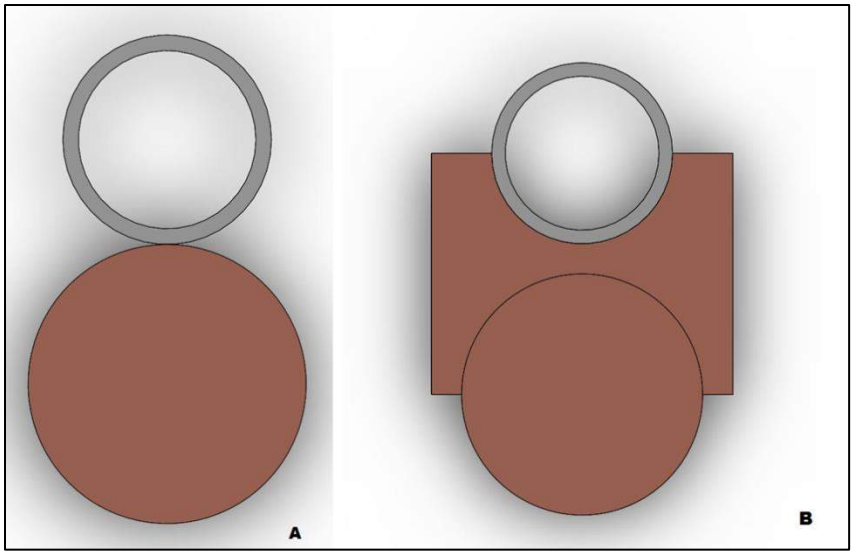

Figure 25. A) TXV/line contact without saddle B) TXV/line contact with saddle

With the TXV saddles fabricated and installed, a heating test was implemented under the same operating conditions in an effort to analyze the discrepancy in temperature between the TXV bulb and evaporator outlet refrigeration line. The increase in contact surface area was found to reduce the thermal gradient between the TXV bulb and refrigeration line as intended. Figure 26 portrays a test under the same operating conditions as demonstrated in Figure 24 only with the TXV saddle installed.

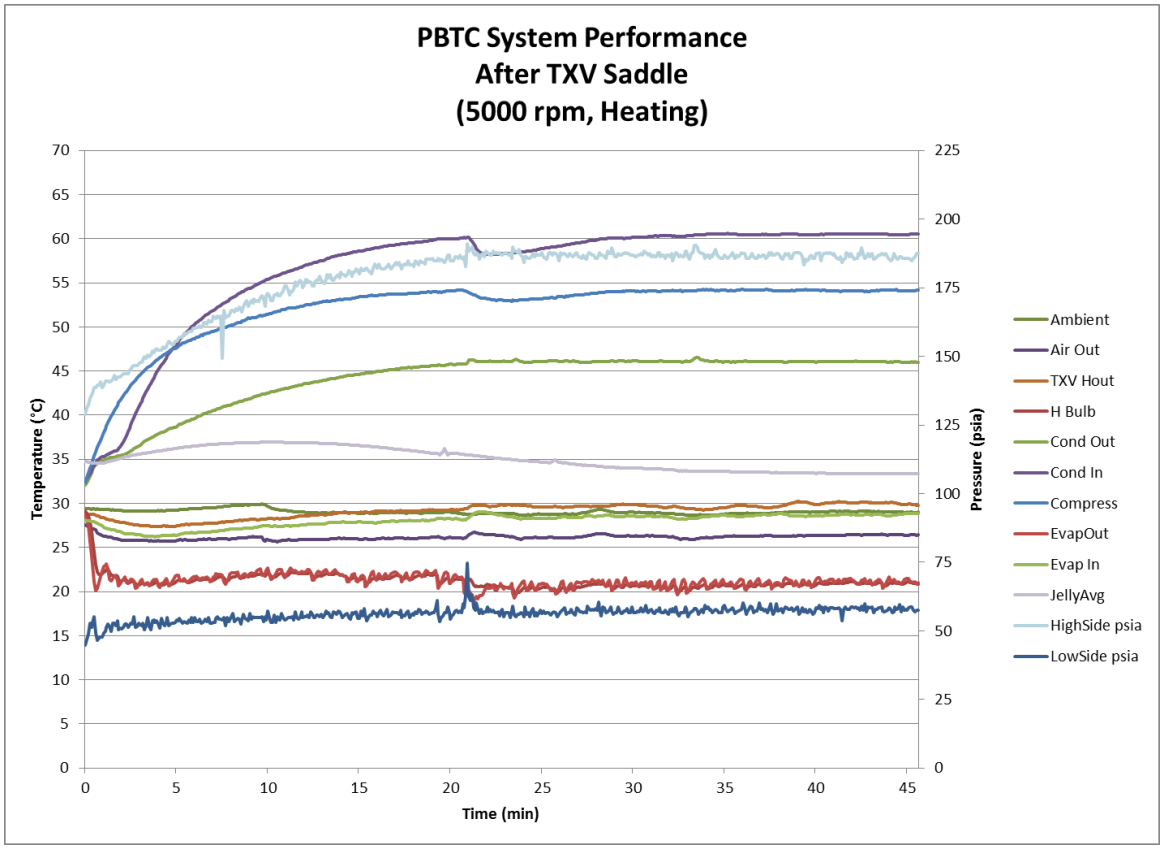

Figure 26. PBTC testing with TXV bulb saddle installed

Figure 26 demonstrates that with the saddle installed, the steady-state temperatures of the TXV bulb and the evaporator outlet refrigeration line temperature were nearly identical. Both were demonstrated to be close to 20°C, allowing the TXV to properly function as designed. Consequently, a fluctuation in evaporator outlet temperature resulted in an almost instantaneous response in TXV bulb temperature. The advantage is that the TXV can quickly respond to instabilities in the system operation, maintaining target thermodynamic operating conditions.

Thermistor saddles have also been designed, fabricated, and evaluated to effectively secure the temperature sensors to the copper plumbing of the system. The saddle contains a hole through the center to fit tightly over the copper tubing, allowing the saddle to be directly sweated to the copper tubing. The surface mount flag terminal probe can then be bolted to the saddle via a mounting hole. The durability of the appliance and integrity of the temperature reading is preserved by robustly fastening the thermistor saddle to the plumbing. The design also allows for good heat transfer between the circulating fluid and the temperature sensor itself. Such a characteristic is essential for accurate water temperature readings being delivered to the blanket as well as the response time of the control scheme. Faster response time directly correlates to tighter temperature modulation of the delivered fluid. Presented in Figure 27 is a drawing of the thermistor saddle.

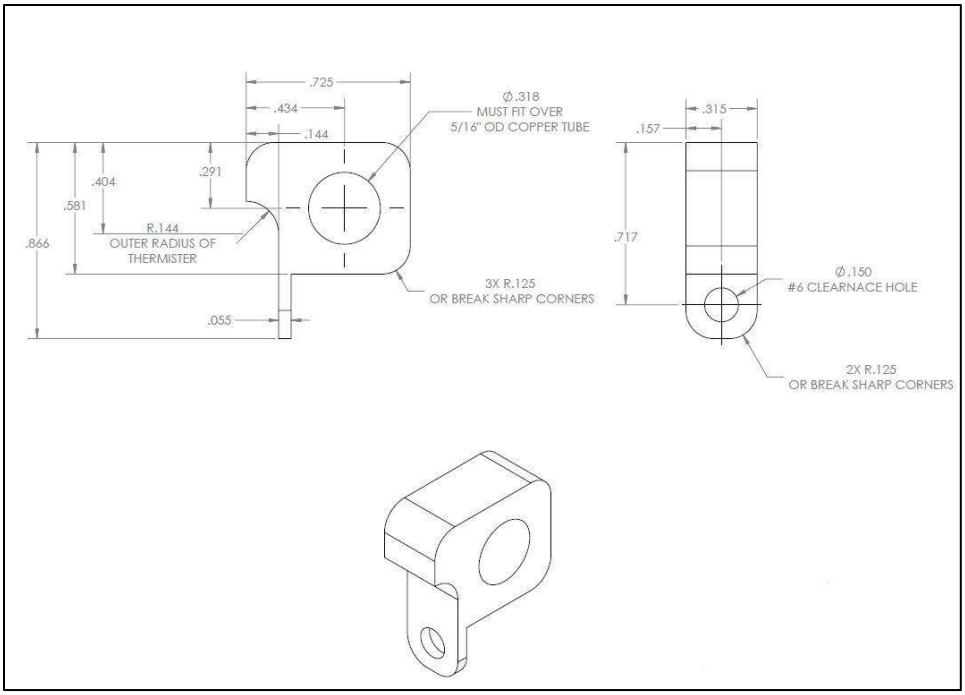

Figure 27. Thermistor saddle

Under identical operating conditions, inconsistencies in water flow rates through the PBTC and the adult sized Maxi-Therm® blanket resulted in further investigations pertaining to the water side plumbing of the system. It was found that pockets of air were being trapped throughout the blanket and system. In order for the PBTC to operate most effectively it is critical that air be purged from the system. A bench scale test was configured with transparent Tygon® tubing so that the removal of air could be visually observed for various plumbing configurations. The results of the bench scale testing led to the requirement of smaller tubing sizes and the recirculation of water through the reservoir of the case. It was established that a higher fluid velocity was required to purge the air effectively from the blanket and system.

Smaller tubing allowed the required fluid velocity to be achieved, but resulted in a larger pressure drop reducing overall water mass flow. Consequently, the change in water temperature was increased by reducing the tubing size. Resultantly, the capacity of the system could be limited to less than maximum capabilities as a result of the safety functions. To increase the mass flow rate, reducing the change in temperature of the water across the unit and allowing the maximum capabilities of the system to be utilized, a larger pump was selected. The new pump is of the same physical dimensions but provides an increased flow rate up to a maximum capacity of 7.9 L/min. The pump has been thoroughly tested in conjunction with the modified plumbing configuration on the system, allowing the full capacities of the system to be obtained without concerns of large water temperature gradients across the appliance. Presented in Figure 28 is a model representation of the system design enhancements. The rendering portrays the updated air

coil and fan as well as the new pump and thermistor saddle. Additionally, the modified plumbing is depicted along with the TXV bulb saddles.

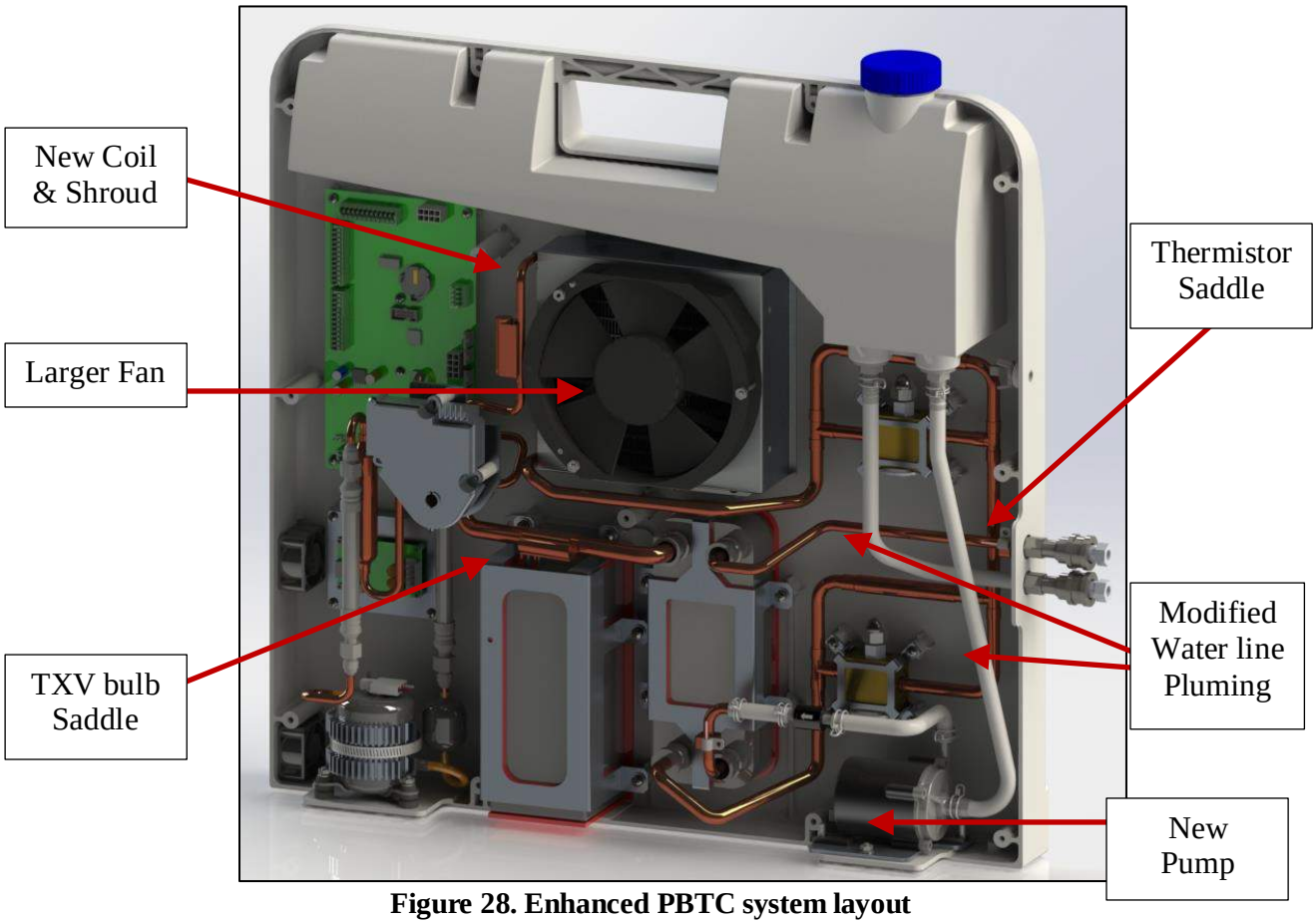

Figure 28. Enhanced PBTC system layout

As a result of replacing the air pockets with water, eliminating air from the system and blanket requires a larger water volume. Consequently, the water reservoir integrated into the case was modified to hold the additional water necessary for a fully purged system. The supplementary volume was accomplished by lengthening the height of the reservoir on the right side near the water ports, and by reducing the gap size for the handle. Both modifications accommodate the system design by not interfering with the placement of other system components. Custom threaded inserts are utilized to connect the water reservoir to the inlet and outlet tubing lines. The modifications to the reservoir are integral to the back half of the case. In an effort to mitigate concerns of a large pressure drop across the coil, the inlet air ports on the front of the case were relocated directly in front of the air coil and fan. The open volumes of the inlet and outlet ports were also increased to reduce pressure drops across the case. Figure 29 is a rendering of the modified case. The picture on left depicts the inside of the back half of the case with the enhancements to the reservoir implemented. On the right is a representation of the inside of the front half of the case with the inlet air ports moved and the open volume increased. The first fully functional prototype was constructed with the presented case design.

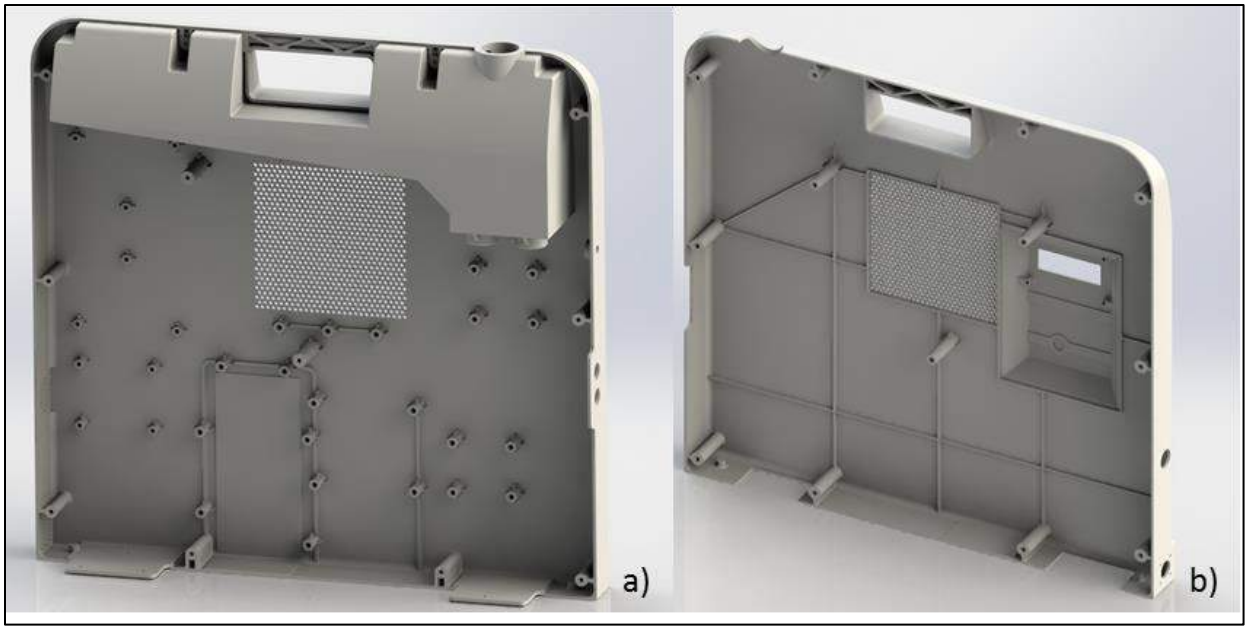

Figure 29. Modified PBTC a) back of case b) front of case

Feet for the PBTC case, designed to enhance system stability, were constructed and integrated into the case design. Two feet mount to the base of the appliance, one on each side. Figure 30 illustrates the feet design and how they are installed on the PBTC. On the left is a representation of the installed feet on the prototype. On the right is an exploded view portraying how the feet attach. Figure 31 demonstrates the estimated geometry specifications of the appliance prior to fabrication.

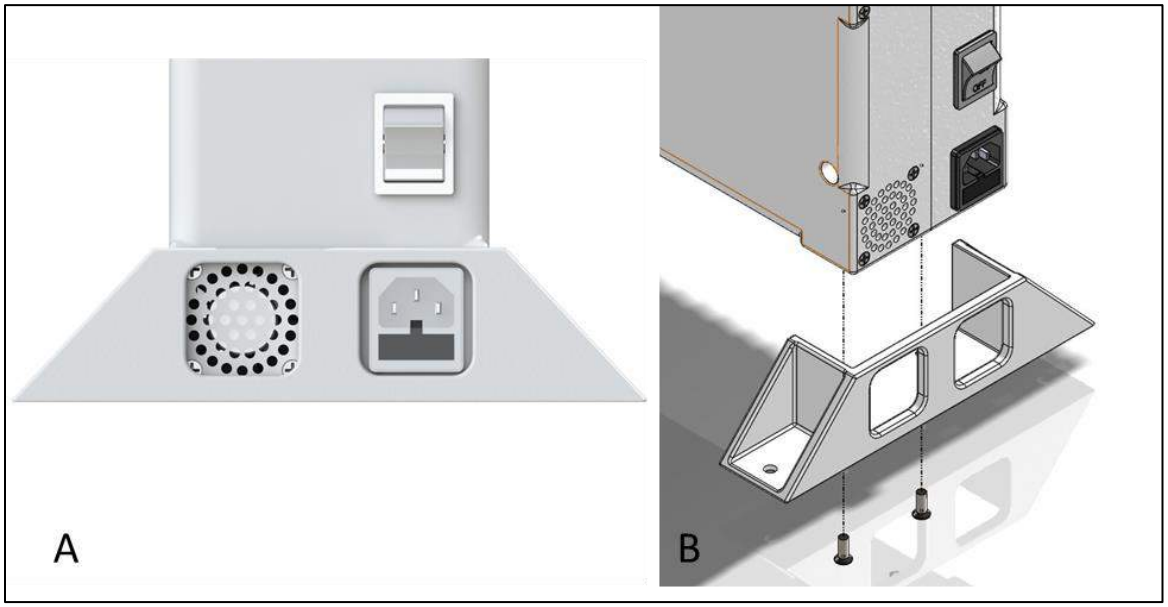

Figure 30. PBTC removable feet

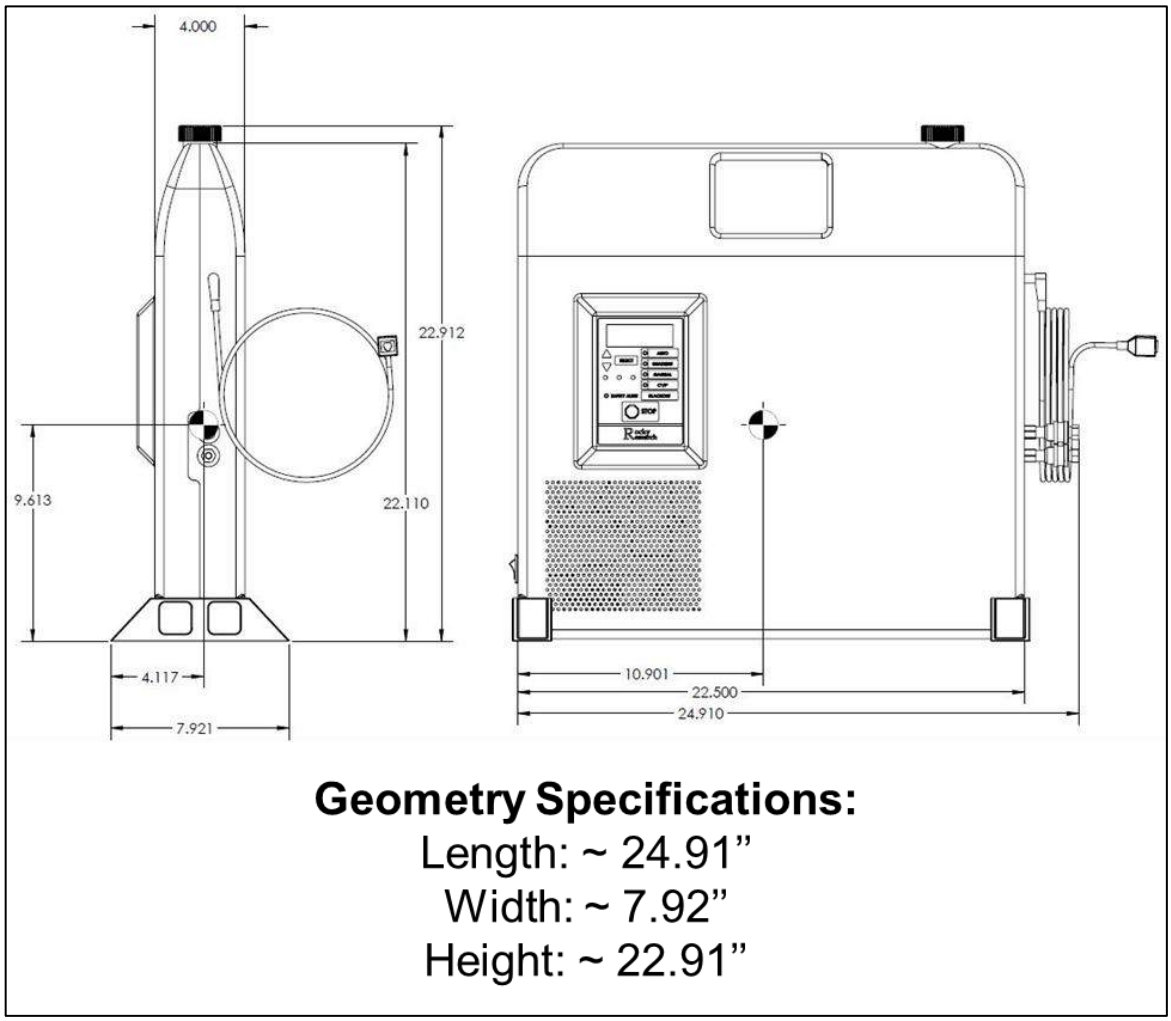

Figure 31. PBTC geometry specifications

With several alterations made to the system design, a comprehensive functional and performance testing matrix was implemented incorporating the improvements. The matrix covered both heating and cooling modes at different compressor operating speeds and ambient temperatures. The compressor was operated at speeds of 2000rpm, 3000rpm, 4000rpm, 5000rpm, and 6000rpm each at ambient temperatures of 10°C, 20°C, 30°C, 40°C, and 50°C. The unit was plumbed directly to a bath with a water mass flow rate equivalent to that producible by the newly selected pump installed on the system. For the cooling tests the recirculating water temperature to the unit was maintained at 25°C and both the performance and power consumption of the system contrasted for the different conditions. Presented in Figure 32 is a plot depicting the system cooling capacities at different compressor speeds and ambient temperatures. Capacities were taken as a steady-state average after a minimum of 10 minutes of system operation. Figure 33 is representative of the coefficient of performance (COP) of the system at the same conditions. The COP was calculated utilizing the battery DC power consumption.

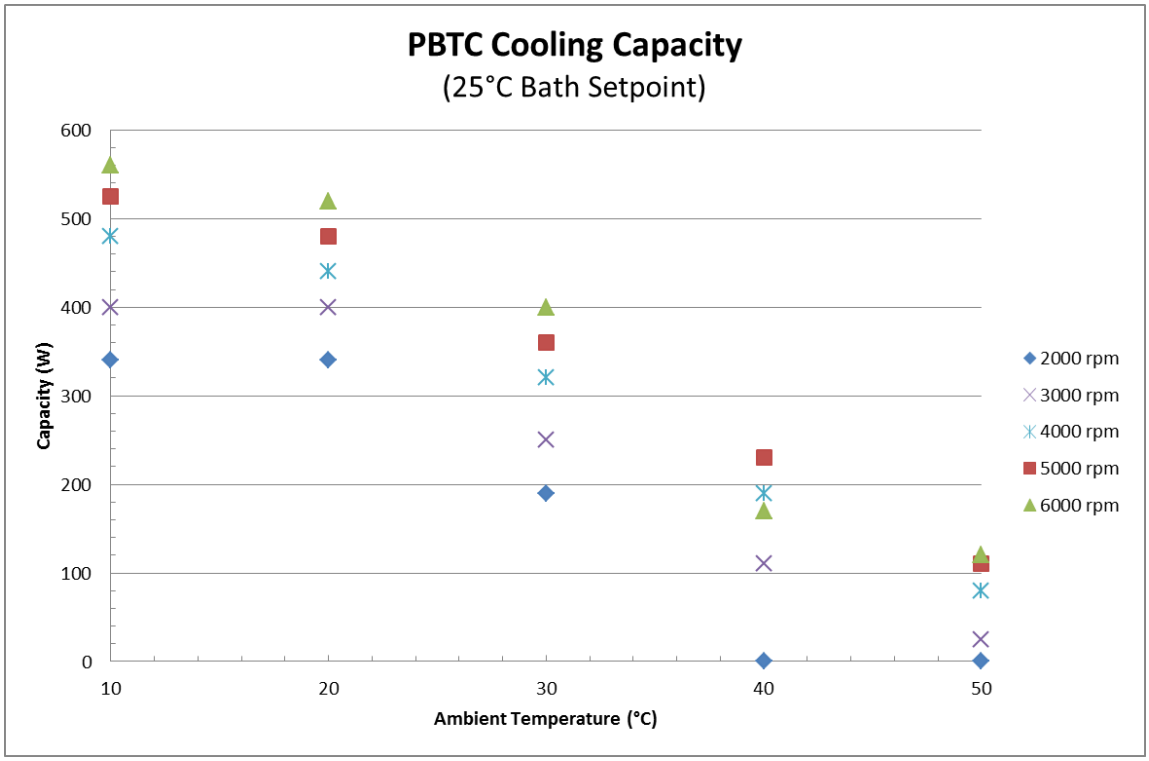

Figure 32. PBTC cooling capacities

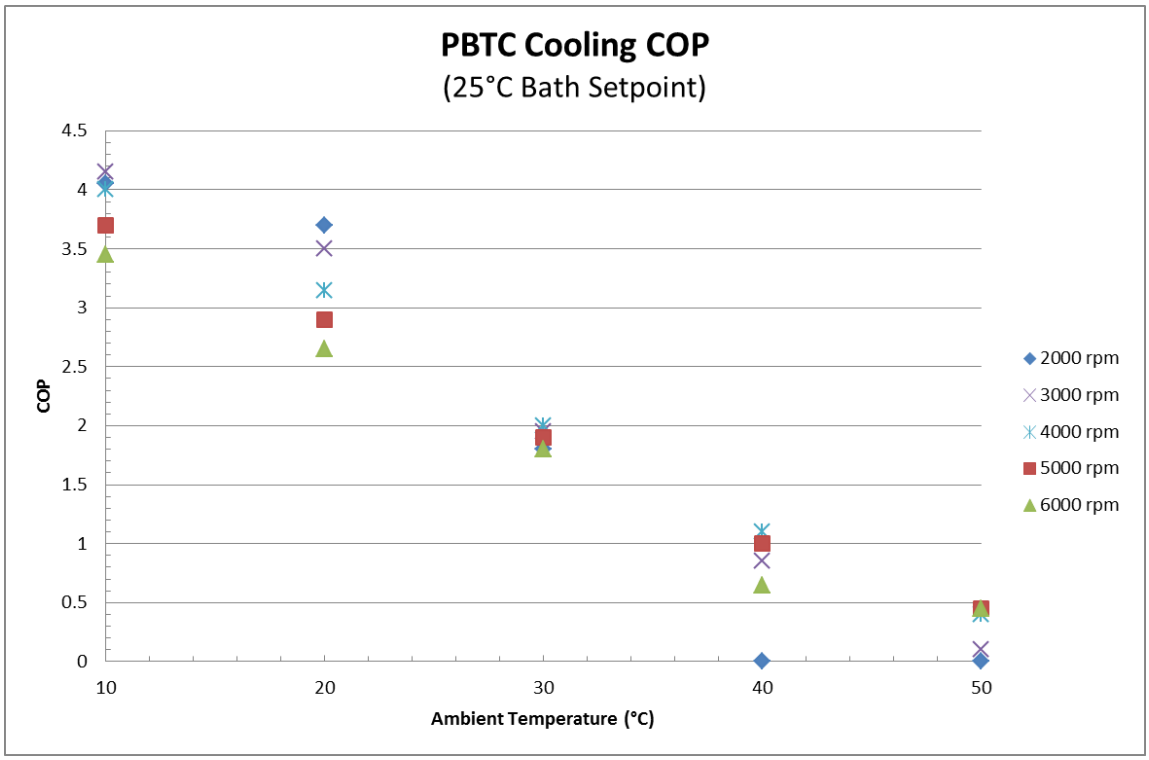

Figure 33. PBTC cooling COP

Figure 32 demonstrates the achievability of cooling capacities up to 560W for the specified 25°C inlet water temperature maintained to the PBTC. As a general observation, the capacities tend to improve as the compressor speed is increased, and the ambient temperature is decreased. From a thermodynamic perspective both of these observations are intuitive and as expected. Figure 33 demonstrates that the higher the operating temperature, and the faster the compressor runs, the more power it consumes, which is also expected.

Heating tests were also implemented for the same compressor speeds and ambient temperatures. Again, the water flow rate through the system was set to maintain that achievable from the newly installed pump. The return load set point temperature of the bath was specified to 40°C. Similar to the cooling tests, capacities were documented after 10 minutes of operation at steady-state conditions. Figure 34 portrays the heating capacity of the PBTC at different ambient temperatures and compressor speeds while figure 35 depicts the COP under identical testing conditions.

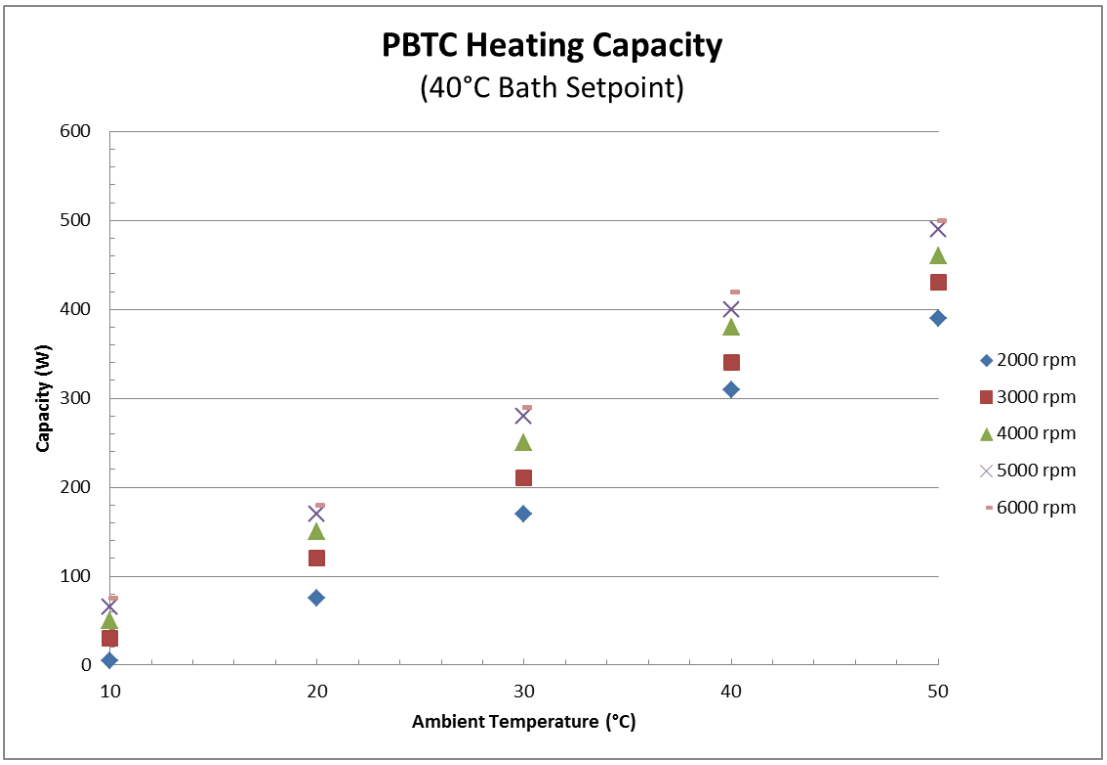

Figure 34. PBTC heating capacities

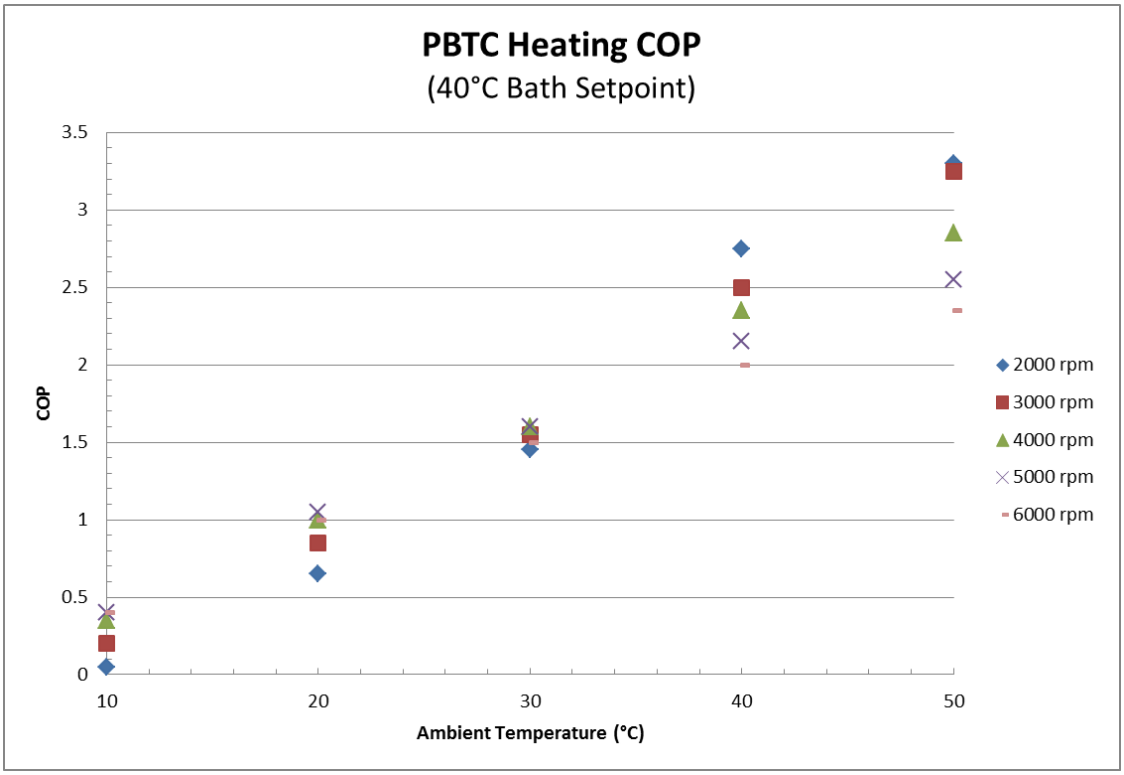

Figure 35. PBTC heating COP

Heating capacities of the PBTC using the vapor compression system ranged from 137W to 561W as presented in Figure 34. The trend of the heating capacities as a function of temperature performs in a predictable behavior, the higher the ambient temperature the more effective the heat pump cycle becomes. Such a pattern is also demonstrated in Figure 34. An interesting observation is that unlike the cooling capacities the heating capacities are nearly identical regardless of compressor speed. This observation points to a volumetric efficiency scenario resulting in a compression ratio limitation of the compressor. It also shows that there is no advantage to running the compressor at a speed of 6000rpm instead of 4000rpm for the given testing conditions. In later testing, oil level in the compressor was closely monitored to ensure preventable leakage is not preluding a subsequent loss of efficiency. Similar to the cooling test, Figure 35 portrays that the higher the compressor speed the more power consumed. Resultantly, based on these results it appears to be a disadvantage to run the compressor at higher speeds than 4000rpm because the system is less efficient and has no gained capacity.

System power consumption has been broken down and examined on an individual component basis. Power utilization analysis was based on maximum power consumption of each system component. Both the higher capacity pump and larger fan draw more power than the initially selected components. Although pump and fan require significantly less power than the compressor, they are the second and third largest consumers of power respectively in the system. Presented in Figure 36 is a pie chart depicting the comparison in power consumption for all

electrical system components. Each electrical component is portrayed along with its power utilization in watts and the percent of total power within the system that each component consumes. Below the pie chart is the summation of all components operating and maximum power consumption and rounded to the nearest watt.

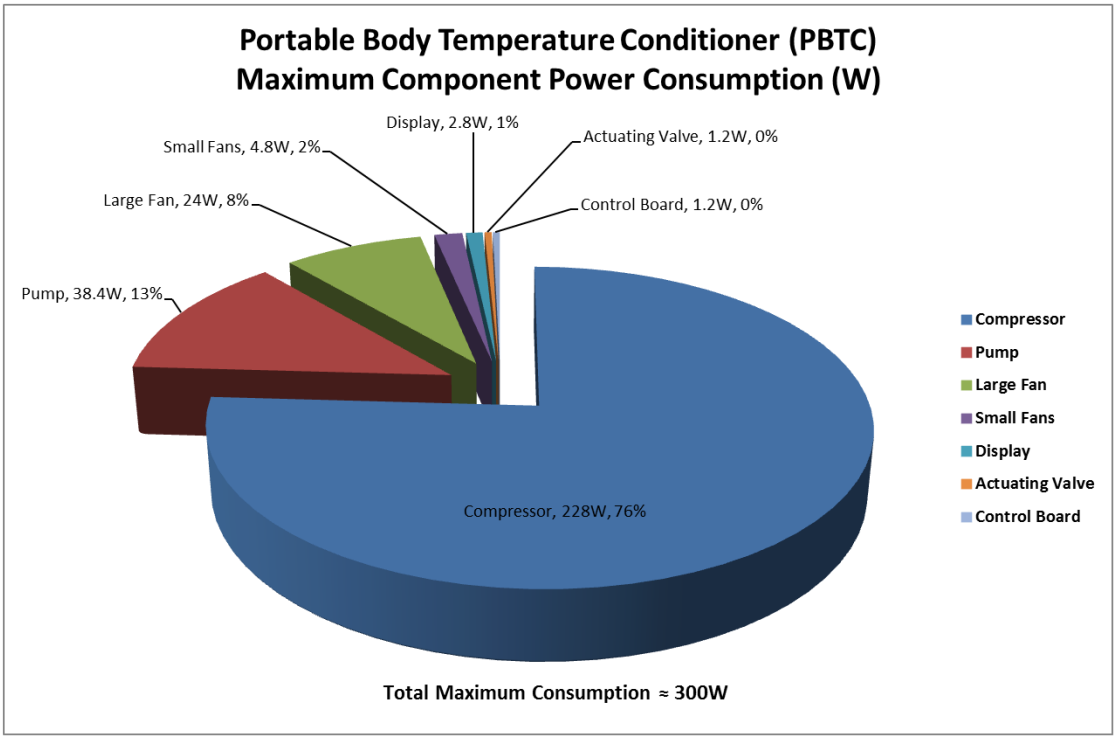

Figure 36. PBTC power consumption breakdown of electrical components

As demonstrated from the figure, the majority of the power consumption is attributed to the compressor at 79% and 228 W. The second largest draw comes from the pump at 38.4 W and only 13% of overall power consumption. Again, it is important to recognize that these are worst case operating conditions. The actuating valve, for example, only has a current draw when switching between heating and cooling modes. The time frame required switching between heating and cooling is minimal, approximately 10 seconds, and otherwise the actuator consumes no power. Furthermore, the power consumption for the compressor, pump, and fans are all calculated assuming maximum operating speeds.

The total power consumption of all system components is approximated at 300W, assuming maximum power draw from each component and all electrical components running simultaneously. It essentially represents a worst case scenario in terms of power utilization. The sized polymer Li-Ion battery pack for the PBTC is rated at 326 Wh and is intended to accommodate an hour of appliance operation. Analysis was performed to determine how long the appliance can run on battery power even at extreme conditions where the battery may become de-rated. Tests were performed at compressor speeds of 6000rpm, for both heating and cooling, because at higher speeds the compressor consumes more power. Minimum and maximum

temperatures of 10°C and 50°C respectively were evaluated for both heating and cooling modes. The concept was to ensure that the battery back is capable of powering the system for the target length of time even under the worst case circumstances of the performance test matrix. The 6000rpm and 50°C cooling test is portrayed in Figure 37 and demonstrates that the breadboard prototype was capable of operating for 70 minutes on battery power.

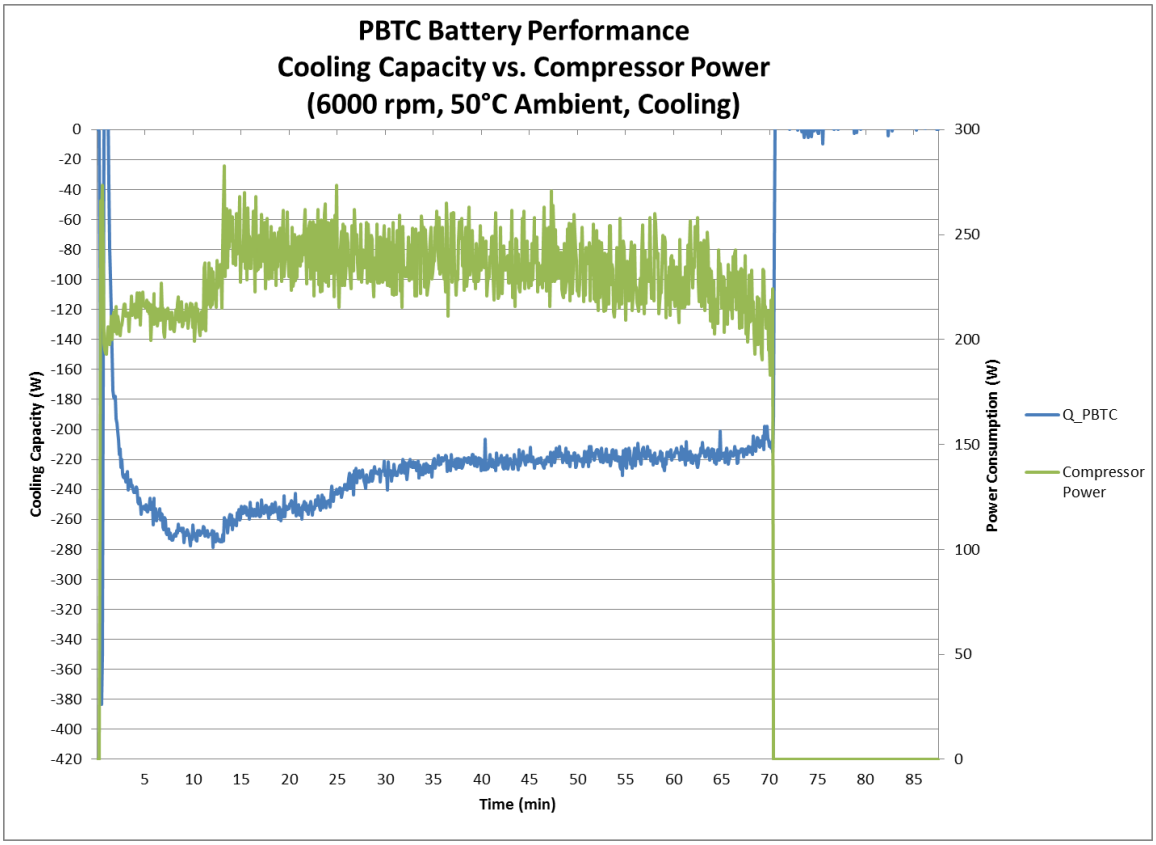

Figure 37. PBTC battery life test with new components

Stability analysis on the PBTC prototype was investigated to evaluate the steadiness of the appliance. The feet have been sized to allow the device to tilt 15° before the center of gravity of the PBTC surpasses its base, the point at which the device will tip over. Since the center of gravity is skewed slightly towards rear of the appliance it is more susceptible to tipping backwards than forwards. The feet support tipping 15° backwards, not forwards. Presented in Figure 38 is a drawing showing the tilt perspective of the point at which the appliance will tip over. The center of gravity is clearly indicated on the drawing along with a line that shows at the 15° tilt angle the center of gravity is vertically in line with the base edge of the foot. Units of length are depicted in inches.

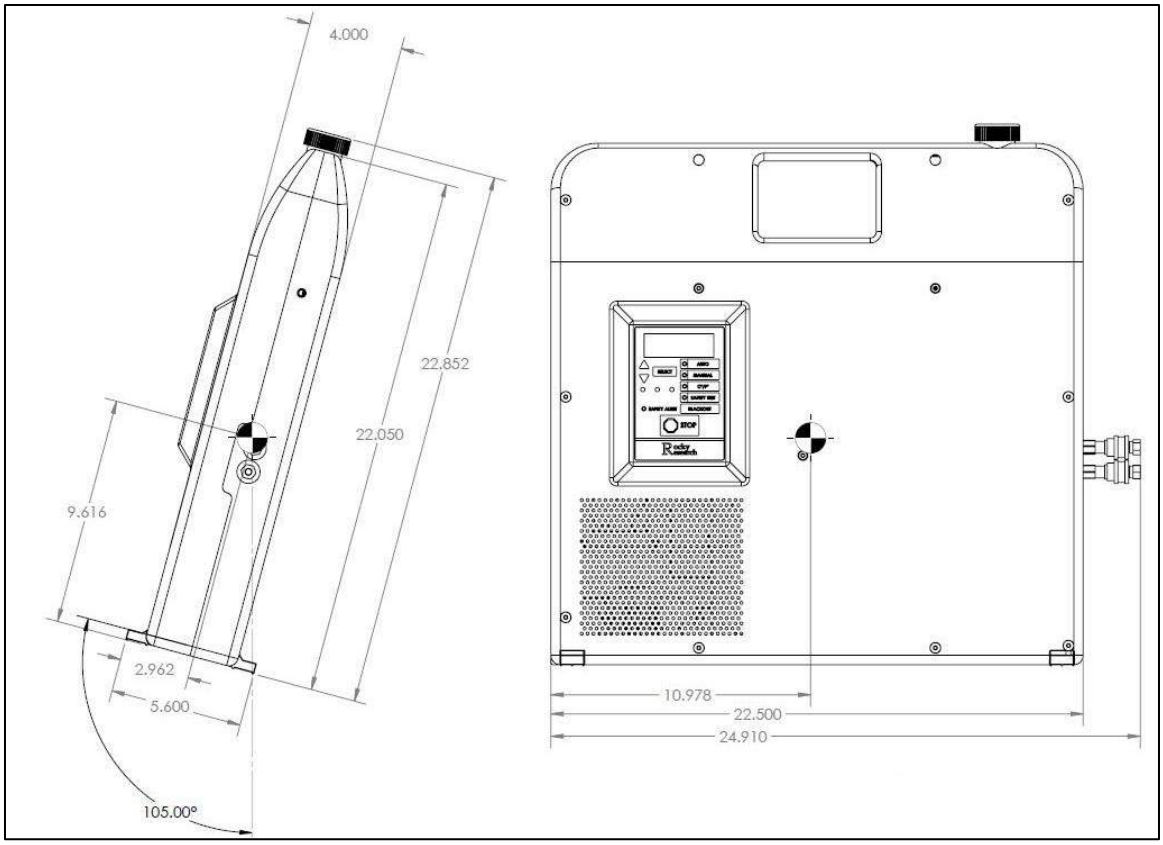

Figure 38. PBTC tipping diagram

The PBTC prototype before fabrication was predicted to weigh approximately 28 pounds empty. The feet length required to accommodate a 15° tilt is 0.8in. Free body diagram analysis leads to a required force of approximately 3.6lbs in the plane normal to the front display at the top of the fill cap in order to tip over the appliance. The case design was fabricated with removal and interchangeable feet of different lengths. Such an approach allowed final system design to be employed with an optimal balance between stability, transportability, and aesthetics. The following figure is a pie chart depicting the weight distribution of the PBTC based on individual system components. The heaviest individual component is the case itself. The miscellaneous component encompasses objects such as insulation, shock rubber, and fittings. Utilizing highly efficient components allows the weight accumulation of the compressor and battery to be relatively minimized.

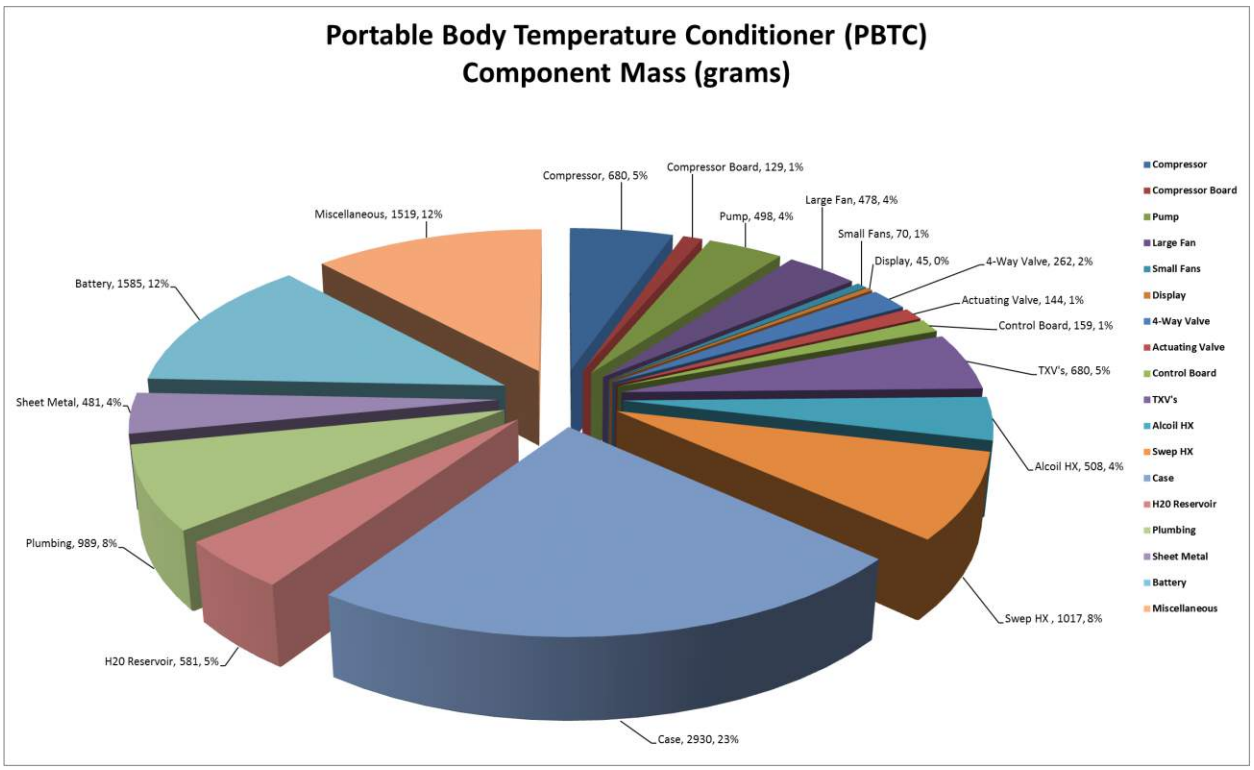

Figure 39. PBTC weight distribution chart

3c. Control Logic Development and Testing

Rocky Research developed a custom microcontroller PC board specifically for controlling the PBTC. The board has been designed exclusively for control of the PBTC required system components. The board consists of three integrated power supplies, an LED display driver, a field-effect transistor (FET) array, a membrane keypad with power controls, eight optically isolated inputs, eight analog inputs, and four analog outputs. These control board features are intended to extend the level of safety, accuracy, and performance quality of the PBTC in a single comprehensive control solution. The board has been enhanced and updated in an iterative process to optimize reliability, safety, and performance.

A control logic flow diagram has been developed for the PBTC. The diagram has been structured in a decision tree hierarchy format resulting in thirteen different operation modes, based on three different control algorithms. Presented is a list of the defined operating modes along with a brief description of each, followed by a description of each of the three control algorithms and how they are utilized:

1) **Off Mode** – The appliance is off and non-operational
2) **Idle Mode** – The appliance is on, displaying system temperatures, but not operational

3) **Gradient Heating Mode** – The appliance is heating according to the gradient heating algorithm
4) **Gradient Maintain Mode** – The appliance is maintaining temperature according to the gradient maintain algorithm
5) **Gradient Cooling Mode** – The appliance is cooling according to the gradient cooling algorithm
6) **Auto Heating Mode** – The appliance is heating according to the auto heating algorithm
7) **Auto Maintain Mode** – The appliance is maintaining temperature according to the auto maintain algorithm
8) **Auto Cooling Mode** – The appliance is cooling according to the auto cooling algorithm
9) **Manual Heating Mode** – The appliance is heating according to the manual heating algorithm
10) **Manual Maintain Mode** – The appliance is maintaining temperature according to the manual maintain algorithm
11) **Manual Cooling Mode** – The appliance is cooling according to the manual cooling algorithm
12) **Safety Default Mode** – The appliance is non-operation due to a safety default
13) **Connection Default Mode** – The appliance is non-operational due to a connection default

The operating modes for the control logic diagram have been developed such that they are suitable for boolean logic implementation. The boolean expressions for the different operating modes were first defined. Control algorithms for the heating, cooling, and temperature maintenance modes were then implemented. Dynamic proportional-integral-derivative (PID) controls were tuned for each control mode and each algorithm was optimized for premium temperature maintenance under varying operating conditions. Each algorithm was then tested and evaluated for performance integrity and reliability utilizing different load sources including a bath as well as the thermal manikin.

Manual mode has been defined to strictly control the water outlet temperature, T_{H2O_OUT}, as specified by the user. If the manual mode is selected the user is prompted to specify a set point temperature. By pressing the "SELECT" button the PBTC attempts to achieve target outlet water set point temperature by allocating whether heating, cooling or maintaining the current temperature is required. Consequently, the user does not specify whether the appliance heats or cools, heating or cooling is determined by the relationship of the measured temperature compared to the set point temperature. This is consistent for all operating modes. Auto mode is defined by controlling to the patient temperature, $T_{PATIENT.}$ Similar to Manual mode, if the user selects the Auto mode they are then prompted to specify a set point temperature. The PID algorithm then attempts to achieve that set point temperature for the patient regardless of the water outlet temperature.

In Gradient mode the operator specifies the patient's set point temperature and the unit operates as in Auto mode except for the following. The system monitors the patient's temperature and maintains the temperature of the water out of the unit at a user programmable temperature difference from the patient's temperature reading. This temperature is set by the user as the gradient value ($T_{PATIENT} \pm T_{H2O\_OUT}$). Once the patient temperature is close enough to set point temperature that it transitions from cooling or heating to maintain the appliance switches to just Auto mode, as to not infringe on the patent, but still portrays to the user Gradient mode. The algorithm stays in this mode until the stop button is selected or the set point temperature is modified. Cooling or heating is determined the same as in Manual or Auto mode, the set point temperature relative to the patient temperature specifies to cool or heat. The PID constants are tuned to maintain the proper user specified gradient, $T_{PATIENT} \pm T_{H2O\_OUT}$.

Safeties for operating the PBTC, whether heating or cooling, have been formulated and integrated into the control scheme. In terms of the high temperature safeties, the highest set point temperature that a user is able to specify for the circulating water is 42°C (107.6°F). A visual safety alert of high temperature occurs at 45°C (113°F) by illumination of the "SAFETY ALERT" LED. If the high temperature of the circulating water reaches 47°C (116.6°F) the user will be alerted with the "SAFETY ALERT" LED as well as a buzzer. For the low temperature safeties, the lowest that a user is able to specify for the circulating water temperature is 8°C (46.4°F). A visual safety alert of low temperature occurs at 6°C (42.8°F). A visual & audio safety alert of low temperature occurs at 4°C (39.2°F). Furthermore, if a connection to the patient temperature sensor is not established the user will not be able to operate the appliance in either a heating or a cooling mode. The display will portray a "CONNECTION DEFAULT" error and indicate to the user that the patient temperature connection has been lost and needs to be reestablished. A safety has also been incorporated to ensure that the water delivery temperature to the blanket is accurately monitored. If water temperature reading faults the user is presented a "H2O SENSOR FAULT" error and informed to remove the appliance from service. Furthermore, the system will not allow the compressor to operate or the system to run. A high pressure switch is also included as an additional precaution to shut down the system if unsafe operating conditions are ever reached, and inform the user to remove the PBTC from service.

They keypad for the PBTC has been developed to offer maximum functionality in an easy to utilize minimalistic design. Touch pad activation has been implemented to strategically guide the user through selecting one of the appropriate user specified operating modes as described above. All three algorithms have a dedicated button for easy selection and operation of the appliance. The keypad consists of buttons as well as indicator LEDs. The "AUTO" button allows the user to achieve Auto control mode, regulating to a user specified patient temperature. The up and down arrows can be utilized to scroll through available set point temperatures and

chose the desired temperature with the “SELECT” button. Once a set point temperature is specified the control logic automatically determines whether to heat or cool based on the set point temperature relative to the measured temperature. If the user presses the “GRADIENT” button the default for gradient set point temperature is displayed. They then scroll up or down to choose their desired set point temperature of the patient relative to the default. If they press the “SELECT” button they are then prompted to input the gradient. Once they press the “SELECT” button again, after specifying the gradient, the compressor and system starts. While running, if they press “SELECT” button the system toggles between setting the gradient and setting the set point temperature. The “MANUAL” button allows the user to specify set point temperature for the water circulating through the blanket utilizing the up and down arrows along with the “SELECT” button. The “C°/F°” button allows the user to switch between the depicted units of temperature on the display. The “BLACKOUT” button allows the LCD backlight of the display to be dimmed and shutoff for discreteness when operating the device in the field. The “STOP” button shuts off heating or cooling of the appliance and puts the device in an idle mode where the temperatures are still displayed. LEDs serve as indicators for varying system functionality and are labeled based on whether the appliance is heating, cooling, or maintaining temperature. The blue LED implies the unit is cooling, the green that the unit is maintaining target temperature, and the orange that the unit is heating. The red LED is a visual safety alert indicator. Presented in Figure 40 is model rendering of the initial keypad design.

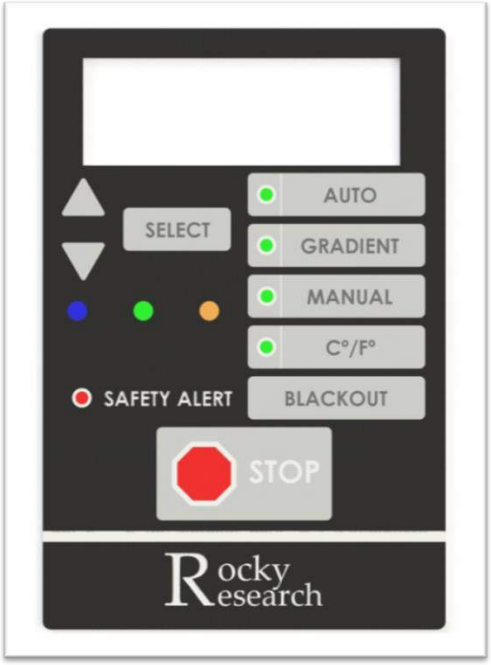

Figure 40. Initial PBTC keypad design

Feedback from qualified medical personnel resulted in modifications to the keypad design. The original keypad for the PBTC has since been enhanced from the initial design to incorporate such changes. The safety alert indicator and stop button have been relocated to a location that increases the aesthetics of the keypad while at the same time making it more intuitive to the user. Additionally, labels have been put on each of the LED functional indicators to inform the user whether the appliance is cooling, heating, or maintaining temperature. Furthermore, the LED indicator for the "C°/°F" button has been removed to eliminate user confusion. The keypad has been tested to validate all the buttons and LED's function as desired. It has been deemed appropriate that at startup the PBTC run a safety diagnostic to ensure properly functionality of the appliance before allowing the user to operate. The diagnostic ensures that all safety LED indicators are functional and that the appliance is safe and reliable to operate. A picture of the final keypad installed on all prototypes is presented in Figure 41.

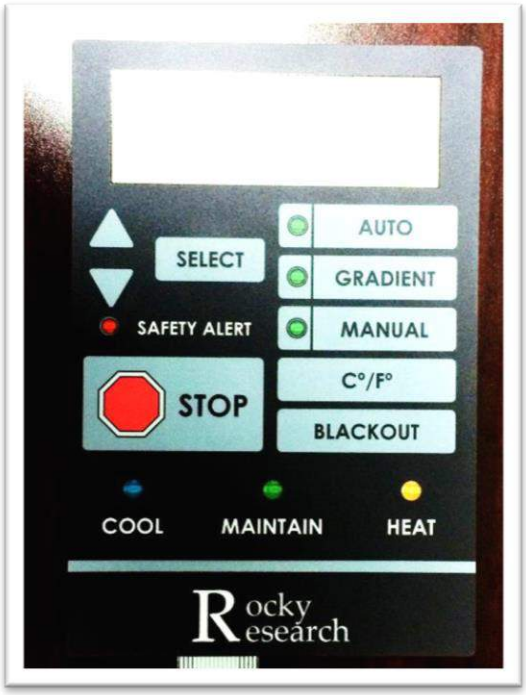

Figure 41. Finalized PBTC keypad

The display for the PBTC is a four line, twenty characters per line display. The first line describes both the operating mode as well as the power source. The second line designates the set point temperature as well as the units of temperature, either ℃ or ℉. As previously described, the set point temperature has different implications depending on the operating mode. The third line depicts the patient temperature while the fourth line portrays the water outlet temperature from the PBTC being delivered to the blanket. Temperatures are displayed to a resolution of 0.1°C. Presented in Figure 42 is a pictorial representation of the display and keypad while the PBTC is operating in Manual mode. The figure demonstrates that the PBTC is

operating off of DC power, in Manual mode, and is heating because the water outlet temperature is less than the set point temperature. Both the display and keypad have been thoroughly evaluated and tested in conjunction with one another for proper functionality and reliability.

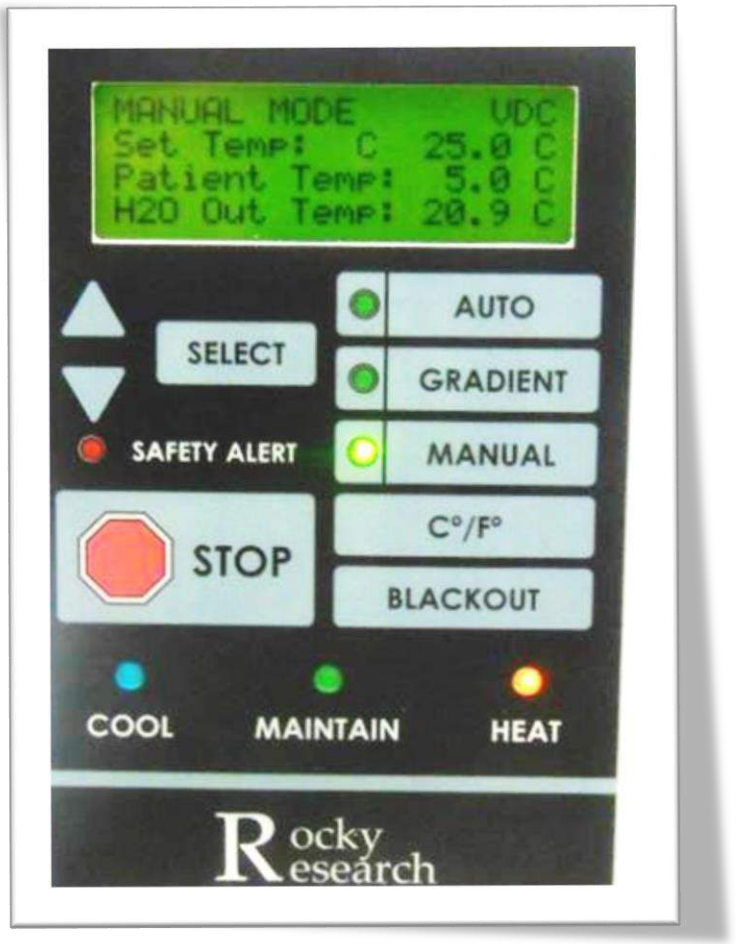

Figure 42. Functional PBTC display & keypad

The temperature probe utilized to measure patient body temperature has been acquired, tested, and assimilated into the system design. The sensor is a YSI 400 series reusable probe that has been approved by the Food and Drug Administration (FDA) for applications such as that of the PBTC. Furthermore, the sensor is currently utilized in comparable patient thermal management devices to that of the PBTC. The YSI 400 has an operation temperature range of 0°C to 60°C with an accuracy ±0.2°C from 0°C to 60°C and an accuracy of ±0.1°C in the 25°C to 45°C range. The probes are considered to be dependable, repeatable, and interchangeable making them ideal for utilization in the PBTC. The YSI 400 supports the utilization of disposable skin, esophageal, oral, and rectal probes. Currently, Measurement Specialties MEAS 4400 series

surface temperature sensors have been utilized for system performance and control evaluations. Figure 43 is a model portraying how the probe is integrated into the case design.

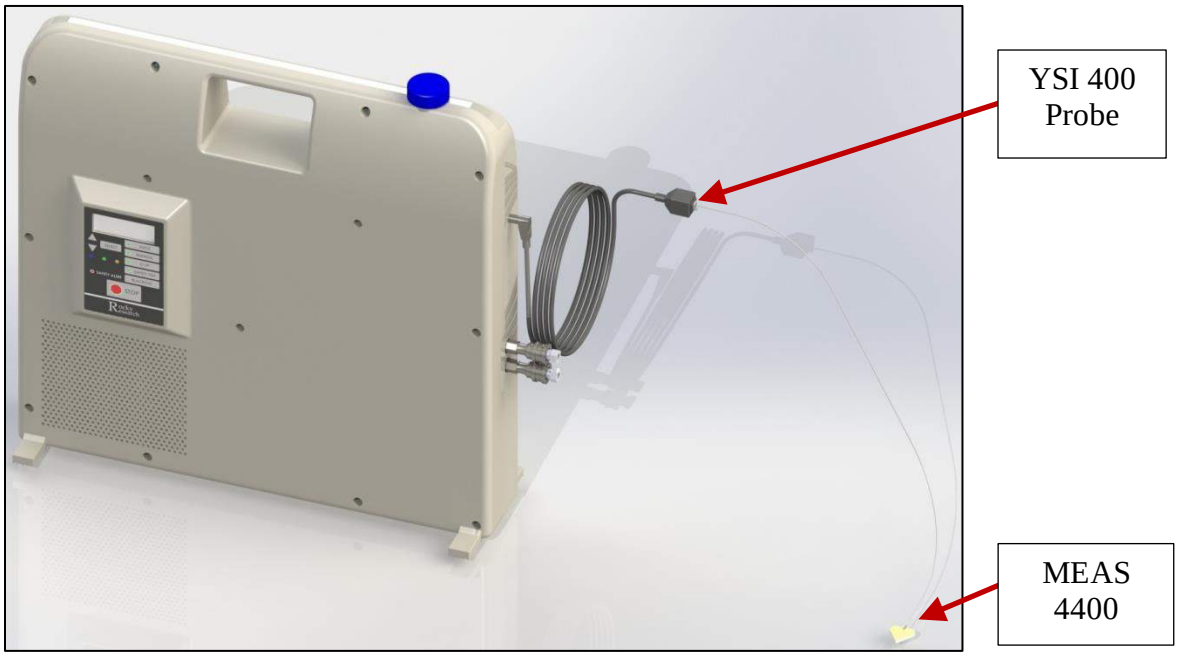

Prototype Fabrication and Testing

Starting with the case, fabrication of the final prototype design was initiated. Military connectors have been integrated into the case design along with a push button for powering the appliance on and off. Both the inlet power as well as the on and off button are located on the side of the case. An experiment was implemented to determine whether or not the cap of the reservoir required venting in order for the system to function correctly. The results of the bench top test determined that a vented cap was not necessary. The case is constructed out of glass filled nylon and is painted white upon completion. The interior is coated with an EMI copper shielding. In order for the reservoir to hold water without leaking it is lined with a Zyvax sealer. Figure 44 shows on the left the final design of the case and on the right the side of the case where the power button and military connector are located. The rendering portrays the final model of the case design from which the first initial prototype was fabricated.

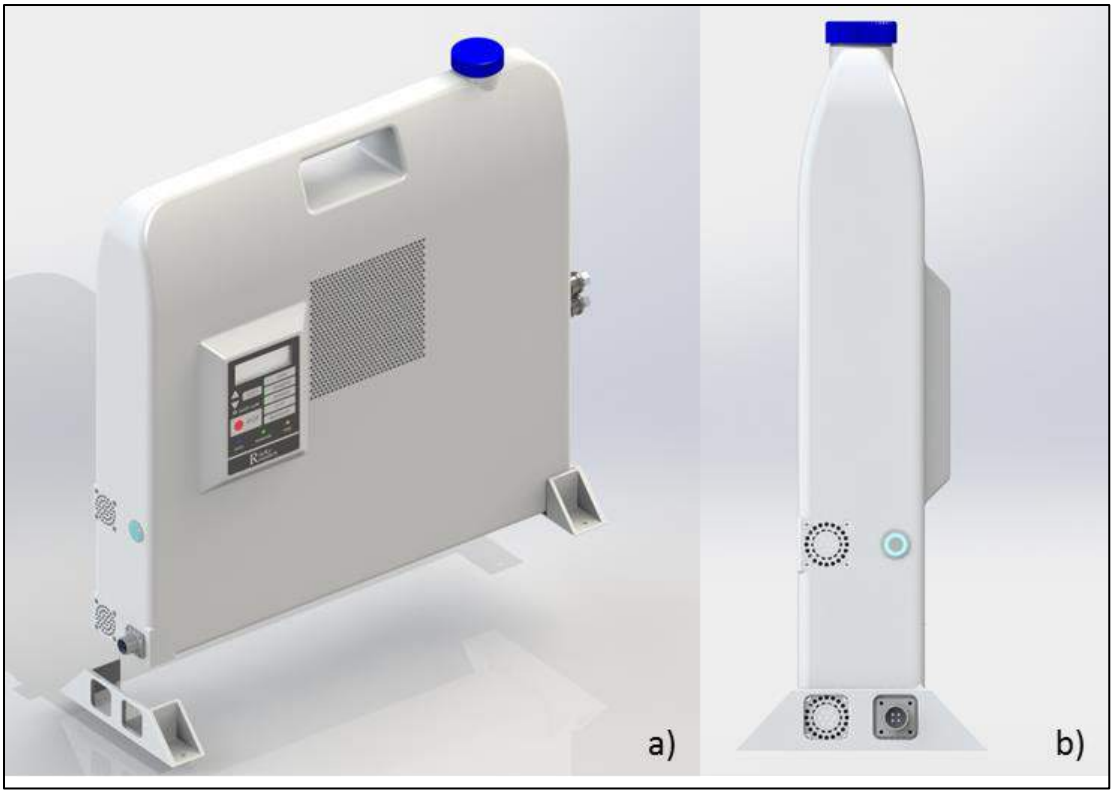

Figure 44. Final PBTC prototype design

Upon complete fabrication of the case the first prototype was plumbed, wired, ruggedized, fully assembled, and performance evaluated. The plumbing, wiring, and component placement was based directly off of the fabricated breadboard design. During system fabrication, however, several modifications were identified to enhance ease of assembly as well as improve the durability of the appliance. The majority of the modifications could be implemented during prototype assembly; however, some adjustments required modification to the case to be implemented on the next generation of the system. Those alterations have subsequently been integrated into the fabrication of the following two prototype cases. The adjustments to the case are strictly to improve the ease of fabrication and have no bearing on the heating and cooling capabilities or performance of the PBTC. Presented in Figure 45 is a picture depicting the inside of the first fabricated prototype fully plumbed, wired, and insulated. As can be observed, the water reservoir is directly integrated into the back half of the case. Presented in figure 46 is a front picture of the fully assembled and closed prototype.

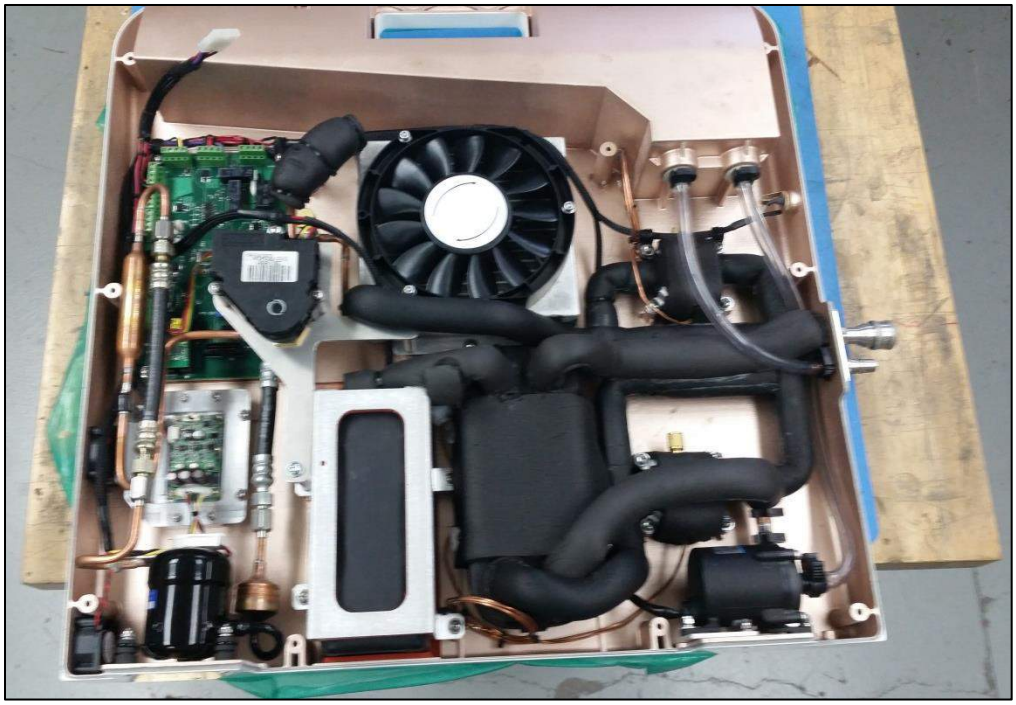

Figure 45. Fully assembled prototype interior

Figure 46. Assembled & closed PBTC prototype

Once assembled, each component was validated for proper performance utilizing the PCB. The appliance was put in diagnostic mode and set to varying speeds ranging from 2000rpm to 6000rpm, in 1000rpm increments. The signal voltage from the compressor control board was then measured to ensure consistency with the manufacturer specifications confirming that the compressor was operating at the correct speed. Performance of the prototype was then evaluated for each of the compressor speeds. Ambient temperature was specified at 30°C and the circulating water temperature was set to 25°C. The PBTC compressor speed was initially specified at 2000rpm and ran to achieve at least 10 minutes of steady-state capacity data. The compressor was then increased in speed, by 1000rpm increments up to 6000rpm, documenting steady-state capacities for each increment in compressor speed. Along with cooling capacity of the system the compressor speed, DC wattage, and COP is also depicted. The testing data is presented in figure 47.

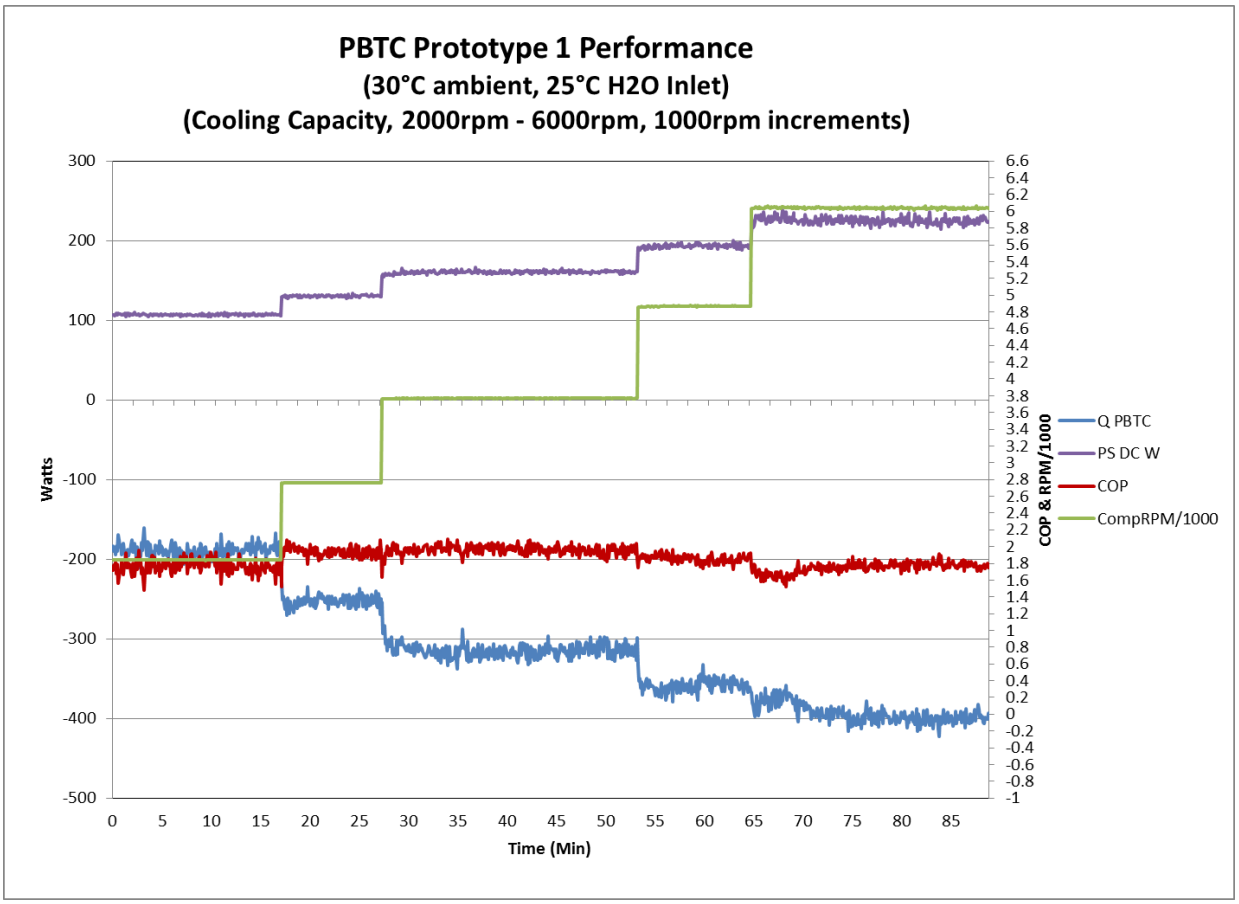

Figure 47. PBTC varying speed cooling performance

The test demonstrates, for the specified operating conditions, a range in performance from approximately 200W at 2000rpm to 400W at 6000rpm. Depending on compressor speed, for the given operating conditions, the COP of the system ranged from approximately 1.7 -2. In terms of energy efficiency, the increase in cooling capacity is not always justified by the increase in

power consumption required to achieve the additional capacity of the PBTC. Consequently, the PBTC control logic was subsequently developed with an effort to minimize power consumption while providing enough heating or cooling capacity to achieve target set point temperatures.

Similar diagnostic mode analysis was also implemented for heating, again starting with a compressor speed of 2000rpm and increasing the speed by increments of 1000rpm up to 6000rpm and monitoring steady-state performance at each interval. The water inlet temperature for cooling was set to 40°C and the ambient temperature the same as the cooling test presented in figure 47 at 30°C. The 40°C inlet water temperature is more realistic for a normal steady-state heating condition than the 25°C inlet water temperature utilized for the cooling analysis. Presented in Figure 48 is the heating capacity, DC power consumption, compressor speed, and COP for the described test.

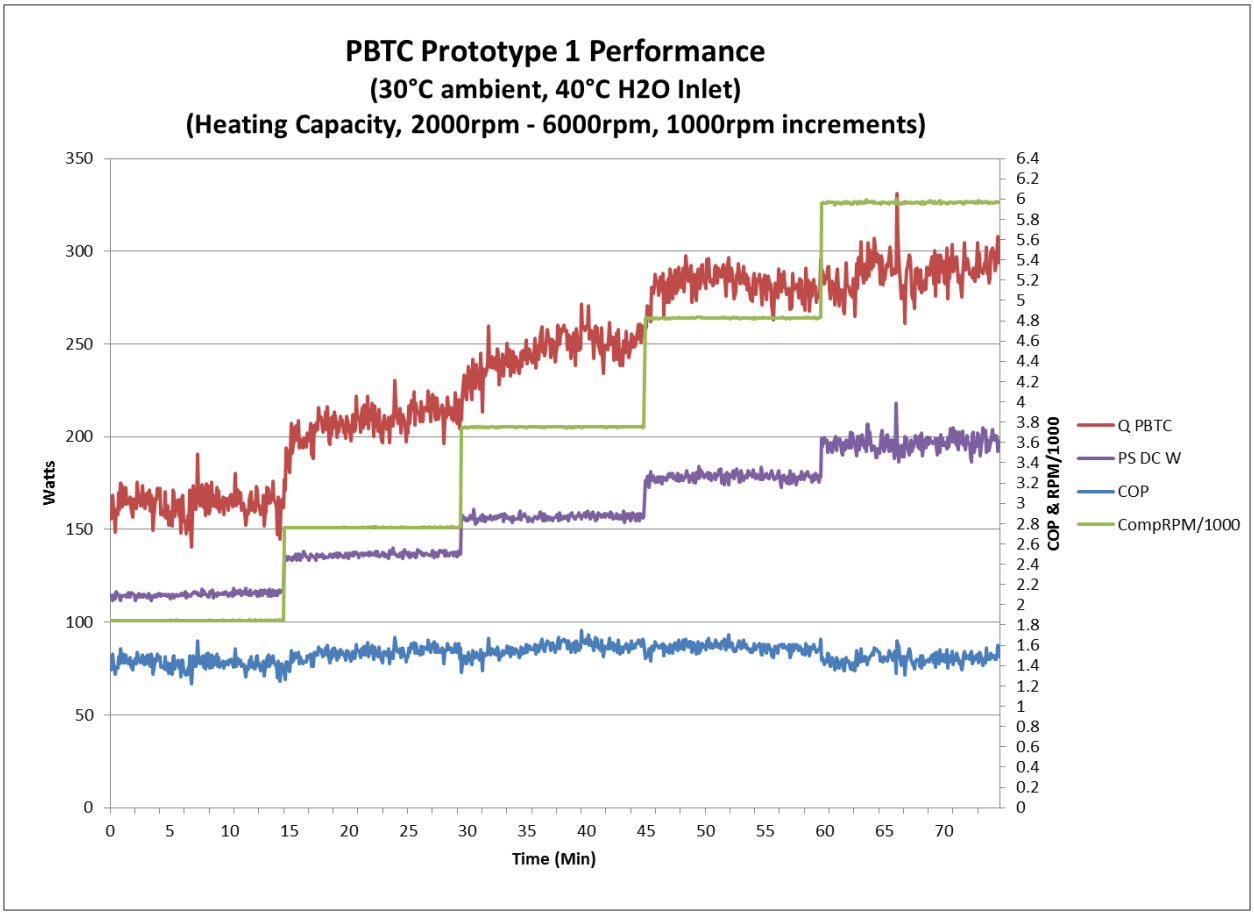

Figure 48. PBTC varying speed heating performance

The figure establishes that for the quantified working conditions, the PBTC prototype was able to achieve an approximate heating capacity range from 170W – 300W when varying the compressor speed from 2000rpm – 6000rpm. Additionally, the COP ranges from approximately 1.4 – 1.7 for the given heating test. With the assembled prototype operating as designed in the diagnostic mode focus was directed towards developing the controls for each of the practical

operating modes, starting with the manual mode, which controls to the outlet water temperature distributed from the PBTC to the blanket.

For initially tuning the manual control mode algorithm the PBTC unit was plumbed in conjunction with a bath containing approximately 16 gallons of water to simulate the heat capacity of a person. The ambient temperature was set to 30°C and the circulating water temperature was set to 20°C. A 170W cartridge heater, simulating the heat production rate of a person, was placed inline of the circulating water stream at a location between the bath and the inlet to the PBTC. The heater for the bath was shut off while simultaneously turning on the PBTC in manual mode along with the 170W cartridge heater. The PID constants were then tuned real time to achieve target performance. Figure 49 portrays the manual algorithm performance in cooling mode once the PID was tuned. The set point temperature was specified at 17°C.

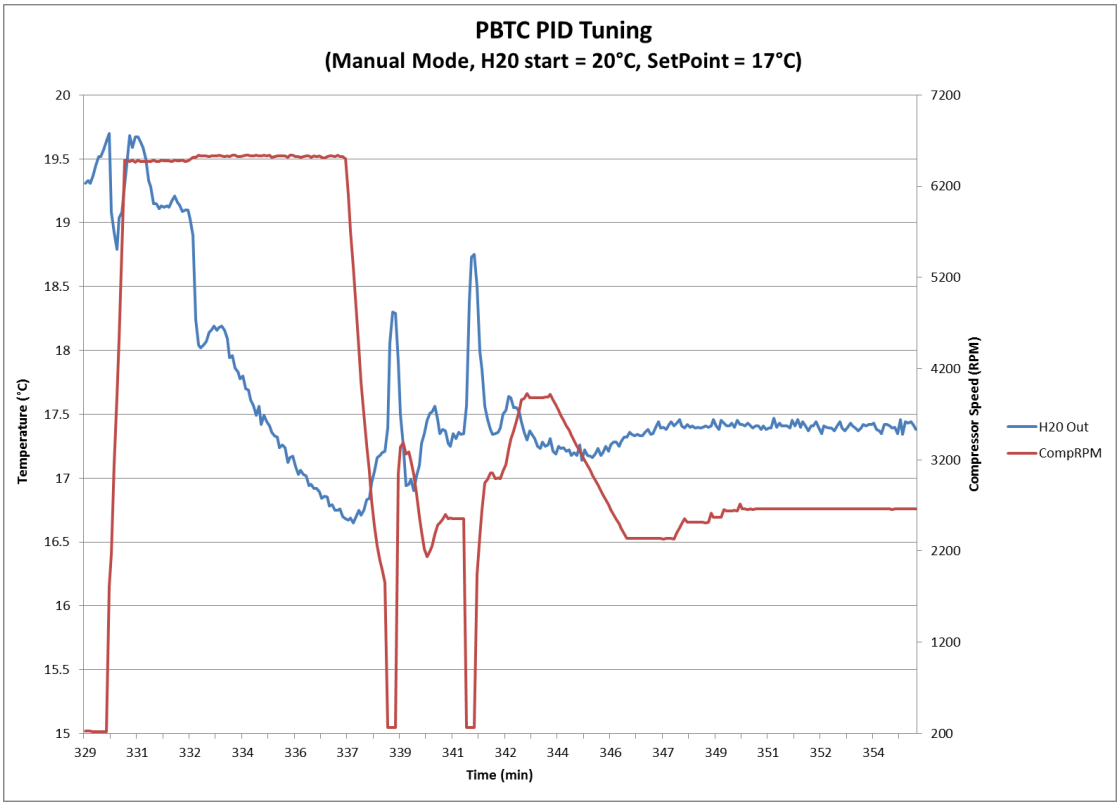

Figure 49. PBTC cooling manual mode algorithm performance with bath

The figure demonstrates that the manual algorithm brings the water temperature down close to the specified set point temperature and is then able to hold that temperature. A 0.3°C discrepancy exists between the data acquisition utilized to produce the plot and the temperature sensors on the appliance for which the PBTC is controlling to. Consequently, the actual temperature is 0.3°C below what is presented in the plot. Considering the discrepancy in temperature, the plot demonstrates that once steady-state conditions were achieved the algorithm

was capable of modulating the water outlet temperature to approximately 17.1°C. Since the cooling capacity of the PBTC at the lowest compressor speed is greater than the 170W heat generation rate utilized to simulate a patient, the appliance will inevitably at some point shut off, as demonstrated in the figure. When the compressor shuts off there is a momentary spike in temperature. However, it is important to recognize that the brief temperature fluctuation is not realizable to the patient because the compressor is only off for a very short duration, not long enough to have an impact on the patient's temperature. This can be visualized in the auto mode test presented below; in which the compressor has to be off for several minutes before a fluctuation in patient temperature is realizable. The manual algorithm was then evaluated on Newton, the thermal manikin, for performance robustness. The results of that test are presented in Figure 50, along with the testing conditions.

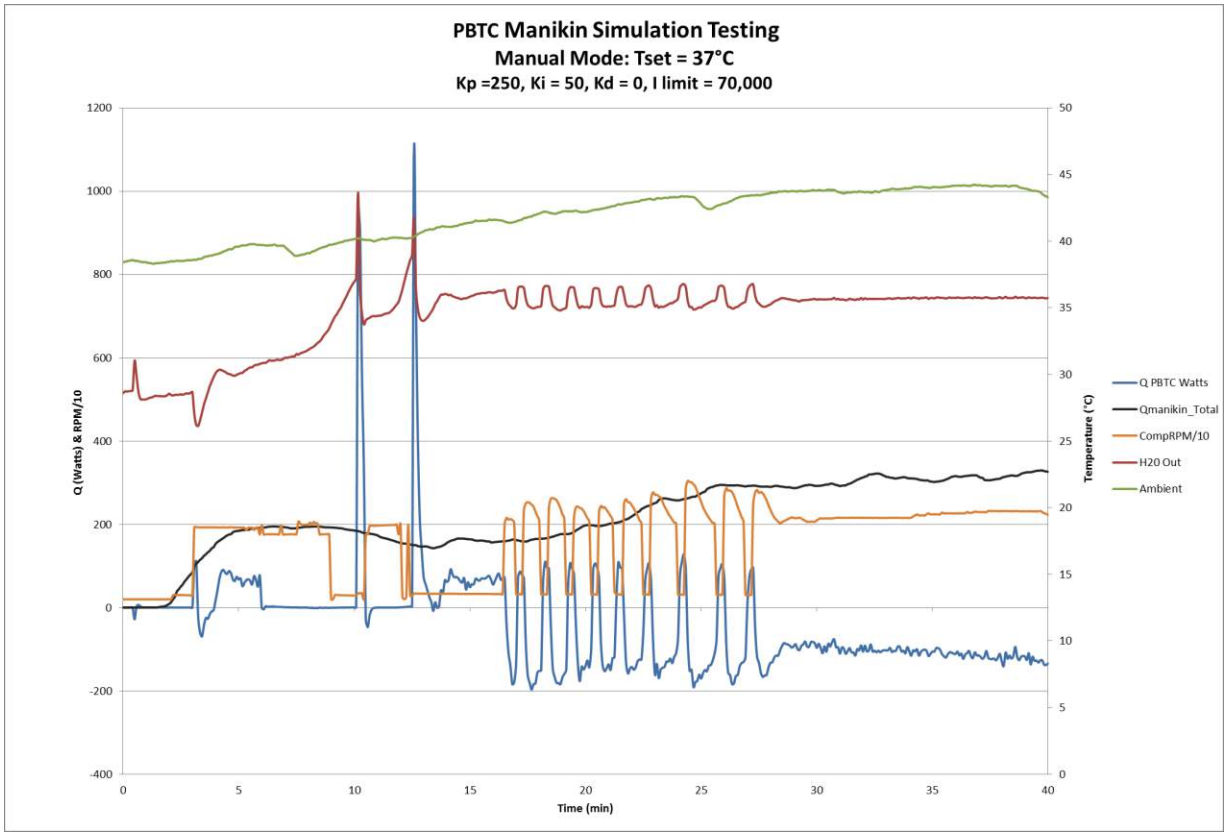

Figure 50. PBTC manual mode algorithm performance on thermal manikin

The results demonstrate that the manual mode PID algorithm is robust enough to respond to the transient conditions of the test, as well as the varying load of the manikin, and still able to achieve a steady-state compressor speed. Additionally, the algorithm attained equilibrium by reaching a constant outlet water temperature at the specified set point. Consequently, the PBTC is utilizing minimum power consumption required to achieve the user specified set point temperature. With validation of proper performance of the manual mode algorithm and PID constants focus was directed towards the refinement of the auto control mode algorithm.

Tuning of the auto mode algorithm, which controls to the patient set point temperature, was implemented in a similar manner as the manual mode. Analogous to the manual tuning approach, a 170W cartridge heater, simulating the heat production rate of a person, was placed inline of the circulating water stream at a location between the bath and the inlet to the PBTC. The heater for the bath was shut off while simultaneously turning on the PBTC in auto mode along with the 170W cartridge heater. The PID constants were then tuned real time to achieve target performance. Since it takes longer to have an impact on the actual patient temperature, in comparison to the water outlet temperature, the set point was specified 2°C below starting temperature instead of 3°C. Presented in Figure 51 is a plot depicting the tuning and performance of the auto mode control algorithm while cooling, by specifying a temperature set point of 27°C, when the initial patient temperature was approximately 29°C.

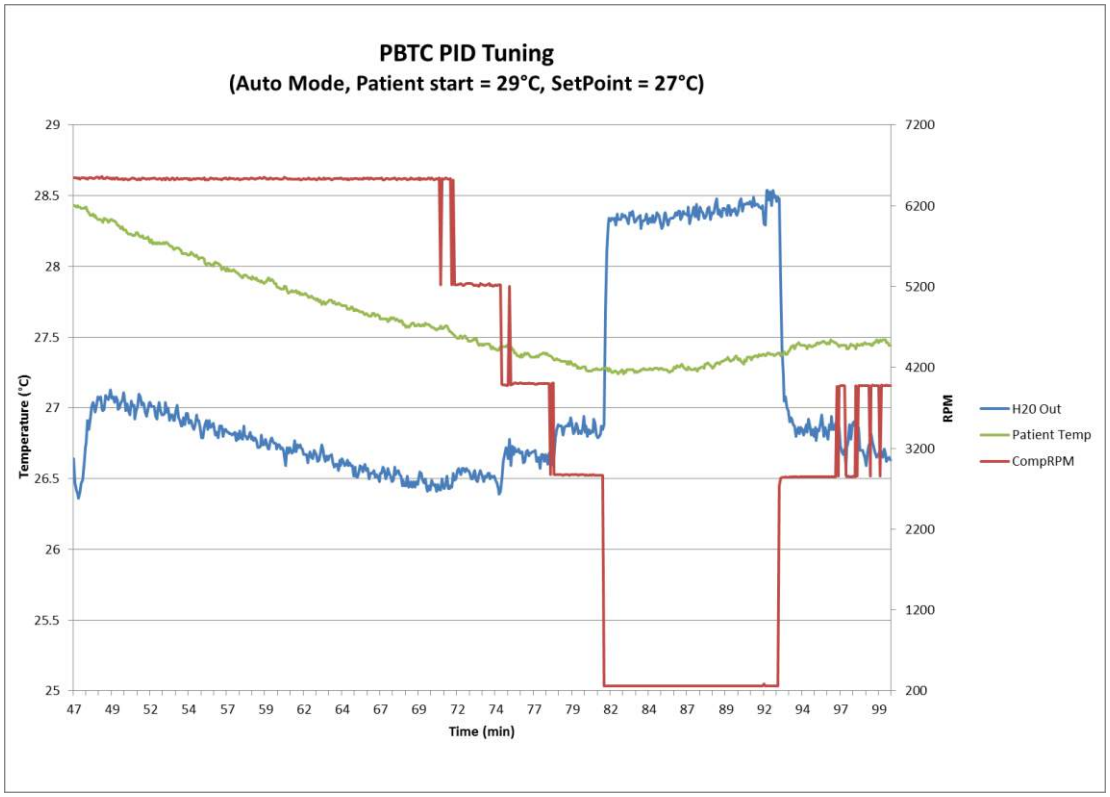

Figure 51. PBTC cooling auto mode algorithm performance

Figure 51 shows that in auto mode as the patient temperature approaches set point the compressor begins to step down in speed, reducing cooling capacity to accommodate the load demand. Similar to the manual mode plot presented in figure 4, there is an approximate 0.3°C discrepancy between the data acquisition utilized to construct the plot and the real time temperature the appliance is controlling to. The data demonstrates that as the appliance achieves set point the compressor is turned off, therefore conserving energy by minimizing power consumption. Once the patient temperature begins to drift above set point temperature the

compressor turns back on at less than maximum capacity to balance the load requirement. As expected, Figure 51 demonstrates that cycling the compressor has a much more drastic effect on water outlet temperature from the PBTC than it does on patient temperature.

Both the manual and auto modes are efficient and effective in achieving and maintaining target set point temperatures. The gradient algorithm has also been tuned with the same PID constants as the auto algorithm. The performance of the gradient mode algorithm is consequently very close to that of the auto mode, with the addition of the gradient parameter to prevent over and undershoot of patient set point temperature. Consequently, the achievability of set point temperature while operating in gradient mode may take longer than that of the auto control algorithm. Upon completion of tuning all three algorithms the prototype was released to UMC to be evaluated with their performance and control tests. The additional testing will help validate the accuracy and robustness of the control algorithms and performance of the PBTC under a barrage of varying testing conditions.

Modifications and System Enhancements

Development of the PBTC was implemented in an iterative process, incorporating modifications and system enhancements throughout the development of the prototype in order to optimize functionality, reliability, and safety of the appliance. In addition, Rocky Research completed the development of an improved and more compact dedicated PCB for the management and control of the PBTC. The controller incorporates a mixture of analog and digital circuits to achieve optimal control of the system. Additionally, refinements have been integrated into the board to accommodate the control of electrical resistance cartridge heaters to be utilized at low ambient temperatures when the heat pump cycle is less efficient. Based on the COP and performance heating analysis the heaters were deemed appropriate to be utilized in replace of the heat pump cycle at 18°C. Four 60W cartridge heaters are utilized, allowing a total of 240W heating. The new board also accommodates the utilization of the high pressure switch integrated into the system as an additional safety precaution. The control firmware incorporates several algorithms intended to optimize the delivery of thermal energy while also optimizing power consumption. The algorithms have been refined in an effort to optimize system performance. These modifications provide the system with maximized performance and longevity endurance when operating on the internal DC battery.

The performance was reevaluated with the cartridge heaters, both in terms of capacity and system efficiency, at ambient temperatures of 20°C and 15°C respectively. The water inlet temperature for the lower ambient heating evaluations with the cartridge heaters was specified at 40°C to maintain consistency with the vapor compression testing parameters. Presented in Figure 52 is the final PBTC performance utilizing the cartridge heaters at lower ambient temperatures. Figure 53 is the COP for the same tests.

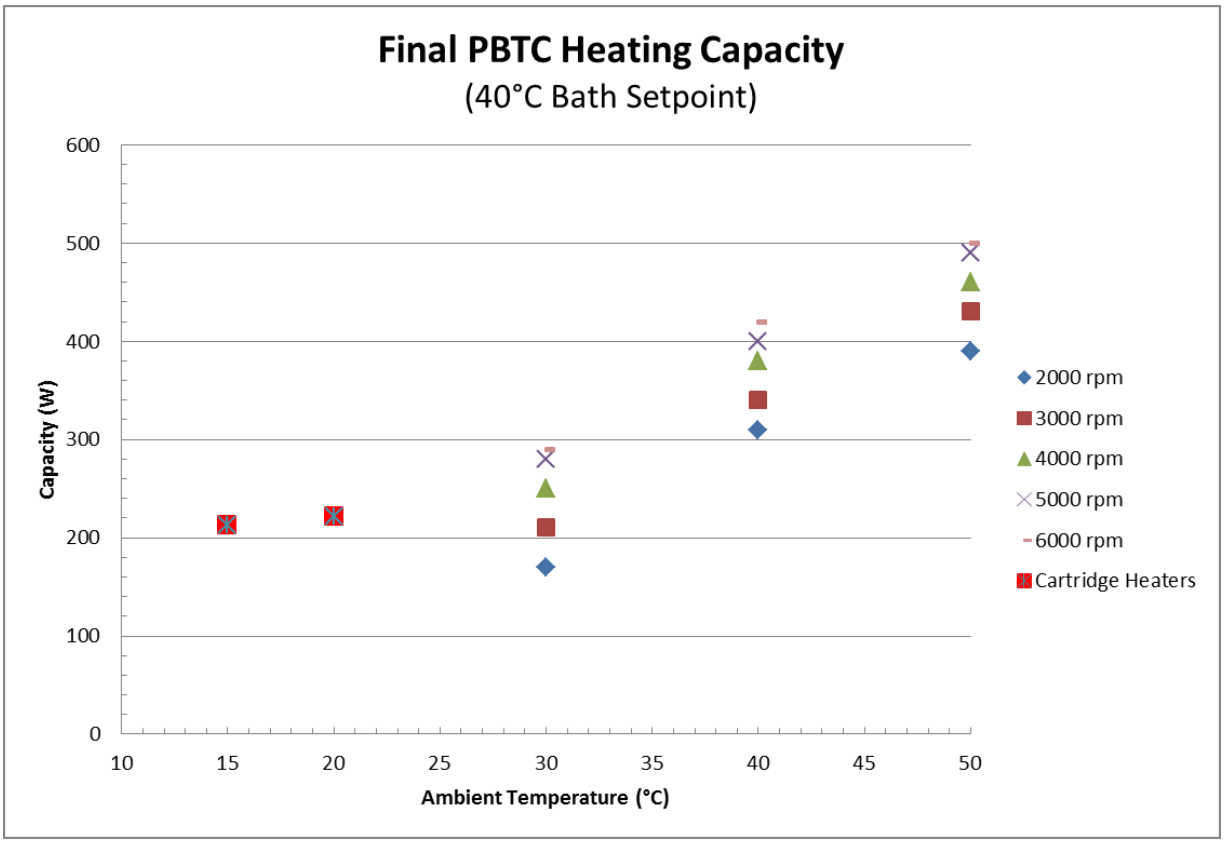

Figure 52. Final PBTC heating capacity

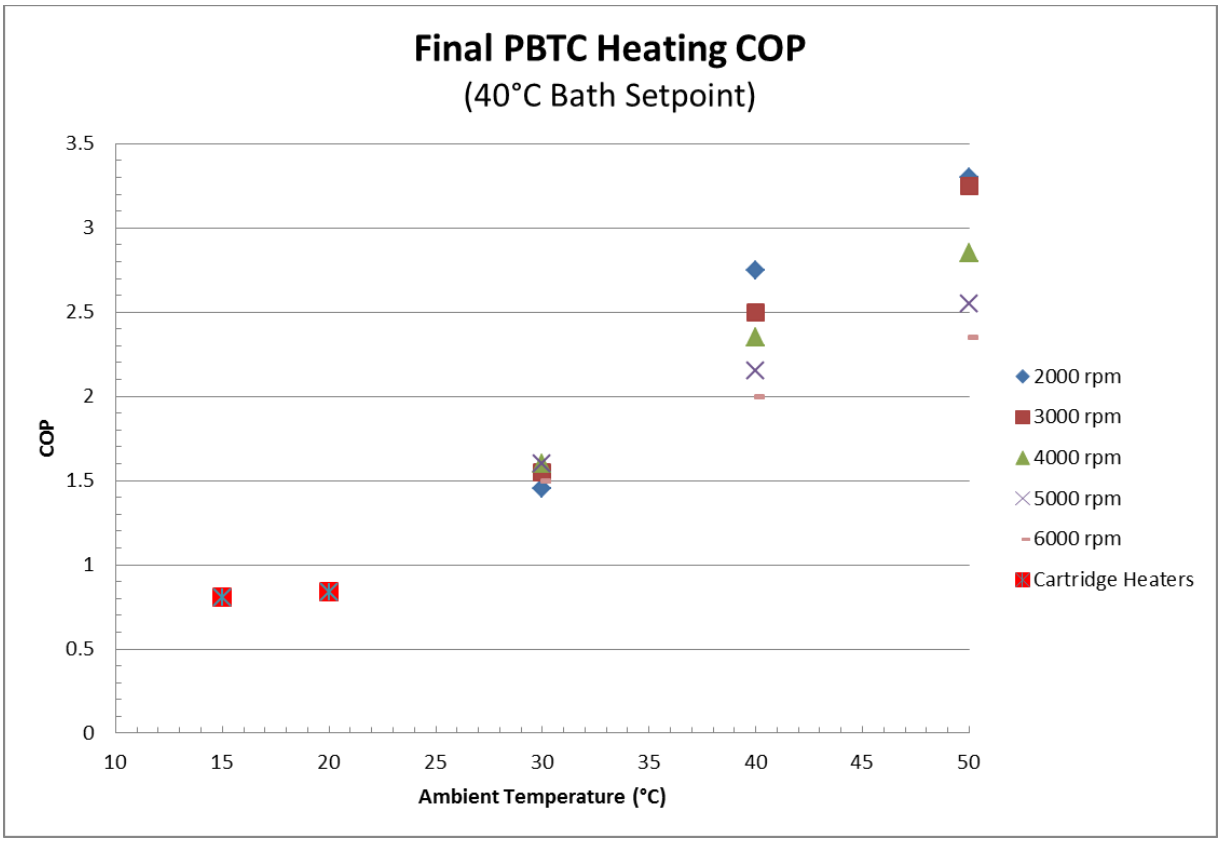

Figure 53. Final PBTC heating COP

Figure 52 demonstrates an effective heating capacity of 221W at an ambient temperature of 20°C and 213W at an ambient temperature of 15°C. In comparison to the heat pump cycle, as presented in Figure 34, there is significant increase in heating capacity at ambient temperatures of 20°C and below. Figure 53 portrays COP's of 0.84 and 0.81 at ambient temperatures of 20°C and 15°C respectively. Depending on the compressor speed, the COP at 20°C is comparable or slightly less than that utilizing the vapor compression system. Consequently, for system implementation the transition temperature for switching to the cartridge heaters was chosen to be 18°C, a justifiable balance between the operational longevity and heating capacity of the PBTC. Overall, the utilization of the cartridge heaters provides a significantly impactful improvement on the PBTC design, specifically at lower ambient temperatures of 20°C or below. The colder the ambient temperature is the better the heating capacity and efficiency of the PBTC becomes utilizing the cartridge heaters in comparison to the vapor compression system.

The current method for producing the case of the PBTC, 3D printing, is not economical for mass production. Consequently, the case design has been altered to lend itself to be more conducive to blow molding. The primary modification consists of having the water reservoir as a separate component instead of being directly integrated into the back half of the case. Having the reservoir as a separate component will allow the reservoir to be blow molded, which was not

possible with the previous implementation design. Presented in the following figure is a rendering of the newly designed water reservoir.

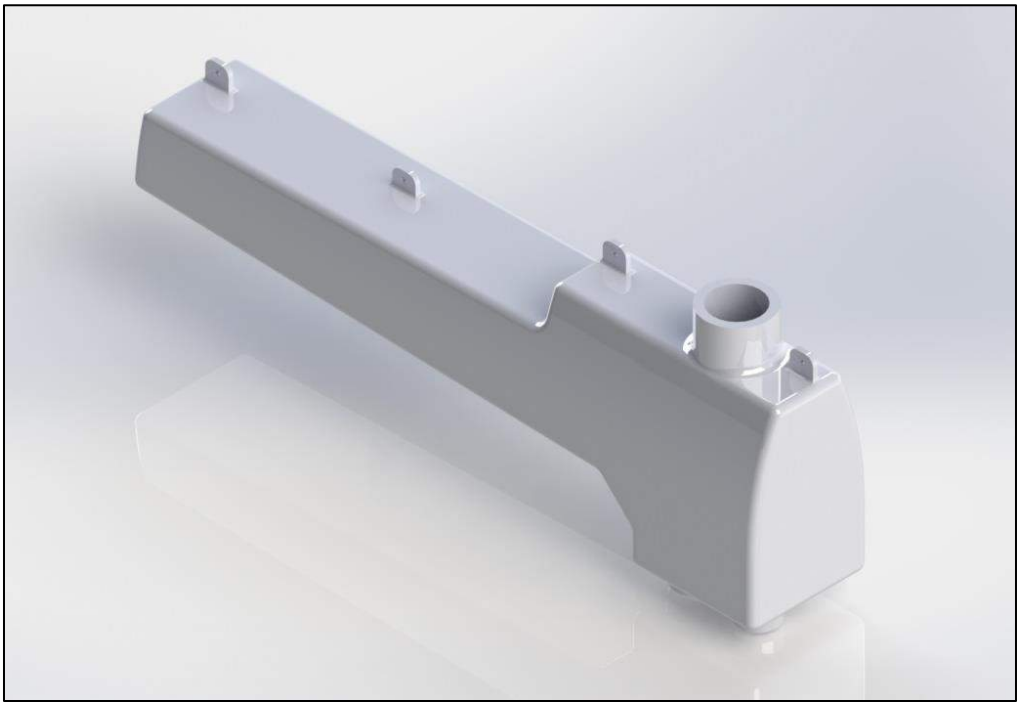

Figure 54. PBTC water reservoir conducive to molding fabrication

As portrayed in the figure, the reservoir contains external mounting tabs so that it can be fastened to the interior back half of the case. The reservoir storage capacity volume is nearly identical to that of the previous design in which the reservoir was integrated directly into the back half case. The newly modified reservoir and case are being fabricated and have been evaluated for fit and performance. The enhanced PBTC case design incorporating the separate reservoir is presented in Figure 55.

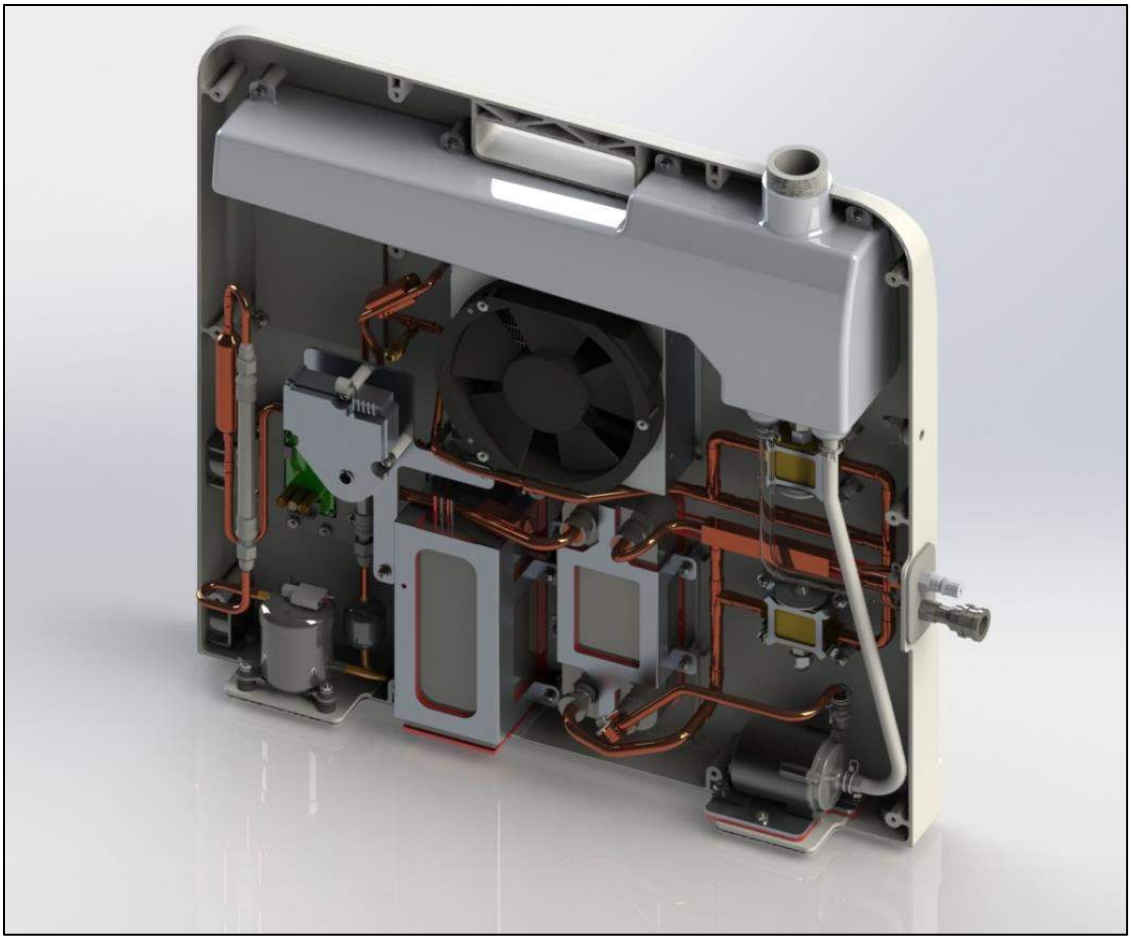

Figure 55. Modified PBTC case with independently mounted water reservoir

Task 4: Patient Load Simulation Testing

UNSOM has completed the necessary FDA documents for this phase of the project. Both Quality Systems (QS) Standard Operating Procedures (SOPs) have been implemented and design history working documents have been created for future FDA 510(k) submission. User Requirements, Product Specifications, Project Plan, Regulatory Plan, Regulatory Standards list, and Risk Management Plan are working documents that were created by a medical device consultant for the PBTC. An FDA consulting firm was hired to assist UNSOM in setting up a quality system to meet CFR Title 21 Part 820 requirements. A custom built thermal manikin was purchased from Measurement Technology Northwest. A training/installation session was held with personnel from MTNW. UNSOM and Rocky Research personnel were trained on the basic use and maintenance of the thermal manikin. Additionally, Installation, Operational, and Performance qualifications were completed for validating the thermal manikin. This testing provides documented evidence that the thermal manikin was installed and operating according to manufacturer's specifications and meets the requirements to successfully complete the patient simulation testing. Three patient simulation tests were designed and performed to evaluate

thermal load and efficacy of PBTC, which are as follows: 1) Heating/Cooling fraction test, 2) Comparison of PBTC to commercial hyper-hypothermia system test, and 3) Head cooling Test.

FDA 510(k) Documentation

The Quality Systems (QS) and design history documents have been prepared for future FDA 510(k) submission of Rocky Research PBTC. An FDA consultant was hired to assist UNSOM to implement basic SOPs and quality systems. The QS will be ongoing throughout the duration of the project. A medical device expert was hired to write a User Requirements Document, Product Specification Document, Project Plan, Regulatory Plan, Regulatory Standards List, and Risk Management Plan. These documents are design history documents and are also considered working documents. These working documents will go through several revisions throughout the various design stages of the medical device. Pending future funding; the next phase will incorporate design changes from the simulated patient testing into a second generation prototype, final production design manufacturing, and commercialization with FDA 510(k) clearance.

1. Quality Systems

UNSOM, Surgery Research Laboratory began work to implement current Good Manufacturing Practice (cGMP) requirements associated with medical devices as defined by the Code of Federal Regulations (CFR) Title 21 Part 820 – Quality System (QS) Regulation for future submission of FDA 510(k) of portable body temperature conditioner. The cGMP requirements set forth in the QS regulation are proclaimed under Section 520 of the Federal Food, Drug and Cosmetic (FD&C) Act. The medical device quality system regulation requires an "umbrella" quality system intended to encompass the design, production, and distribution of all medical devices. It specifies general requirements such as the use of trained employees, design reviews, design validation, calibrated equipment process controls, etc. and allow the individual companies/institutions to implement systems that demonstrate they are in control.

A consulting firm was hired to assess the quality systems and good manufacturing practice compliance within UNSOM, Surgery Research Laboratory. A gap analysis was conducted to determine what quality systems, processes, and basis documents would be required for FDA 510(k) submission. A gap analysis report was provided detailing the gaps in the organization QS.

List of Signed and Approved SOPs, Policies, and test methods created and implemented in UNSOM Surgery Research Laboratory:

- Creation, Format and Review of SOPs SOP
- Quality Policy
- Management Responsibility and Organization Policy
- Validation Policy
- Instrument & Equipment Calibration and Maintenance Policy

- Regulatory Inspection Policy
- Records Retention Policy
- Training SOP
- Corrective and Preventive Actions (CAPA) SOP
- Change Control SOP
- Issuance & Control of Notebooks/Logbooks SOP
- Qualification of Vendors & Contract Facilities SOP
- Internal Audits SOP
- Laboratory Notebook Entry & Review Guide SOP
- Significant Figures and Rounding SOP
- Investigating Out of Specifications (OOS) Test Results SOP
- Personal Hygiene SOP
- Central Documentation SOP
- Equipment Validation Procedure SOP
- Data Integrity SOP
- Thermal Manikin Use and Maintenance SOP
- Thermal Manikin Fluidics Calibration Test Method
- Thermal Manikin Fixed Temperature Test Method

Completed Instrument Validation Qualifications

- Newton 26 zone thermal manikin system

2. User Requirements Document

A medical device consultant wrote a User Requirements Document by gathering information from UNSOM and Rocky Research. The purpose of this working document is to provide user needs and intended use for PBTC. The User Requirements document is basically the customers' input for certain features and requirements to be developed into the device. A meeting was held with military experts to discuss their questions and requests in designing the device. See Appendix A for the information that was covered in the meeting.

The User Requirements document includes device description, intended use and user specifications. The user specifications section was broken down into the following categories:

- Device Description and Overview
- Intended Use
- Users
- Intended Markets
- Minimum Requirements for User Needs and Intended Use Matrix

A Market review of hyper-hypothermia systems was researched and compared to Rocky Research's PBTC to identify technical and performance specifications found in Table 5. This information assisted UNSOM and Rocky Research in identifying specifications in the development of Rocky Research's PBTC.

Table 5. Comparison of Rocky Research PBTC to Commercial Hyper-Hypothermia Systems

Attribute	Rocky Research PBTC	CSZ Blanketrol III Model 233	Gaymar Medi-Therm MTA7900
Dimensions	23" (58.42 cm) H, 24" (60.96 cm) W, 4" (10.16 cm) D [1]	37.5" (95.25 cm) H, 17" (43.18 cm) W, 17" (43.18 cm) D	37" (93.98 cm) H, 14" (35.56 cm) W, 18.25" (46.36 cm) D
Weight	27 lbs (12.2 kg) empty, 34 lbs (15.4 kg) full	131 lbs (59.4 kg) empty, 147 lbs (66.7 kg) full	121 lbs (54.9 kg) empty, 141 lbs (64 kg) full
Cooling Capacity	200W - 500W [2]	Unknown	Unknown
Heating Capacity	300W - 800W [2]	800W heater	500W heater
Power Consumption	~300W	~1200W	~1380W
Power Source	24 VDC, 12.5 Amps & 120 VAC, 2.8 Amps	115 VAC, 10.2 Amps & 230 VAC, 5.2 Amps	120 VAC, 11.5 Amps
Battery Life	Minimum 60 min.[3], continuous on external power	No battery option	No battery option
Operating Temperature	-40°C-60°C (-40°F-140°F)[4]	15°C-30°C (59°F-86°F)	Unknown
Operating Locations	Hospital & Field deployable	Hospital only	Hospital only
Designed Mil Specs	Shock, Vibration, & EMI	None	None
Water Temperature Range	3°C-42°C (37.4°F-107.6°F)	4°C-42°C (39.2°F-107.6°F)	4°C-42°C (39.2°F-107.6°F)
Patient Temperature Range	30°C-40°C (86°F-104°F)	30°C-40°C (86°F-104°F)	30°C-41°C (86°F-105.8°F)

Attribute	Rocky Research PBTC	CSZ Blanketrol III Model 233	Gaymar Medi-Therm MTA7900
Physical Representation			

[1] Depth of detachable feet is 8", feet can be detached for hard mounting

[2] Target capacity

[3] Battery life minimum based on all components running at full speed, the intelligent electronics of the system vary compressor speed based on the load demand to conserve power consumption

[4] Requires glycol solution to prevent H_20 freezing at cold ambient temperatures

3. Product Specifications Document

A medical device consultant wrote a Product Specifications document by gathering information from UNSOM and Rocky Research. The purpose of this working document is to provide product specifications for PBTC. It is a technical document describing the device. The document includes device description and intended use, device biological safety evaluation classification, and product specifications. The product specifications section was broken down into similar categories as the user requirements document except for the following additional categories:

- Device Description and Intended Use
- Device Biological Safety Evaluation Classification
- System Diagram
- Product Specifications
    - Users
    - Operational Environmental Requirements
    - Operational Transport
    - Physical Specifications
    - Performance and Functional Requirements
    - Reliability
    - Serviceability
    - Biocompatibility & Materials Characterization Requirements
    - Transit, Packaging, Shelf-Life

    - Labeling
    - Suppliers
- Design Inputs and Outputs

4. Project Plan/Schedule
   A project plan was written to outline the tasks to be completed for launching the product and obtaining FDA 510(k) clearance. It is estimated that it will take an additional 4 years to commercialize this device. The plan task categories include the following: Proof of Concept, Concept Phase, Design Input Phase, Design Verification, Design Transfer, and Product Launch. It is estimated this plan will take 4 years to complete.

5. Regulatory Plan
   The purpose of this working document is to provide a regulatory strategy and identify regulatory requirements for future FDA 510(k) submission of Rocky Research's PBTC.

6. Regulatory Standards List
   A working document has been created which lists the regulatory standards to be met for Rocky Research PBTC's future FDA 510(k) submission.

7. Risk Management Plan
   Two documents were created for the Risk Management plan. First, a risk management plan work instruction document was created to provide the framework to implement a risk management plan. Second, a risk management plan template. The risk management process is a systematic approach to document the identification of medical device hazards, estimating and evaluating the associated risks, controlling these risks, and monitoring the effectiveness of the controls by conducting production and post-market surveillance throughout the life cycle of the medical device.

4a. Write Test and Validation Methods

UNSOM has completed writing the patient simulation and validation test methods. Protocols for the thermal manikin validation methods and the SOP for the "Equipment Validation Procedure" have been finalized. This SOP describes the procedure for the Installation Qualification and Operational Qualification portion of the thermal manikin validation. This procedure ensures that the thermal manikin is installed and operating according to its intended use as outlined by the manufacturer. The Performance Qualification portion of the manikin validation has been finalized and the procedure tested by UNSOM personnel**.** Three patient simulation tests were designed and performed to evaluate thermal load and efficacy of PBTC, which are as follows: 1) Heating/Cooling fraction test, 2) Comparison of PBTC to commercial hyper-hypothermia system test, and 3) Head cooling Test.

4b. Receive/Training on Thermal Manikin/Software

The thermal manikin "Newton – 26 zones" was purchased from Measurement Technology Northwest (MTNW), which is a Seattle based company specializing in the manufacture of thermal manikins and associated accessories. The thermal manikin is a human body simulator that consists of surface sensors capable of independently measuring the rate of heat transfer across various controlled zones. The total surface area available for measurement is 1.8 sq/m. The skin heat transfer rates are coupled to a computerized physiological model using two software platforms. The ThermDAC control software is the primary operating system that maintains full thermal control and data acquisition of the sensor data. The Manikin PC2 software is used for modeling predicted physiologic and metabolic responses of healthy individuals over time in response to environmental control systems.

UNSOM and Rocky Research completed training on the thermal manikin and software provided by Measurement Technology Northwest (MTNW). This included system set-up and startup procedures, operation of the various control modes, basic safety precautions/procedures, and general maintenance/calibration procedures. Also included with the training session, MTNW personnel assembled and tested the thermal manikin "Newton" and the associated accessories/software. This testing was a part of the installation and operational qualification portion of the manikin validation.

4c. Validation of Thermal Manikin

Calibration Thermal Manikin

Prior to the start of the patient simulation testing, the thermal manikin was sent back to Measurement Technology Northwest (MTNW) for yearly calibration to ensure consistency and accuracy of the future testing. Calibration of the thermal manikin consists of a complete evaluation of all manikin systems and components, which ensures that the thermal manikin was operating according to manufacture specifications. UNSOM sent the thermal manikin back to MTNW at the end of April 2014 and received the calibrated manikin from MTNW early May 2014.

Procedure for Manikin Validation

The objective of the validation was to provide documented evidence that the thermal manikin "Newton" had been installed and was operating according to manufacturer's specifications and meets UNSOM's requirements to successfully complete the patient simulation testing. Validation of the thermal manikin encompasses three parts; Installation Qualification (IQ), Operational Qualification (OQ), and Performance Qualification (PQ). MTNW performed part of the validation procedure for the thermal manikin (IQ and OQ) during the assembly/training

session. Additional documentation for thermal manikin operation was received from MTNW following the annual calibration. The installation qualification included documentation of the activities necessary to establish that the manikin was received and functions as was designed and specified. The operational qualification included the documentation of the testing necessary to establish that the manikin will function according to its operational specifications. The performance qualification consisted of documentation of activities necessary to establish that the manikin consistently performs according to defined user specifications. All the parts of the validation procedure was completed, reviewed and compiled together into a single validation report.

UNSOM completed the validation protocol for the thermal manikin and the test methods for the performance qualification. The performance qualification consisted of three tests; evaluation of the environmental chamber, the sweating fluidics system test, and fixed temperature testing with the thermal manikin.

1. Evaluation of the environmental chamber
   The purpose of this test was to measure for consistent control of the ambient temperature and humidity within the chamber. The thermal manikin system includes two ambient temperature sensors and relative humidity (RH) sensors. The manikin system was set up in the environmental chamber. The chamber's ambient temperature was set to 25^{o}C and an industrial humidifier (Mini Mister; Air & Water Systems; Lake Elsinore, CA) was set to 50% RH. Temperature and RH measurements were taken every minute for 180 minutes after the room reached steady state. The testing passed the acceptance criteria limits set at $\leq \pm 1^{o}$C as shown in Table 6.
2. Sweating Fluidics system Test
   The sweating system fluidics test procedure calibrates the volumetric flow of the manikin's sweating system, which ensures precise and consistent delivery of fluid. During the fluidics calibration procedure, each of the 26 zones was calibrated individually. All zones were initially set to maximum sweating, so no fluid was recirculated back to the holding reservoir. Next, one zone was chosen to be calibrated. That zone was set to 100% recirculation, so all water delivered to that zone was recirculated back to the reservoir. A pipet was attached to the return line of the manikin. The recirculated water from the zone was collected in the pipet for a period of 1 minute. The volume collected in the pipet was then compared to the software calculated recirculation volume. A new flow conductance value was calculated according to the following equation:

$$\text{New Flow Conductance} = \frac{\text{Total Volume Collected}}{\text{Recirculation Volume}} \times \text{Old Flow Conductance} \qquad [1]$$

This procedure was repeated for the rest of the zones. The new flow conductance values were then entered into the software and saved. Measurement Technology Northwest suggested that the feeder tube on the zone controller should be replaced when the new flow conductance value was approximately 20% less than the previous flow conductance value. This metric was chosen as part of the acceptance criteria for validation of the thermal manikin's sweating system. The new flow conductance value was less than 20% and passed the acceptance criteria as shown in Table 7.

3. Thermal Manikin Fixed Temperature Test

The last part of the performance qualification was the fixed temperature test, which evaluated repeatability of the thermoregulatory response of the thermal manikin at a fixed ambient temperature over three days. To encompass the range of the temperature to be used during the Patient Simulation testing ($15^oC – 40^oC$); cold (15^oC), neutral (25^oC), and hot (40^oC) ambient conditions were evaluated as part of the validation. Each temperature was tested on three separate days to evaluate consistency. As part of the testing procedure, the environmental chamber was set to the desired ambient temperature and allowed to reach steady state. Once the chamber reached temperature, the manikin was allowed to acclimate to the ambient conditions for 30 minutes. After the acclimation period, the manikin was set to model control mode, which is controlled by the physiological software, and the experiment was allowed to run for 90 minutes. The acceptance criteria for the fixed temperature tests include ambient temperature tolerance of the environmental chamber and 10% CV of end-point skin temperature/core temperature of the thermal manikin. The testing passed the acceptance criteria limits set within the validation protocol.

The data collected was compared over multiple days for simulated core body temperature and body average skin temperature. The data is depicted in figures 56-61 for cold, neutral, and hot ambient conditions.

Table 6. Environmental chamber ambient room temperature and humidity measurements for Performance Qualification

Item	Acceptance Criteria	Result	Pass/Fail
Room Temperature	Temperature Variation $\leq \pm 1^oC$ at 1 hr, 2 hr, 3 hr	1 hr: 25.33^oC 2 hr: 24.96^oC 3 hr: 24.95^oC	Pass
Humidity	Report variation over 3 hr	1 hr: 52.5% 2 hr: 51.9% 3 hr: 52.5%	Pass

Table 7. Sweating System Fluidics calculated Flow Conductance for Performance Qualification

Item	Acceptance Criteria	Result	Pass/Fail
Fluidics Test Flow Conductance*	Record Results: ≤ 20% lower than previous flow conductance value	Day 1: 23.50 Day 2: 24.18	Pass

*Record results from duplicate runs

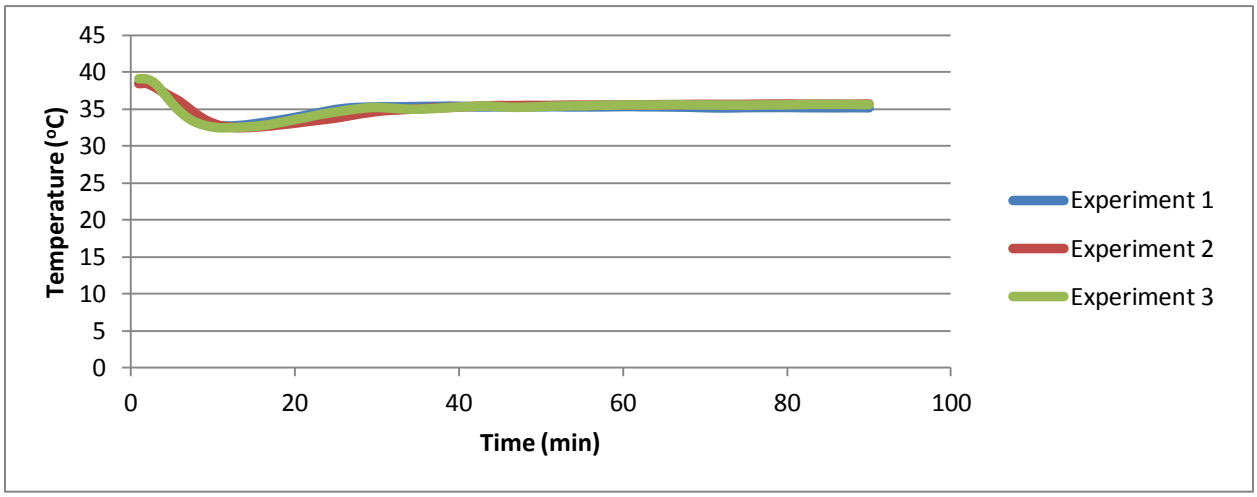

Figure 56. Comparison of body average skin temperature of thermal manikin in hot (40°C) ambient conditions

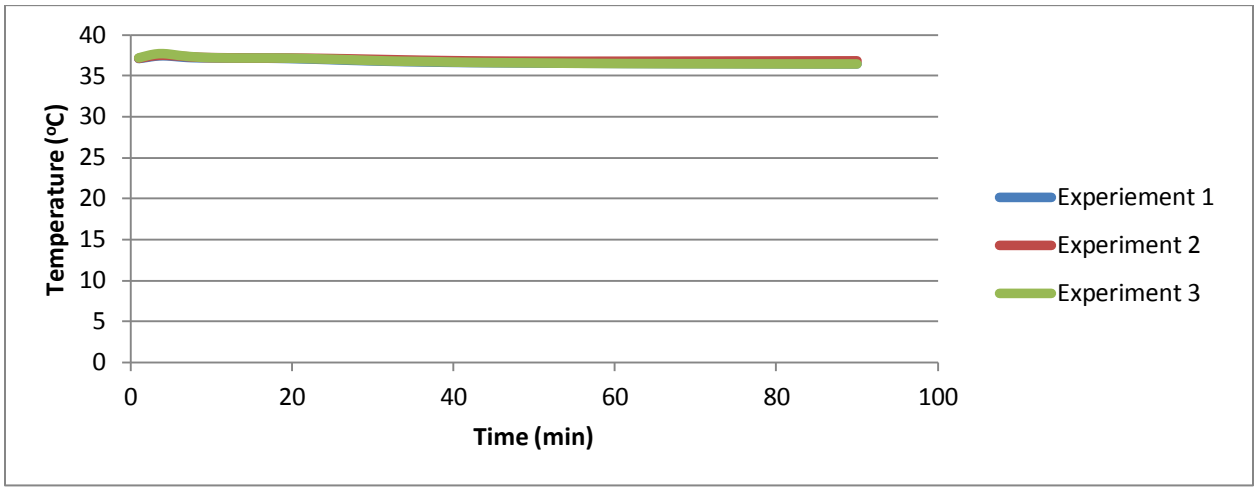

Figure 57. Comparison of core temperature of thermal manikin in hot (40°C) ambient conditions

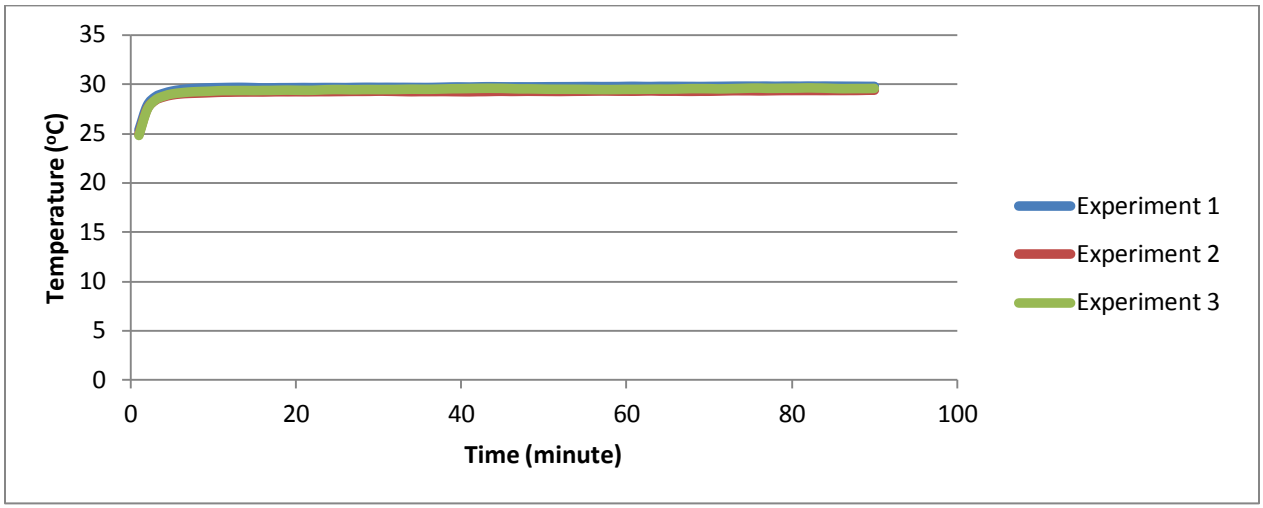

Figure 58. Comparison of body average skin temperature of thermal manikin in neutral (25°C) ambient conditions

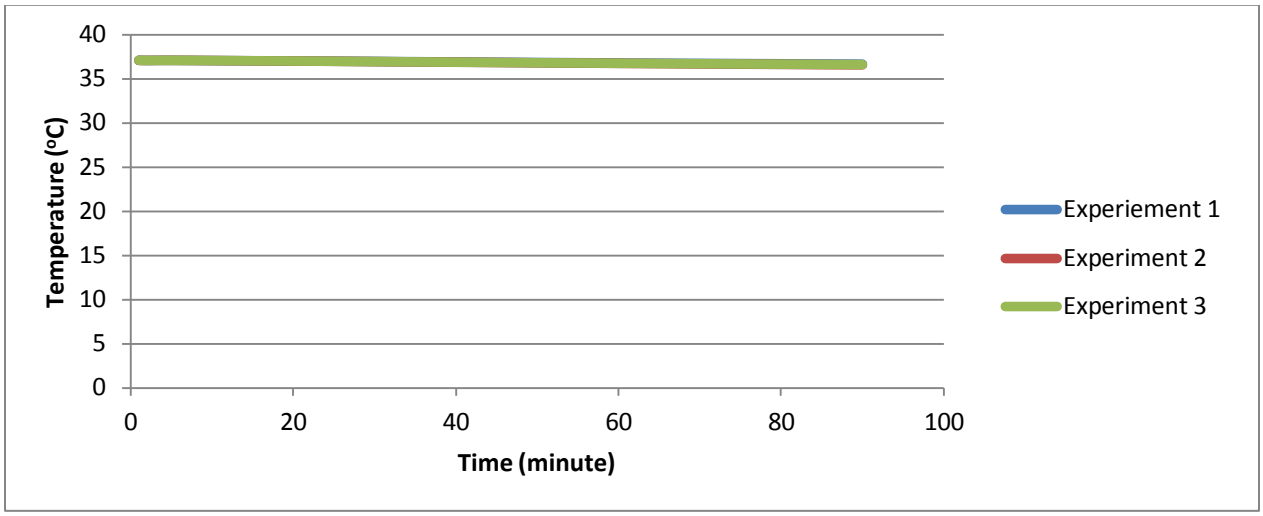

Figure 59. Comparison of core temperature of thermal manikin in neutral (25°C) ambient conditions

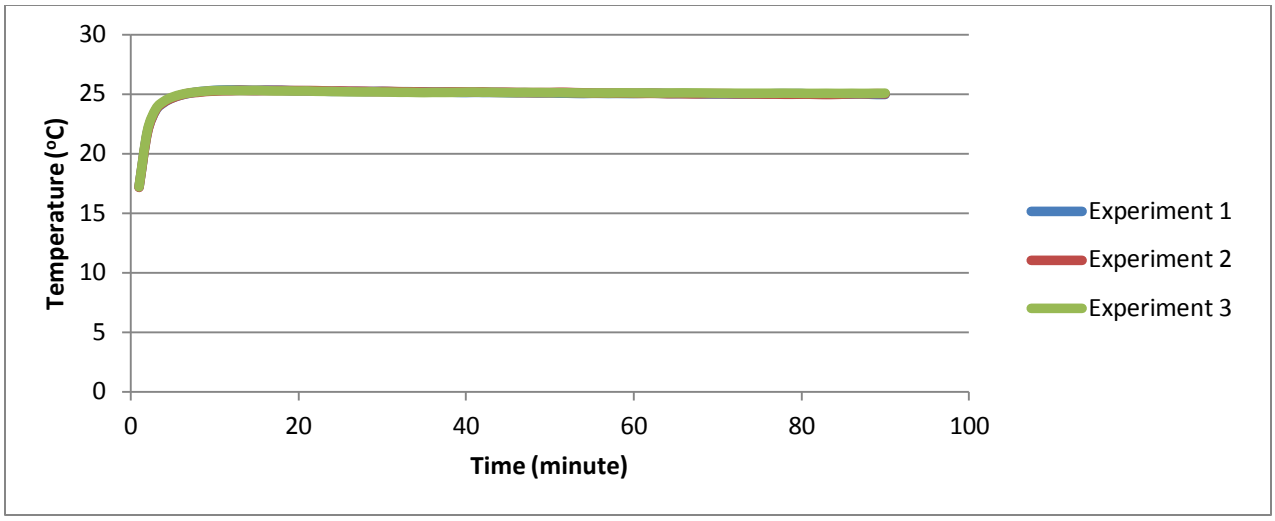

Figure 60. Comparison of body average skin temperature of thermal manikin in cold (15°C) ambient conditions

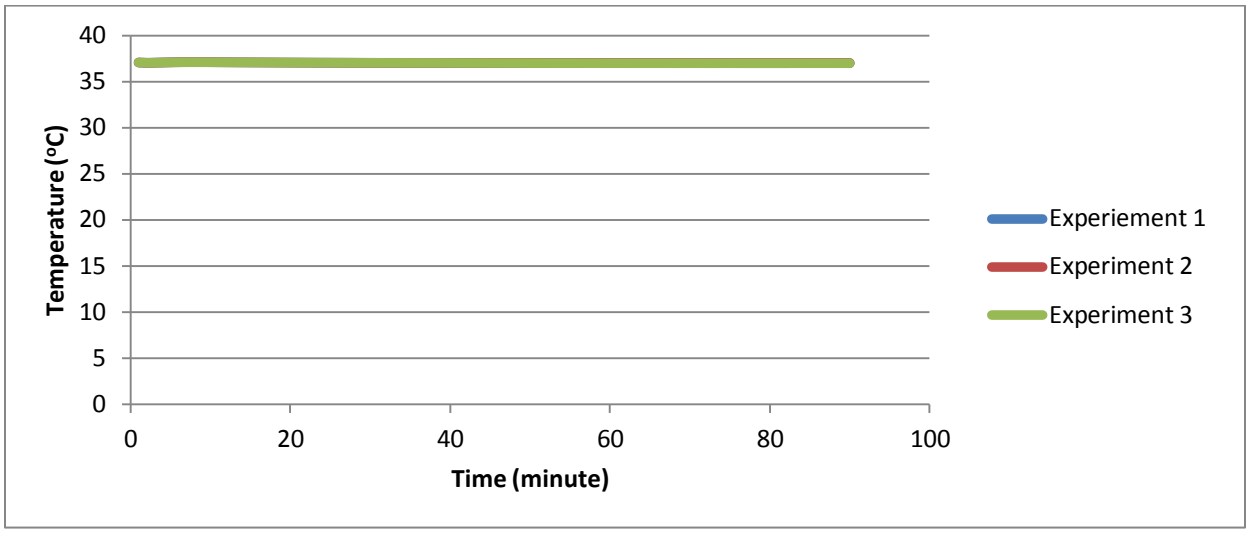

Figure 61. Comparison of core temperature of thermal manikin in cold (15°C) ambient conditions

4d. Patient Simulation Testing

Currently, one of the most effective treatments for patients who are either hypothermic or hyperthermic involves the use of active convective/conductive heating/cooling devices[1-8]. However, these methods require heavy or bulky equipment and are not practical for military applications in the field. The evidence for active heating/cooling treatments for injured or ill patients prompted this study to develop a portable battery operated body temperature

conditioning device for military use in austere environments where access to electrical power is not available.

The patient simulation test method described in the statement of work (SOW) was to evaluate the PBTC. The prototype was to be application tested using simulated patient thermal loads and compare the efficacy of PBTC to current available devices. A circulating water blanket was to be placed on the manikin and then covered with cotton blankets. The device water blanket temperature was to be evaluated at 15°C, 20°C, 25°C, 30°C, 35°C, and 41°C after manikin and environmental chamber reached steady state conditions. Blanket temperature, skin surface temperature, and heat flux (heat flow/unit area) would be sampled over 10 minutes. These measurements would be used to calculate heat transfer between manikin and blanket. Core body temperature would be measured as well.

A mechanical engineer with expertise in bio-heat transfer was hired in June 2013 following approval by United States Army Medical Research Acquisition Activity (USAMRAA) to assist with developing and finalizing the patient simulation testing. The following three tests were designed for evaluating PBTC performance: 1) Heating/Cooling fraction test, 2) Comparison of PBTC to commercial hyper-hypothermia system test, and 3) Head cooling Test. The thermal loads and efficacy of the PBTC were evaluated; however the originally planned test method in the SOW had a few modifications. The first modification was that some of the testing was performed outside of an environmental chamber. The PBTC was compared to a commercial hyper-hypothermia system using commercial off-the-shelf (COTS) circulating water blanket and vest wrap. The data collected from the commercial device was obtained in a local hospital operating room (OR), whereas the PBTC testing was performed in an environmental chamber at Rocky Research. UNSOM was granted access to use the OR and the hyper-hypothermia at the hospital for another study that was applicable to this project. Second modification, test measurements were sampled for at least 60 minutes or longer instead of the original planned 10 minutes. It became evident that 10 minutes was inadequate time to acquire the number of data points necessary for the calculations in cooling/heating fraction testing or to show warming/cooling trends in the other two tests. Finally, the third modification was PBTC circulating water blanket/wraps were evaluated at 15°C and 37.5°C for heating/cooling fraction test, 42°C for comparison of PBTC to commercial device, 10°C for head cooling. These temperatures were selected for clinical relevance. A study performed by Xu et al[15] evaluated the cooling fraction of a liquid cooling garment. The PBTC prototype was ran under similar test conditions described in the study with some modifications. The cooling fraction test temperature (15°C) was selected based on the lowest temperature tested in a liquid cooling garment. Normal core body temperature (37.5°C) was selected for heating fraction testing because it would be an ideal warming temperature used by physicians in maintaining normothermia. The comparison test temperature was selected for warming patients in an intraoperative setting where active warming device would be set to maximum temperature (42°C). The coldest temperature (10°C) setting on the device that would not cause the water to freeze without glycol was selected for the head cooling test.

1. Heating & Cooling Fraction Test

The performance and battery life of the Portable Body Temperature Conditioner (PBTC) were evaluated by performing cooling/heating fraction tests. The PBTC was tested under continuous and battery power to show consistent cooling/heating capacity and sufficient battery life for operation in the field.

Setup of the Heat Flux Sensors and Data Acquisition System (DAQ)

Due to constraints from the DAQ system a total of only seven RdF Micro-Foil® heat flux sensors can be used. Figure 62 shows placement of seven sensors during preliminary testing. The National Instruments (NI) USB-6289 (Mass Termination) data acquisition module, used in experimental testing, has 32 analog inputs (16 analog inputs per terminal block). Two SCB-68A terminal blocks were connected to the NI USB-6289. Each terminal block has eight analog input channels (one positive and one negative input). Each heat flux sensor requires two analog inputs, one for voltage measurement and one for surface temperature measurement. The heat flux sensors used have a built in type K thermocouple to measure the surface temperature of the manikin. Thermocouples work on the principle that dissimilar metals generate voltage, which can be related to temperature. Connecting the leads of the thermocouple to a data acquisition system introduces more dissimilar metal junctions (cold junctions) to the thermocouple resulting in inaccurate temperature measurements. The SCB-68A terminal block, used in experimental testing, has built-in cold junction compensation for accurate temperature measurements. However, the cold-junction compensation requires the use of one analog input. In total, two SCB-68A terminal blocks were used in conjunction with the NI USB-6289 DAQ system resulting in two terminals being used for cold junction compensation (one for each terminal block). As a result, due to the fact that each heat flux sensor requires two terminals, two terminals were used for cold junction compensation, and the NI USB-6289 DAQ system has a total of 32 analog inputs (16 analog inputs per terminal block, 8 positive/negative inputs summing to 16 total) the system was only capable of accommodating seven heat flux sensors[4-5,15].

Figure 62. Example placement of heat flux sensors on a thermal manikin

The heat flux sensors used in the experimental testing generated a voltage proportional to the heat rate applied to the surface of the sensor. The measured heat rate was then divided by the surface area of the sensor to determine the heat flux. Each sensor measured the voltage generated to determine the heat flux (microvolts, µV) and the surface temperature via a thermocouple (°F). Figure 63 shows the DAQ setup with the NI USB-6289 and two SCB-68A terminal blocks. The terminal blocks have the seven heat flux sensor leads connected. Figure 64 shows a zoomed in view of the leads for the first heat flux sensor. The voltage leads, white positive and red negative, are connected to analog inputs 33 and 66 respectively (1a in the figure). The thermocouple leads, yellow positive and red negative, are connected to analog inputs 65 and 31 respectively (1b in the figure). Analog inputs 68 and 34 are used for cold junction compensation as discussed previously. The rest of the heat flux sensors are connected to the remaining analog inputs.

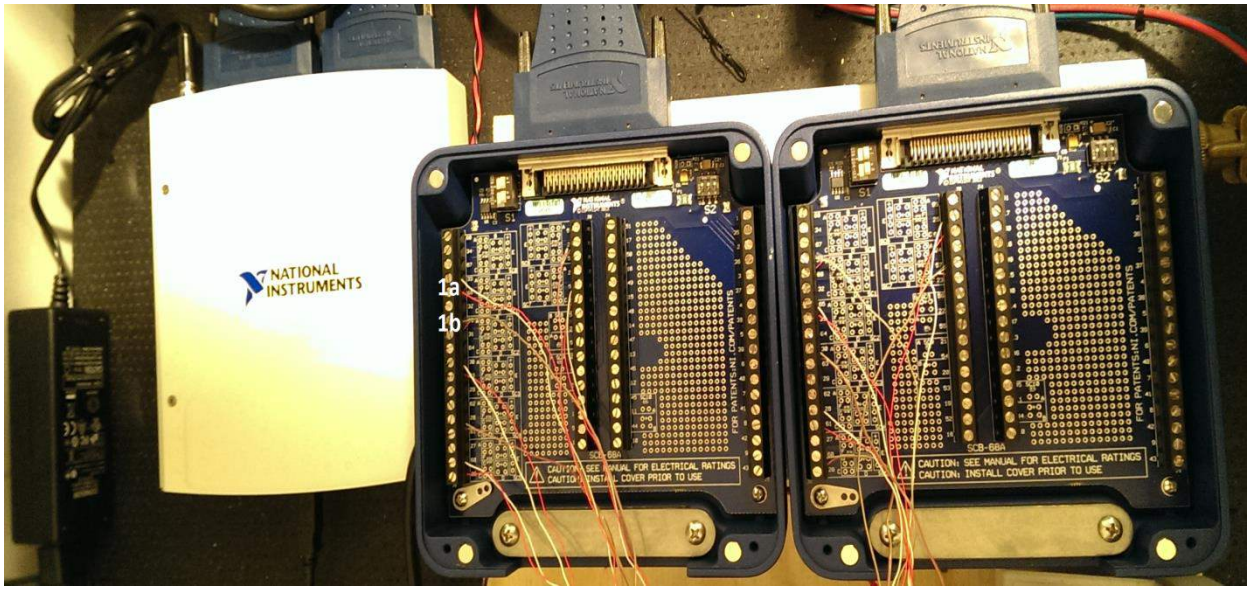

Figure 63: DAQ setup with the seven heat flux sensor leads connected to the terminal blocks

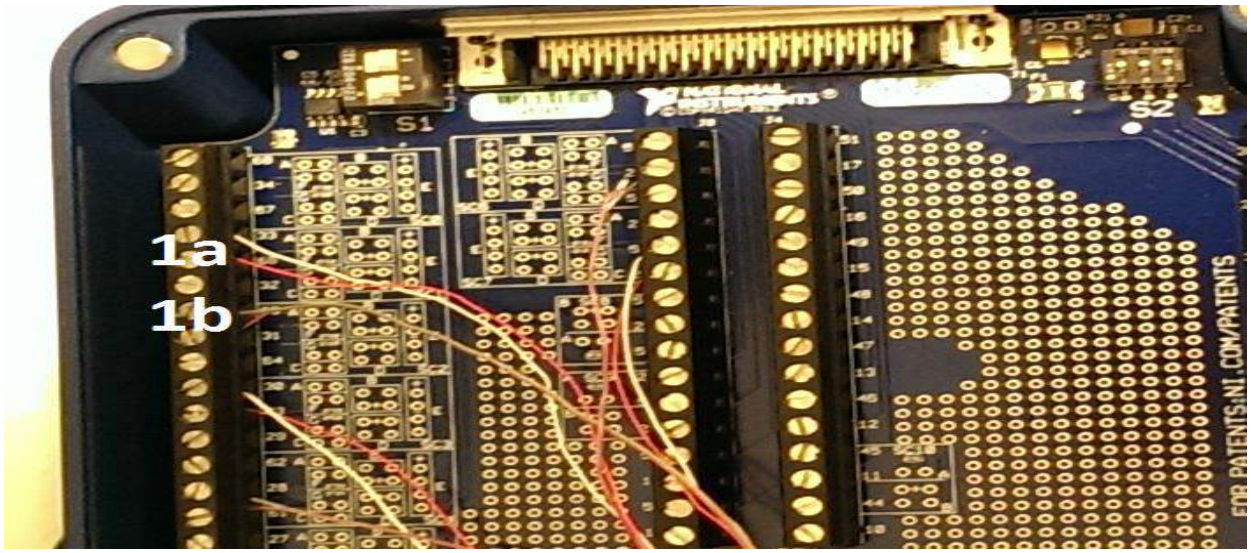

Figure 64: Zoomed in view of the heat flux sensor leads connected to the terminal block

The DAQ system was controlled using LabVIEW software. Figures 65 and 66 show the block diagram programmed to record the measurements from the heat flux sensors used in the experimental testing. Each heat flux sensor records the voltage generated and the surface temperature of the manikin. The heat flux sensors were calibrated using a fifth order polynomial based on a surface temperature of 70°F. This calibration value converts the voltage outputted (µV) into the heat flux (BTU/ft^2·hr) recorded. The fifth order polynomial gives a multiplication factor based on the surface temperature recorded from the thermocouple attached to the heat flux sensor. The voltage output of the sensor was divided by a conversion factor to output the heat flux and then multiplied by the output of the fifth order polynomial, which was based on the surface temperature of the manikin, to output the heat flux recorded by the sensor. Finally the

outputted heat flux was converted to W/m^2 for data analysis. The DAQ system records the heat flux and surface temperature for each of the seven sensors and saves the data to a .txt file.

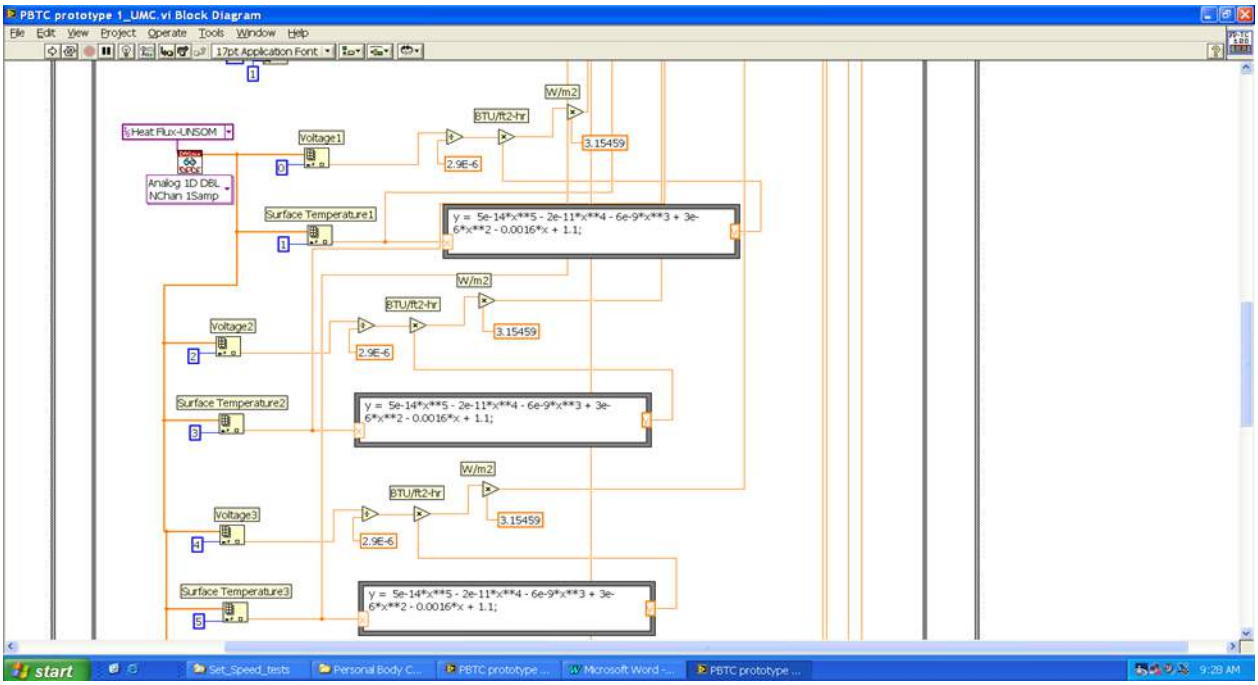

Figure 65. LabVIEW block diagram program for recording the heat flux sensor measurements

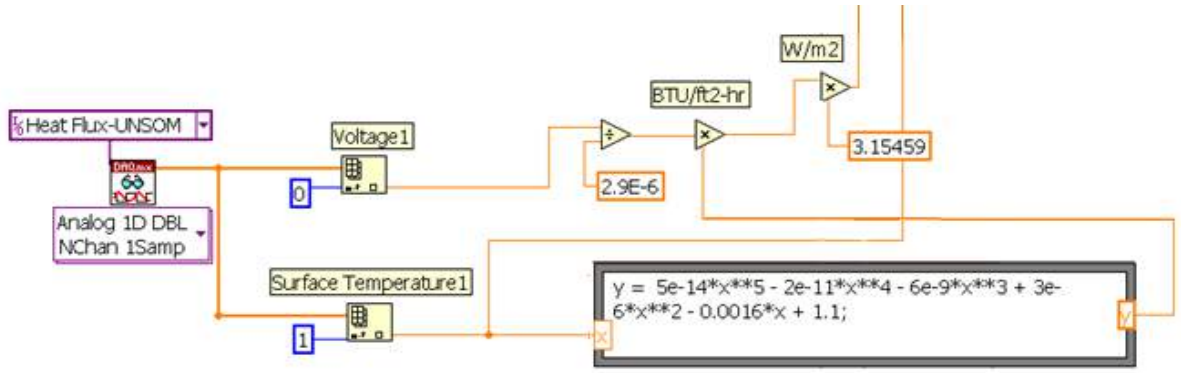

Figure 66. Zoomed in view of the LabVIEW block diagram program for recording the heat flux sensor measurements

Cooling/Heating Modes and Battery Life Experimental Testing

To determine how well the Portable Body Temperature Conditioner (PBTC) functions and the battery life operating under extreme conditions, cooling/heating mode tests were performed to determine the heating/cooling fraction (fraction of heat transfer between the circulating water blanket and thermal manikin) Each day of testing consisted of running four individual tests; a

fixed temperature test, control test, and cooling/heating mode tests running on continuous and battery power[3-6,11,15,16].

Fixed Temperature Test

First a fixed ambient temperature test was run at 15°C (Heating) and 30°C (Cooling). This test was performed to show that the environmental chamber can maintain a constant ambient temperature for the duration of an experimental run and to demonstrate consistent thermoregulatory response of the thermal manikin at a fixed ambient temperature. Figure 67 shows the environmental chamber located at Rocky Research used for the experimental testing. The environmental chamber was heated by baseboard heaters and cooled by a NESLAB HX-750 Refrigerated Recirculator connected to a heat exchanger/fan setup. Four sensors were used to record the ambient temperature, relative humidity, and wind speed. The relative humidity and one temperature sensor were positioned six feet from the ground (A, figure 67) and the wind speed and a second temperature sensor were positioned two feet from the ground (B, figure 67). All measurements were recorded by the ThermDAQ software and saved as a .csv file.

Figure 67. Environmental chamber at Rocky Research

For the fixed temperature testing procedure the thermal manikin was placed supine on a table within the environmental chamber as shown in figure 67. The absorbent pad placed between the table and the manikin was there to collect any water loss from sweating. The sweating skin was not used during experimental testing because of obstruction from the heat flux sensors. Prior to

the start of the experiment the environmental chamber was set to the specified ambient temperature (15℃ for heating and 30℃ for cooling) and allowed to reach steady state. After initial setup of the environmental chamber, the thermal manikin flow pump and power supply were powered on and the ThermDAQ software was started. The thermal manikin was then allowed to acclimate to the ambient conditions for 30 minutes, at which time the physiological software "Manikin PC2" was started and the experiment "Model Control" was run. The manikin was then running under the control of the physiological software which accounts for conditions such as; vasodilation, vasoconstriction, sweating, metabolic activity, circulation, and conduction/convection/radiation heat loss. The physiological software simulates the thermoregulatory response of a healthy individual based on the environmental conditions. The activity level, which is measured in terms of metabolic rate (met), was set to 1 met (the equivalent of an individual walking) and the Activity Type was set to 0 (indicating the individual is lying down). The experiment was run for one hour. Figure 68 shows the average ambient temperature of the environmental chamber during five runs of the fixed temperature test in cooling mode (30°C ambient temperature). The data showed that the environmental chamber maintained the designated 30 ± 1°C ambient temperature for an extended period of time. Figures 69 and 70 shows the total heat generated by all 26 zones of the thermal manikin during the fixed temperature test in cooling mode (30°C ambient temperature) for five runs. The data from the ThermDAQ software shows that the environmental chamber produced a constant ambient temperature and the manikin produced a consistent thermoregulatory response for each of the five runs. This indicates that the manikin was functioning properly and that data from cooling mode tests will be valid for a constant ambient temperature[3-6,11,15,16].

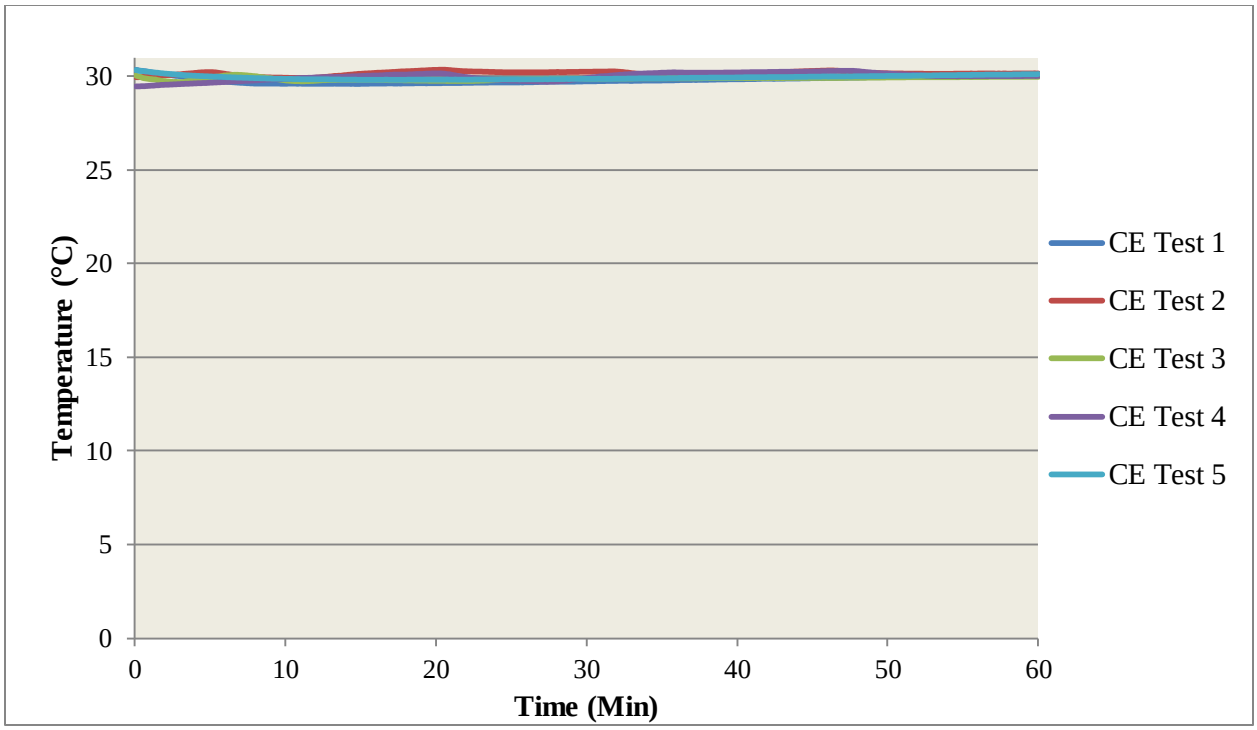

Figure 68. Average ambient temperature from fixed temperature test in cooling mode (30°C ambient temperature)

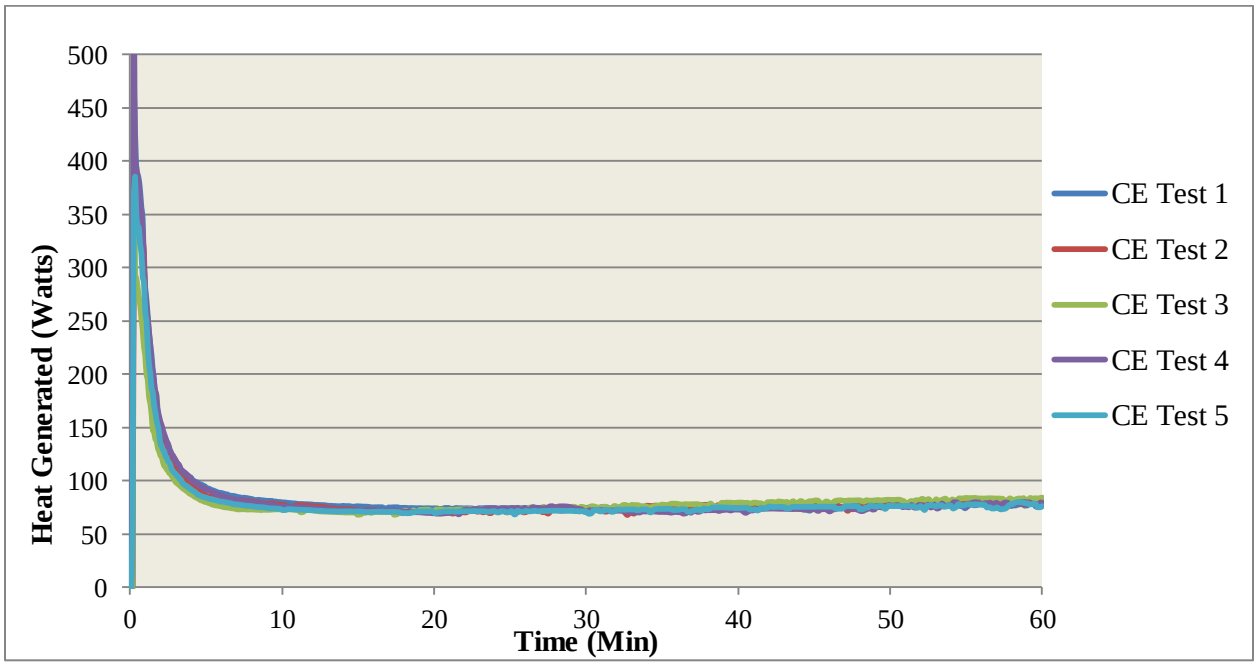

Figure 69. Total heat generated by manikin's 26 zones for the fixed Temperature test in cooling mode (30°C ambient temperature)

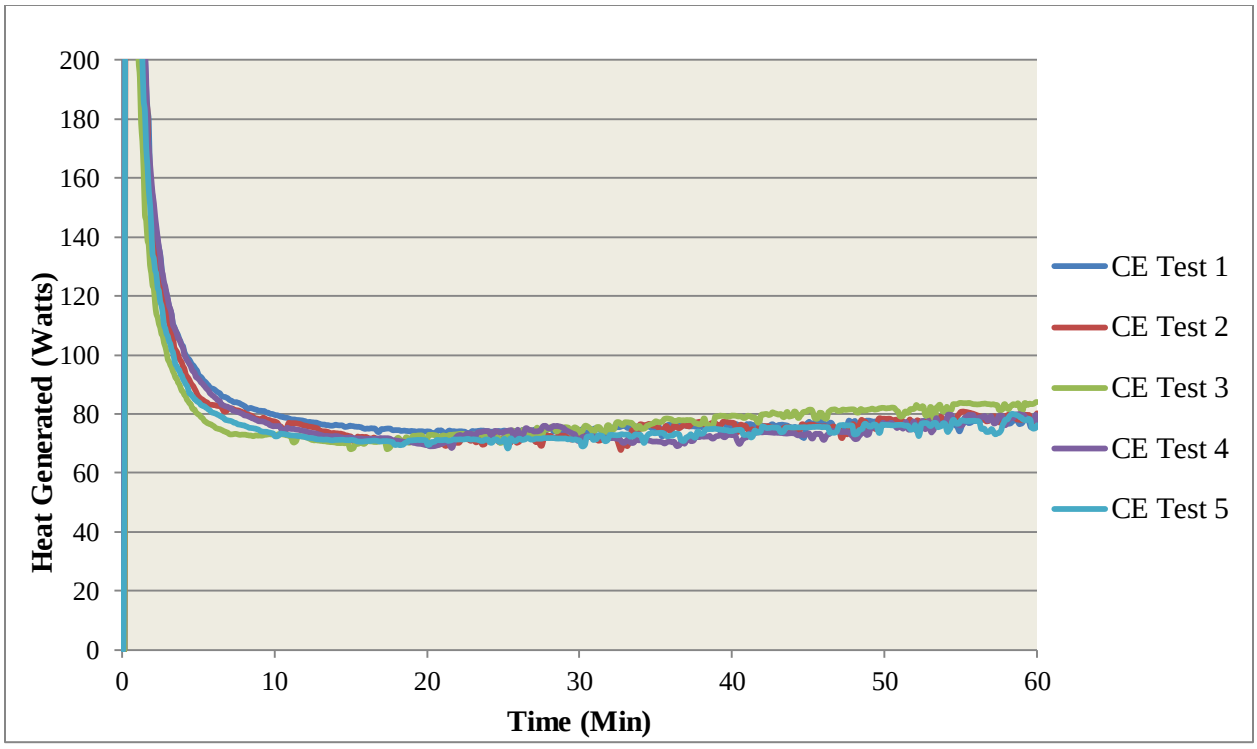

Figure 70. Zoomed in view of the total heat generated by manikin's 26 zones for fixed temperature test in cooling mode (30°C ambient temperature).

Figure 71 shows the average ambient temperature of the environmental chamber during five runs of the fixed temperature test (Heating, 15°C). The data shows that the environmental chamber maintained the designated 15°C ± 1°C ambient temperature for an extended period of time. Figures 72 and 73 show the total heat generated by all 26 zones of the thermal manikin during the fixed temperature test (Heating, 15°C) for five runs. The data from the ThermDAQ software shows that the environmental chamber produced a constant ambient temperature and the manikin produced a consistent thermoregulatory response for each of the five runs. This indicates that the manikin is functioning properly and that data from heating mode tests will be valid for a constant ambient temperature.

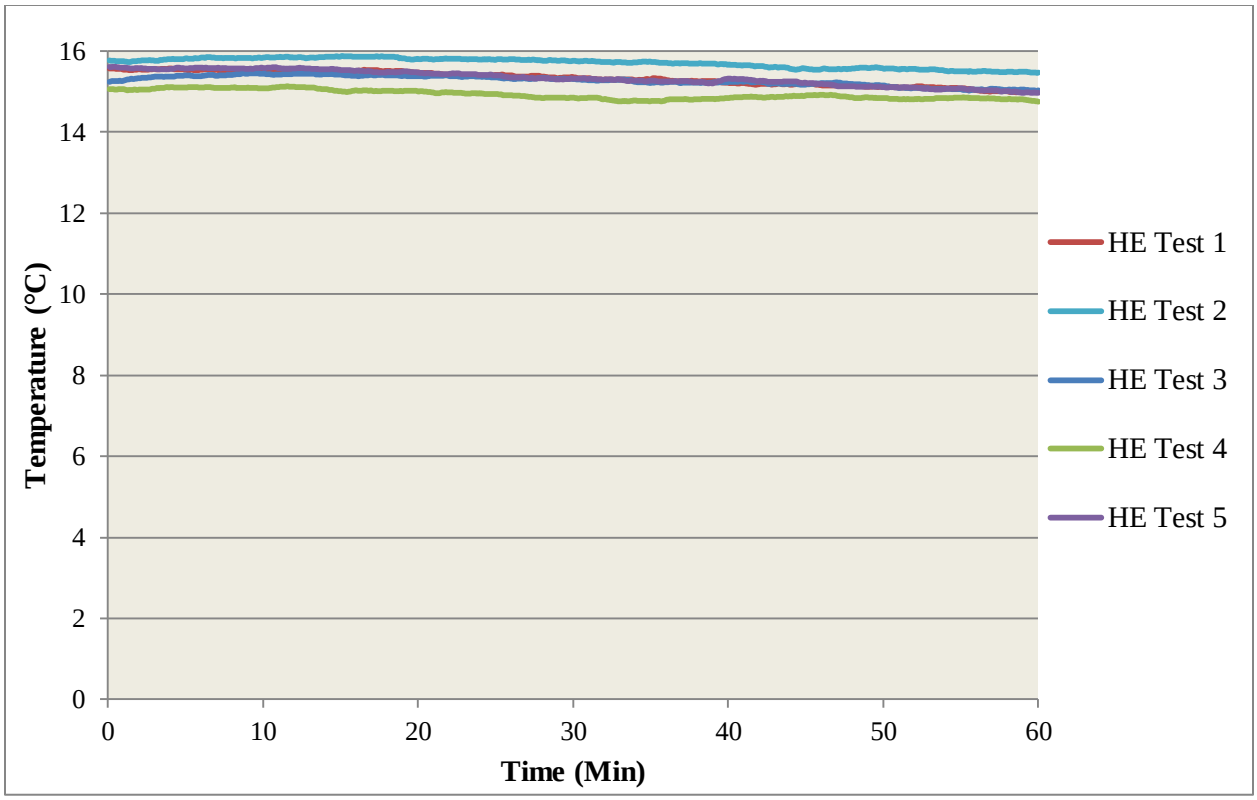

Figure 71. Average ambient temperature from the fixed temperature test in heating mode (15°C ambient temperature)

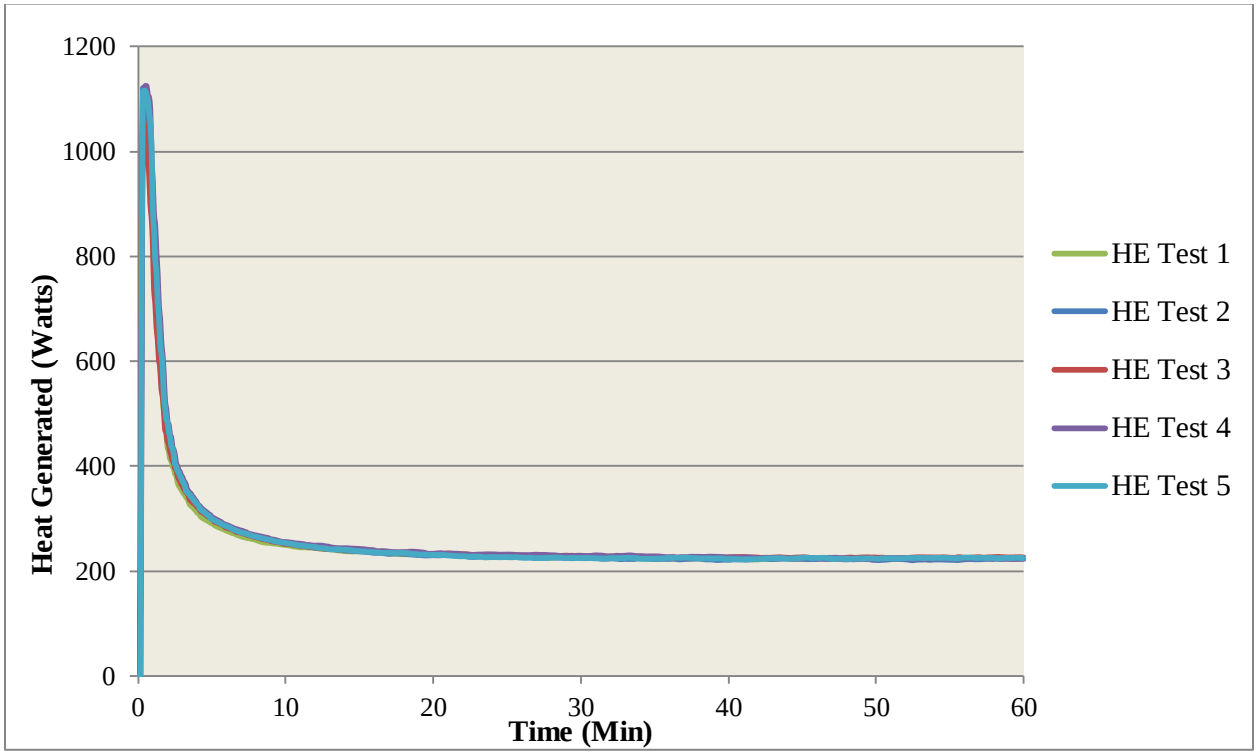

Figure 72. Total heat generated by the manikin's 26 Zones for the fixed

Temperature test in heating mode (15°C ambient temperature).

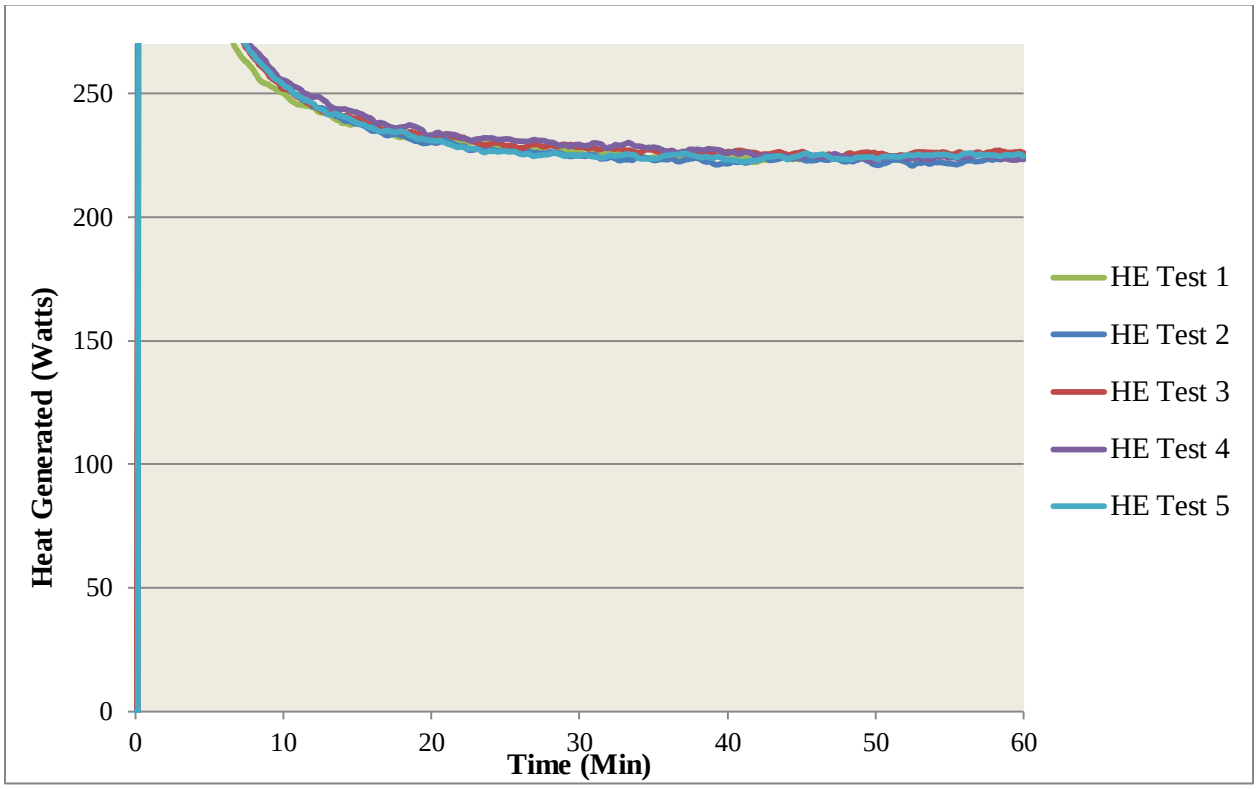

Figure 73. Zoomed in view of the total heat generated by manikin's 26 zones for the fixed temperature test in heating mode (15°C ambient temperature).

Control Experimental Runs for Heating/Cooling Modes

The next step for the experimental testing was to run a control test to record baseline measurements for the cooling/heating fraction of the PBTC. The thermal manikin setup and environmental chamber ambient conditions for the control runs were the same as the fixed temperature tests. For the control test an industrial humidifier was used to maintain a relative humidity of 50% ± 5%. Due to weather conditions during the experimental testing, some days the humidity could not be maintained at the designated percentage. The data for those days was still consistent with the other days of testing or it was disregarded. For the control test a Maxi-Therm® circulating water blanket (Cincinnati Sub-Zero Products, Inc.; Cincinnati, OH**)**, connected to the PBTC, was placed over the thermal manikin. Toothpaste was applied to each heat flux sensor before the water blanket was placed over the manikin to ensure thermal contact between the two surfaces. A wool blanket was then placed over the circulating water blanket for insulation. The sweating function of the thermal manikin was not used during experimental testing because the water effected the measurements taken by the heat flux sensors. However, with the minimal amount of liquid produced during basal sweating and the low air flow velocities over the manikin, the amount of heat lost through evaporation can be neglected. For the control runs the PBTC was not switched on to record the baseline measurements for heat flow into/out of the circulating water blanket. The program "Dry Test" was used. This program

maintains the thermal manikin surface temperature at 33°C ± 1°C by varying the heat generated by each of the 26 individual zones of the thermal manikin. Once the environmental conditions reached steady state, the thermal manikin was allowed to acclimate at those conditions for 30 minutes before testing began. Once the manikin acclimated to the ambient conditions the LabVIEW software program controlling the measurements for the PBTC was started and then the ThermDAQ software was started. The LabVIEW program also controls the DAQ system for the heat flux sensors. The test was run for one hour. The LabVIEW data was saved as a .txt file and the ThermDAQ data was saved as a .csv file. Figures 78 and 79 show data from the ThermDAQ software for the cooling and heating mode control tests respectively. The software records the heat flux generated by each of the 26 zones of the thermal manikin. The total heat generated by the manikin can then be calculated by summing the heater power being delivered to each manikin zone:

$$\dot{Q} = \sum_{i=1}^{n=26} \dot{q}_i \dot{A_i} \qquad (2)$$

Where,

q_i = Zone Heat Flux [W/m^2]

A_i = Surface Area of Manikin Zone [m^2]

The power consumed by the thermal manikin when the circulating water blanket is not running was calculated for both cooling and heating mode control tests and is displayed in figures 74 and 75 below. From the figures you can see that steady state portion of the curve is consistent for each experimental run[3-6,11,15,16].

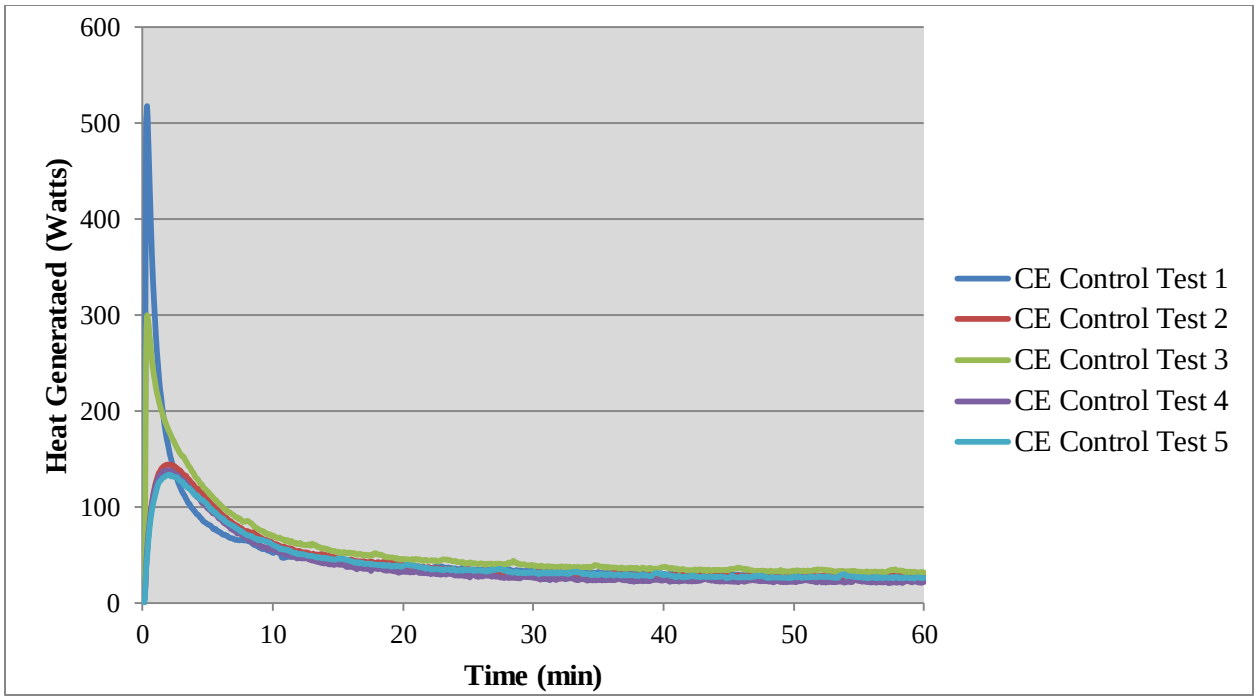

Figure 74. Total Heat Generated for the 26 Zones of the Thermal Manikin During a Control Test (Cooling Mode)

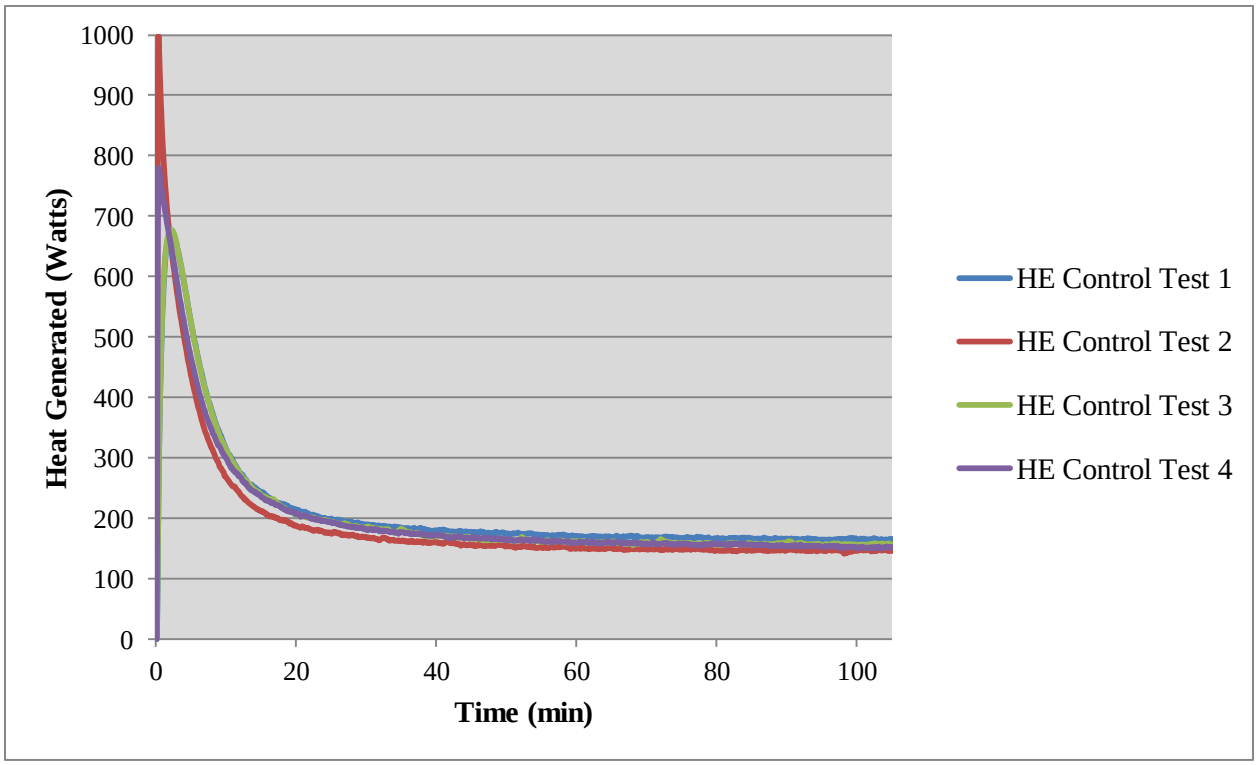

Figure 75. Total Heat Generated for the 26 Zones of the Thermal Manikin During a Control Test (Heating Mode)

Cooling/Heating Modes

The final step in the experimental testing protocol was to perform cooling/heating mode tests with the PBTC running on continuous or battery power. The goal of these experimental runs was to evaluate the battery life and cooling/heating fraction of the PBTC running at both temperature extremes. The continuous and battery powered experimental data were then compared to show comparable functionality while operating under battery power. The thermal manikin setup and environmental chamber ambient conditions for the continuous/battery powered runs were the same as the control test runs. The PBTC manual mode was used for the cooling/heating mode tests. The PBTC water setpoint temperature was set to 15°C for the cooling mode tests and 37°C for the heating mode tests. Once the environmental conditions reached steady state, the thermal manikin was allowed to acclimate at those conditions for 30 minutes before testing began. Once the manikin acclimated to the ambient conditions the LabVIEW software program controlling the measurements for the PBTC and heat flux sensors was started, then the ThermDAQ software was started, and finally the PBTC was started. For the battery powered tests the experiment ran until the battery exhausted (≈90 minutes for cooling mode and ≈105 minutes for heating mode). The continuous power experimental runs were allowed to run for the same period of time as the battery powered runs. The LabVIEW data was saved as a .txt file and the ThermDAQ data was saved as a .csv file. Tables 8 and 9 shows the battery life of the PBTC for cooling and heating mode tests respectively. Rocky Research battery life performance testing for the PBTC running at maximum compressor speed and extreme ambient temperatures showed a battery life of 70 minutes (figure 37). The experimental testing runs performed at less extreme ambient temperatures with constant outlet water temperature showed a battery life that was longer then during the performance testing performed by Rocky Research[3-6,11,15,16].

Table 8. Battery life for the cooling fraction experimental runs

Date	Test 1	Test 2	Test 3	Test 4	Test 5	
Time (min)	89.3	81.9	86.9	90.3	91.8	
					88.0	**Average**

Table 9. Battery life for the heating fraction experimental runs

Date	Test 1	Test 2	Test 3	Test 4	
Time (min)	111.2	111.0	110.4	110.6	
				110.8	**Average**

Figures 76-83 shows the data for the PBTC running on continuous and battery power for five runs of the cooling mode test. Figures 76 and 77 shows the thermal capacity of the PBTC running on continuous and battery power respectively for a cooling mode test. A moving average was taken for the data, averaged at two minute intervals (continuous power) and three minute intervals (battery power), to improve visibility of the data and remove noise. The negative direction indicates that the PBTC is cooling the thermal manikin (removing heat). The cooling

capacity of the PBTC during experimental testing is consistent with the performance testing done by Rocky Research, shown in figure 32, indicating that the empirical data for calculating the cooling capacity is valid. Experimental testing showed no significant difference between the cooling capacity of the PBTC running on continuous power versus battery power. Figures 78 and 79 shows the inlet/outlet water temperature to the PBTC for five cooling test runs. The water temperature is consistent with the cooling capacities shown in figures 76 and 77 for each experimental run. Experimental testing showed no significant difference between the inlet/outlet water temperature to the PBTC running on continuous power versus battery power. Figures 80 and 81 shows the compressor speed of the PBTC running on continuous and battery power for five cooling mode tests. A moving average was taken for the data, averaged at two minute intervals (continuous power) and three minute intervals (battery power), to improve visibility of the data and remove noise. The compressor speed is controlled by an algorithm optimized to maintain the required cooling capacity to maintain constant outlet temperature and maximum battery life (when operating under battery power). The compressor speeds recorded in figures 80 and 81 are consistent with the control algorithms designed by Rocky Research. At around the 57 minute mark for continuous power experimental run (Test 5), the compressor shut off for about 30 seconds. This affected the cooling capacity slightly for that run. However, the data was still consistent to the other experimental results and the inconsistent data recorded for that run was only a small portion of the data analyzed for that test. Figures 82 and 83 shows the flow rate of water flowing through the circulating water blanket and PBTC. For test 3 of the battery powered runs (Figure 83) the lower flow rate is likely the result of pinching or other constriction of the thermal blanket or the connecting lines. The flow rate for the unit is essentially fixed, but may be influenced slightly by differences in voltage between converted AC power and battery power. The flow rate can also be influenced by constrictions in the thermal blanket and connection tubes. For both the continuous and battery powered runs the water temperature, reached at steady-state, were consistent for each individual run. The slightly different water flow rates, with negligible impact on capacity, is attributed to small discrepancies in signal voltage provided to the pump when operating on external vs. battery power.

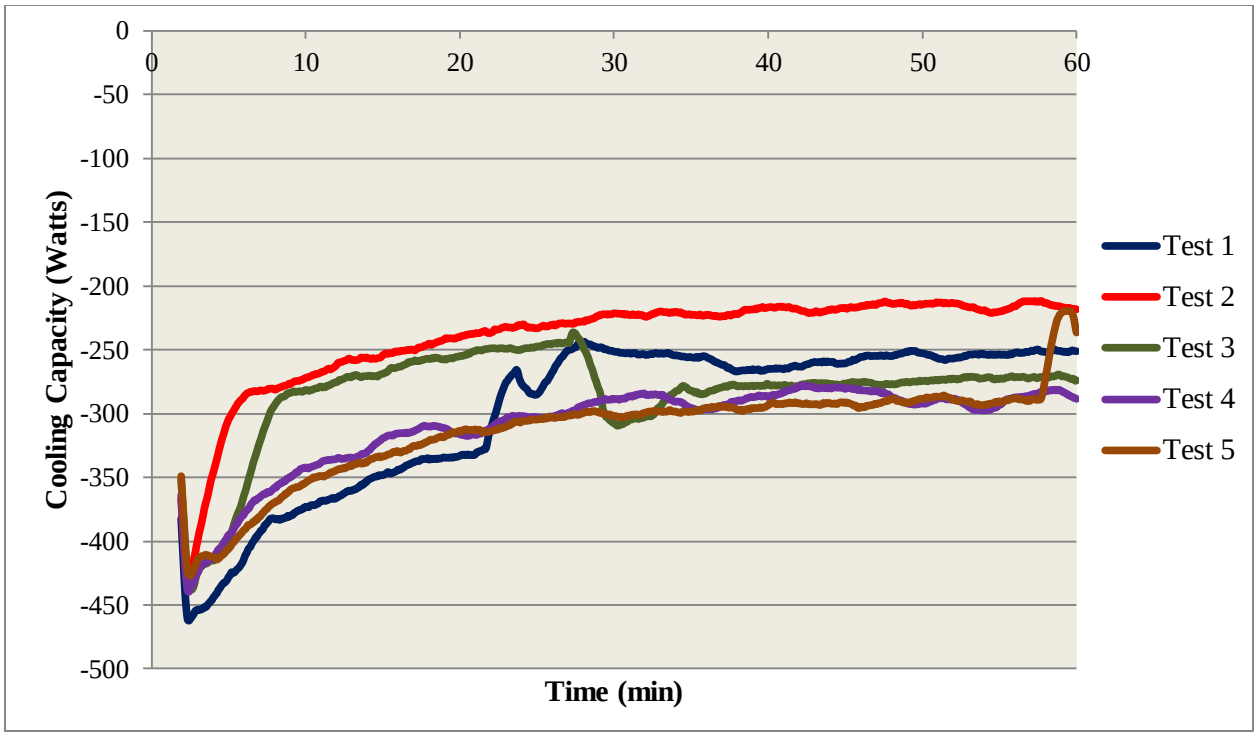

Figure76. Thermal Capacity of the PBTC Running on Continuous Power (Cooling Mode)

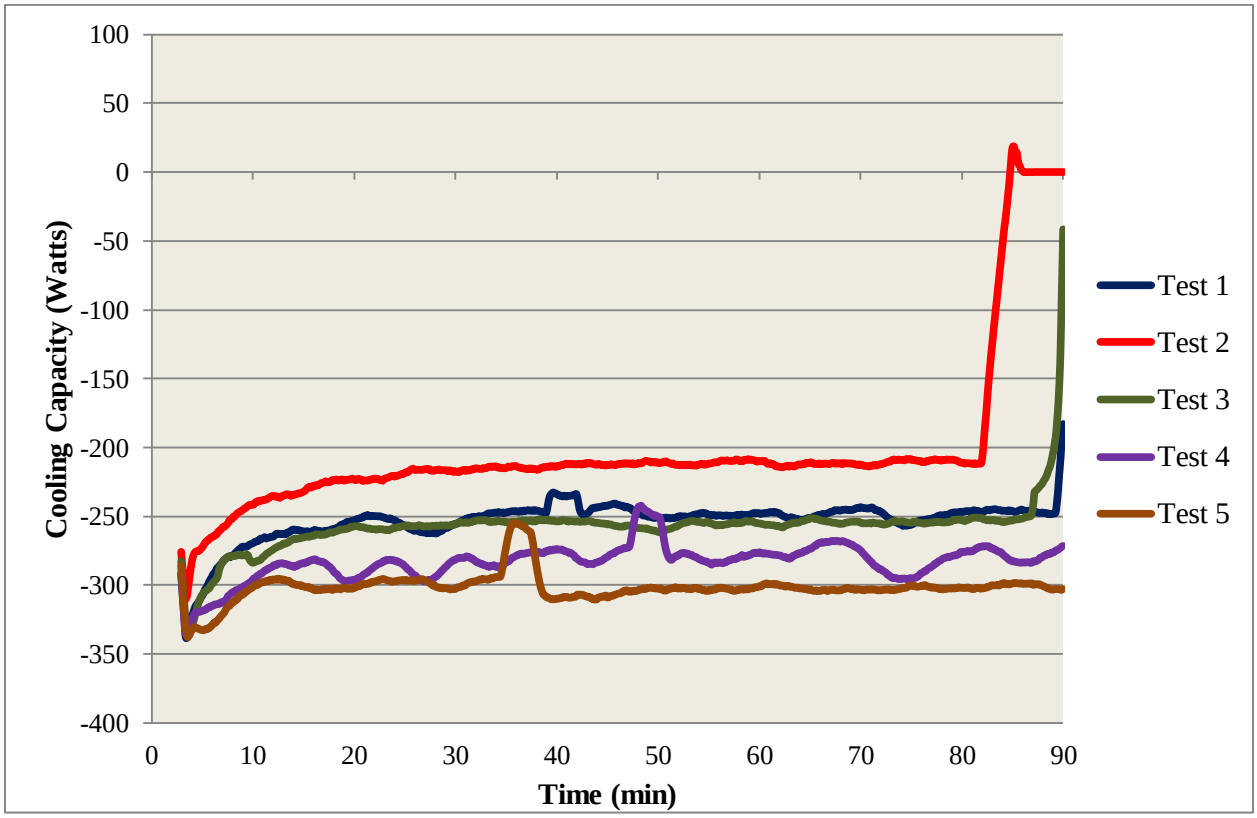

Figure 77. Thermal Capacity of the PBTC Running on Battery Power (Cooling Mode)

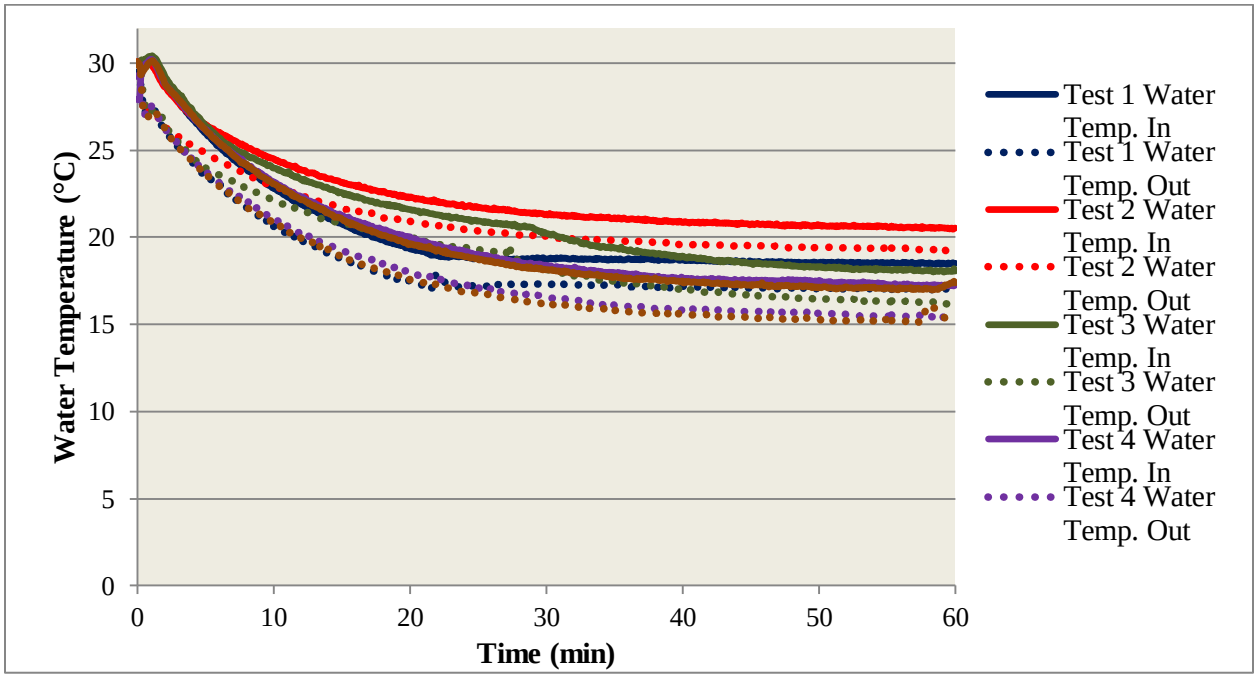

Figure 78. Inlet/Outlet Water Temperature to the PBTC Running on Continuous Power (Cooling Mode)

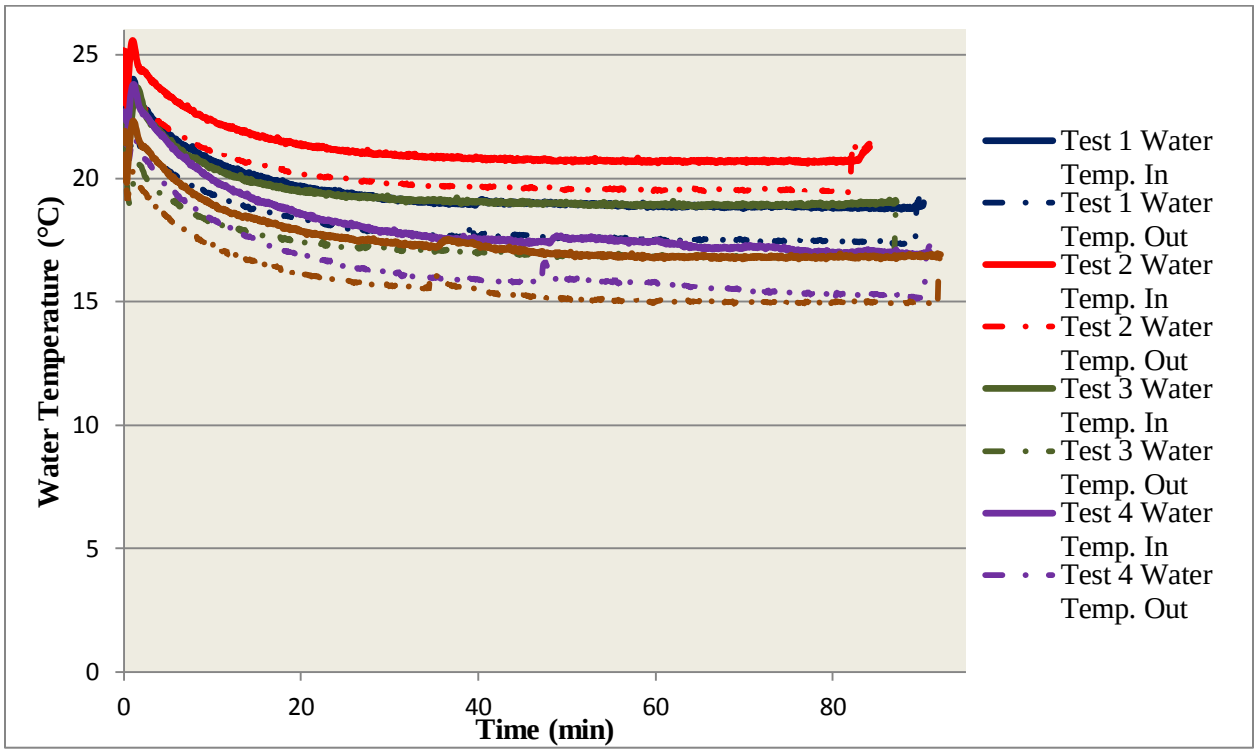

Figure 79. Inlet/Outlet Water Temperature to the PBTC Running on Battery Power (Cooling Mode)

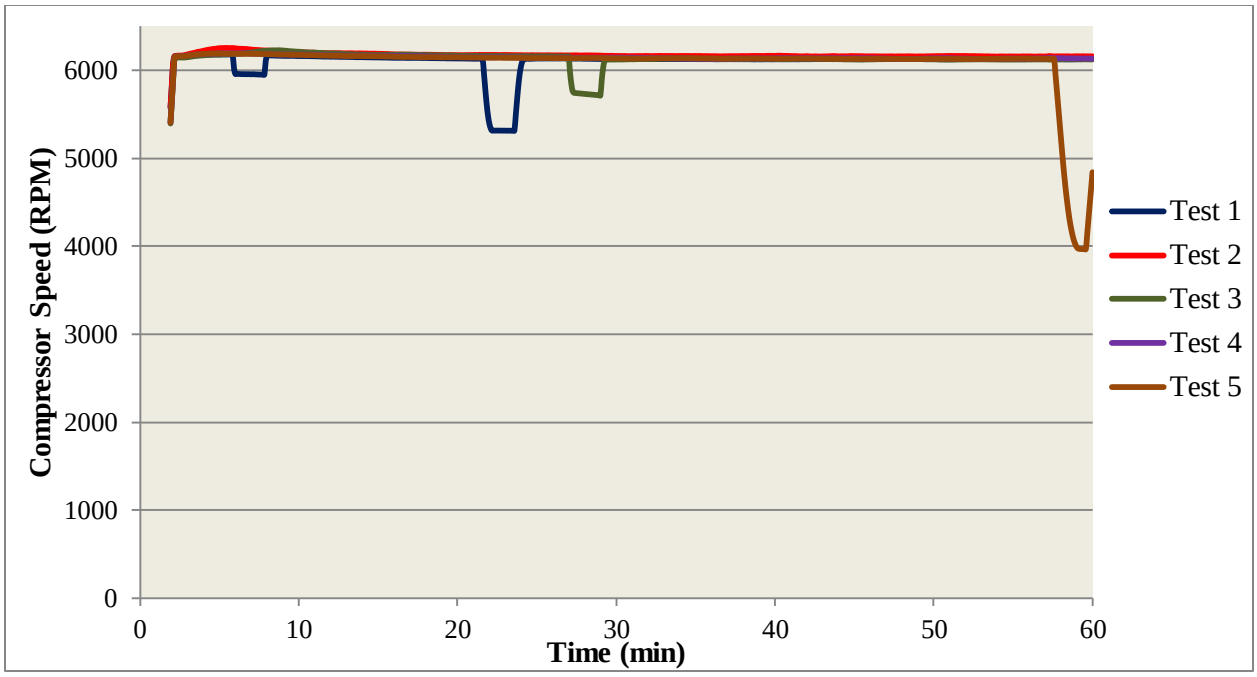

Figure 80. Compressor speed of the PBTC running on continuous power (Cooling Mode)

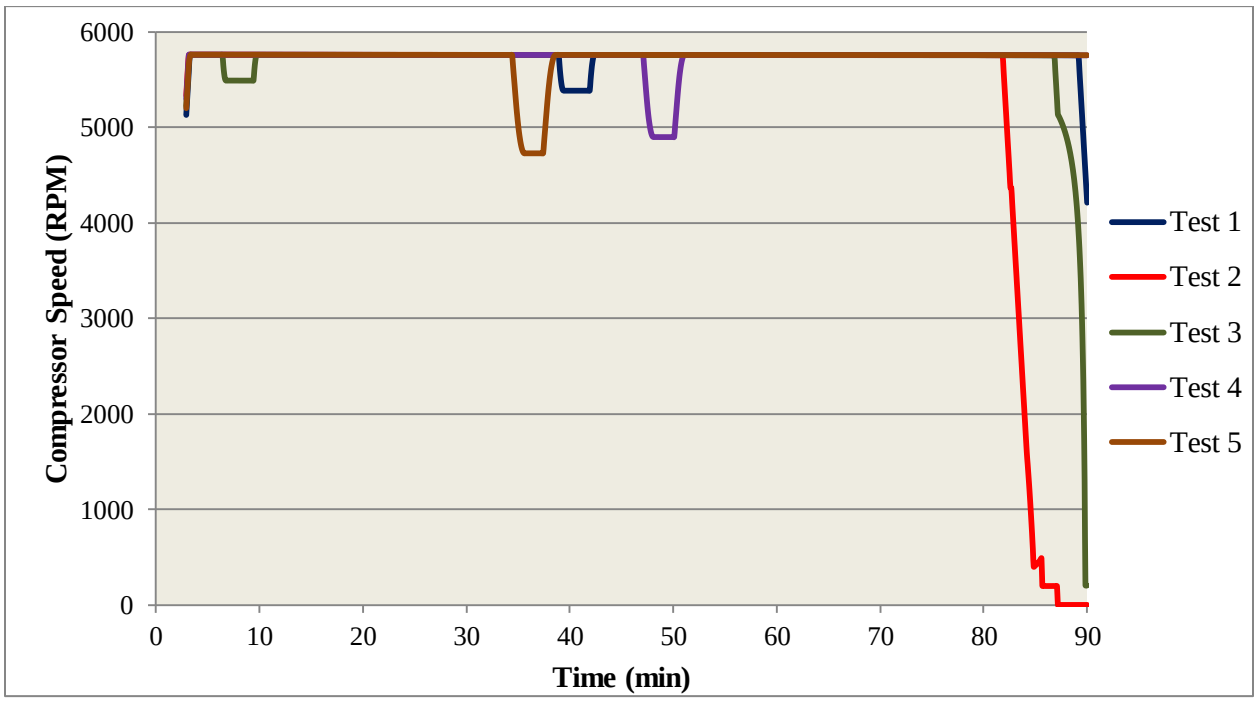

Figure 81. Compressor speed of the PBTC running on battery power (Cooling Mode)

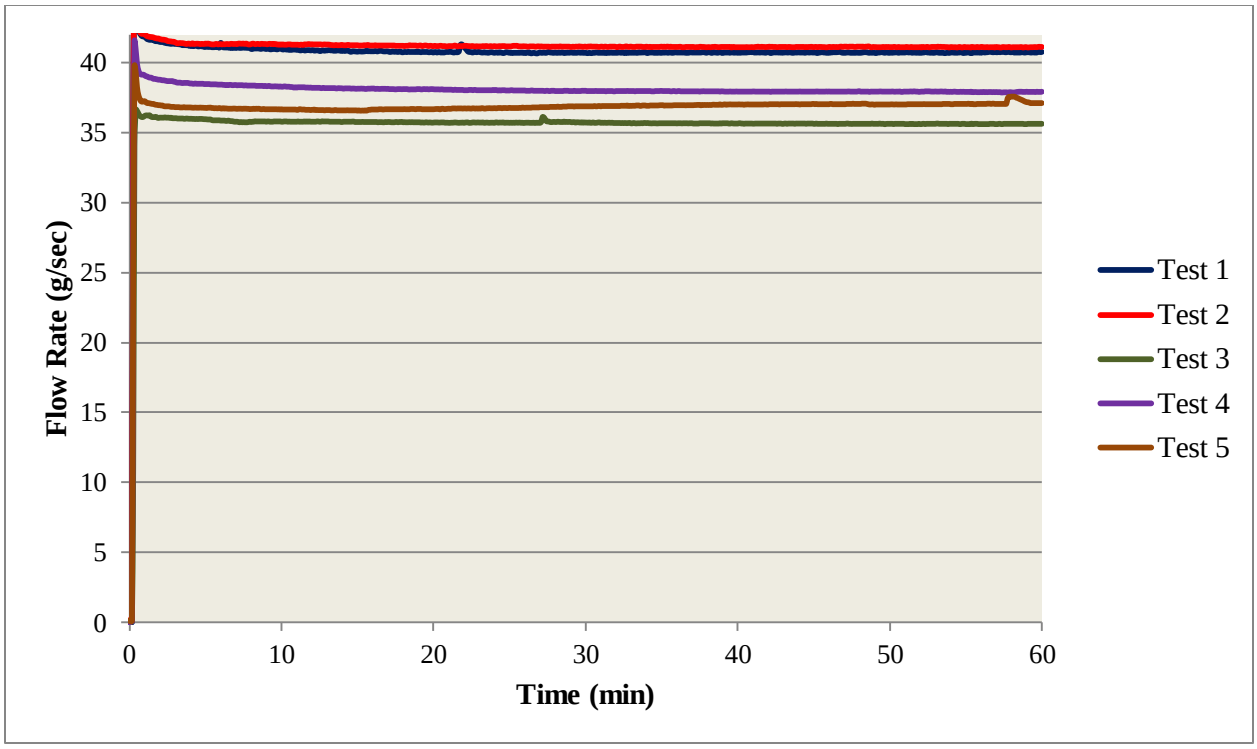

Figure 82. Circulating Water Blanket Flow Rate Running on Continuous Power (Cooling Mode)

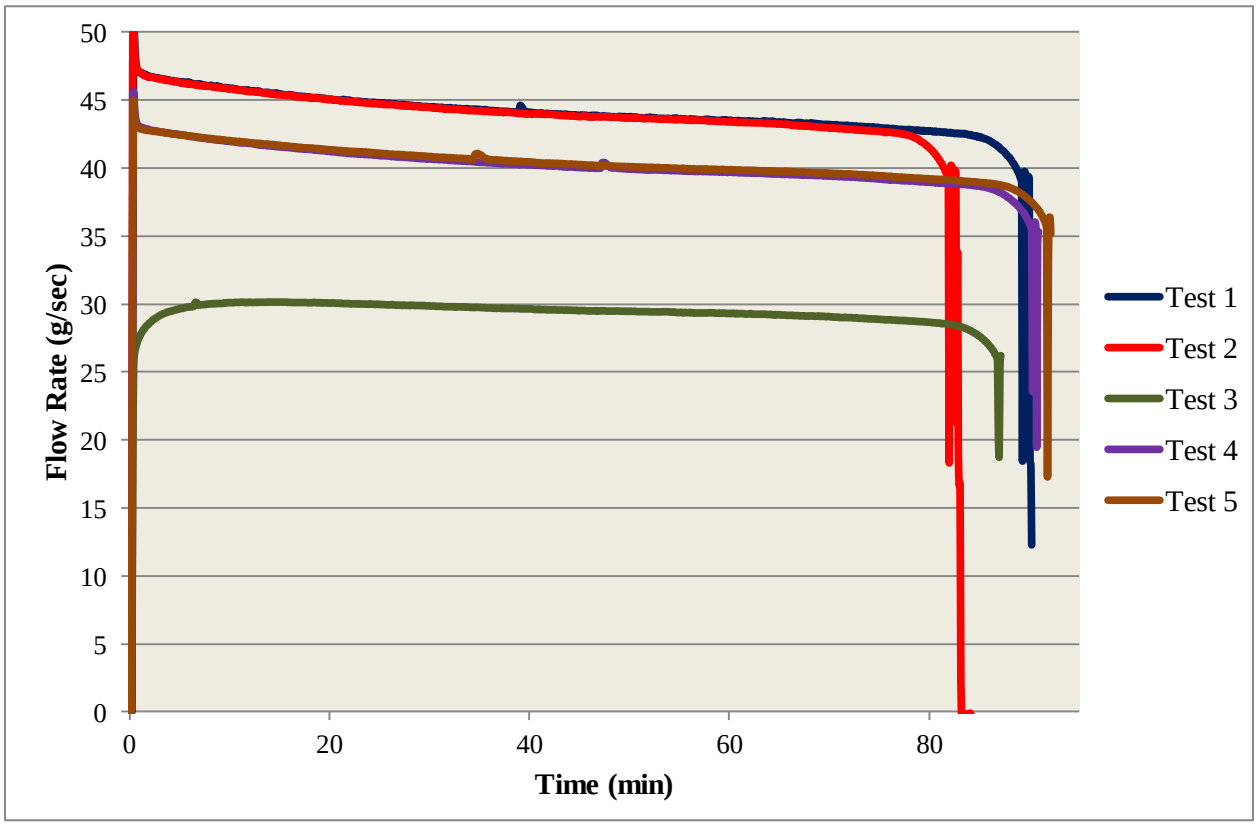

Figure 83. Circulating Water Blanket Flow Rate Running on Battery Power (Cooling Mode)

Figures 84-91 shows the data for the PBTC running on continuous and battery power for four runs of the heating mode test. An additional battery powered run was performed (Test 5) to confirm assumptions about why the flow rate was higher for the battery powered experimental runs. Initially the continuous power experimental runs were allowed to run for one hour. After analysis of the data the PBTC did not reach steady-state within that time period, as a result additional continuous power runs were performed at a later date and allowed to run for 105 minutes (average battery life for heating mode tests). Figures 84 and 85 shows the heating capacity of the PBTC running on continuous and battery power respectively for a heating mode test. The experimental runs were performed with the heat pump cycle only, not the external 240W electric resistance heaters. The heating capacity of the PBTC utilizing both the heat pump cycle and electric resistance heaters will be higher than the values shown in figures 84 and 85. A moving average was taken for the data, averaged at three minute intervals, to improve visibility of the data and remove noise. The positive direction indicates that the PBTC is heating the thermal manikin (adding heat). The heating capacity of the PBTC during experimental testing is consistent with the performance testing done by Rocky Research, shown in figure 34, indicating that the empirical data for calculating the heating capacity is valid. Experimental testing showed no significant difference between the heating capacity of the PBTC running on continuous power versus battery power. Figures 86 and 87 shows the inlet/outlet water temperature to the PBTC for four runs of the heating mode test. The water temperature is consistent with the heating capacities shown in figures 84 and 85 for each experimental run. Experimental testing showed no significant difference between the inlet/outlet water temperature to the PBTC running on continuous power versus battery power. Figures 88 and 89 shows the compressor speed of the PBTC running on continuous and battery power for four runs of the heating mode test. A moving average was taken for the data, averaged at three minute intervals, to improve visibility of the data and remove noise. The compressor speed is controlled by an algorithm optimized to maintain required outlet temperature and maximum battery life (when operating under battery power). The compressor speeds recorded in figures 88 and 89 are consistent with the control algorithms designed by Rocky Research. The higher compressor speed associated with the continuous power run performed (Test 4) can be attributed to an updated version of the software, designed by Rocky Research, being uploaded prior to testing for that day. The results for the experimental runs on that day showed no significant difference between the other empirical data. Figures 90 and 91 shows the flow rate of water flowing through the circulating water blanket and PBTC for experimental runs of the heating mode test. The figures show slightly higher flow rates for the battery power runs, likely due to slightly higher DC voltage.

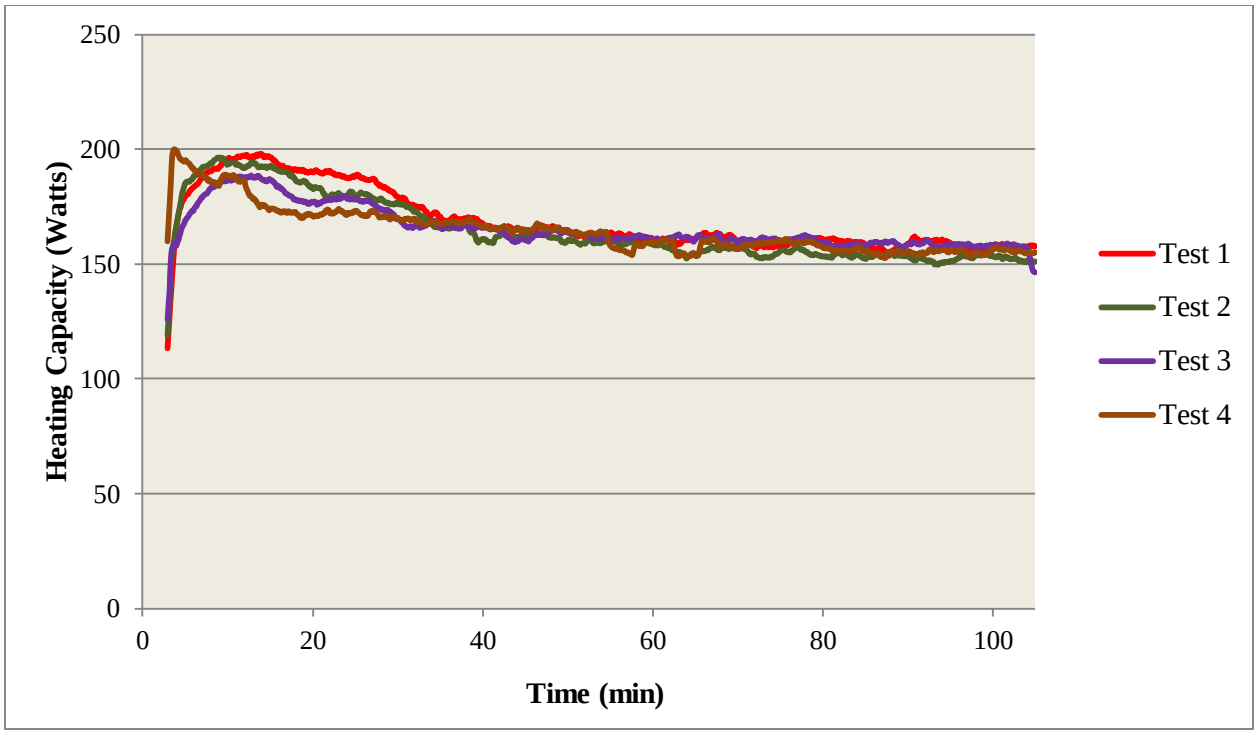

Figure 84. Thermal capacity of the PBTC Running on Continuous Power (Heating Mode). Tests performed with the heat pump cycle only, not the external 240W electric resistance heaters

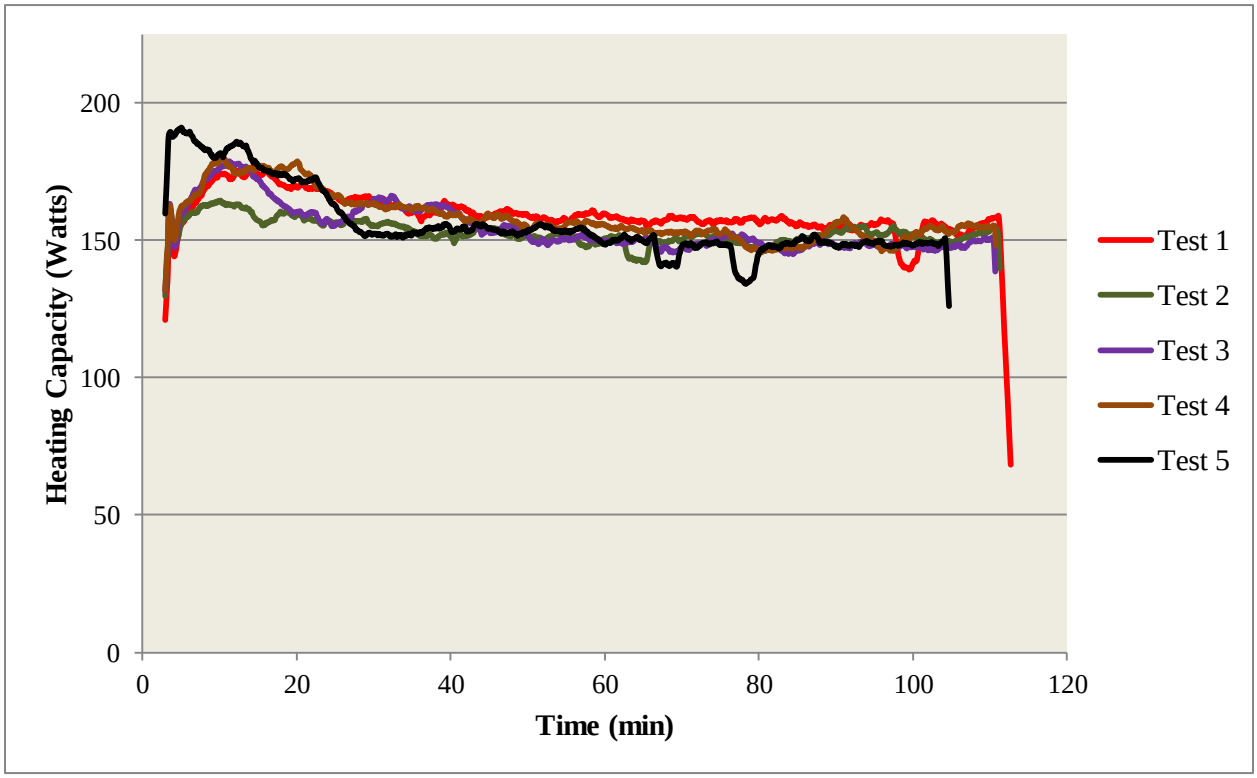

Figure 85. Thermal capacity of the PBTC Running on Battery Power (Heating Mode). Tests performed with the heat pump cycle only, not the external 240W electric resistance heaters

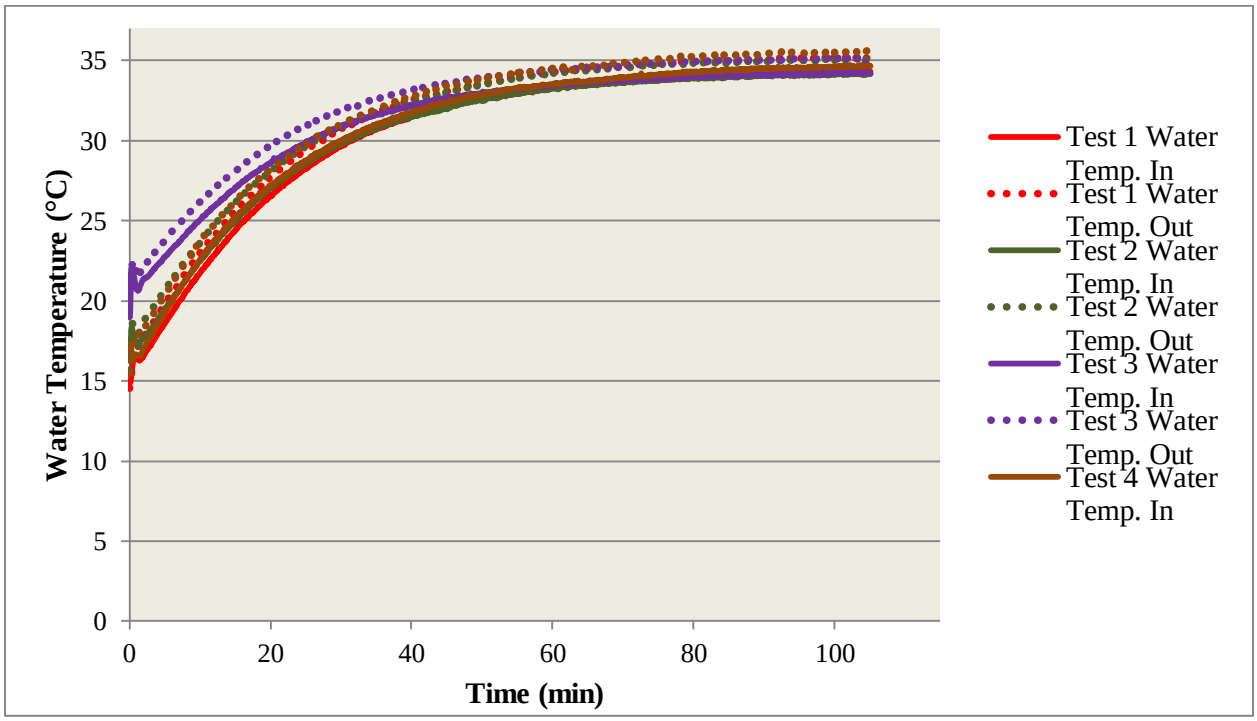

Figure 86. Inlet/Outlet Water Temperature to the PBTC Running on Continuous Power (Heating Mode)

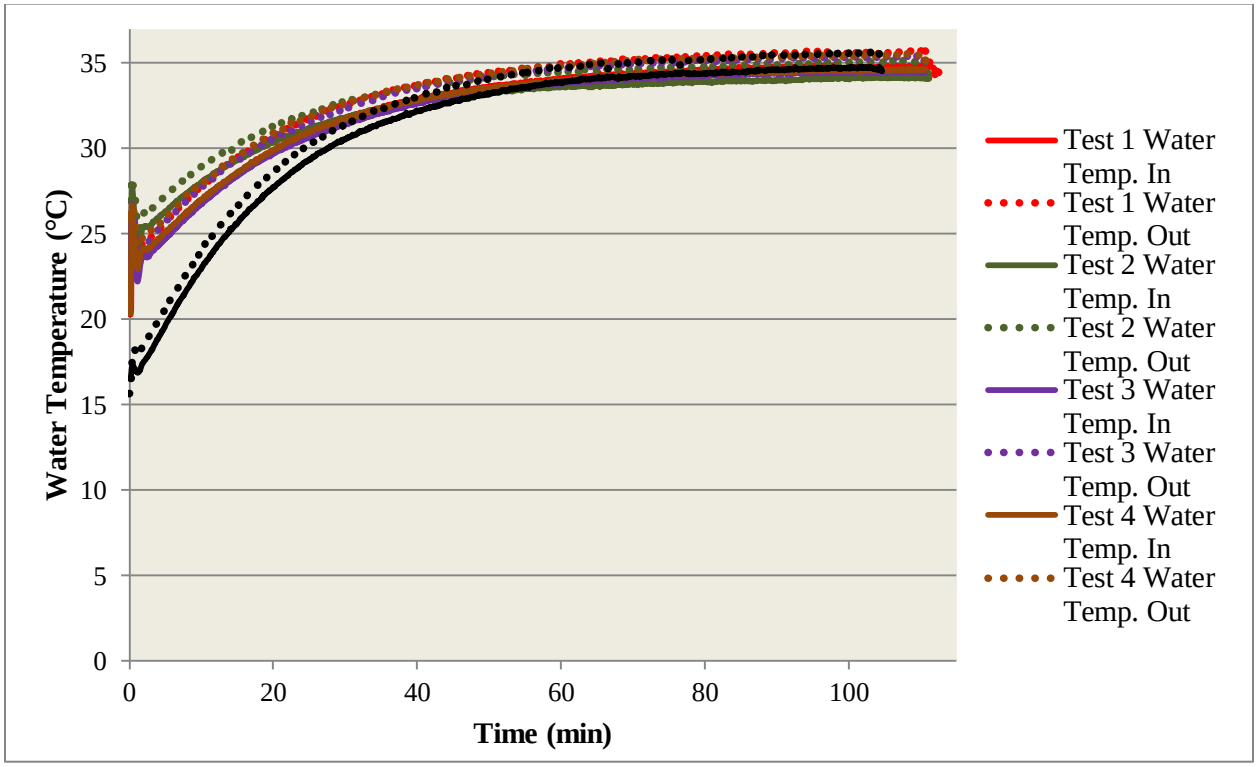

Figure 87. Inlet/Outlet Water Temperature to the PBTC Running on Battery Power (Heating Mode)

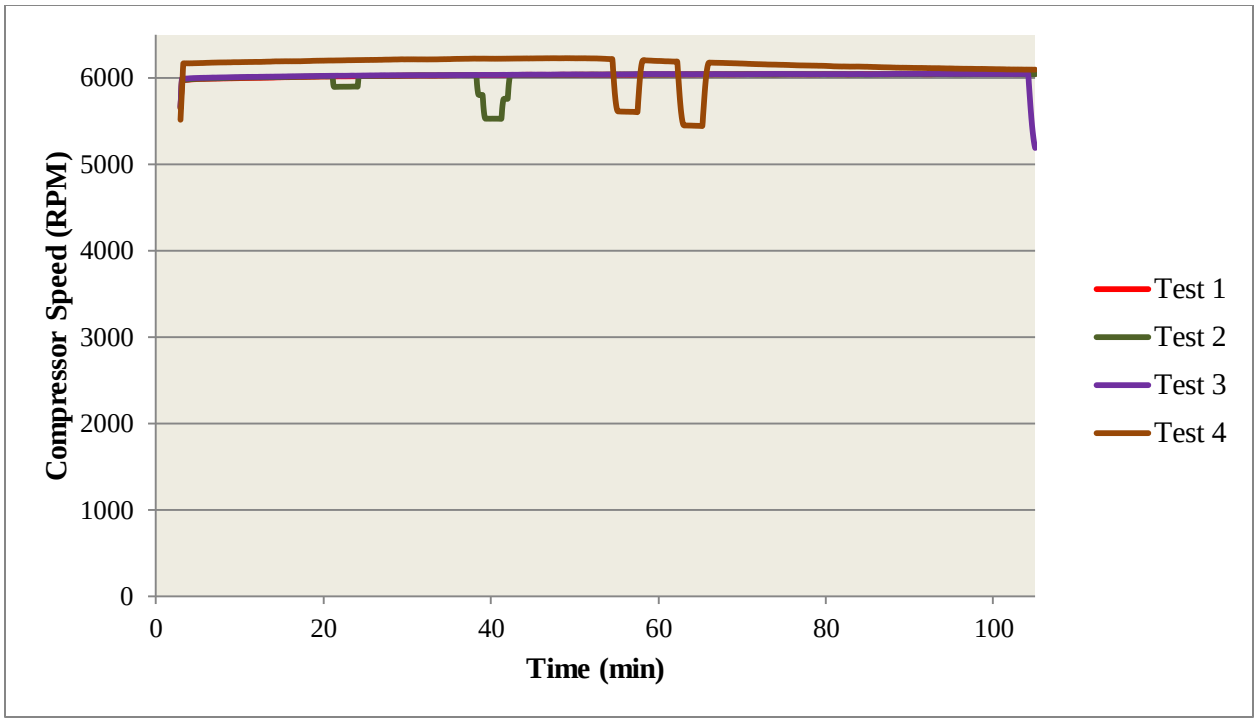

Figure 88. Compressor speed of the PBTC running on continuous power of the heating mode test

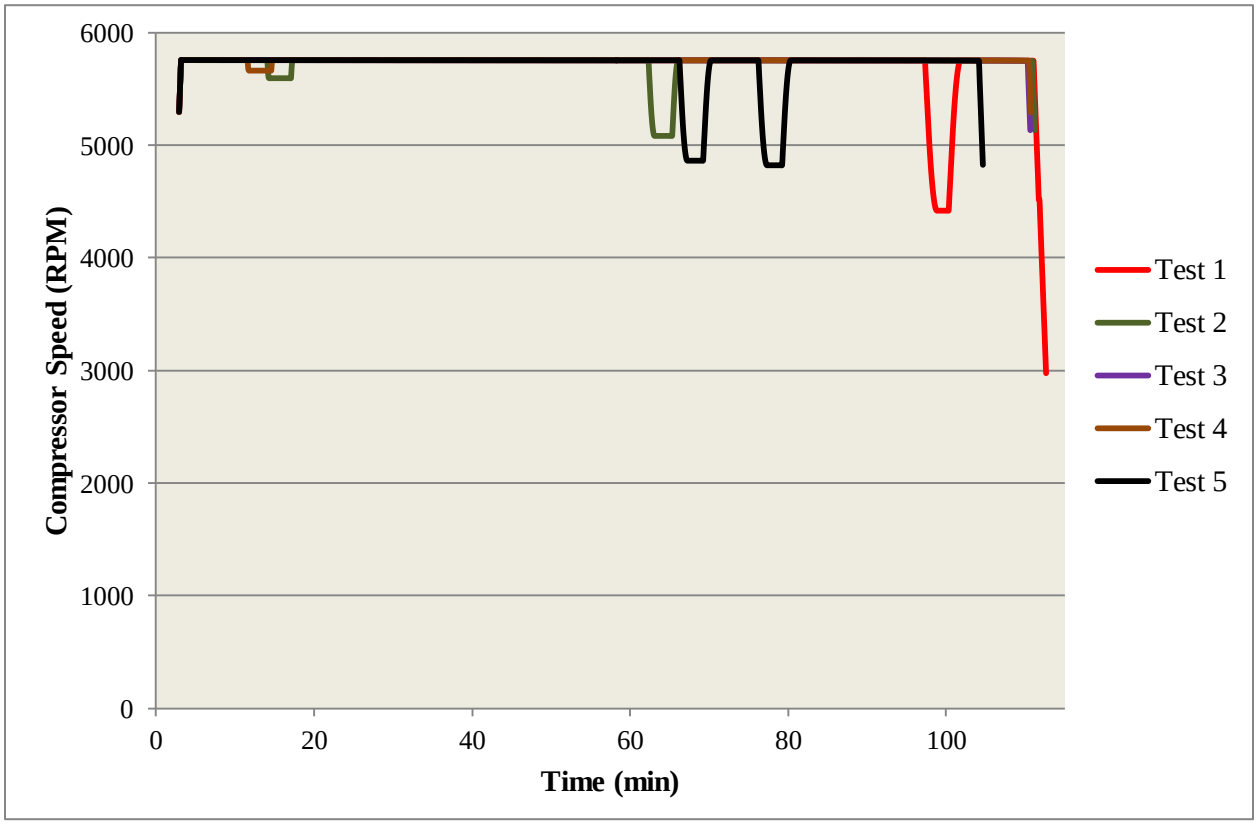

Figure 89. Compressor speed of the PBTC running on battery power of the heating mode test

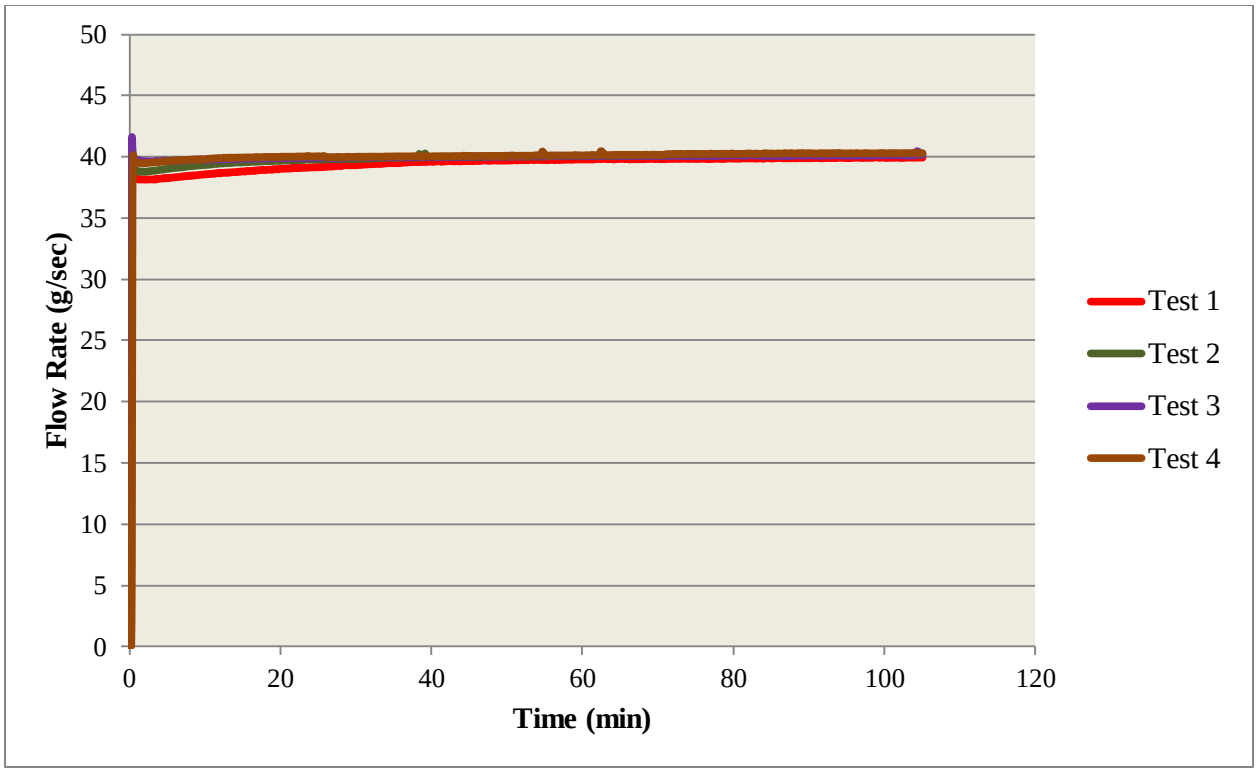

Figure 90. Circulating Water Blanket Flow Rate Running on Continuous Power of the heating mode test

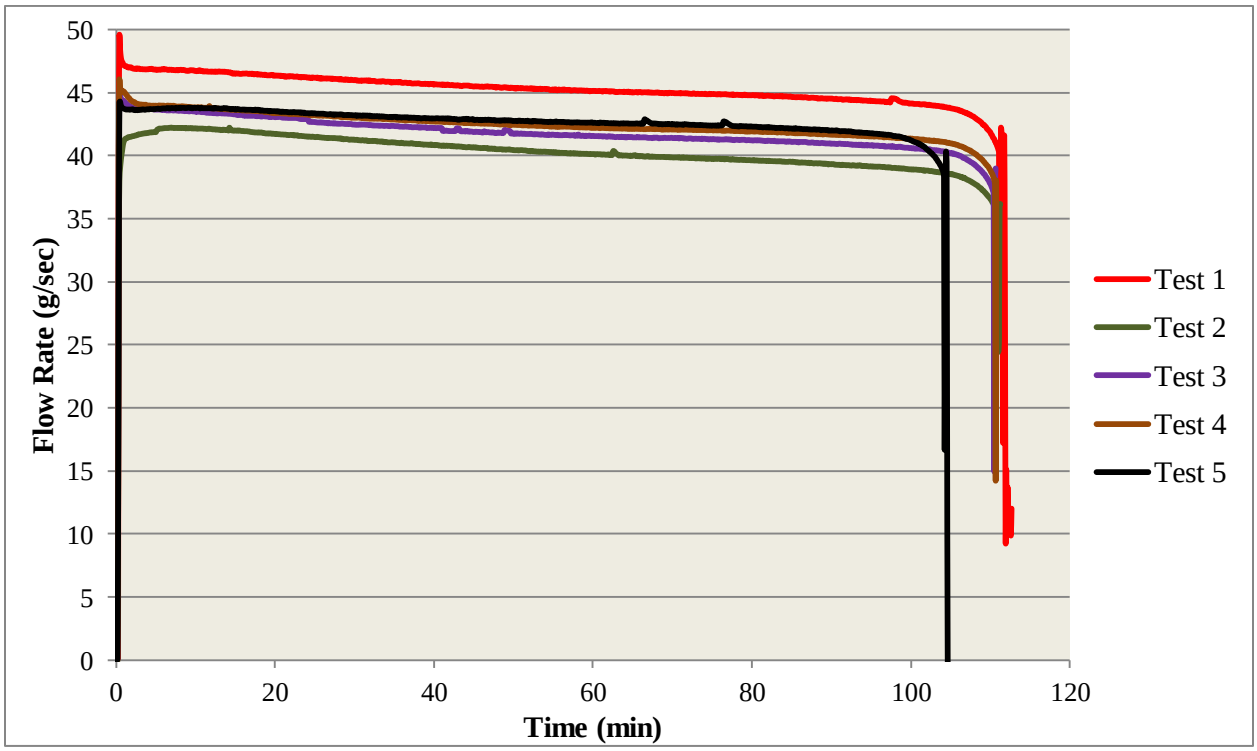

Figure 91. Circulating Water Blanket Flow Rate Running on Battery Power of the heating mode test

The performance of the PBTC for cooling/heating mode tests were calculated from experimental runs (Q_{PBTC}). The calculations also measured the heat transfer from the thermal manikin into the circulating water blanket (cooling fraction) and from the circulating water blanket into the thermal manikin (heating fraction) to determine the cooling fraction. The cooling fraction is calculated according to the following equation:

$$Cooling\ Fraction = \frac{\dot{Q}}{Q_{PBTC}} \qquad (3)$$

Where,

$\dot{Q}$ = Actual Measured Heat Removal

Q_{PBTC} = Heat Removal by the PBTC

The actual heat removal $\dot{Q}$ is calculated by measuring the power consumed by the thermal manikin when the circulating water blanket is running minus the power the manikin is using when the circulating water blanket is not running. This can be done simply by recording the heater power being delivered to each of the 26 manikin zones, for control and continuous/battery power runs, utilizing the ThermDAQ software. This total heat flux generated by the manikin can then be calculated using equation 2, shown above. The heat removal by the Portable Body Temperature Conditioner Q_{PBTC} is calculated using the following equation:

$$Q_{PBTC} = \dot{m} C_p (T_{in} - T_{out}) \qquad (4)$$

Where,

$\dot{m}$ = Mass Flow Rate [Kg/s]

C_p = Specific Heat of Water [4.18 KJ/Kg – ^oC]

T_{in} = Inlet Water Temperature to Blanket [^oC]

T_{out} = Outlet Water Temperature from Blanket [^oC]

The heat removal by the PBTC was calculated using the data recorded from the PBTC LabVIEW software for each day of testing to determine the performance of the PBTC. It was calculated for the steady-state portion of the data only. The maximum value for this portion of data was recorded for each run and used to calculate the cooling fraction for each day of testing respectively. Figure 92 shows the calculated cooling fraction for five experimental runs with the PBTC running on continuous and battery power. The cooling fraction was calculated from the steady-state portion of the recorded data (≈50-60 minutes into testing). For the continuous powered run (Test 5) the PBTC compressor shut off at around minute 57 into testing for about 30 seconds (shown in figure 80). This drop in compressor speed corresponds to the drop in cooling

fraction below that of the battery run for the same day of testing as can be seen in figure 92. Figure 93 shows the average value for each run running on continuous and battery power. Table 10 shows the average values for the cooling fraction for each individual run and the average value for running on continuous and battery power. The data shows slightly higher values for when the PBTC is running on continuous power. A lot of factors contribute to the cooling fraction of the PBTC and without clinically relevant data to compare to the overall performance of the PBTC was evaluated. Figure 37 shows the average cooling capacity of the PBTC from the five runs of continuous and battery powered experimental tests. The average cooling capacity is fairly consistent for the device running on continuous versus battery power. The spike in the capacity for the continuous average is again attributed to the compressor speed dropping for Test 5. The drop in compressor speed impacted the cooling capacity for that particular run. The purpose of running cooling mode tests was to compare the response of the thermal blanket with the PBTC operating under continuous/battery power. Figure 94 shows no significant difference in performance of the PBTC, in regards to cooling capacity, when running on continuous/battery power. Overall the PBTC performed as intended and sufficiently cooled the thermal manikin, as shown in figures 95 and 96, by the increased heat generation on the front side of the manikin. The areas in direct contact with the circulating water blanket are generating more heat to maintain the surface skin temperature of the manikin indicating that the PBTC is functioning as designed[3-6,11,15,16].

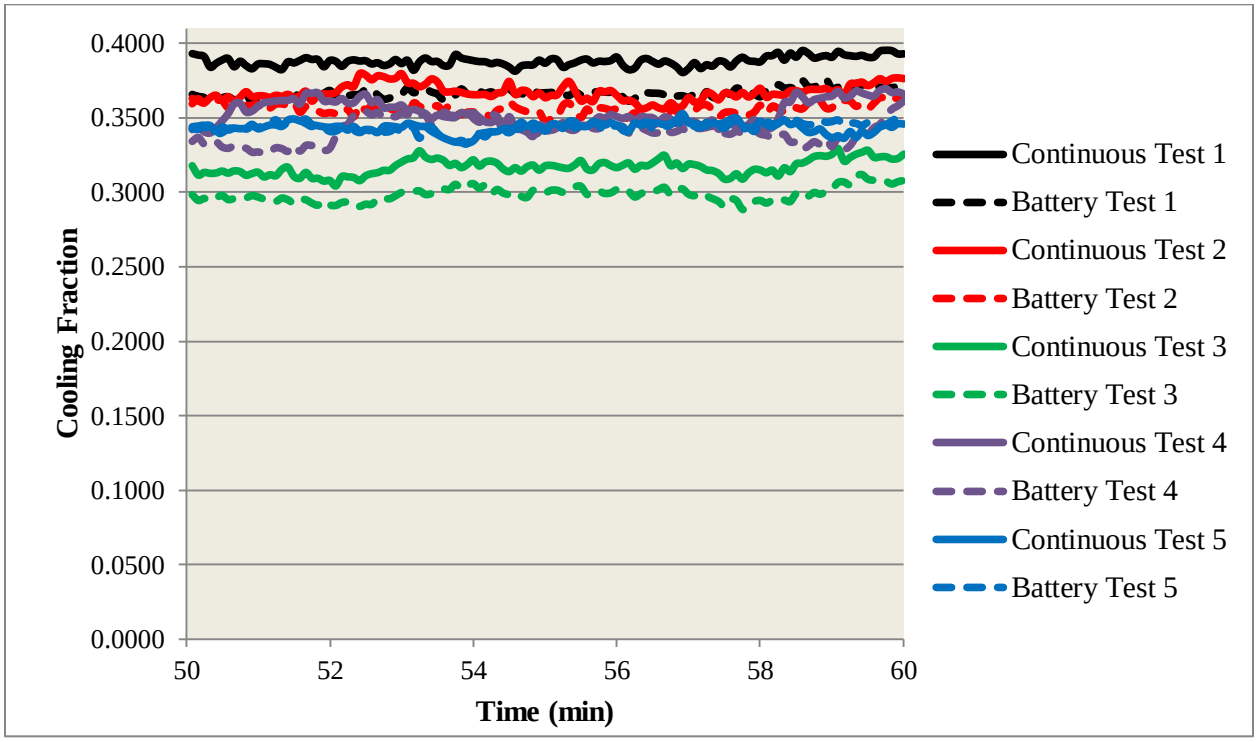

Figure 92. Cooling Fraction of the thermal blanket with the PBTC running on continuous and battery power (30°C Ambient, 15°C Water Temp.)

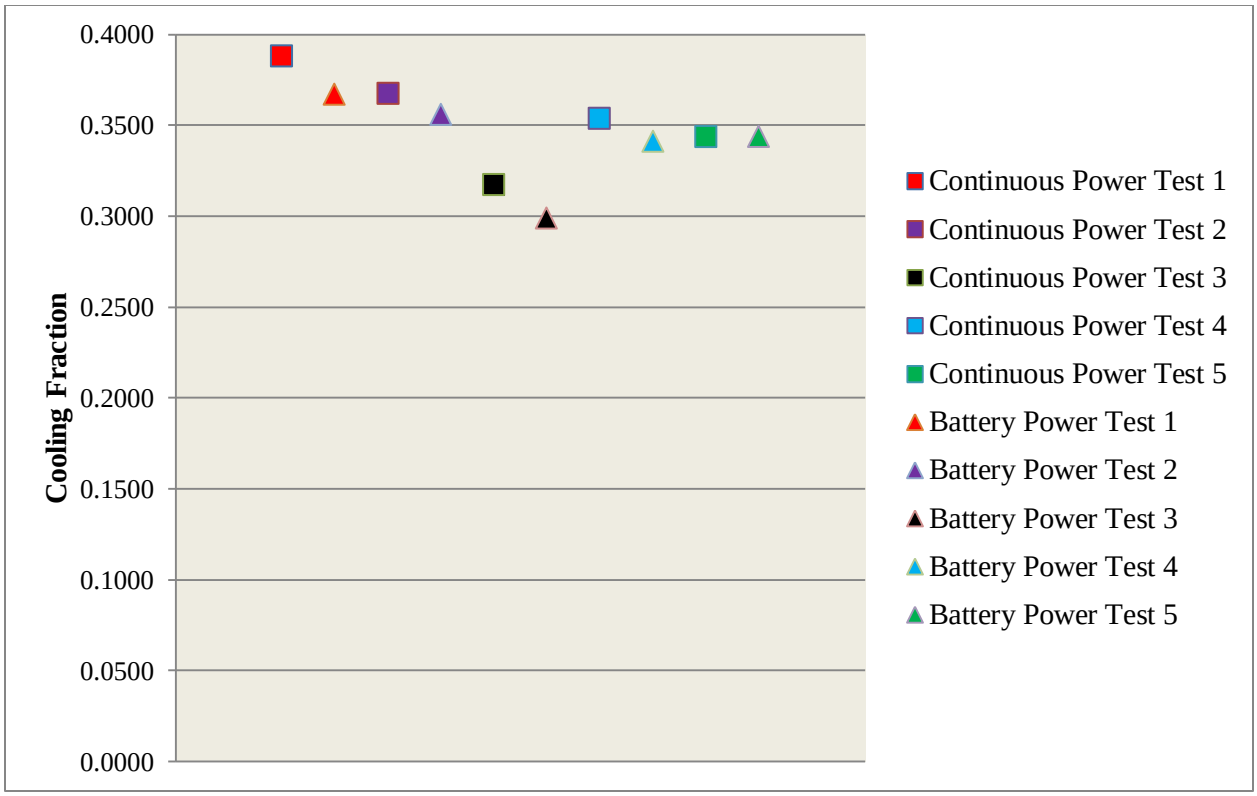

Figure 93. Average cooling Fraction of the thermal blanket with the PBTC running on continuous and battery power

Table 10. Average cooling fraction of the thermal blanket with the PBTC for each experimental run and overall average for continuous/battery powered runs

Continuous Test 1	Continuous Test 2	Continuous Test 3	Continuous Test 4	Continuous Test 5
0.39	0.37	0.32	0.35	0.34
Average: 0.35				
Battery Test 1	**Battery Test 2**	**Battery Test 3**	**Battery Test 4**	**Battery Test 5**
0.37	0.36	0.30	0.34	0.34
Average: 0.34				

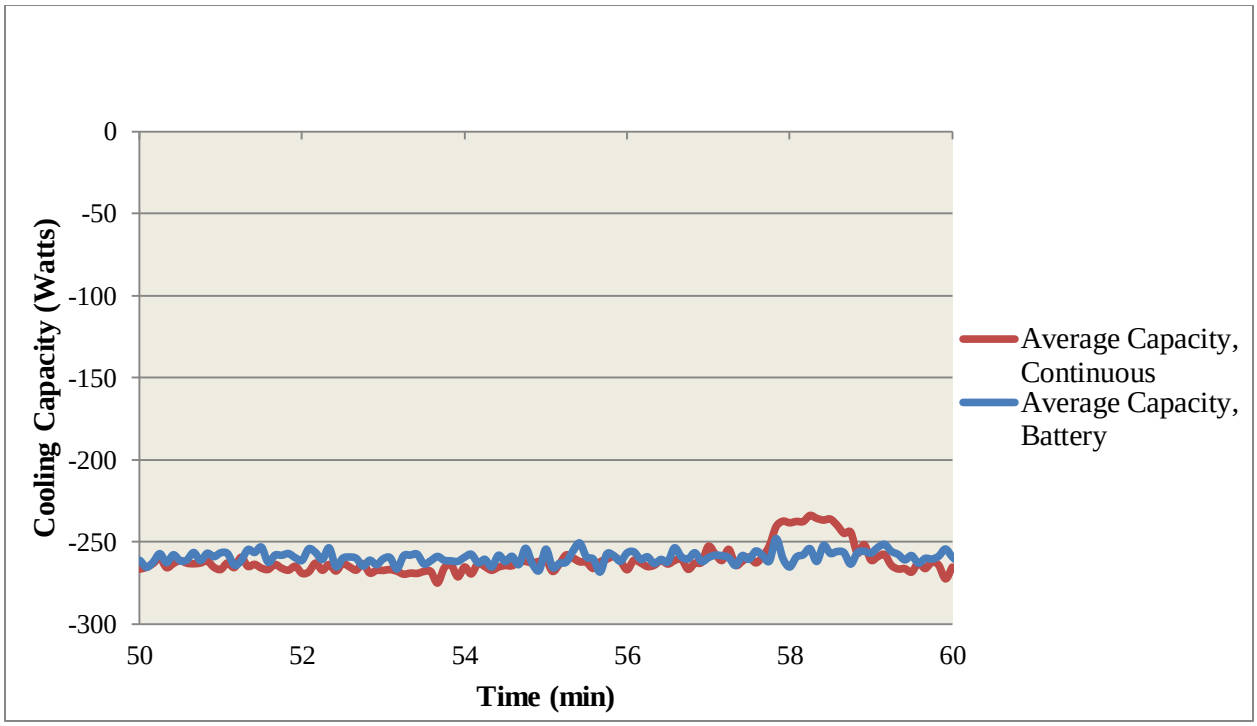

Figure 94. Average cooling capacity of the PBTC running on continuous and battery power for five experimental runs (Cooling)

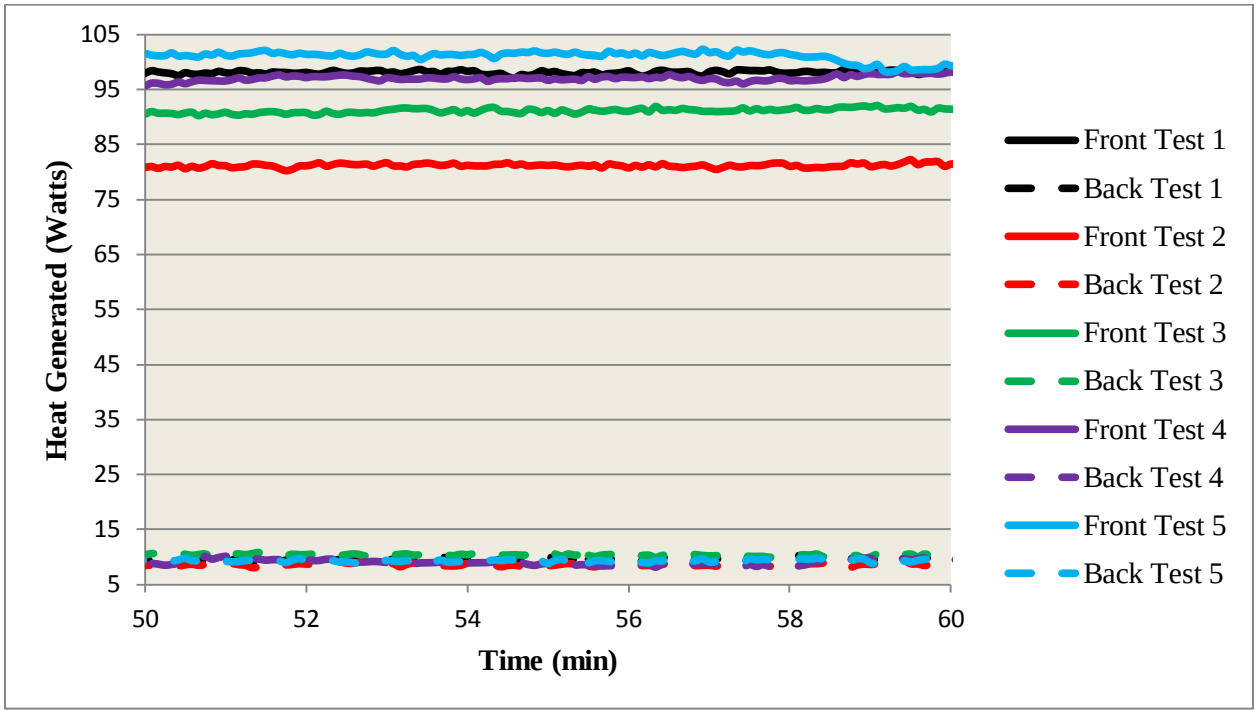

Figure 95. Total heat generated by the front and backside of the thermal manikin running on continuous power (cooling)

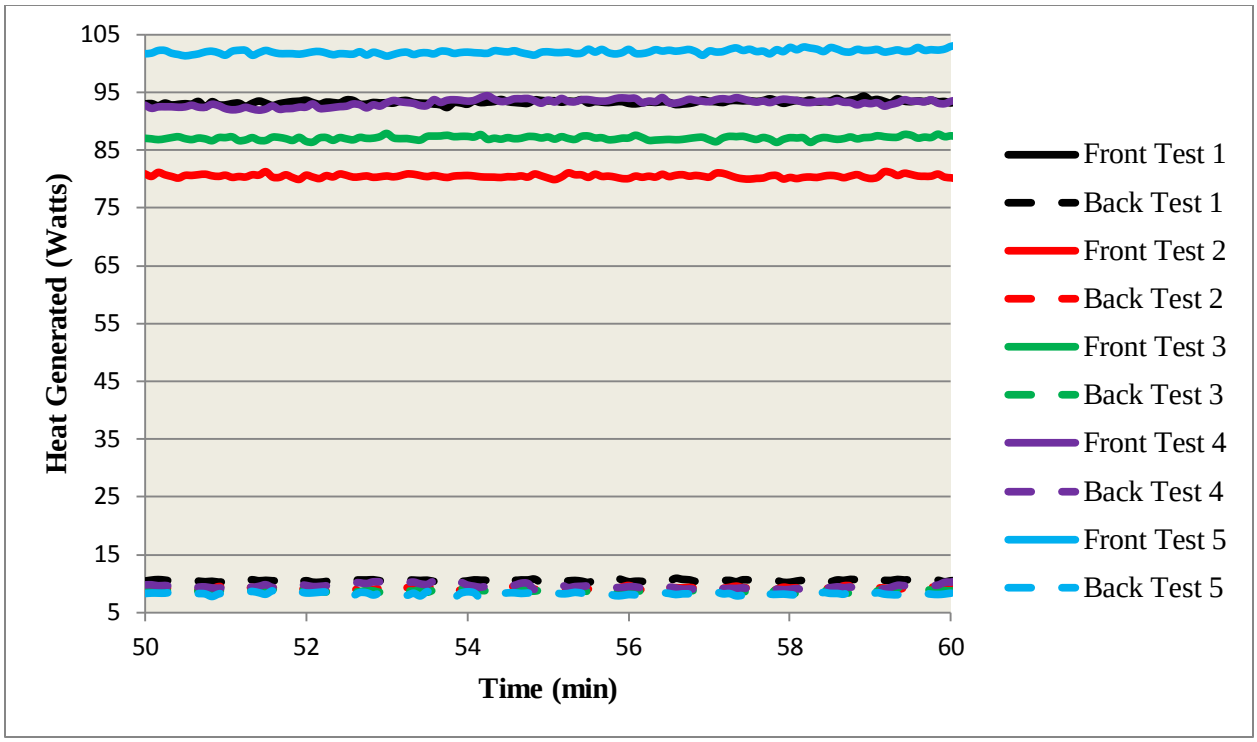

Figure 96. Total heat generated by the front and backside of the thermal manikin running on battery power (cooling)

The heating fraction for the thermal blanket is calculated according to the following equation:

$$Heating\ Fraction = \frac{\dot{Q}}{Q_{PBTC}} \qquad (5)$$

Where,

$\dot{Q}$ = Actual Measured Heat Input

Q_{PBTC} = Heat Supplied by the PBTC

The actual heat supplied $\dot{Q}$ is calculated by measuring the power consumed by the thermal manikin when the circulating water blanket is not running minus the power the manikin is using when the circulating water blanket is running. This can be done simply by recording the heater power being delivered to each of the 26 manikin zones, for control and continuous/battery power runs, utilizing the ThermDAQ software. This total heat flux generated by the manikin can then be calculated using equation 2, shown above. For the heating fraction testing, as discussed early, additional continuous powered runs were performed at a later date than the control and battery powered runs. For this reason an average value for the actual measured heat gained was taken for the control runs and used to calculate the actual measurements for the continuous and battery powered runs. For the cooling fraction runs the control data for each day of testing was used and

not an average. The heat output by the Portable Body Temperature Conditioner Q_{PBTC} is calculated using the following equation:

$$Q_{PBTC} = \dot{m} C_p (T_{out} - T_{in}) \qquad (6)$$

Where,

$\dot{m}$ = Mass Flow Rate [Kg/s]

C_p = Specific Heat of Water [4.18 KJ/Kg – ^oC]

T_{in} = Inlet Water Temperature to Blanket [^oC]

T_{out} = Outlet Water Temperature from Blanket [^oC]

The heat output of the PBTC was calculated using the data recorded from the PBTC LabVIEW software for each day of testing. It was calculated for the steady-state portion of the data only. The largest value for this portion of data was recorded for each run and an average was taken for all runs. The average value was then used to calculate the heating fraction. Figure 97 shows the calculated heating fraction for four experimental runs with the PBTC running on continuous and battery power. The heating fraction was calculated from the steady-state portion of the recorded data (≈95-105 minutes into testing). Figure 98 shows the average value for each run of both continuous/battery power. Table 11 shows the average values for heating fraction for each individual run and the average value for running on continuous and battery power. The data shows higher values for when the PBTC is running on battery power than on continuous power. This can be attributed to slightly higher flow rates obtained when the PBTC was running on battery power (figures 90 and 91). The slightly different water flow rates, with negligible impact on capacity, is attributed to small discrepancies in signal voltage provided to the pump when operating on external vs. battery power. As discussed early, the higher starting water temperature for the battery runs was ruled out as a possibility for the higher flow rates. Figure 99 shows the average heating capacity of the PBTC from the four runs of continuous and battery powered experimental tests. The average heating capacity is fairly consistent for the device running on continuous versus battery power. The dip in capacity for the battery run at around 97 minutes is associated with the drop in compressor speed similar to the event for the cooling fraction runs explained above. Overall the PBTC performed as intended and sufficiently warmed the thermal manikin, as shown in figures 100 and 101, by the minimal heat generation on the front side of the manikin. The areas in direct contact with the circulating water blanket are generating little to no heat because the blanket is transferring enough heat to maintain the set skin surface temperature. The heating fraction runs were performed to compare the performance of the PBTC while operating under continuous/battery power. Figure 98 shows consistent performance of the PBTC over four experimental runs and the standard deviation error bars show very little variation throughout the steady-state portion of the data. Overall the PBTC maintained a constant heating

capacity and sufficiently heated the thermal manikin to help maintain the skin surface temperature in the cold ambient conditions[3-6,11,15,16].

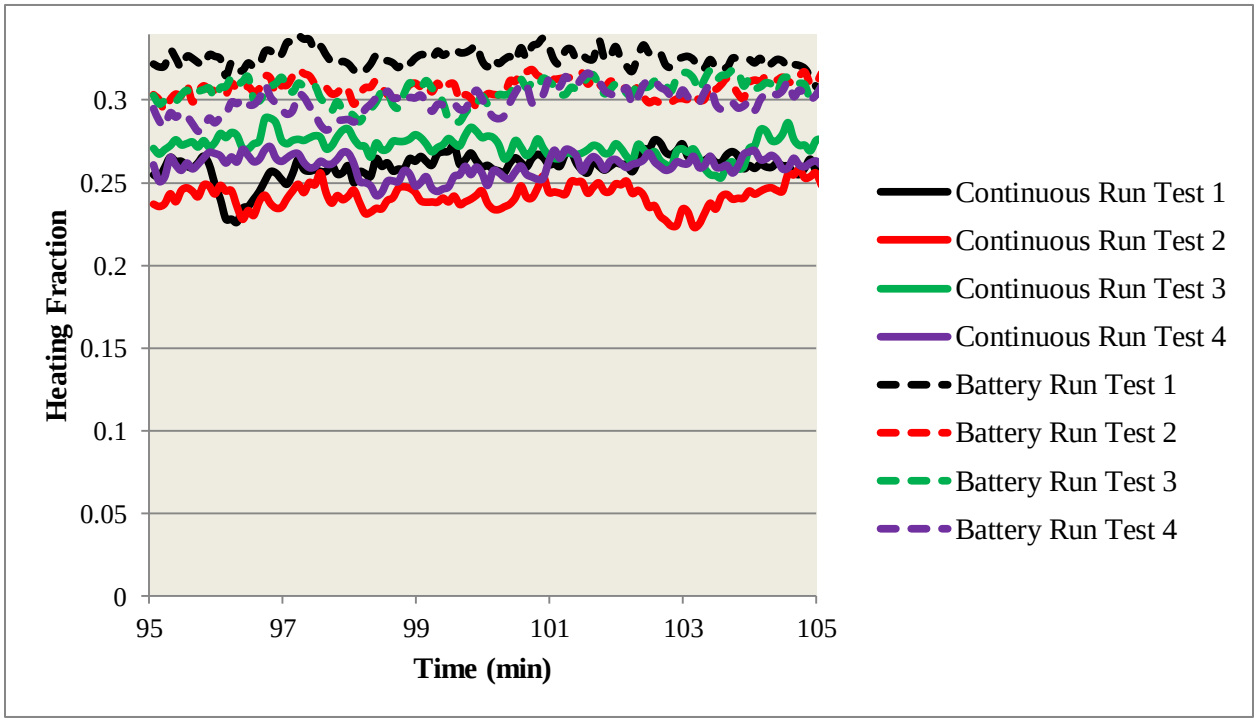

Figure 97. Heating fraction of the thermal blanket with the PBTC running on continuous and battery power for four experimental runs (15°C Ambient, 37°C Water Temp.)

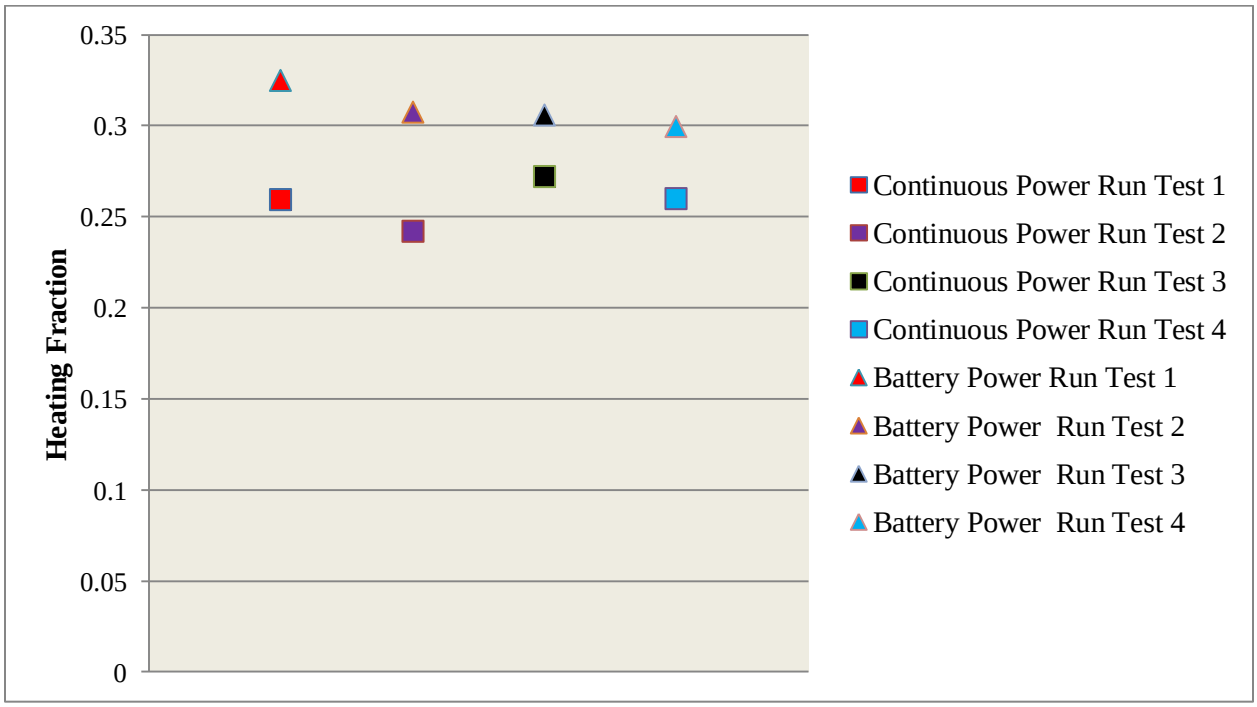

Figure 98. Average heating fraction of the thermal blanket with the PBTC running on continuous and battery power for five experimental runs

Table 11. Average heating fraction of the thermal blanket with the PBTC for each experimental run and overall average for continuous/battery powered runs

Continuous Test 1	Continuous Test 2	Continuous Test 3	Continuous Test 4
0.26	0.24	0.27	0.26
Average: 0.26			
Battery Test 1	**Battery Test 2**	**Battery Test 3**	**Battery Test 4**
0.32	0.31	0.31	0.30
Average: 0.31			

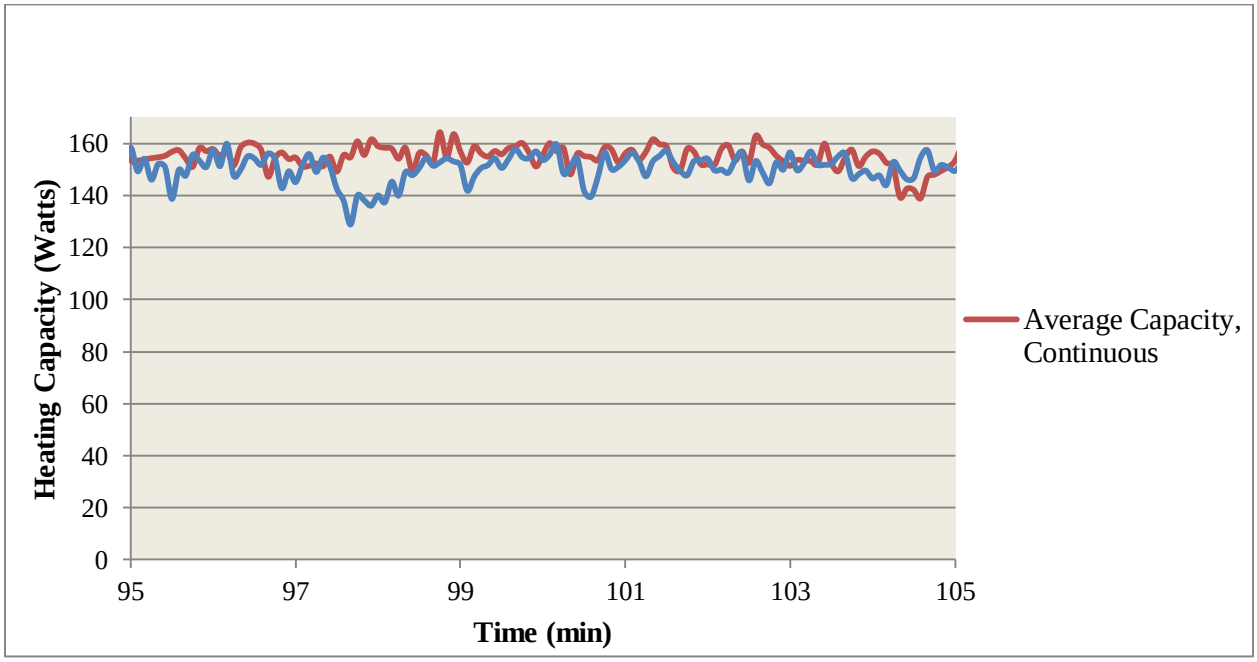

Figure 99. Average heating capacity of the PBTC running on continuous and battery power for four experimental runs. (heating)

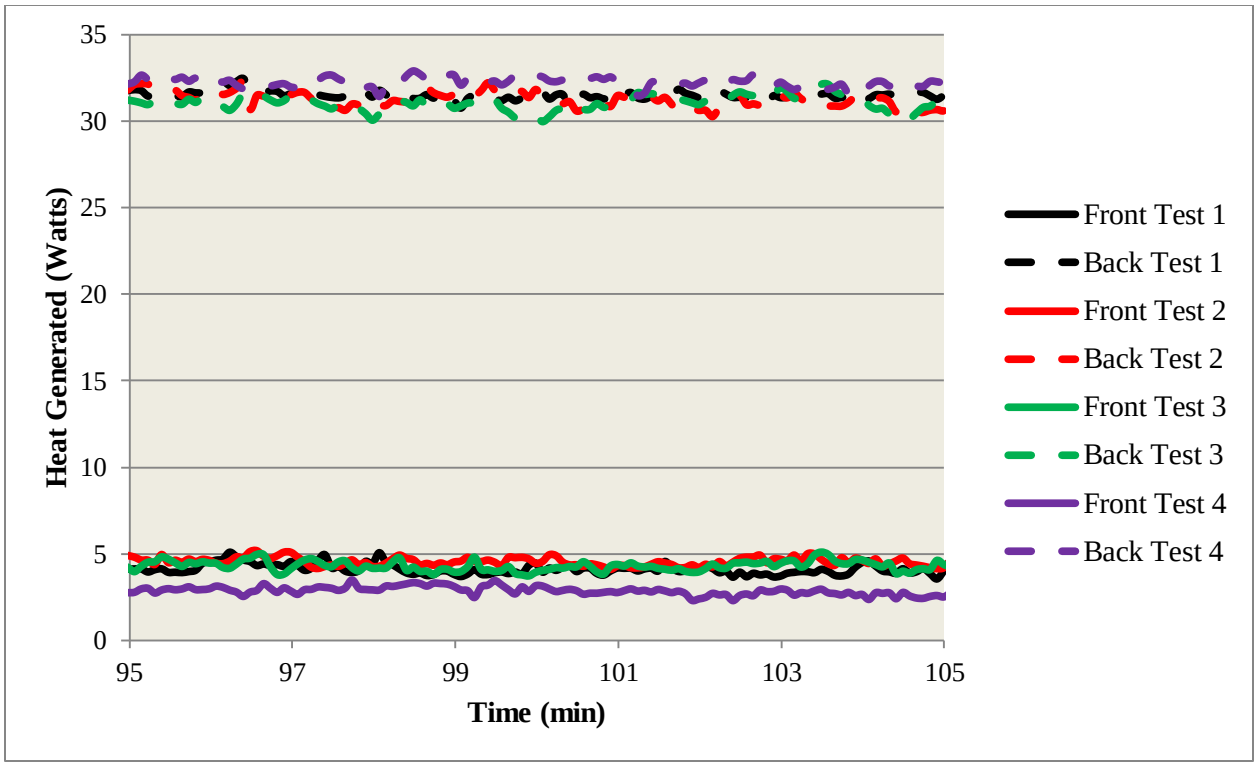

Figure 100. Total heat generated by the front and backside of the Thermal manikin running on continuous power (heating)

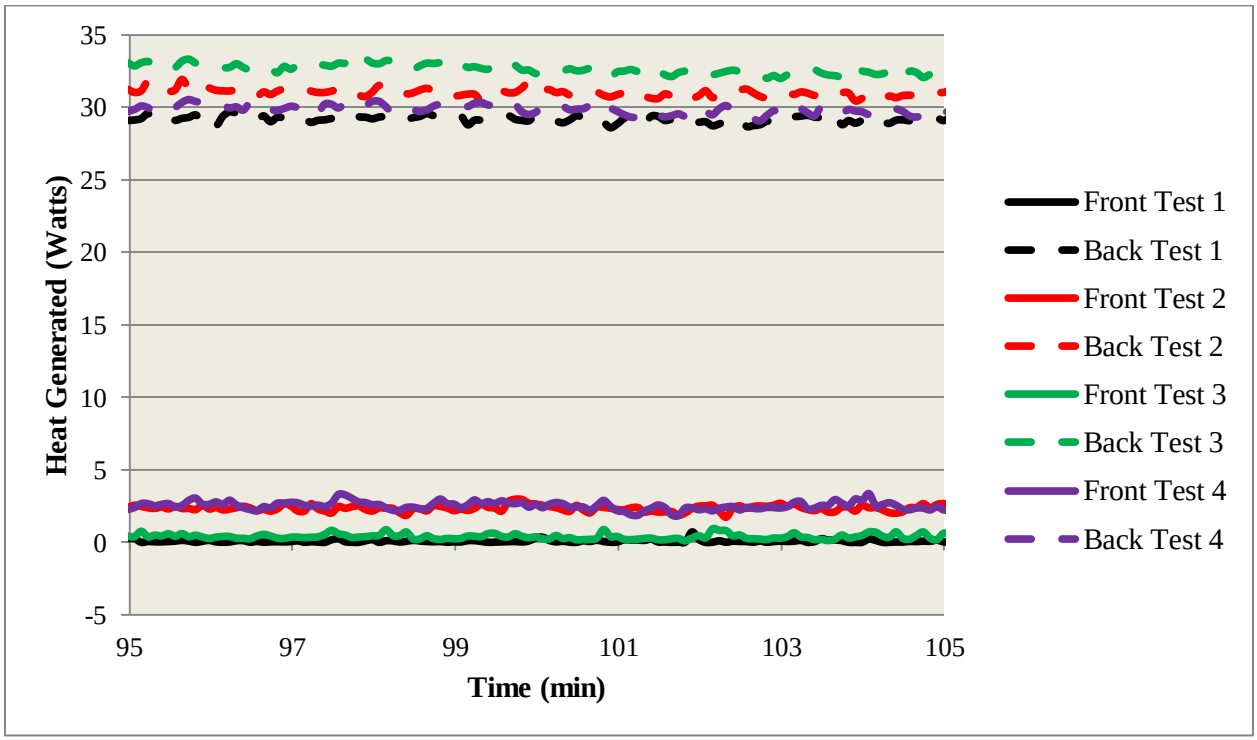

Figure 101. Total heat generated by the front and backside of the Thermal manikin running on battery power (heating)

The calculations for the cooling/heating fraction were found assuming negligible heat loss through the table on which the thermal manikin was placed. To account for this assumption, heat flux sensors were placed on the front and back of the thermal manikin and the heat flux measurements were compared. For comparison three heat flux sensors recorded the heat transfer through the front of the thermal manikin and four sensors recorded the heat transfer through the back of the manikin. The heat flux sensors placed on the chest and right thigh (shown in figure 62) recorded the heat flow into/out of the circulating water blanket. Two sensors were placed on the shoulders and two were placed on the backside of the hip. These four locations were chosen because the manikin is in direct contact with the table at these locations. Figures 102-111 shows the measurements recorded from the heat flux sensors placed on the front and back of the thermal manikin. A moving average was taken for the control data and all heating fraction data, averaged at three minute intervals, recorded by the heat flux sensors to reduce the fluctuations resulting from imperfect thermal contact between the blanket and manikin. A control run and two runs of both continuous and battery power was performed to ensure that the assumption of negligible heat loss through the table was valid for all experimental data. The figures show a notable difference between the heat flux measurements recorded from the front and back of the thermal manikin. During the transient portion of the graph, the heat flux through the back side of the manikin either shows no response to the circulating water blanket or shows a significantly smaller response than that of the sensors placed on the front of the manikin for all experimental runs. During the steady-state portion of the graph, for the cooling mode runs (figures 102-106), the heat flux through the backside is much lower than the heat flux recorded from the sensors placed on the front. For theses runs the manikin is programmed to maintain a set skin surface temperature. The circulating water blanket is set to cool the thermal manikin and as a result the manikin is generating more heat to maintain the set skin surface temperature, shown by the large heat flux values recorded by the sensors on the front of the manikin. The small values recorded by the sensors placed on the backside indicate that a majority of the heat generated on the backside is being directed toward the blanket and any heat loss through the backside is negligible compared to the front side. The large spike in heat flux measurement for the cooling mode battery run performed on 11/5/14, shown in figure 106, is attributed to readjustment of the circulating water blanket during the transient portion to ensure proper thermal contact. Only the steady-state portion of the data was analyzed, so the spike did not affect the calculations for heat loss. During the steady-state portion of the graph, for the heating mode runs (figures 107-111), the heat flux recorded from the sensors placed on the front side drops below zero indicating that heat is flowing into the thermal manikin. For these runs the circulating water blanket is transferring heat into the manikin, as expected. The values recorded by the sensors placed on the backside were small, but larger than zero, so the actual heat lost through the table was calculated for both the heating and cooling mode runs. Figures 112 and 113 show the average heat flux measured by the four sensors located on the back of the thermal manikin. A moving average was taken for the data, averaged at three minute intervals, recorded by the heat flux sensors to reduce the fluctuations resulting from imperfect thermal contact between the blanket and manikin. Table

12 shows the average heat flux for each of the experimental runs performed to determine the heat loss through the table. The values for the steady-state portion of the data are close to zero indicating little heat loss through the table. The data shows higher values for the heating mode tests. This makes sense because the circulating water blanket is transferring heat into the manikin for these runs; as a result the heat flow is toward the table. For the cooling mode runs the heat transfer is flowing toward the blanket[4-5,15].

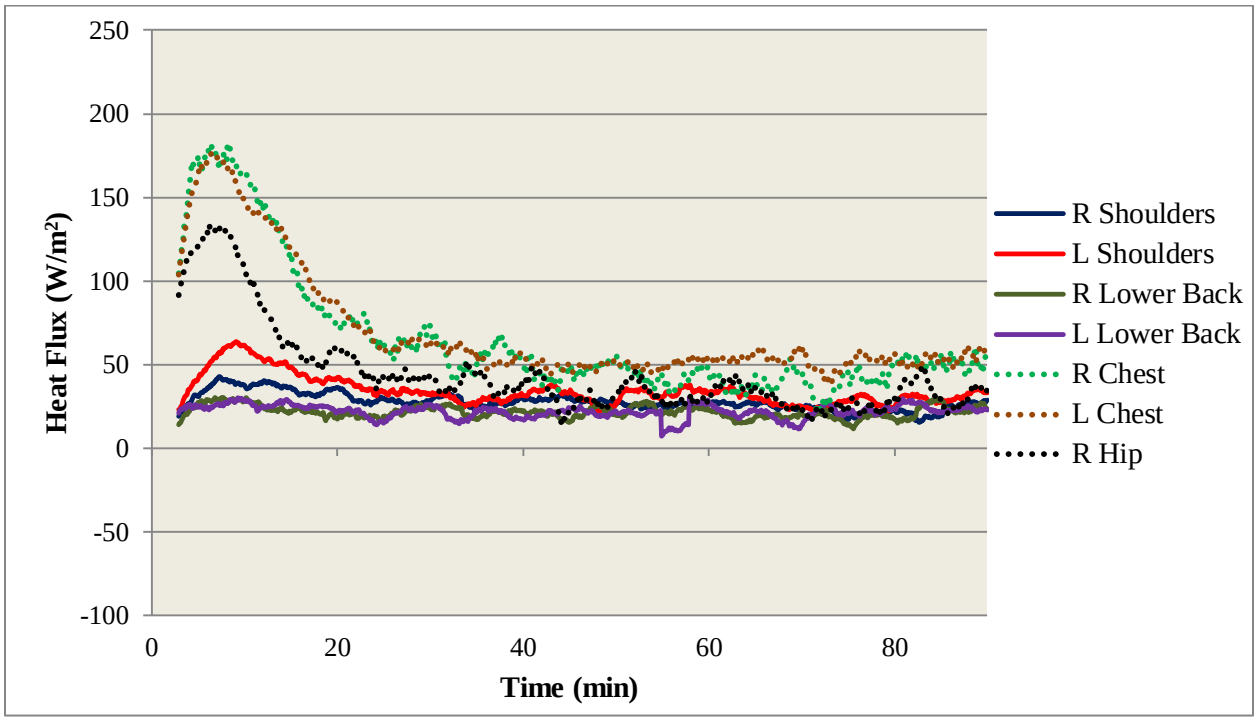

Figure 102. Heat flux measurements recorded form heat flux sensors placed on the front and back of the thermal manikin for a control test (cooling fraction, control test)

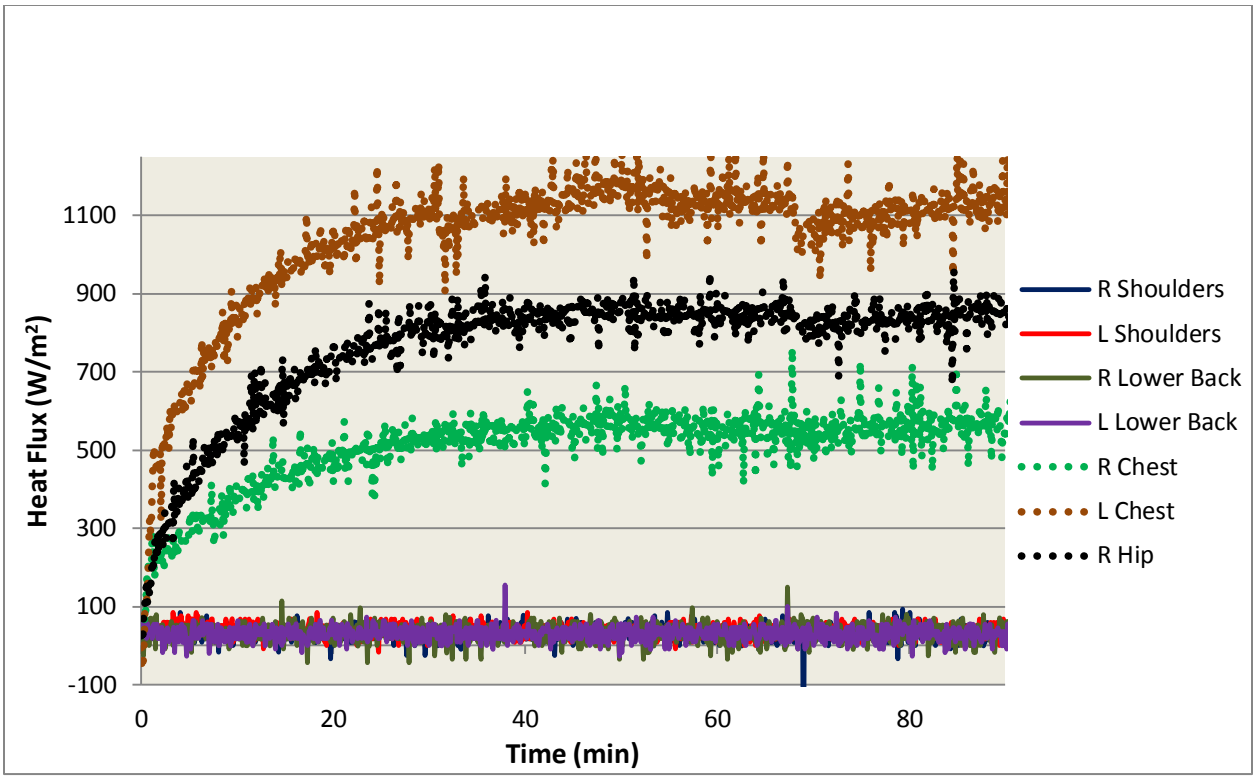

Figure 103. Heat flux measurements recorded form heat flux sensors placed on the front and back of the thermal manikin for a continuous power test (cooling fraction, Continuous Power Test 1)

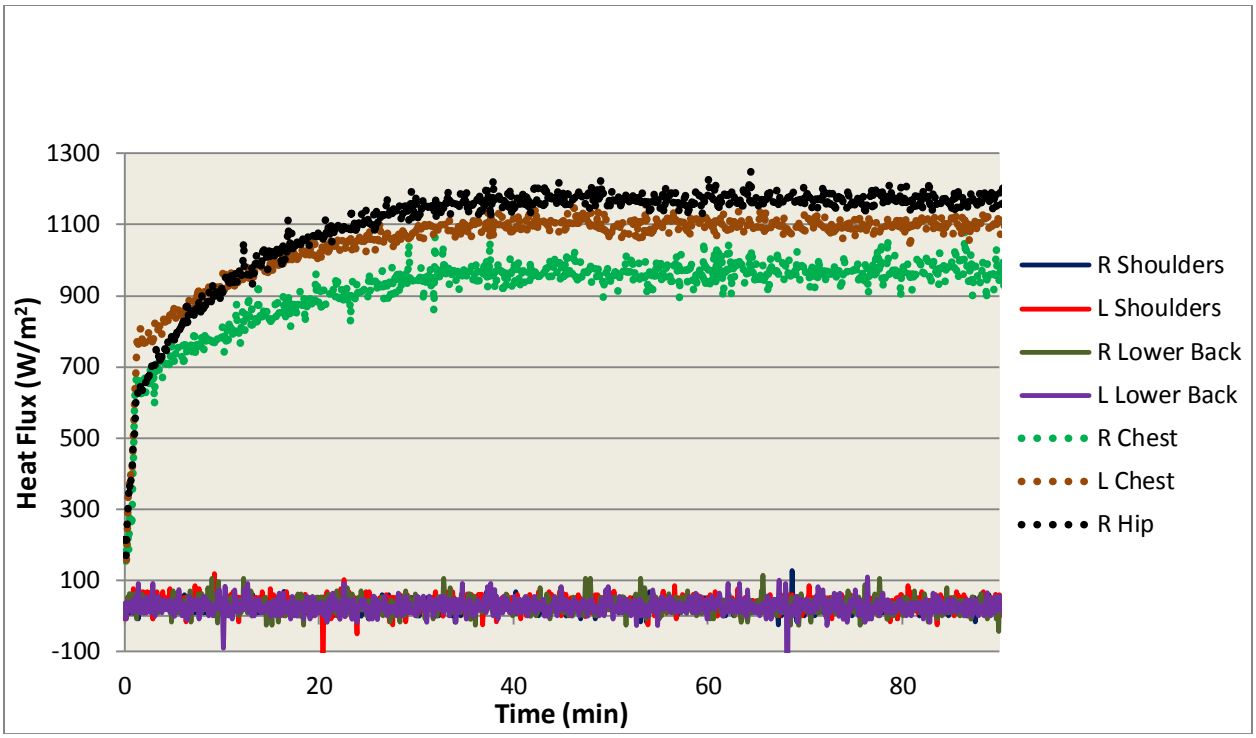

Figure 104. Heat flux measurements recorded from heat flux sensors placed on the front and back of the thermal manikin for a continuous power test (cooling fraction, Continuous Power Test 2)

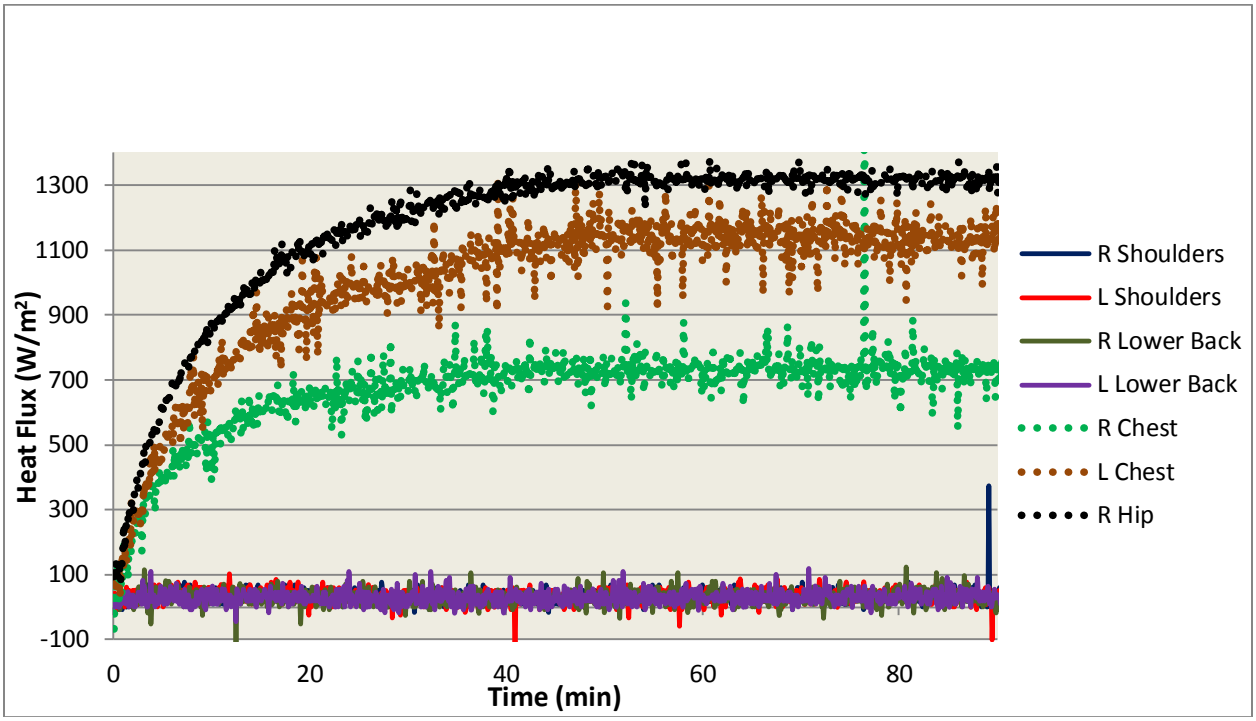

Figure 105. Heat flux measurements recorded form heat flux sensors placed on the front and back of the thermal manikin for a battery power test (cooling fraction, Battery Power Test 1)

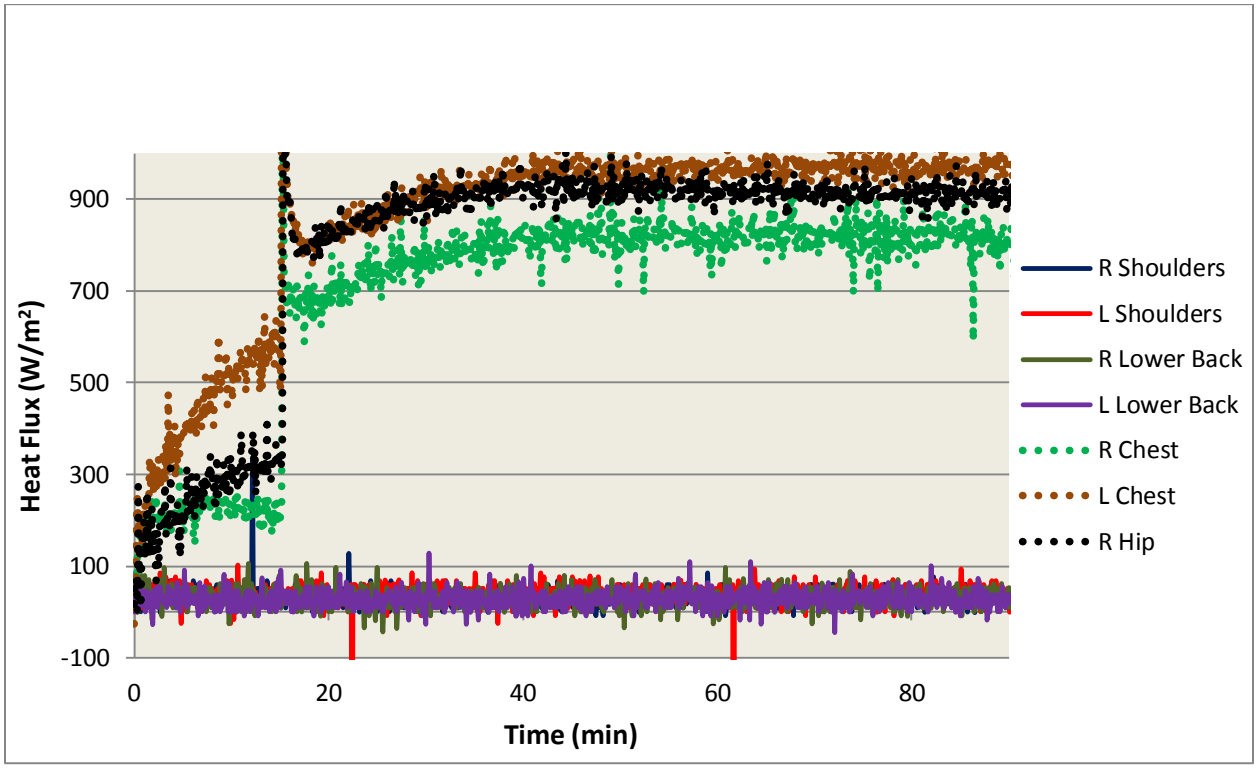

Figure 106. Heat flux measurements recorded from heat flux sensors placed on the front and back of the thermal manikin for a battery power test (cooling fraction, Battery Power Test 2)

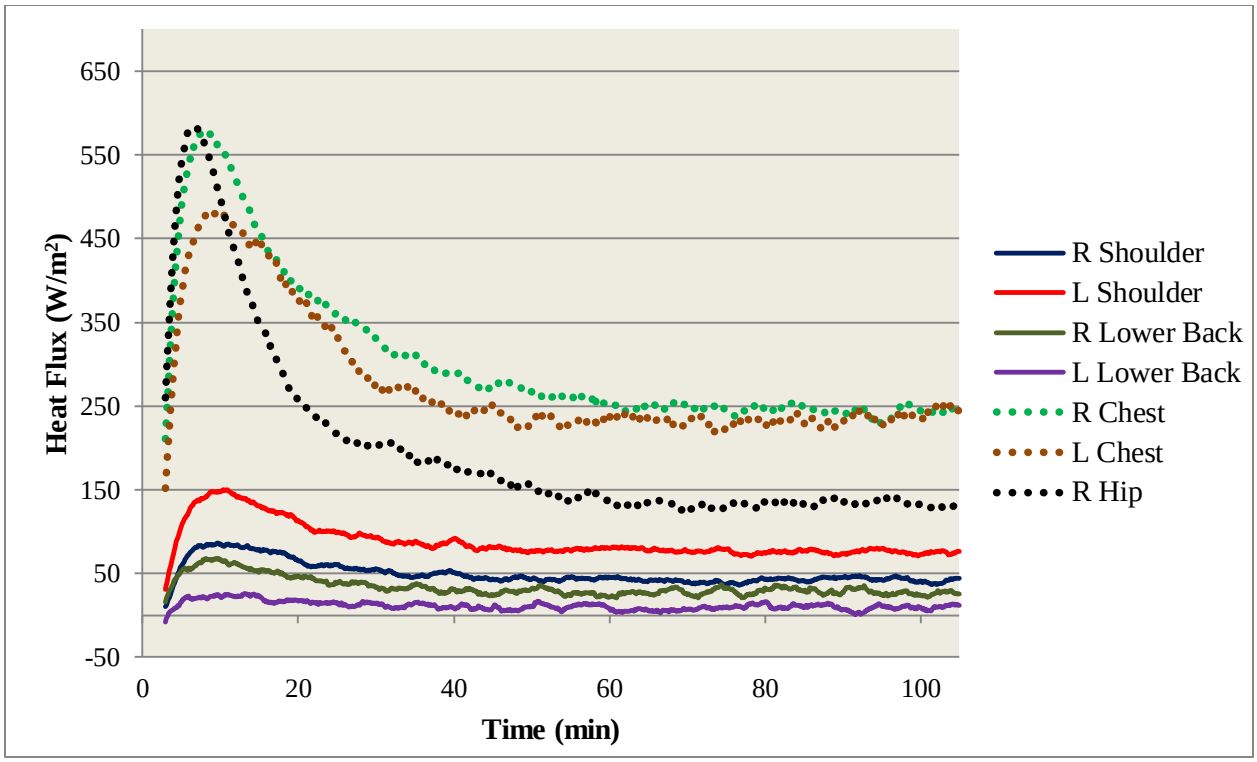

Figure 107. Heat flux measurements recorded from heat flux sensors placed on the front and back of the thermal manikin for a control test (heating fraction, Control Test)

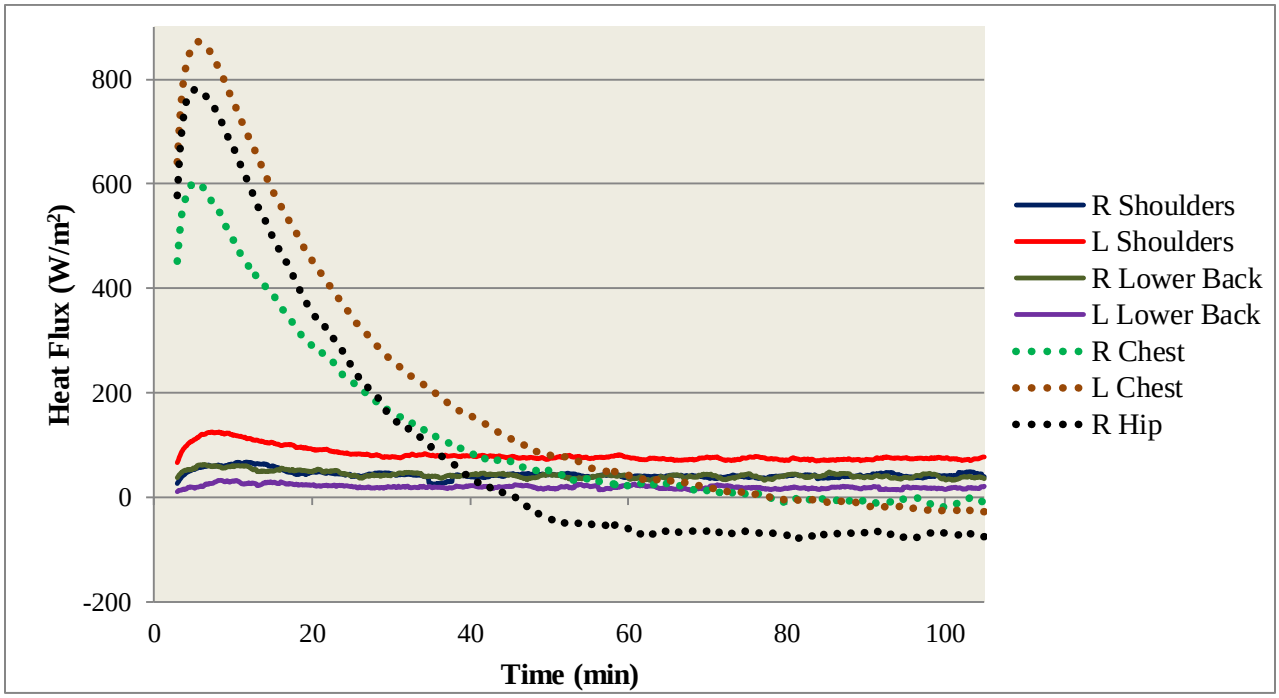

Figure 108. Heat flux measurements recorded from heat flux sensors placed on the front and back of the thermal manikin for a continuous power test (heating fraction, Continuous Power Test 1)

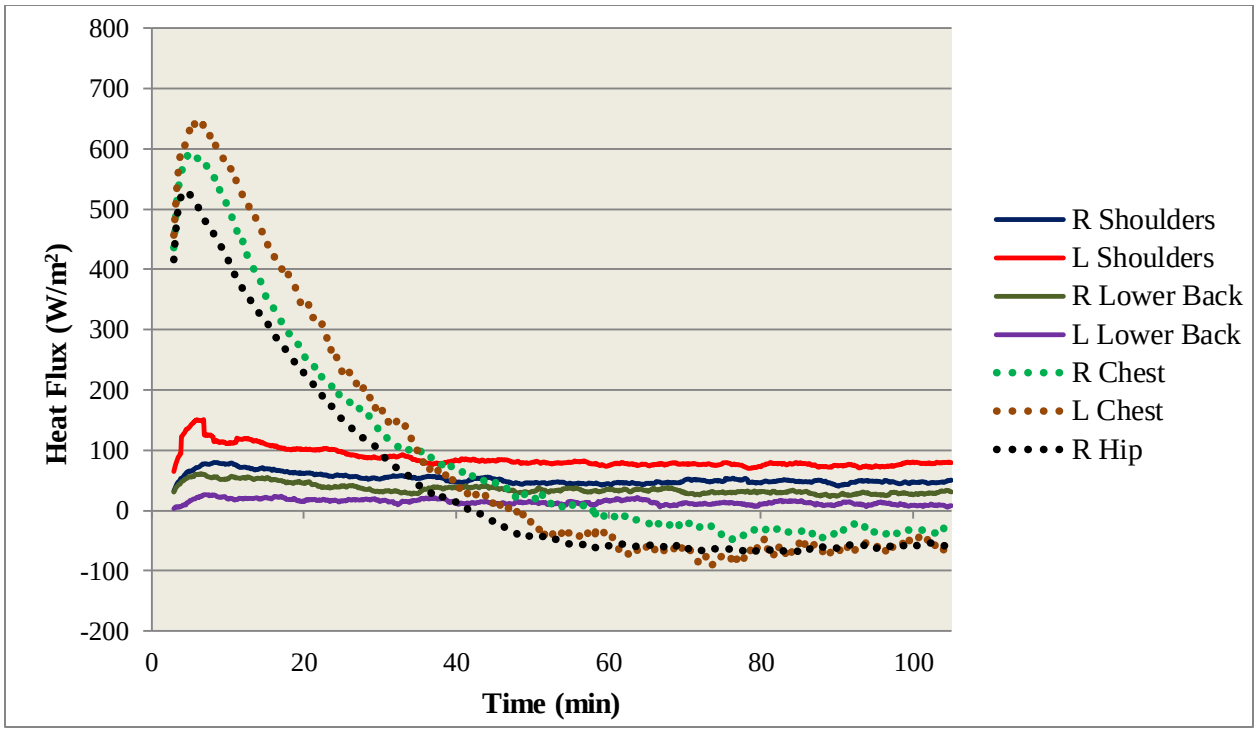

Figure 109. Heat flux measurements recorded from heat flux sensors placed on the front and back of the thermal manikin for a continuous power test (heating fraction, Continuous Power Test 2)

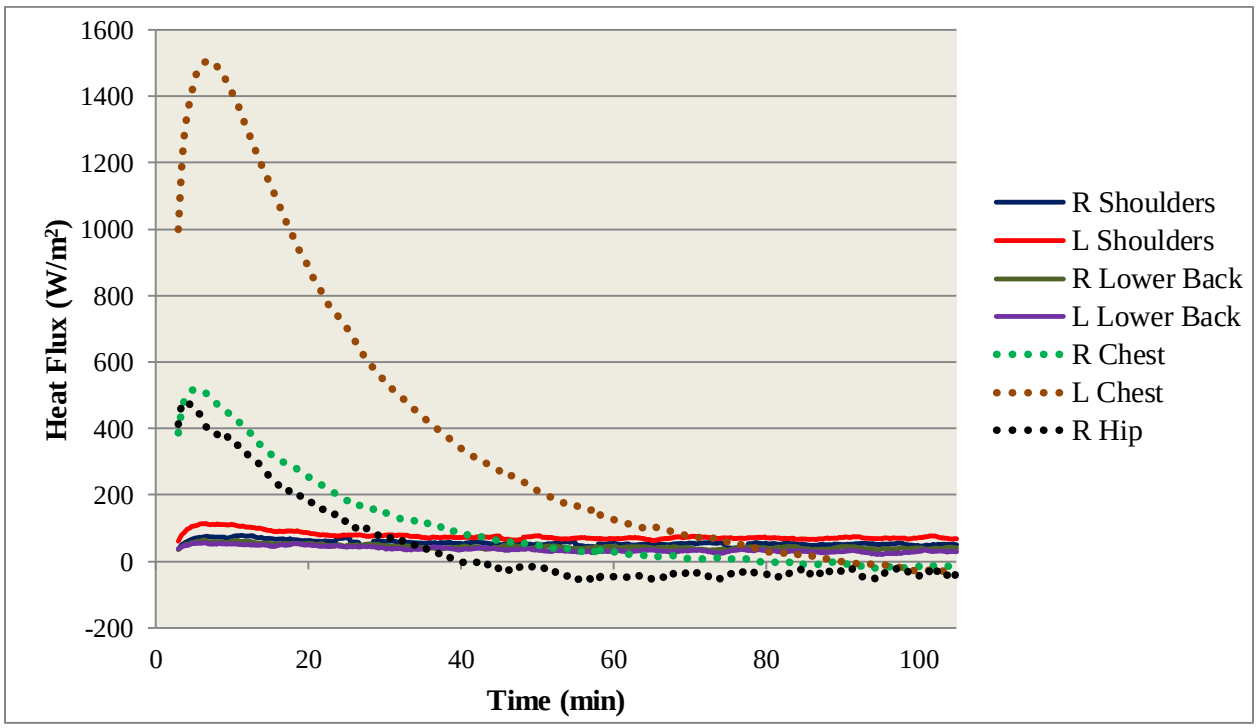

Figure 110. Heat flux measurements recorded form heat flux sensors placed on the front and back of the thermal manikin for a battery power test (heating fraction, battery power Test 1)

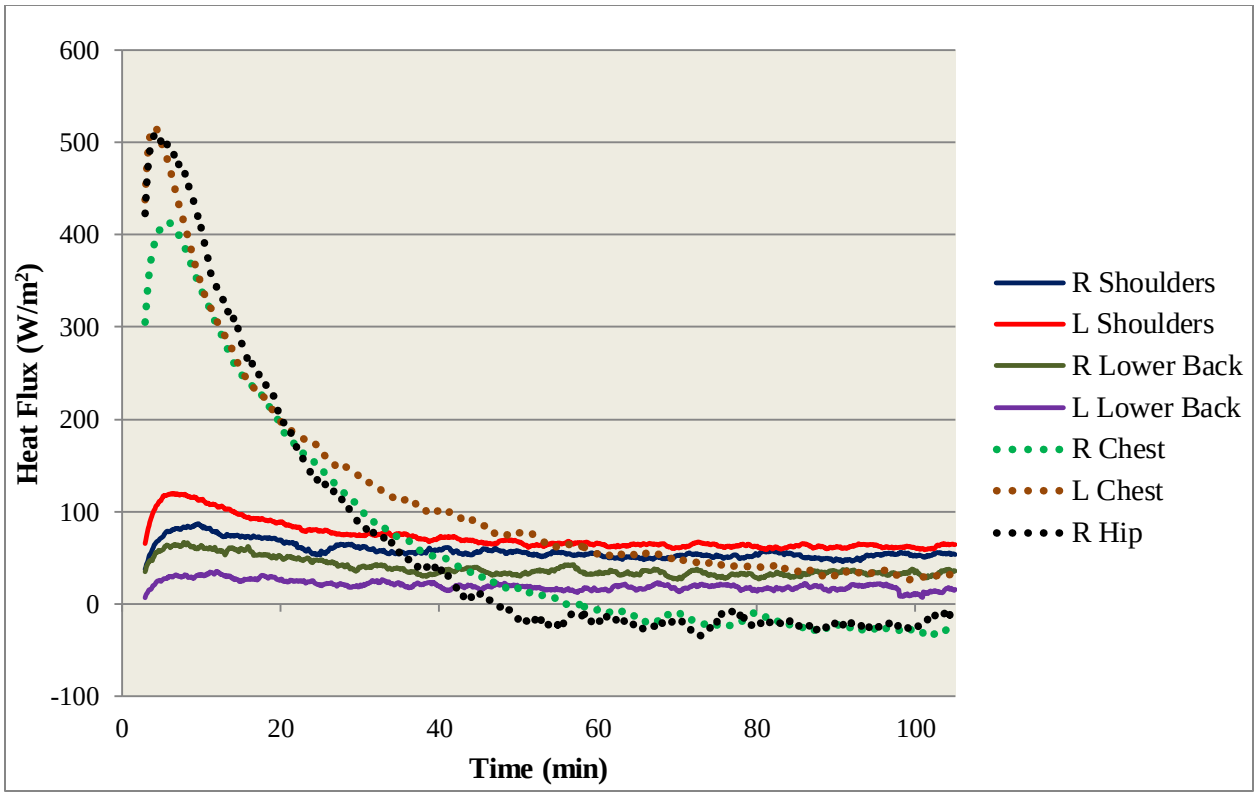

Figure 111. Heat flux measurements recorded from heat flux sensors placed on the front and back of thermal manikin for a battery power test (heating fraction, Battery Power Test 2)

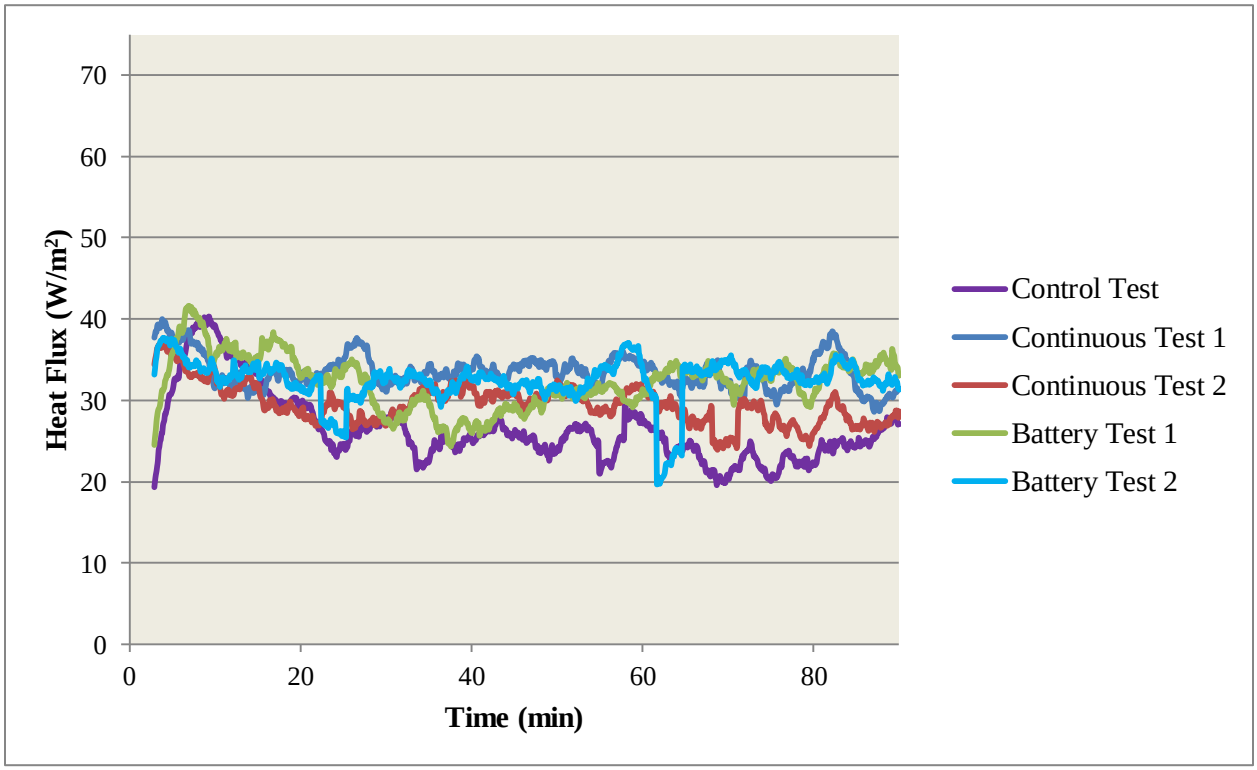

Figure 112. Average heat flux for the four sensors placed on the backside of Thermal Manikin (cooling)

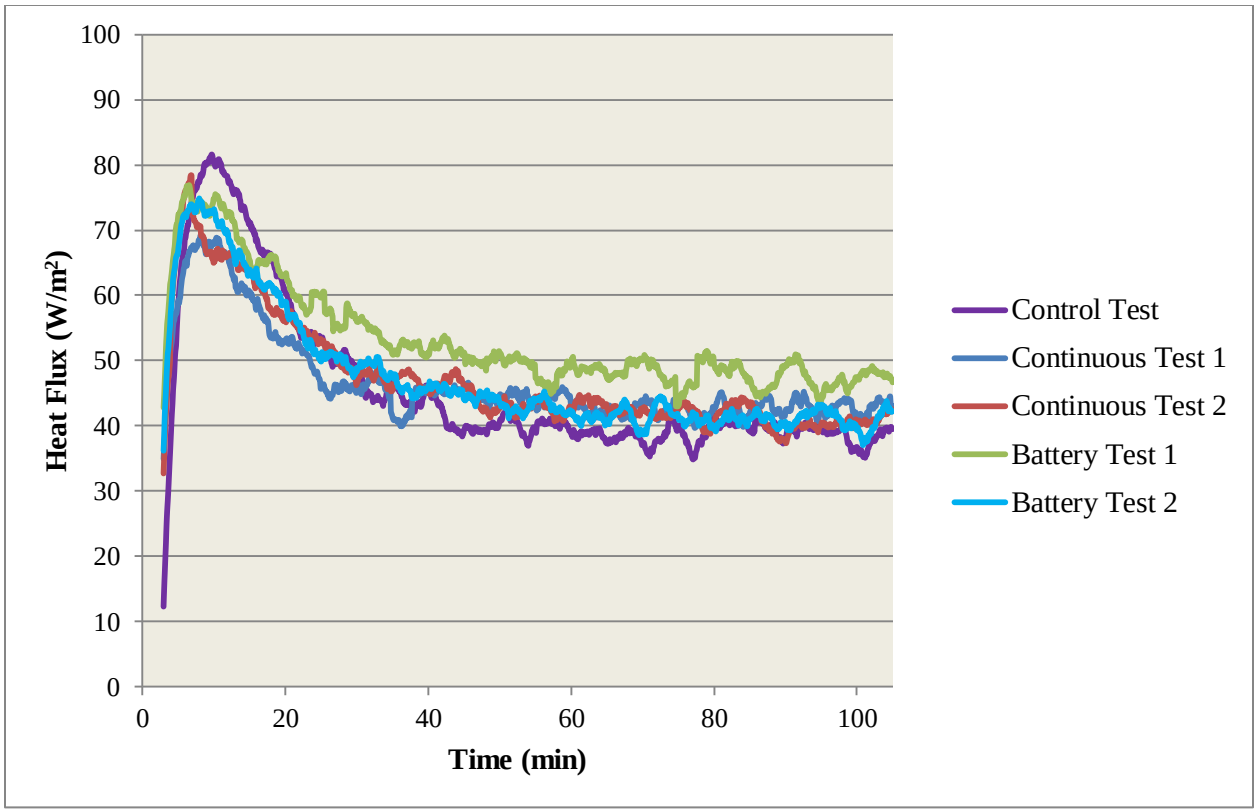

Figure 113. Average heat flux for the four sensors placed on the backside of Thermal Manikin (heating)

Table 12. Average heat flux for the four sensors located on the backside of the thermal manikin

Average Heat Flux Cooling Fraction	**Control**	**Continuous Test 1**	**Continuous Test 2**	**Battery Test 1**	**Battery Test 2**
W/m^2	26.2	34.3	30.1	31.0	33.4
Average Heat Flux Heating Fraction	**Control**	**Continuous Test 1**	**Continuous Test 2**	**Battery Test 1**	**Battery Test 2**
W/m^2	42.1	43.1	41.0	47.3	40.3

Along with the comparison between the heat flux recorded from sensors placed on the front and backside of the thermal manikin, the heat transfer through the table was also calculated to ensure a negligible heat loss assumption was valid. The table on which the thermal manikin was placed is a laminate table made of particle board and sealed with melamine. To calculate the heat transfer through the table, the table is first considered as a composite material and a thermal

resistance is then associated which each component. The heat flux can be found from the following equation:

$$\frac{q}{A} = \frac{T_{in} - T_{out}}{\frac{L_1}{k_1} + \frac{L_2}{k_2} + \frac{1}{h}} \qquad (7)$$

Where,

$\frac{q}{A}$ = Heat Flux [W/m^2]

T_{in} = Inside Table Surface Temperature [^{o}C]

T_{out} = Outside Table Surface Temperature [^{o}C]

L_1 = Thickness of the Melamine Layer [m]

k_1 = Thermal Conductivity of Melamine [0.345 W/m·K]

L_2 = Thickness of the Particle Board Layer [m]

k_2 = Thermal Conductivity of Particle Board [0.17 W/m·K]

h = Convective Heat Transfer Coefficient of Air [W/m^2·K]

The inside and outside surface temperatures are found from the heat flux sensors placed on the back of the thermal manikin and the second temperature sensor placed two feet off the ground respectively. The total thickness of the laminate table measures 17 mm (Melamine layer: 1 mm and Particle board: 16mm). As described previously, the environmental chamber is cooled using a Refrigerated Recirculator connected to a heat exchanger/fan setup. Cold air is circulated throughout the room using the fan setup. In order to calculate the convective heat transfer coefficient a forced convection correlation equation was utilized because of the external force applied by the fan to induce air flow. The table was modeled as air flow over a flat plate. The Reynolds number was calculated first to determine the type of flow, laminar or turbulent. The Prandtl number was also calculated to determine which correlation equation would be valid for this particular situation. The Reynolds and Prandtl numbers are dimensionless quantities that characterize the flow and determine whether momentum or thermal diffusivity dominate respectively. The Reynolds number is calculated from the following equation:

$$Re = \frac{vL}{\nu} \qquad (8)$$

Where,

v = Mean Fluid Velocity [m/s]

L = Characteristic Length [m]

ν = Kinematic Viscosity [m^2/s]

The critical Reynolds number for this situation, point at which the flow becomes turbulent, is equal to 5 x 10^5. The Prandtl number is calculated from the following equation:

$$Pr = \frac{\nu}{\alpha} \qquad (9)$$

Where,

ν = Kinematic Viscosity [m^2/s]

α = Thermal Diffusivity [m^2/s]

For a Prandtl value < 1 thermal diffusivity dominates and for a Prandtl value > 1 momentum diffusivity dominates. Table 13 shows the air properties at ambient temperatures of 15°C and 30°C and the calculated values for the Prandtl number. Table 14 shows the average wind speed values recorded for the experimental runs performed to determine heat loss through the table and the calculated values for the Reynolds number. The values for the dimensionless numbers indicate laminar flow and that thermal diffusivity is dominate[10].

Table 13. Air Properties at an ambient temperature of 15°C and 30°C

	Thermal Conductivity of Air (W/m·K)	**Kinematic Viscosity of Air (10^{-5} m^2/s)**	**Thermal Diffusivity of Air (10^{-6} m^2/s)**	**Prandtl Number**
Ambient Temperature (30°C)	0.026	1.6	22.5	0.71
Ambient Temperature (15°C)	0.025	1.5	20.6	0.71

Table 14. Average wind speed and Reynolds number for various runs of cooling/heating fraction

Cooling Fraction	Continuous Test 1	Continuous Test 2	Battery Test 1	Battery Test 2
Average Air Velocity (m/s)	0.08	0.12	0.12	0.09
Reynolds Number	9258	13733	13968	10261
Heating Fraction	**Continuous Test 1**	**Continuous Test 2**	**Battery Tests 1**	**Battery Test 2**
Average Air Velocity (m/s)	0.07	0.07	0.07	0.06
Reynolds Number	7966	7981	7965	6957

For laminar flow over a flat plate the following forced convection correlation equation for determining the convective heat transfer coefficient can be applied:

$$Nu = \frac{hL}{k} = 0.664 Re_L^{1/2} Pr^{1/3} \qquad (10)$$

The previous equation is valid for $Re < 5 \times 10^5$ and $Pr \geq 0.6$

Where,

Nu = Nusselt Number [dimensionless]

h = Convective Heat Transfer Coefficient of Air [$W/m^2 \cdot K$]

L = Characteristic Length [m]

k = Thermal Conductivity of Air [$W/m \cdot K$] [10]

Table 15 shows the calculated values for the convective heat transfer coefficient for the experimental runs performed to determine the heat loss through the back of the manikin. The values are low, but considering the very low air flow rates the values make sense.

Table 15. Convective heat transfer coefficient of air calculated for each run

Cooling Fraction	**Continuous Test 1**	**Continuous Test 2**	**Battery Test 1**	**Battery Test 2**
h ($W/m^2 \cdot K$)	0.82	1.00	1.01	0.87
Heating Fraction	**Continuous Test 1**	**Continuous Test 2**	**Battery Test 1**	**Battery Test 2**
h ($W/m^2 \cdot K$)	0.73	0.73	0.73	0.69

Figures 114 and 115 show the calculated heat flux through the table for the cooling and heating fraction runs respectively. A moving average was taken for the data, averaged at three minute intervals, recorded by the heat flux sensors to reduce the fluctuations resulting from imperfect thermal contact between the blanket and manikin. The larger values associated with the heating fraction runs are due to the transfer of heat from the circulating water blanket as discussed previously. Tables 16 and 17 show the percentage of heat lost through the table for cooling/heating fraction. For the cooling fraction runs the only heat generated was from the thermal manikin. The values were calculated using equation 2 and an average value was taken from the steady-state portion of the data (50-60 minutes). The heat transfer through the table was calculated by multiplying the average value for the calculated heat flux from figure 114 by the area of the laminate folding table on which the thermal manikin was placed. The percentage of heat lost through the table for the cooling fraction runs is not negligible, but is very small compared to the actual heat generated by the manikin. For the heating fraction runs the manikin and the circulating water blanket generated heat. The heat generated by the circulating water blanked was calculated using equation 6 and an average value was taken from the steady-state portion of the data (95-105 minutes). The other values were calculated in the same way as the cooling fraction data. The percentage of heat lost through the table for the heating fraction runs, again is not negligible and is higher than that of the cooling fraction runs, but it is significantly less than the total heat generated by the manikin and circulating water blanket. The larger values of heat loss again are associated with the heat flowing toward the table for the heating fraction runs.

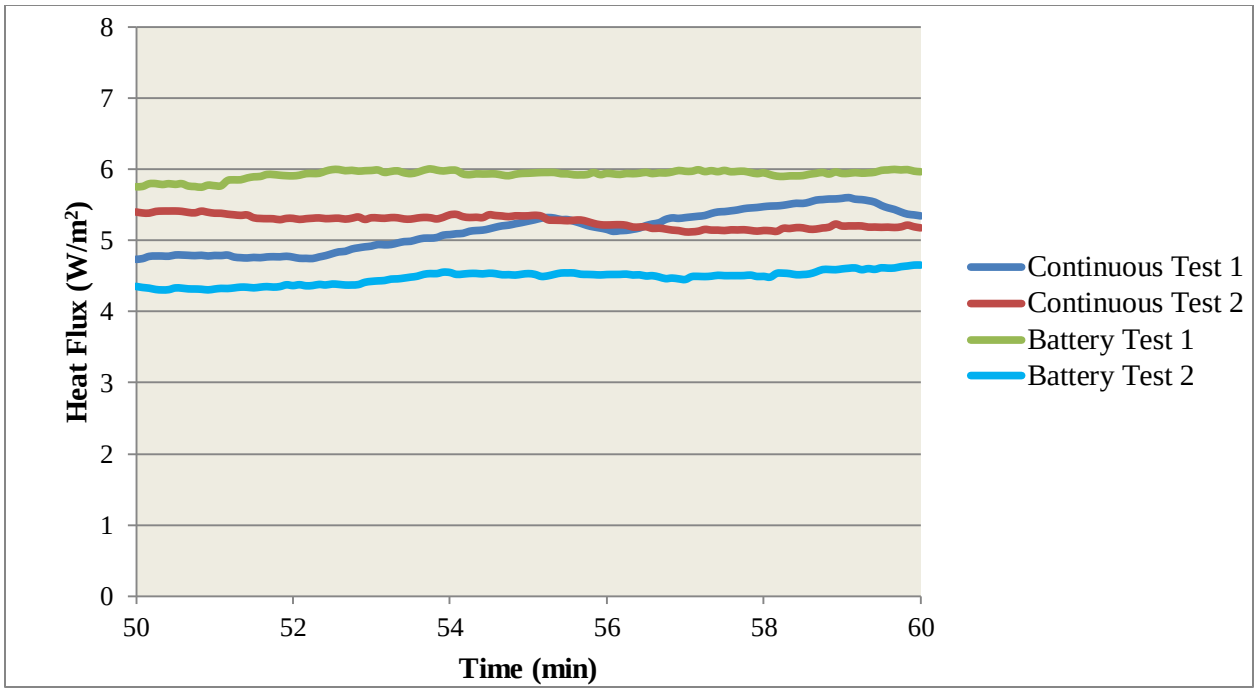

Figure 114. Calculated heat loss through the table (Cooling Fraction).

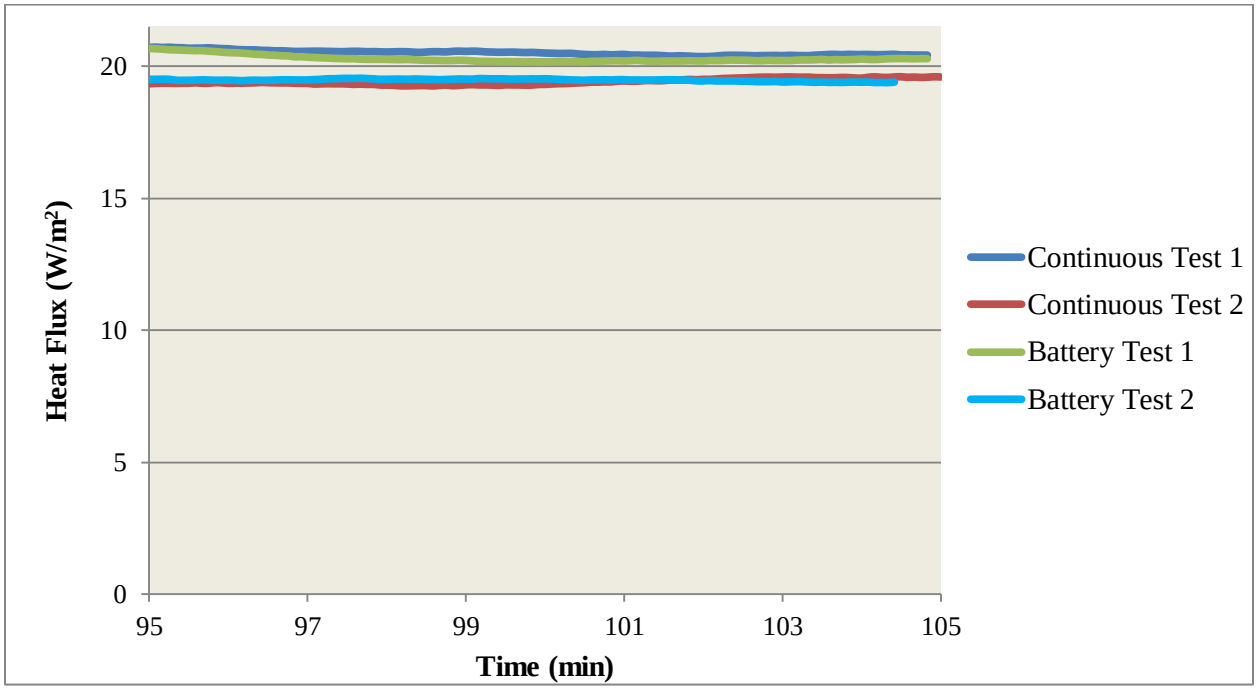

Figure 115. Calculated heat loss through the table (Heating Fraction)

Table 16. Calculated percentage of the heat generated lost through the table (cooling fraction)

Cooling Fraction	Continuous Test 1	Continuous Test 2	Battery Test 1	Battery Test 2
Heat Generated by Manikin (Watts)	140.0	141.9	145.5	146.2
Heat Transfer Through Table (Watts)	7.3	7.3	8.3	6.3
Percentage of Heat Lost (%)	5.2	5.1	5.7	4.3

Table 17. Calculated percentage of the heat generated lost through the table (heating fraction)

Heating Fraction	Continuous Test 1	Continuous Test 2	Battery Test 1	Battery Test 2
Heat Generated by Manikin (Watts)	110	118	116	104
Heat Generated by Blanket (Watts)	155	190	155	149
Total Heat Generated (Watts)	265	308	271	253
Heat Transfer Through Table (Watts)	28.5	27.1	28.2	27.1
Percentage of Heat Lost (%)	10.8	8.80	10.4	10.7

The purpose of performing the cooling/heating fraction tests was to show the impact of the thermal blanket on system performance with the PBTC operating under continuous/battery power. Analysis of the experimental data showed consistent performance of the thermal blanket with the PBTC operating under both continuous and battery power. The empirical data showed no significant difference for the cooling/heating capacity of the PBTC operating under continuous/battery power. Overall the PBTC functioned as designed and sufficiently cooled/heated the water flowing through the circulating water blanket allowing for sufficient heating/cooling of the thermal manikin.

2. Comparison of PBTC to Commercial hyper-hypothermia Test

The primary objective of this test was twofold. First, compare the performance of Rocky Research PBTC prototype to another commercial hyper-hypothermia system. Second, gain knowledge of the prototype's capabilities for future design improvements in a reiterative process between UNSOM and Rocky Research.

Test Design and Set Up

UNSOM surgery research laboratory personnel performed a study evaluating a thermal regulatory response of a thermal manikin within an operating room (OR) using various warming devices. A local county hospital granted use of their OR and Blanketrol III Model 233 (Cincinnati Sub-Zero Products, Inc.; Cincinnati, OH) hyper-hypothermia system. The data collected from this study would be beneficial for comparing to the PBTC.

According to the Association of Operating Room Nurses (AORN), the recommended temperature range for an OR is between 20^{o}C (68^{o}F) and 23^{o}C (73^{o}F). A study on operating room temperature and the effect on patients were performed by Morris[17]. He showed that all patients became hypothermic in rooms below 21^{o}C whereas patients remained normothermic in rooms between 24 – 26^{o}C. The OR warming test methods were conducted at two different ambient temperatures, 20^{o}C $\pm$ 1^{o}C and 26^{o}C $\pm$ 1^{o}C (79^{o}F). The thermal manikin was dressed in a sweating suit and placed supine on OR table. Two surgical lights were turned on and placed 90 cm over manikin's chest and front hips for the surgery simulation. The purpose of the lights was to provide sufficient illumination of surgical site to the surgeon. However, it was thought that some heat would be produced and may have an effect on warming the manikin. Due to availability and scheduling of the OR, only one test was run per warming method per ambient temperature (20^{o}C and 26^{o}C). PBTC tests were performed three times per group. The following three groups were tested: 1) control-nude manikin, 2) whole body water circulating blanket (Maxi Therm® Lite; Cincinnati Sub-Zero Products, Inc.) placed underneath manikin and 3) combination of a head, vest, and leg water circulating wraps (Kool Kit®, Cincinnati Sub-Zero Products, Inc.) A laparotomy surgical drape was placed over the manikin for groups 2 and 3. A commercial hyper-hypothermia medical device was set to maximum temperature of 42^{o}C in manual mode.

Prior to each experiment, the OR room temperature was set to the specified temperature and allowed to reach steady state. After OR room reached temperature, the thermal manikin was powered on and heated to a thermoneutral set point (See Figure 116). These set points are typical human skin temperatures in a thermoneutral state. Once the manikin was preheated to thermoneutral conditions, the physiological model software, Manikin PC2 (ThermoAnacalytics, Calumet, MI) was started. The Manikin PC2 software is imbedded into the ThermDAC software

and runs simultaneously. The physiology software ran for 1 hour for each of the warming methods and control. Skin surface and core body temperature measurements were sampled ever 1 minute for 60 minutes. The Rocky Research experiments were set up and ran in the exact same manner as the hospital experiments using the PBTC with three exceptions. First, overhead surgical lamps were not available to use in the environmental chamber. Second, only the vest wrap was used in group 3, because the PBTC provided one inlet/outlet water connection hose. The commercial device provided three inlet/outlet water connection hoses. Third, skin surface and core body temperature measurements were sampled over 5 seconds for 60 minutes.

Statistics

Statistics were performed using ANOVA and a paired t-test. A p-value $\leq$ 0.05 was considered statistically significant. Analysis was conducted using Statistical Analysis System (SAS) (version 9.3) software.

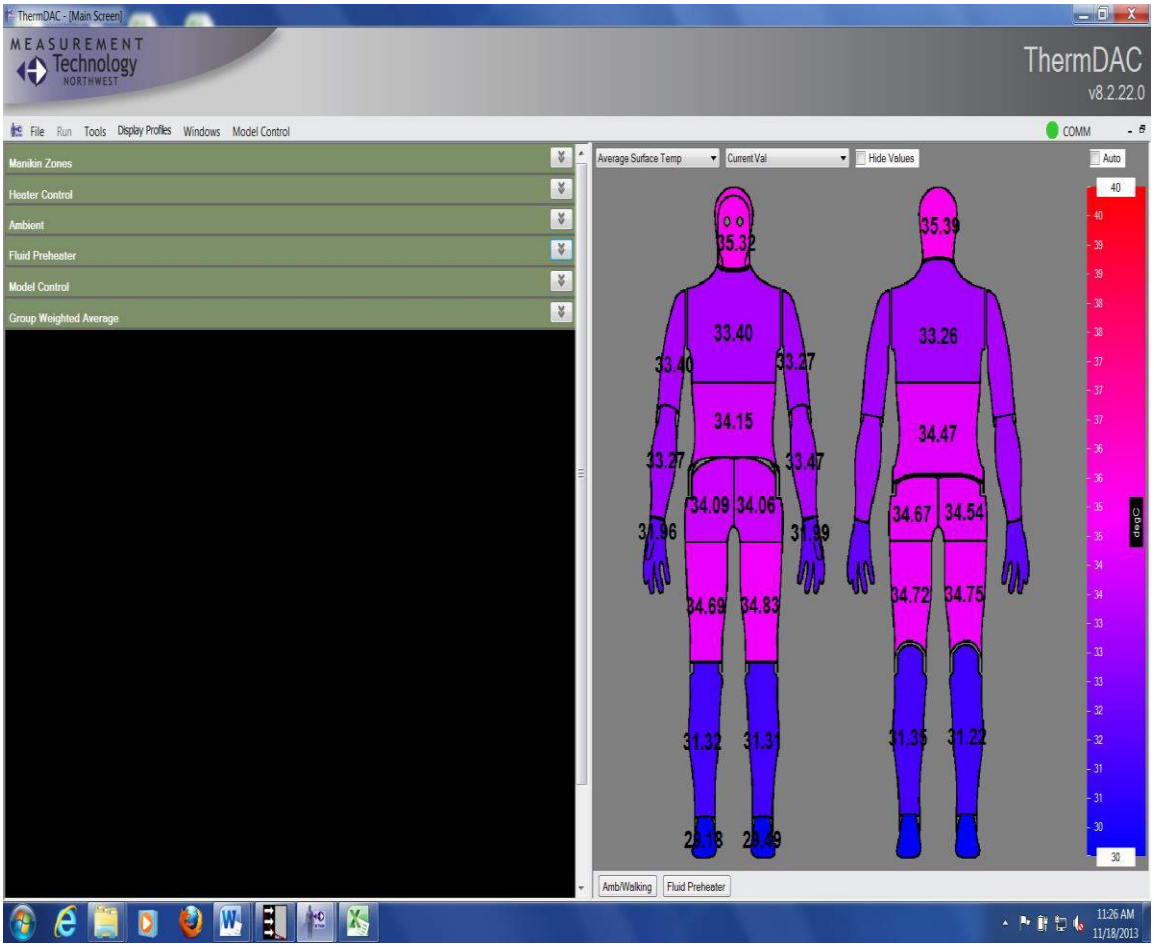

Figure 116. ThermDaq screen shot of thermoneutral set point

Results

The OR and environmental chamber nude manikin controls were compared at both 20^{o}C and 26^{o}C ambient temperatures. Relative humidity was measured but could not be controlled in the OR setting. It did not impact skin surface temperature readings. The manikin was dressed in sweating skin and placed supine on table. Table 18 compares the skin surface temperatures of a 26 zone thermal manikin for each zone and average of all zones in a 20^{o}C ambient temperature OR vs. environmental chamber. Table 19 compares the skin surface temperatures of a 26 zone thermal manikin for each zone and average of all zones in a 26^{o}C ambient temperature OR vs. environmental chamber. The manikin's skin surface temperature for each 26 zones and the all zone average had a statistically significant higher temperature in the OR than environmental chamber for both 20^{o}C and 26^{o}C ambient temperatures. The manikin's average of all zones skin surface temperature was 1.7^{o}C higher at 30 minutes and 2.1^{o}C higher at 60 minutes in OR than environmental chamber with ambient temperature set at 20^{o}C. The manikin's average of all zones skin surface temperature was 1^{o}C higher at 30 minutes and 1.5^{o}C higher at 60 minutes in OR than environmental chamber with ambient temperature set at 26^{o}C. It appears that the surgical lights may increase the skin surface temperature of the manikin by at least 2 $\pm$ 1^{o}C. Core body temperature measurements were sampled and all readings were normal (37.5 $\pm$ 0.5^{o}C) for control nude manikin.

Table 18. Comparing Nude Manikin Skin Surface temperatures in 20°C Operating Room vs. Rocky Research Environmental Chamber

Zone	Operating Room (°C)		Environmental Chamber (°C)	
	30 minutes	**60 minutes**	**30 minutes**	**60 minutes**
Head*	31.7	31.1	29.0	28.0
Face*	31.9	31.1	30.6	29.6
R Upper Arm*	30.6	30.6	29.7	29.4
L Upper Arm*	31.2	31.1	29.9	29.5
R Forearm*	30.3	30.3	30.0	29.8
L Forearm*	31.4	31.5	29.7	29.3
R Hand	27.8	26.9	27.7	26.6
L Hand*	28.9	28.3	27.6	26.6
Chest*	32.8	32.8	30.3	29.8
Shoulders*	33.3	33.3	31.2	30.8
Stomach	31.8	31.6	30.8	30.4
Back*	33.1	33.0	31.9	31.1
R Hip Front*	32.2	31.9	30.4	30.0
R Hip Back*	33.5	33.3	31.4	30.3
L Hip Front*	33.6	33.5	31.8	29.6
L Hip Back*	33.9	33.7	30.7	30.2
R Thigh Front*	31.4	31.1	30.3	29.8
R Thigh Back*	32.7	32.2	30.0	29.6
L Thigh Front*	31.6	31.2	30.0	29.5
L Thigh Back*	32.9	32.5	29.8	29.2
R Calf Front*	30.4	30.7	29.3	29.2
R Calf Back*	31.1	31.3	29.2	29.0
L Calf Front*	30.2	30.6	28.9	28.5
L Calf Back*	31.4	31.8	28.5	27.9
R Foot*	25.7	25.1	24.6	23.9
L Foot*	25.9	25.5	24.3	23.5
Average of All Zones*	**31.2**	**31.0**	**29.5**	**28.9**

*$p \leq 0.05$ Operating Room vs. Environmental Chamber

Table 19. Comparing Nude Manikin Skin Surface temperatures in 26°C Operating Room or Rocky Research Environmental Chamber

Zone	Operating Room (°C)		Environmental Chamber (°C)	
	30 minutes	**60 minutes**	**30 minutes**	**60 minutes**
Head*	32.2	33.3	32.0	31.6
Face*	33.7	33.7	32.6	32.3
R Upper Arm*	32.1	32.6	31.6	31.7
L Upper Arm*	32.2	32.8	31.6	31.7
R Forearm*	31.9	32.6	31.5	31.7
L Forearm*	32.2	33.2	31.1	31.4
R Hand*	30.3	30.5	29.5	29.2
L Hand*	31.1	31.5	29.7	29.5
Chest*	34.0	34.7	32.2	32.1
Shoulders*	33.4	34.2	32.7	32.8
Stomach*	33.2	33.6	32.4	32.4
Back*	33.3	33.8	32.8	33.0
R Hip Front*	33.5	34.0	32.2	32.1
R Hip Back*	33.2	33.8	32.6	32.7
L Hip Front*	34.1	34.8	32.0	31.8
L Hip Back*	33.2	33.9	32.2	32.2
R Thigh Front*	33.1	33.4	32.0	31.8
R Thigh Back*	33.5	33.9	31.8	31.6
L Thigh Front*	33.2	33.5	31.7	31.6
L Thigh Back*	33.3	33.7	31.6	31.5
R Calf Front*	31.7	32.6	31.0	31.5
R Calf Back*	31.7	32.8	30.9	31.4
L Calf Front*	31.6	32.5	30.8	31.1
L Calf Back*	31.9	32.9	30.6	30.9
R Foot*	28.2	28.8	27.8	27.9
L Foot*	28.3	28.8	27.7	27.8
Average of All Zones*	**32.3**	**32.9**	**31.3**	**31.4**

*$p \leq 0.05$ Operating Room vs. Environmental Chamber

Group 2, the whole body water circulation blanket was placed under the manikin. A laparotomy surgical drape was placed over the manikin. Tables 20 and 21 compares the skin surface temperatures of a 26 zone thermal manikin warmed by whole body water circulating blanket connected to a commercial hyper-hypothermia system or PBTC at two different ambient temperatures. The manikin's skin surface temperature for each 26 zones and the all zone average had a statistically significant higher temperature using the commercial device than PBTC for both 20^{o}C and 26^{o}C ambient temperatures. The manikin's average of all zones skin surface temperature was 2.9^{o}C higher at 30 minutes and 3.1^{o}C higher at 60 minutes using commercial device than the PBTC in 20^{o}C room (See Table 20). The manikin's average of all zones skin surface temperature was 1.5^{o}C higher at 30 minutes and 1.8^{o}C higher at 60 minutes using commercial device than the PBTC in 26^{o}C room (See Table 21). Core body temperature measurements were sampled and all readings were normal (37.5 $\pm$ 0.5^{o}C) for group 2.

The thermal manikin warmed by whole body blanket connected to a medical device was compared to the nude manikin control at both ambient temperatures. The manikin's skin surface temperature for each 26 zones and the all zone average had a statistically significant higher temperature in manikin warmed by medical device system than control nude manikin for 20^{o}C and 26^{o}C ambient temperatures. The manikin's average of all zones skin surface temperature was 3.4^{o}C higher at 30 minutes and 4.1^{o}C higher at 60 minutes using commercial device than control nude manikin in 20^{o}C room (See Table 22). The manikin's average of all zones skin surface temperature was 3.0^{o}C higher at 30 minutes and 3.3^{o}C higher at 60 minutes using commercial device than control nude manikin in 26^{o}C room. The manikin's average of all zones skin surface temperature was 2.2^{o}C higher at 30 minutes and 3.1^{o}C higher at 60 minutes using PBTC than control nude manikin in 20^{o}C room. The manikin's average of all zones skin surface temperature was 2.1^{o}C higher at 30 minutes and 2.3^{o}C higher at 60 minutes using PBTC than control nude manikin in 26^{o}C room.

Overall, both the PBTC and commercial device warmed the thermal manikin's all zone average skin surface temperature at least > 2 - 3^{o}C higher than nude control manikin temperatures in 60 minutes.

Table 20. PBTC compared to a commercial hyper-hypothermia system using a whole body blanket underneath manikin. Skin Surface temperatures measured at 20°C ambient temperature

Zone	Commercial Device in Operating Room (°C)		PBTC in Environmental Chamber (°C)	
	30 minutes	60 minutes	30 minutes	60 minutes
Head*	34.0	34.5	31.1	30.6
Face*	34.3	34.4	31.9	31.5
R Upper Arm*	34.5	35.2	31.6	32.1
L Upper Arm*	34.2	35.0	31.3	31.7
R Forearm*	33.8	34.5	32.2	32.9
L Forearm*	34.1	35.0	31.5	32.1
R Hand*	31.5	32.8	29.9	30.0
L Hand*	32.3	33.8	29.9	29.8
Chest*	35.1	35.5	32.0	31.9
Shoulders*	39.1	39.1	33.9	35.1
Stomach*	34.8	35.0	32.3	32.3
Back*	37.0	36.7	34.1	35.0
R Hip Front*	34.8	35.3	32.2	32.2
R Hip Back*	36.3	36.5	34.4	35.2
L Hip Front*	35.0	35.4	31.9	31.8
L Hip Back*	36.3	36.5	33.8	34.5
R Thigh Front*	34.8	35.2	32.4	32.4
R Thigh Back*	37.4	37.3	33.4	33.9
L Thigh Front*	34.6	35.1	32.2	32.1
L Thigh Back*	37.1	36.8	32.9	33.3
R Calf Front*	33.7	34.9	31.0	31.9
R Calf Back*	37.2	36.8	32.5	33.8
L Calf Front*	33.4	34.5	30.4	31.0
L Calf Back*	37.1	36.3	31.4	32.6
R Foot*	28.7	30.3	26.9	27.2
L Foot*	28.5	30.1	26.0	26.1
Average of All Zones*	**34.6**	**35.1**	**31.7**	**32.0**

*$p \leq 0.05$ commercial device vs. PBTC

Table 21. PBTC compared to a commercial hyper-hypothermia system using a whole body blanket underneath manikin. Skin Surface temperatures measured in 26°C ambient temperature room

Zone	Commercial Device in Operating Room (°C)		PBTC in Environmental Chamber (°C)	
	30 minutes	60 minutes	30 minutes	60 minutes
Head*	35.1	35.6	33.7	33.7
Face*	35.3	35.5	34.2	34.2
R Upper Arm*	35.3	36.0	33.9	34.7
L Upper Arm*	35.3	36.1	33.6	34.2
R Forearm*	34.7	35.6	33.9	34.6
L Forearm*	34.8	35.9	33.5	34.1
R Hand*	33.4	35.5	31.8	32.7
L Hand*	33.7	35.5	32.0	32.6
Chest*	35.9	36.3	34.2	34.6
Shoulders*	38.7	39.0	37.1	37.3
Stomach*	35.5	36.0	34.1	34.9
Back*	36.6	36.9	35.5	35.8
R Hip Front*	35.8	36.4	34.2	34.7
R Hip Back*	36.5	36.7	35.6	36.0
L Hip Front*	35.7	36.3	34.0	34.4
L Hip Back*	36.4	36.5	35.1	35.1
R Thigh Front*	35.8	36.3	34.4	34.8
R Thigh Back*	37.2	37.4	35.4	35.7
L Thigh Front*	35.6	36.2	34.2	34.5
L Thigh Back*	36.4	36.4	35.0	35.2
R Calf Front*	34.7	35.9	33.2	34.6
R Calf Back*	36.8	37.2	35.7	36.3
L Calf Front*	34.4	35.7	32.8	33.6
L Calf Back*	36.5	36.3	34.1	34.7
R Foot*	31.1	34.3	29.3	30.4
L Foot*	31.0	34.1	28.6	29.3
Average of All Zones*	**35.3**	**36.1**	**33.8**	**34.3**

*$p \leq 0.05$ commercial device vs. PBTC

Table 22. Thermal manikin all zones average skin surface temperature difference between control nude manikin and medical device

Ambient Temperature (^{o}C)	Commercial Device		PBTC	
	30 minutes	60 minutes	30 minutes	60 minutes
20	3.4^{o}C	4.1^{o}C	2.2^{o}C	3.1^{o}C
26	3.0^{o}C	3.3^{o}C	2.1^{o}C	2.3^{o}C

*p $\leq$ 0.05 medical device vs. control

Group 3, the vest wrap was placed around the manikin. A laparotomy surgical drape was placed over the manikin. Skin surface temperatures were sampled for all zones as well as core body temperature. Vest wrap came into direct contact with chest, shoulders, stomach and back. Only these zones were reported for PBTC comparison to commercial device at both 20^{o}C and 26^{o}C ambient temperatures (See Figures 117 – 124). Chest and Shoulders skin surface temperatures had a statistically significantly higher temperature in commercial device than PBTC at 20^{o}C ambient temperature. The manikin's chest skin surface temperature was 1.4^{o}C higher at 30 minutes and 0.4^{o}C higher at 60 minutes using commercial device than the PBTC in 20^{o}C room (See Figure 117). The manikin's shoulders skin surface temperature was 3.4^{o}C higher at 30 minutes and 2.0^{o}C higher at 60 minutes using commercial device than the PBTC in 20^{o}C room (See Figure 118). The manikin's stomach skin surface temperature was 0.5^{o}C higher at 30 minutes and 2.7^{o}C higher at 60 minutes using PBTC than commercial device in 20^{o}C room (See Figure 119). The manikin's back skin surface temperature was 0.1^{o}C higher at 30 minutes using commercial device than PBTC and 1.6^{o}C higher at 60 minutes using PBTC than commercial device in 20^{o}C room (See Figure 120). Chest and Shoulders skin surface temperatures had a statistically significantly higher temperature in commercial device than PBTC at 20^{o}C ambient temperature. Shoulders skin surface temperatures had a statistically significantly higher temperature in commercial device than PBTC at 26^{o}C ambient temperature. Stomach skin surface temperatures had a statistically significantly higher temperature in PBTC than commercial device at 26^{o}C ambient temperature. The manikin's chest skin surface temperature was same temperature at 30 minutes in both devices and 0.2^{o}C higher at 60 minutes using PBTC than commercial device in 26^{o}C room (See Figure 121). The manikin's shoulders skin surface temperature was 0.8^{o}C higher at 30 minutes and 1.2^{o}C higher at 60 minutes using commercial device than the PBTC in 26^{o}C room (See Figure 122). The manikin's stomach skin surface temperature was 1.9^{o}C higher at 30 minutes and 2.6^{o}C higher at 60 minutes using PBTC than commercial device in 26^{o}C room (See Figure 123). The manikin's back skin surface temperature was 0.3^{o}C higher at 30 minutes and 0.6^{o}C higher at 60 minutes using PBTC than commercial device in 26^{o}C room (See Figure 124). Core body temperature measurements were sampled and all readings were normal (37.5 $\pm$ 0.5^{o}C) for group 3. Both the PBTC and commercial device

were comparable in warming the thermal manikin's chest, shoulders, stomach, and back to > 34°C skin surface temperature at the two ambient temperatures. Group standard deviations were very small less than 0.5 for all groups.

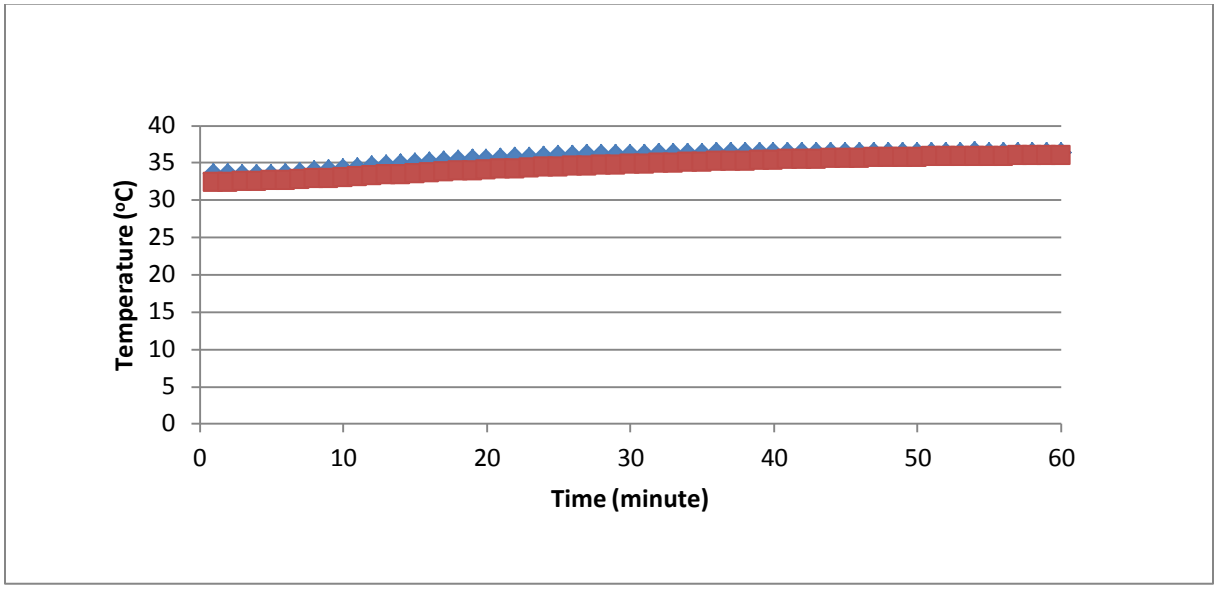

Figure 117. PBTC compared to a commercial hyper-hypothermia system using vest wrap on thermal manikin. Chest skin surface temperatures measured in 20°C ambient temperature room. Rocky Research PBTC is red line. Commercial Device is blue line.
$p \leq 0.05$ commercial device vs. PBTC

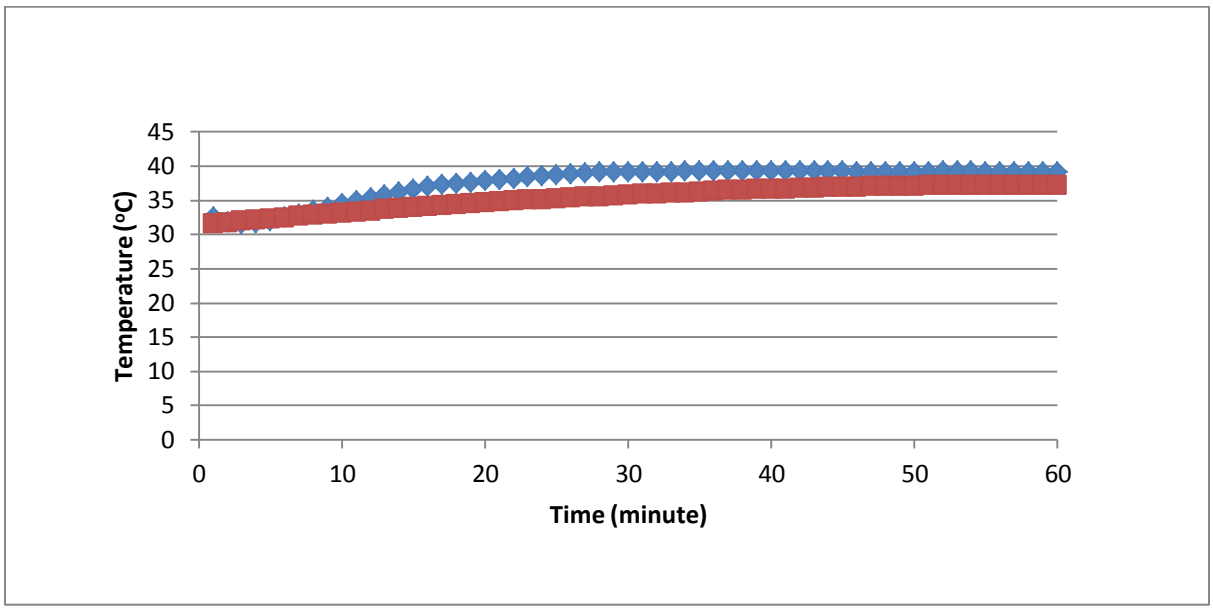

Figure 118. PBTC compared to a commercial hyper-hypothermia system using vest wrap on thermal manikin. Shoulder skin surface temperatures measured in 20°C ambient temperature room. Rocky Research PBTC is red line. Commercial Device is blue line.
$p \leq 0.05$ commercial device vs. PBTC

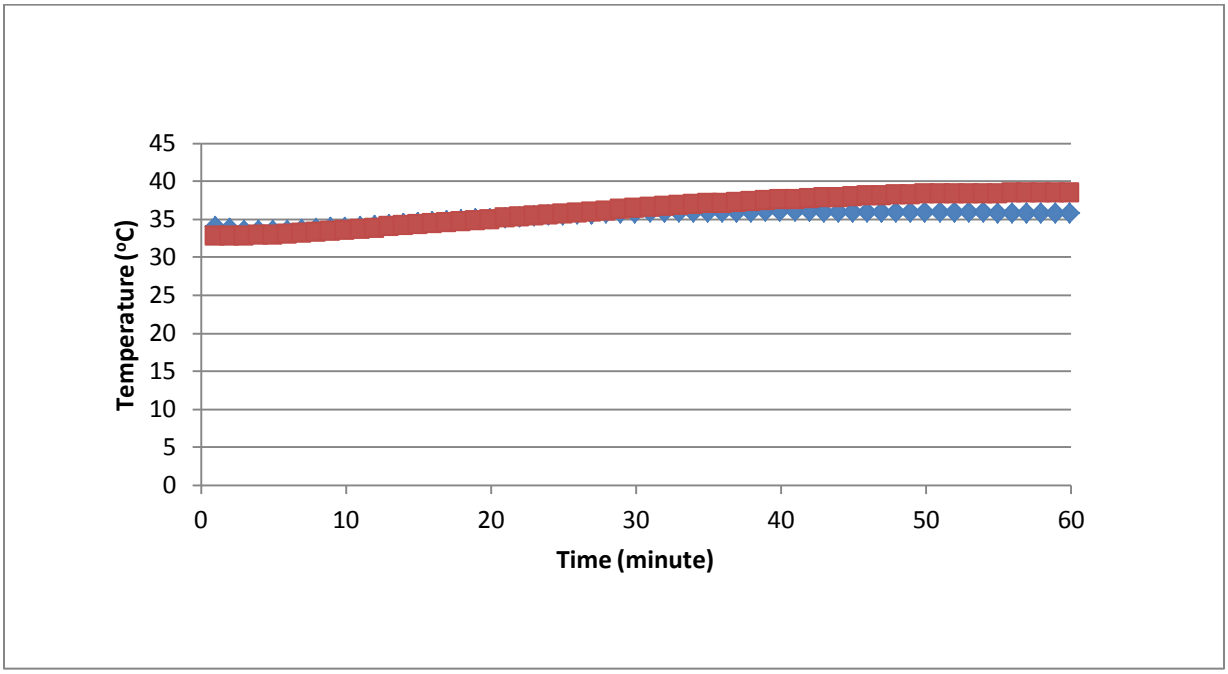

Figure 119. PBTC compared to a commercial hyper-hypothermia system using vest wrap on thermal manikin. Stomach skin surface temperatures measured in 20°C ambient temperature room. Rocky Research PBTC is red. Commercial Device is blue.

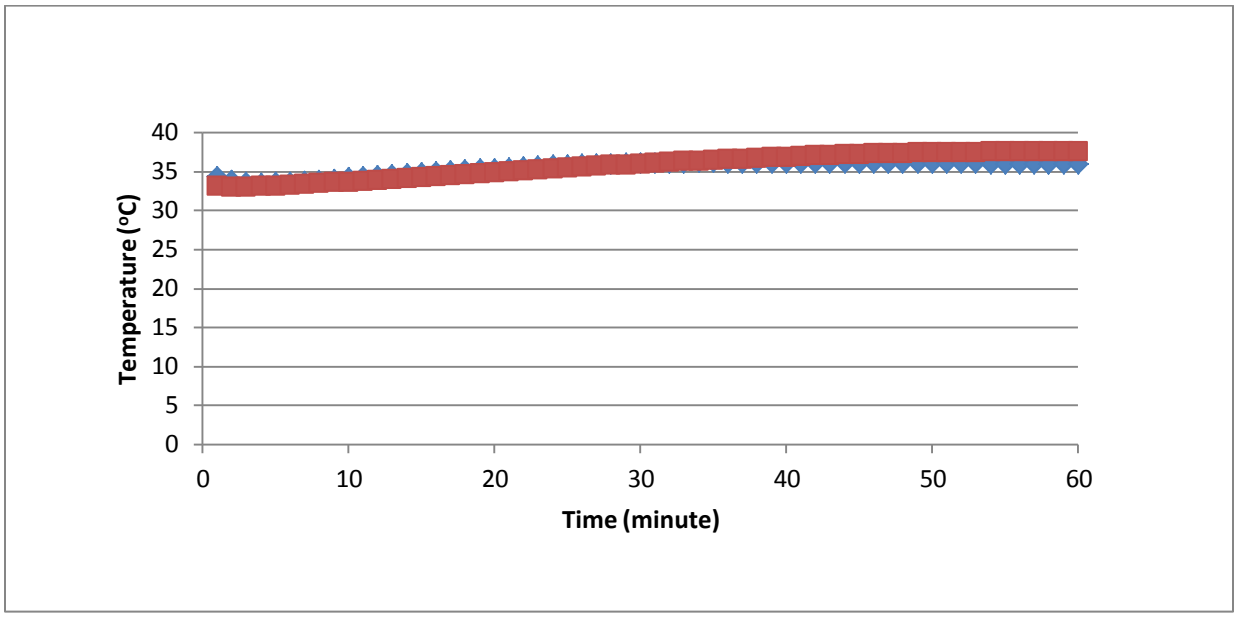

Figure 120. PBTC compared to a commercial hyper-hypothermia system using vest wrap on thermal manikin. Back skin surface temperatures measured in 20°C ambient temperature room. Rocky Research PBTC is red. Commercial Device is blue.

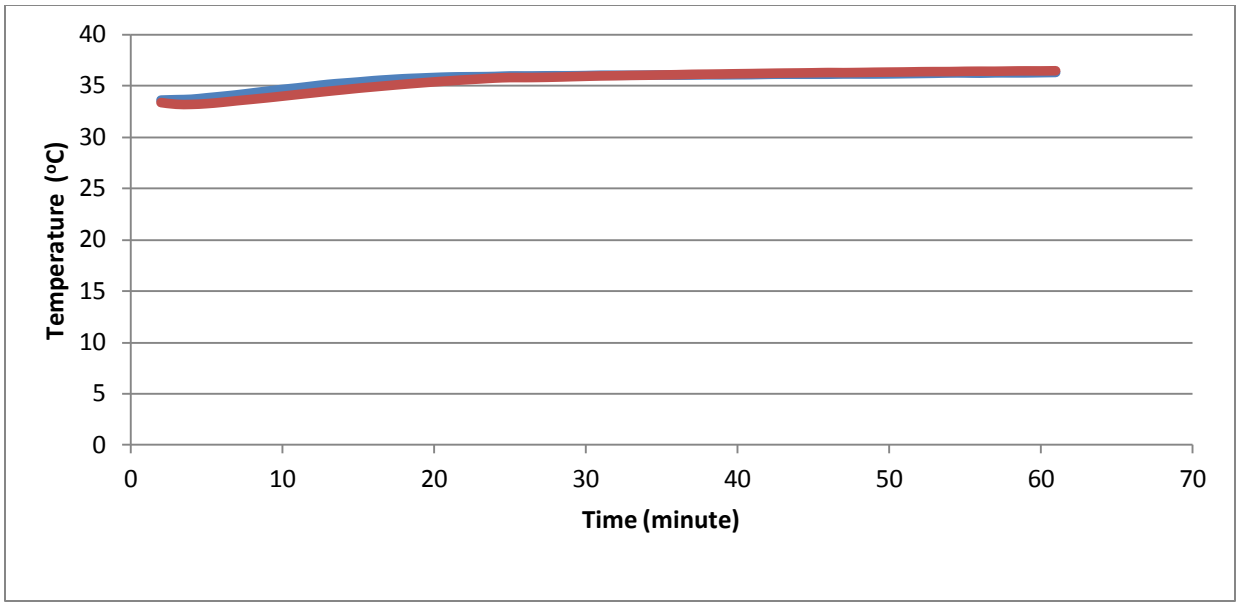

Figure 121. PBTC compared to a commercial hyper-hypothermia system using vest wrap on thermal manikin. Chest skin surface temperatures measured in 26°C ambient temperature room. Rocky Research PBTC is red. Commercial Device is blue.

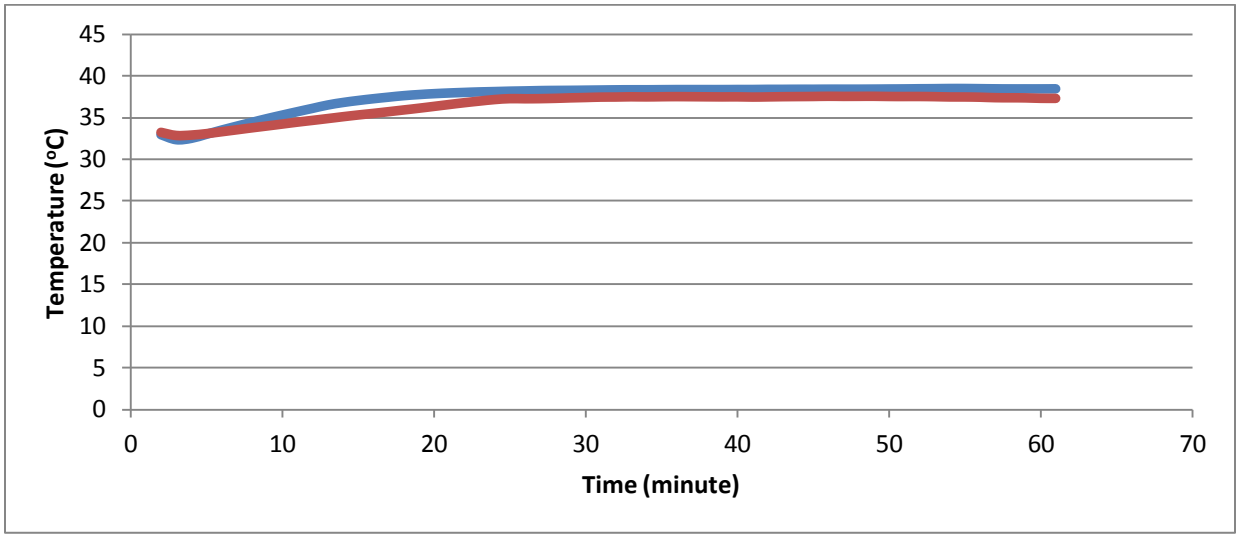

Figure 122. PBTC compared to a commercial hyper-hypothermia system using vest wrap on thermal manikin. Shoulder skin surface temperatures measured in 26°C ambient temperature room. Rocky Research PBTC is red. Commercial Device is blue.
$p \leq 0.05$ commercial device vs. PBTC.

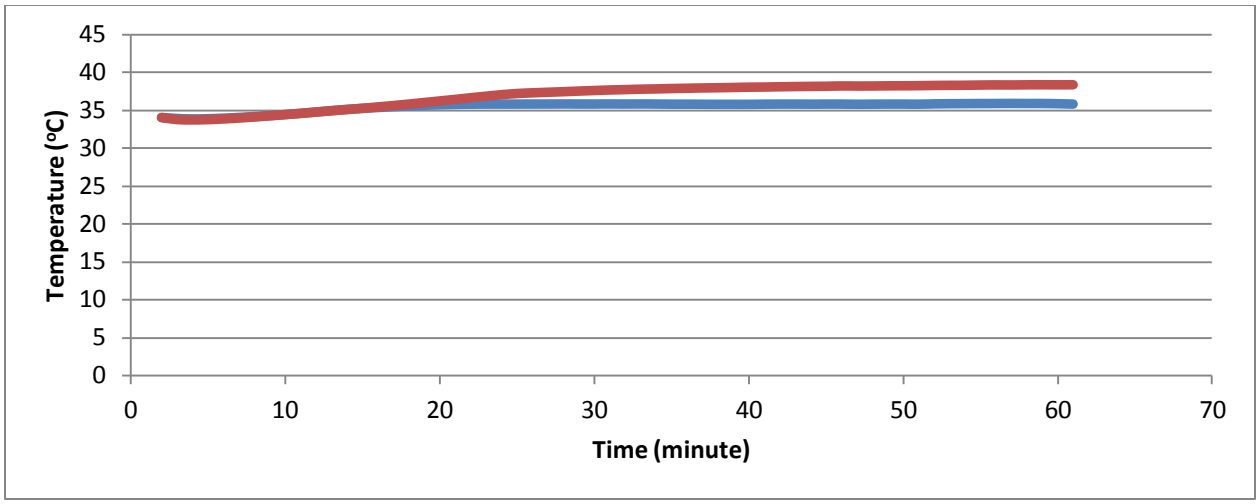

Figure 123. PBTC compared to a commercial hyper-hypothermia system using vest wrap on thermal manikin. Stomach skin surface temperatures measured in 26°C ambient temperature room. Rocky Research PBTC is red. Commercial Device is blue.
$p \leq 0.05$ commercial device vs. PBTC

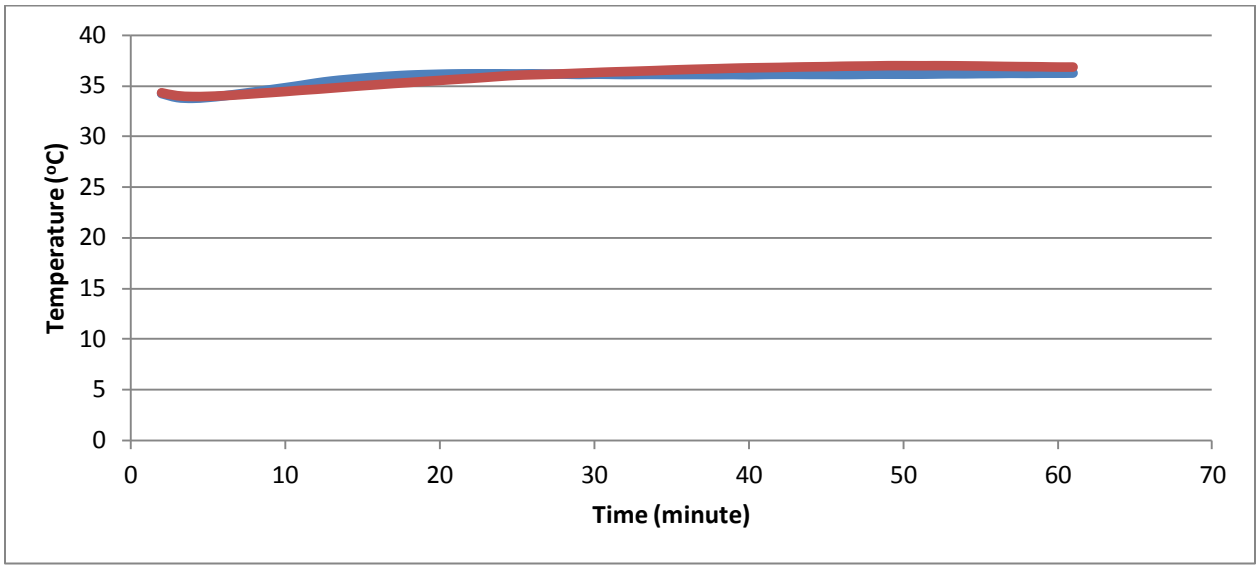

Figure 124. PBTC compared to a commercial hyper-hypothermia system using vest wrap on thermal manikin. Back skin surface temperatures measured in 26°C ambient temperature room. Rocky Research PBTC is red. Commercial Device is blue.

The PBTC and a non-portable commercial device were both ran in manual mode using the same COTS blanket and vest wrap. The water temperature of blanket was set at maximum temperature of 42°C. The non-portable commercial device reached 42°C water blanket temperature in 8 minutes, whereas the PTBC took more time to reach the target temperature (See Table 23).
There are several physical characteristics that are unique to the Rocky Research PBTC when compared to other commercial hyper-hypothermia systems (See Table 5). The PBTC is small, lightweight and transportable device intended for field use where the commercial device is a

large heavy appliance intended for stationary use. The commercial device is 4 times larger in weight and uses 4 times the power consumption than the PBTC.

Table 23. Time for PBTC and Non-Portable Commercial Device to reach blanket water target temperature of 42°C.

Device	20°C Room	26°C Room
PBTC	38.5°C at 60 minutes	27 minutes
Commercial Device	8 minutes	8 minutes

3. Head Cooling Test

Traumatic brain injury (TBI) is a significant cause of death, disability and cost to military combat casualty care[18]. The neurologic damage incurred following TBI is an evolving process that occurs over several hours and days. Evidence has shown that outcomes are improved when secondary, or delayed insults are limited[19]. Treatment therapies are therefore directed at maximizing cerebral oxygen delivery and minimizing episodes of cerebral oxygen debt. Core temperature variations occur frequently following TBI as a result of direct hypothalamus injury and a loss of cerebral autoregulation. The presence of hyperthermia in TBI patients contributes to secondary brain injury. Elevated core body temperature increases metabolic demands of the brain. With each increase in temperature of 1°C, there is a 6-10% increase in cerebral metabolism which subsequently increases cerebral oxygen consumption. Research has confirmed that hyperthermia in combination with TBI results in measurable cerebral damage and worsens neurologic outcome[20]. The ability to reliably and efficiently control temperature variations in the acute TBI patient will improve outcomes. The current method used for hyperthermia management in the head injured soldier is external packing with ice bags. This method is unreliable and potentially dangerous due to the risk of cutaneous injury and the possibility of inducing hypothermia[21].

The primary objective of this test was to determine the prototypes capability to cool the manikin's head using a commercial off the shelf head wrap.

Test Design and Set Up

This test was conducted within a temperature controlled environmental chamber with the ambient temperature set at 26°C ± 1°C. The thermal manikin was dressed in a sweating skin and placed supine on a table. The following two groups were tested: 1) control-nude manikin and 2) circulated water head wrap (Kool Kit®, Cincinnati Sub-Zero Products, Inc.). A commercial off the shelf head wrap was placed on the manikin's head and wrapped around the neck. PBTC was turned on, set to 10°C in manual mode, and started for group 2.

Prior to each experiment, the environmental chamber temperature was set to the specified temperature and allowed to reach steady state. After the chamber reached temperature, the thermal manikin was powered on and heated to a thermoneutral set point (See Figure 116). These set points are typical human skin temperatures in a thermoneutral state. Once the manikin was preheated to thermoneutral conditions. The physiological model software, Manikin PC2 (ThermoAnacalytics, Calumet, MI) was started. The Manikin PC2 software is imbedded into the

ThermDAC software and runs simultaneously. The physiology software ran for 1 hour for each of the cooling and control experiments. Skin surface and core body temperature measurements were sampled over 5 seconds for 60 minutes. PBTC tests were performed three times per group.

Statistics

Statistics were performed using ANOVA and a paired t-test. A p-value ≤ 0.05 was considered statistically significant. Analysis was conducted using Statistical Analysis System (SAS) (version 9.3) software.

Results

Cooling capabilities of PBTC was evaluated by placing a COTS water circulating head wrap on manikin's head and around neck. The manikin's head skin surface temperature had a statistically significant lower temperature in manikin cooled by PBTC than control nude manikin experiment at both 30 and 60 minutes. The manikin's head skin surface temperature was 0.4°C lower at 1minute, 5.4°C lower at 30 minutes, and 6.5°C lower at 60 minutes using PBTC control nude manikin (See Figure 125). Core body temperature measurements were sampled and all readings were normal (37.5 $\pm$ 0.5°C) for head cooling test. Group standard deviations were less than 0.4 for all groups.

The PBTC was capable of cooling the head skin surface temperature to from 34°C to 26°C in 60 minutes.

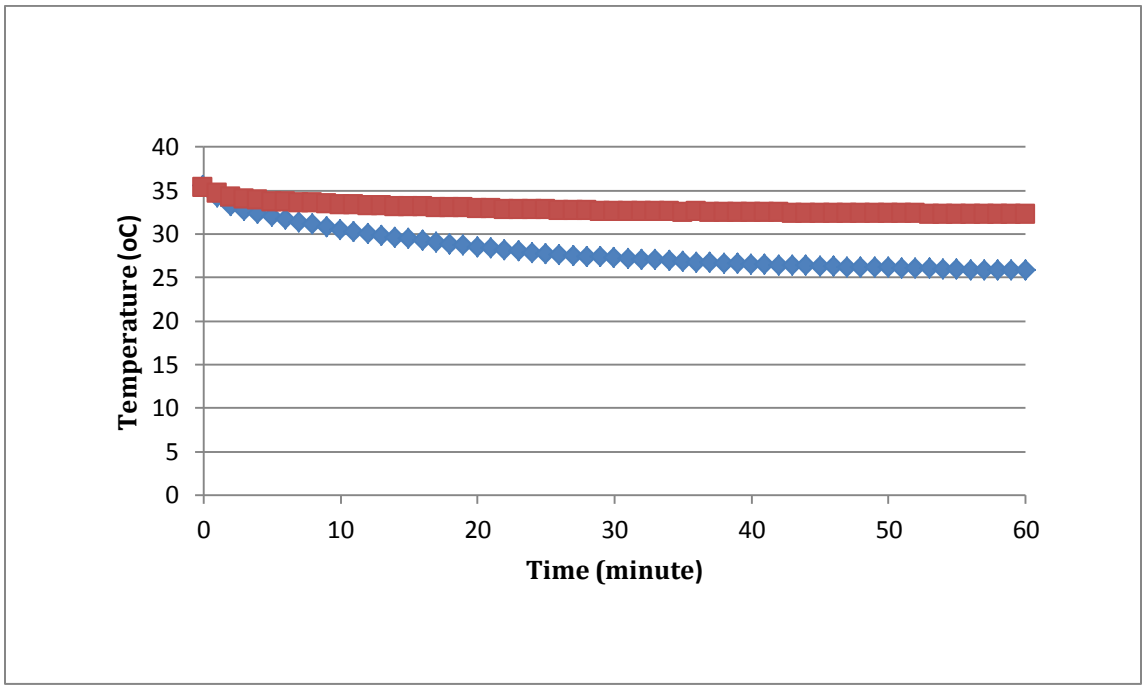

Figure 125. Evaluating cooling capabilities of PBTC set to 10°C in manual mode using a head wrap. Head skin surface temperatures measured in 26°C (79°F) Room. Control is red line. Head wrap is blue line. $p \leq 0.05$ control vs. head wrap at 30 and 60 minutes.

KEY RESEARCH ACCOMPLISHMENTS:

- Methods were developed for utilizing Newton, the thermal manikin, to gauge and quantify PBTC heating and cooling capabilities. System analysis was implemented utilizing these testing procedures to quantify capacities and different ambient and operating conditions.

- Heat sinks for the compressor and compressor control board have been designed, sized, fabricated, and tested for effectiveness in order to mitigate concerns of overheating. The compressor has been operated for extended periods of time to ensure long-term functional integrity of system.

- The TXV orifices on both the heating and cooling sides were modified to better modulate refrigerant flow into the evaporator at an optimal proportion to the evaporation rate of the refrigerant in the evaporator.

- A discrepancy in the required refrigerant charge between optimal performance of the heating and cooling cycles was identified. In order to accommodate the additional charge required for the heating cycle a separate refrigerant reservoir was designed and sized to allow the additional charge to be available during the heating cycle and stored in the reservoir during the cooling cycle.

- An accumulator was designed, assembled, and integrated into the system implementation in order to eliminate liquid refrigerant droplets from flooding the compressor. The accumulator is a custom fabrication specifically designed and tested for the PBTC.

- Vibration dampers have been incorporated into the design of the PBTC at the suction and discharge lines of the compressor to mitigate concerns of mechanical failure.

- A control logic diagram was constructed to identify the operating modes of the appliance. Furthermore, the boolean logic expressions were defined for each operating mode based on the decision tree hierarchy of the logic diagram. Safeties and system defaults were also identified and integrated into the control logic design.

- A keypad design has been developed based on the user inputs require to guide the user through properly selecting an operating mode. An LCD display has also been specified and acquired for the system.

- An actuator valve was identified, sized, and retrofit in order to automate the process of switching between heating and cooling modes.

- Temperature probes were identified, attained, and assimilated into the system design for monitoring patient body temperature. A flowmeter was sized and acquired to be utilized in the control scheme for optimal temperature maintenance by allowing the heat transfer rate to be monitored in and out of the system. It will also be utilized to ensure water flow is present when operating the device.

- Several modifications were made to the case design of the PBTC to accommodate additional system components such as the accumulator, actuator, and refrigerant reservoir. Additionally, a water storage reservoir has been integrated directly into the case design and stability analysis was implemented on the case to evaluate how easily the case may tip over.

- Implemented QSR: Currently, twenty-one SOP's have been implemented. UNSOM worked with an FDA consultant as part of QSR compliance. UNSOM hired a medical device expert to who wrote six design history documents with a focus on meeting necessary regulatory standards/steps towards eventual 510 (k) submission and FDA clearance of the medical device.

- Thermal manikin validation was completed, reviewed and compiled into a single validation report. Validation encompasses three parts: Installation Qualifications (IQ), Operational Qualifications (OQ), and Performance Qualifications (PQ). This testing provides documented evidence that the thermal manikin was installed and operating according to manufacturer's specifications and meets the requirements to successfully complete the patient simulation testing.

- Patient Simulation Testing: Three tests were designed and performed to evaluate thermal load and efficacy of PBTC. Experimental data showed comparable heating/cooling capacity of PBTC operating under continuous or battery power. PBTC warmed a thermal manikin skin surface temperature > 2 – 3^{o}C than a control nude manikin using commercial whole body circulating water blanket at 20^{o}C and 26^{o}C ambient temperature. PBTC cooled the thermal manikin head skin surface temperature > 6^{o}C than a control nude manikin using commercial circulating water head wrap at 26^{o}C ambient temperature.

CONCLUSIONS:

Defense medical installations require efficient and reliable equipment for the thermoregulation of either injured or ill patients. However, effective methods for warming/cooling injured patients under typical conditions encountered in the field and during medical evacuations in the absence of a reliable power source are currently unavailable. Rocky Research and University of Nevada School of Medicine (UNSOM) have developed a new novel Portable Body Temperature Conditioner (PBTC). It is a portable, reliable, intuitive device that will effectively maintain normal core body temperature during transport between various levels of combat casualty care. Similarly, the portable body temperature conditioner will also translate to civilian use as an essential tool for Emergency Medical Service (EMS) crews in response to emergency situations within the general public.

Rocky Research completed the design, development, and hardware implementation of a compact portable appliance capable of cooling or heating water that circulates through a conductive heat transfer wrap or blanket facilitating optimal patient thermal temperature maintenance. The PBTC is distinctly unique from any other product available because it is portable, can operate on AC or DC power, and offers both variable speed heating and variable speed cooling capabilities in a single unique and compact solution. Component selection of the PBTC was evaluated utilizing a system breadboard accommodating the interchangeability of system components. Once breadboard testing was completed, and final component selection identified, fully functional prototypes were assembled. Enhancements were made as necessary, during breadboard testing as well as prototype implementation, to the mechanical components as well as the hardware and software utilized to drive and control the system. The keypad and display were formulated to provide the user with intuitive operation of the appliance, in terms of selecting the proper operating mode as well as specifying the set point temperature. Three distinct operating modes were identified and implemented to provide the caregiver with intimate control of patient temperature therapy. The PCB design was iteratively refined and the control algorithms were written and tested for robustness and reliability. Prototypes were subsequently fabricated and tested for performance. Evaluation testing was completed for control reliability as well as system performance in both heating and cooling modes under different ambient and operating conditions.

UNSOM has completed the necessary FDA documents for this phase of the project. Both Quality Systems (QS) SOPs have been implemented and design history working documents have been created for future FDA 510(k) submission. User Requirements, Product Specifications, Project Plan, Regulatory Plan, Regulatory Standards list, and Risk Management Plan are working documents that were created by a medical device consultant for the PBTC. An FDA consulting firm was hired to assist UNSOM in setting up a quality system to meet CFR Title 21 Part 20 requirements. A custom built thermal manikin was purchased from Measurement Technology Northwest. A training/installation session was held with personnel from MTNW. UNSOM and

Rocky Research personnel were trained on the basic use and maintenance of the thermal manikin. Additionally, Installation, Operational, and Performance qualification were completed for validating the thermal manikin. This testing provides documented evidence that the thermal manikin was installed and operating according to manufacturer's specifications and meets the requirements to successfully complete the patient simulation testing. Three patient simulation tests were designed and performed to evaluate thermal load and efficacy of PBTC, which are as follows: 1) Heating/Cooling fraction test, 2) Comparison of PBTC to commercial hyper-hypothermia system test, and 3) Head cooling Test. Experimental data showed comparable heating/cooling capacity of PBTC operating under continuous or battery power. PBTC was comparable to a commercial device in warming a thermal manikin using a circulating water vest. The thermal manikin's skin surface temperatures were statistically significantly higher using commercial device than PBTC in $20^{o}C$ and $26^{o}C \pm 1^{o}C$ ambient temperatures. However, the PBTC is small, lightweight and transportable device intended for field use where the commercial device is a large heavy appliance intended for stationary use. The commercial device is 4 times larger in weight and uses 4 times the power consumption than the PBTC. PBTC warmed a thermal manikin skin surface temperature $> 2 - 3^{o}C$ than a control nude manikin using commercial whole body circulating water blanket at $20^{o}C$ and $26^{o}C$ ambient temperature. PBTC cooled the thermal manikin head skin surface temperature $> 6^{o}C$ than a control nude manikin using commercial circulating water head wrap at $26^{o}C$ ambient temperature.

Pending future funding; the next phase will incorporate design changes from the simulated patient testing into a second-generation prototype, final production design manufacturing, and commercialization with FDA 510(k) clearance. Additionally, the thermoregulatory and physiological software models utilized by the thermal manikin also represent healthy individuals. The thermoregulatory state, metabolic state, circulation, core temperature, and skin temperature of traumatically injured patients are not optimal and may react differently to active convective warming methods than healthy individuals. The plan is to develop disease state physiological software that would be used in tandem with a thermal manikin to simulate different temperature protocols. UNSOM has been in discussions with software engineers who developed the physiology software used with the thermal manikin. The software engineers are interested to work with UNSOM trauma surgeons to develop a disease state module for the physiology software. UNSOM trauma surgeons would collect trauma patient data related to core temperature, skin temperature, metabolic rate, blood pressure, and respiration rate. This data coupled with patient simulation experiments using the thermal manikin would be utilized to develop physiological software models for injured patients. This software is expected to model core temperature, skin temperature, metabolic rate, shivering, sweating, and thermoregulatory responses of injured patients. This research may also examine the bio-heat transfer mechanisms associated with trauma or surgical patients, which may lead to improvements in hypothermia, hyperthermia, and traumatic brain injury protocols. The benefit of a disease state thermal patient model is that it provides an opportunity to study the influences of different temperature protocols

or treatments, without the risk of exposing patients to unknown conditions. This software could be used to predict the thermal response of trauma/injured patients to active cooling/heating devices, helping to determine their efficacy. Due to the minimized risk, this software could also enhance treatment protocols for traumatic brain injury, hypothermia, and hyperthermia in patients.

PUBLICATIONS, ABSTRACTS, AND PRESENTATIONS:

Conference

DeGuzman, M. Comparison of Several Warming Methods Via Thermoregulatory Simulations With a Thermal Manikin. The American College of Surgeons' Committee on Trauma 2014 Resident Trauma Papers Competition, 2013 Dec 7; Tuscon, AZ.

INVENTIONS, PATENTS AND LICENSES:

No inventions, patents, or licenses have been produced or issued for this report.

REPORTABLE OUTCOMES:

No reportable outcomes to report.

OTHER ACHIEVEMENTS:

Not Applicable

REFERENCES:

1. Aragon D. Temperature management in trauma patients across the continuum of care: the TEMP Group. Temperature Evaluation and Management Project. AACN Clin Issues 1999 Feb; 10(1):113-23.

2. Bernabel AF, Levison MA, Bender JS. The effects of hypothermia and injury severity on blood loss during trauma laparotomy. J Trauma 1992;33:835-9.

3. Brauer A, Bovenshulte H, Perl T, et al. What Determines the Efficacy of Forced-Air Warming Systems? A Manikin Evaluation with Upper Body Blankets. International Anesthesia Research Society 2009; 108: 192-198.

4. Brauer A, English MJM, Sander H, et al. Construction and Evaluation of a Manikin for Perioperative Heat Exchange. Acta Anaesthesiologica Scandinavica 2002; 46:43-50.

5. Brauer A, Pacholik L, Perl T, et al. Conductive Heat Exchange with a Gel-Coated Circulating Water Mattress. International Anesthesia Research Society 2004; 99: 1742-46.

6. English MJ, Hemmerling TM. Heat Transfer Coefficient: Medivance Artic Sun Temperature Management System vs. Water Immersion. European Journal of Anesthesiology 200; 25: 531-537.

7. Fritsch DE. Hypothermia in the trauma patient. AACN Clin Issues 1995 May;6(2):196-211.

8. Gregory JS, Flancbau L, Townsend MC, et al. Incidence and timing of hypothermia in trauma patients undergoing operations, J Trauma 1991;31:795-8.

9. Jurkovich GJ, Greiser WB, Luteman A, et al. Hypothermia in trauma victims: an ominous predictor of survival. J Trauma 1987;27:1019-24.

10. Kreith F, Bohn MS. *Principles of Heat Transfer*. 6th ed., Brooks/Cole, California, 2001.

11. Sessler DI, Moayeri A. Skin-Surface Warming: Heat Flux and Central Temperature. Anesthesiology 1990; 73: 218-224.

12. Sinclair W, Rudzki S, Leicht A, et al. Efficacy of field treatments to reduce body core temperature in hyperthermia subjects. Medicine and Science in Sports and Exercise 2009 March; 1984-1990.

13. Tsuei BJ, Kearney PA. Hypothermia in the trauma patient. Injury, Int. J Care Injured 2004;35:7-15.

14. Smalley B, Janke R, and Cole D. Exertional heat illness in Air Force basic military trainees. Military Medicine 2003;4: 298-303.

15. Xu X, Endrusick T, LaPrise B, et al. Efficiency of Liquid Cooling Garments: Prediction and Manikin Measurement. Aviation, Space, and Environmental Medicine 2006; 77: 644-648.

16. Xu X, Gonzalez J. Determination of the cooling capacity for body ventilation system. European Journal Applied Physiology 2011; 111: 3155-60

17. Morris R. Operating Room Temperature and the Anesthetized Paralyzed Patient. JAMA Surgery 1971; 2(2):95-97.

18. Ling G, Bandak F, Grant G, Armonda R, Ecklund J: Neurotrauma from explosive Blast. Elsayed N, Atkins J, Gorbunuv N eds. Explosion and Blast Related Injuries: Effects of Explosions and Blast from Military Operations and Acts of Terrorism Elsevier, NY. 2008; Chapter 4:91-104.

19. Dubose J, Barmparas G, Inaba K, et al: Isolated severe traumatic brain injuries sustained during combat operations: Demographics, mortality outcomes, and lessons learned from contrasts to civilian counterparts. J Trauma. 2011;70(1):11- 18.

20. Badjatia N. Hyperthermia and fever control in brain injury. Curr Opin Crit Care. 2009 Apr;15(2):79-82.

21. Sinclair W, Rudzki S, Leicht A, et al. Efficacy of Field Treatments to Reduce Body Core Temperature in Hyperthermic Subjects. Medicine and Science in Sports and Exercise 2009 March; 1984-1990.

Appendix A

Notes from May 17, 2012 Teleconference with University of Nevada, Reno

Portable Body Temperature Conditioner

General Questions

The main goal in the development of the portable body temperature conditioner is core temperature maintenance as to prevent further temperature loss. It may be difficult to raise a patient's core temperature in the field due to non-ideal conditions and the patient's injuries. The advantages of the proposed system is that it will provide sufficient heating and cooling power to maintain normothermia under typical conditions encountered in the field and during air transport.

1. Clinical utility in austere environments where ice packs are not available.
   - To promote use in austere environments, the device will be lightweight, of minimal size, and battery operated allowing for maximum portability.

2. Does design address MilSpecs and when will you test device for meeting MilSpecs?
   - **Phase I Technical Objectives**

   The major technical objectives of the proposed project are to design, develop, fabricate, and test a portable body temperature conditioner subject to extreme ambient conditions to determine performance and cost. In order to reach realistic results a compressor breadboard suitable to measure energy consumption and evaluate the feasibility and practicality of the concept will be fabricated and used. The data generated in the compressor breadboard will be used in the design. Based on the compressor and heat exchanger selection a 3-D solid model of the system will be generated using SolidWorks. A prototype will then be fabricated and tested with and without simulated patient body heat loads. Sub-objectives are:

   1. The development of an analytical model of the system
   2. The design of the prototype
   3. SolidWorks 3-D modeling and drawings
   4. The fabrication of the prototype
   5. Testing of the prototype on the workbench
   6. Testing of the prototype with the patient simulated load
   7. Preliminary cost analysis
   8. Begin implementing design and quality regulatory controls required by Food and Drug Administration (FDA)

   - **Military Standards**

   The system will be designed to operate in harsh military environments including airborne, shipboard, and ground mobile conditions. The device will be designed to meet military standards in current phase but not tested for meeting military standards until fabrication of the prototype has been completed. This is scheduled to occur in phase 3 of

the project. The specific Mil-Standards that the system will be designed to pass in the upcoming phase are:

Environmental

- MIL-STD-810G-507.4 HUMIDITY
- MIL-STD-810G-509.4 SALT/FOG
- MIL-STD-810G-510.4SAND/DUST
- MIL-STD-810G-500.4 LOW PRESSURE(ALTITUDE) PROCEDURE II
- MIL-STD-810G-501.4 HIGH TEMPERATURE PROCEDURE I
- MIL-STD-810G-501.4 HIGH TEMPERATURE PROCEDURE II
- MIL-STD-810G-502.4 LOW TEMPERATURE PROCEDURE II
- MIL-STD-810G-514.5 VIBRATION
- MIL-STD-810G-516.5MECHANICAL SHOCK, PROCEDURE

EMI (The following Mil-Standards apply to Air –worthiness in addition to mobile systems on the ground)

- MIL-STD 461E,FCE 102 CONDUCTED EMISSIONS, POWER LEADS
- MIL-STD 461E,FCS 10 CONDUCTED SUSCEPTIBILITY, POWER LEADS
- MIL-STD 461E,FRE 102 RADIATED EMISSIONS
- MIL-STD 461E,FRS 103RADIATED SUSCEPTIBILITY

3. How does system interact with casualty? (Provide diagram of the whole system with casualty)

- The device will be able to interface with a typical core temperature measuring probe, allowing for a direct feedback control system based on the patient's core body temperature. In automatic or gradient temperature mode, the device will provide heating or cooling based on the patient's current core temperature, circulating the appropriate temperature fluid through the convective/conductive blanket. A simple diagram of the interface between the patient and the temperature conditioning device is provided in figure 1. The body temperature conditioning system is connected to the convective blanket with an inlet and exit flow setup. This allows the heated or cooled convective fluid to flow into the blanket, circulate, and then exit back into the temperature conditioning device. The user interface is a generalized schematic and is planned to incorporate a user interface similar to commercial conditioning blanket systems. A simple flow chart describing the interaction between the patient and temperature conditioning device is in gradient or automatic mode is provided in figure 2.

  In just about every scenario where this device would be used the patient will need to be intubated and sedated, as the systems primary function is to maintain core body temperature or warm/cool the patient as part of a resuscitative effort during transport to improve the patient's outcome.

In a cardiac arrest scenario where the idea is to cool the patient and prevent brain injury the patient will need to be intubated and sedated to tolerate cooling. Most patients put into iatrogenic hypothermia will shiver, experience pain, and on a whole be really uncomfortable. If they are sufficiently obtunded to require this therapy then they almost certainly will require intubation. Cooling of a patient is not recommended unless the patient requires intubation and an invasive temperature monitoring probe is required.

- **Clinical Scenario**

A 24 year old male suffers blast wounds to the right upper extremity and torso with 10% total body surface area burns to the chest. The ambient temperature is 22^{o} C. A first responder arrives and upon removing the burned clothing and exposing the areas of injury, severe mangling of the extremity is noted. The patient is moved to a safe location where it is determined his airway is patent, he is breathing without issues and he has palpable pulses in all extremities save the mangled arm. The transport team arrives and IV access is placed in the unaffected limb and room temperature fluids are initiated. The patient is tachycardic and anxious, his blood pressure is normal, skin temperature is 36.0^{o} C. The patient complains of severe abdominal pain and intra-abdominal injury is suspected.

In this scenario the patient is already in the early stages of shock. He is also mildly hypothermic. In a scenario such as this where the ambient temperature is 22^{o} C, the patient is burned, and the patient has had significant blood loss - the patient warmer would be applied with the arrival of transport utilizing a skin temperature probe. In this situation, the body temperature conditioning device is primarily being used for body temperature maintenance, as to prevent any further heat loss. This, in addition to resuscitation would prevent worsening of the hypothermia and subsequent coagulopathy. An invasive core temperature monitor could be placed should the patient require intubation or additional invasive monitoring. In burned patients heat loss can occur quickly. Lastly, this patient may require urgent operative intervention. Acidosis and coagulopathy can be prevented by addressing the issue of heat loss via blanket technology rather than "playing catch-up" in the OR.

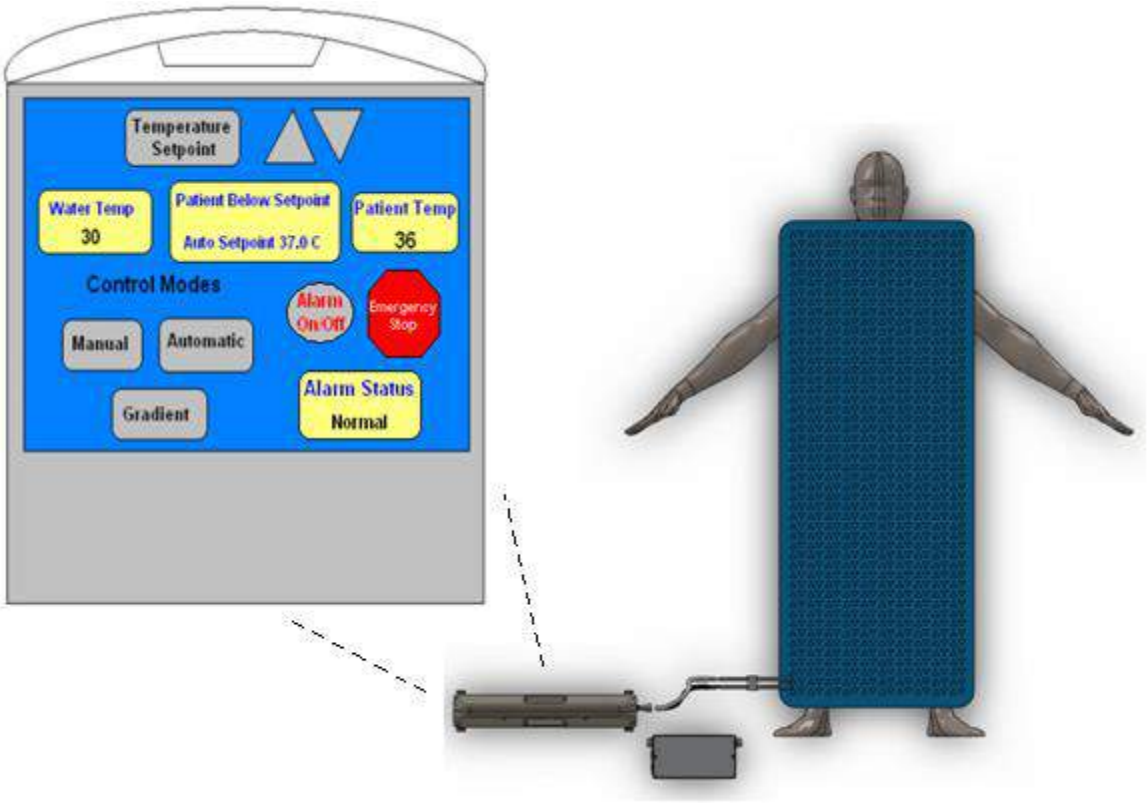

Figure 1. Diagram of body temperature conditioning system interaction with patient

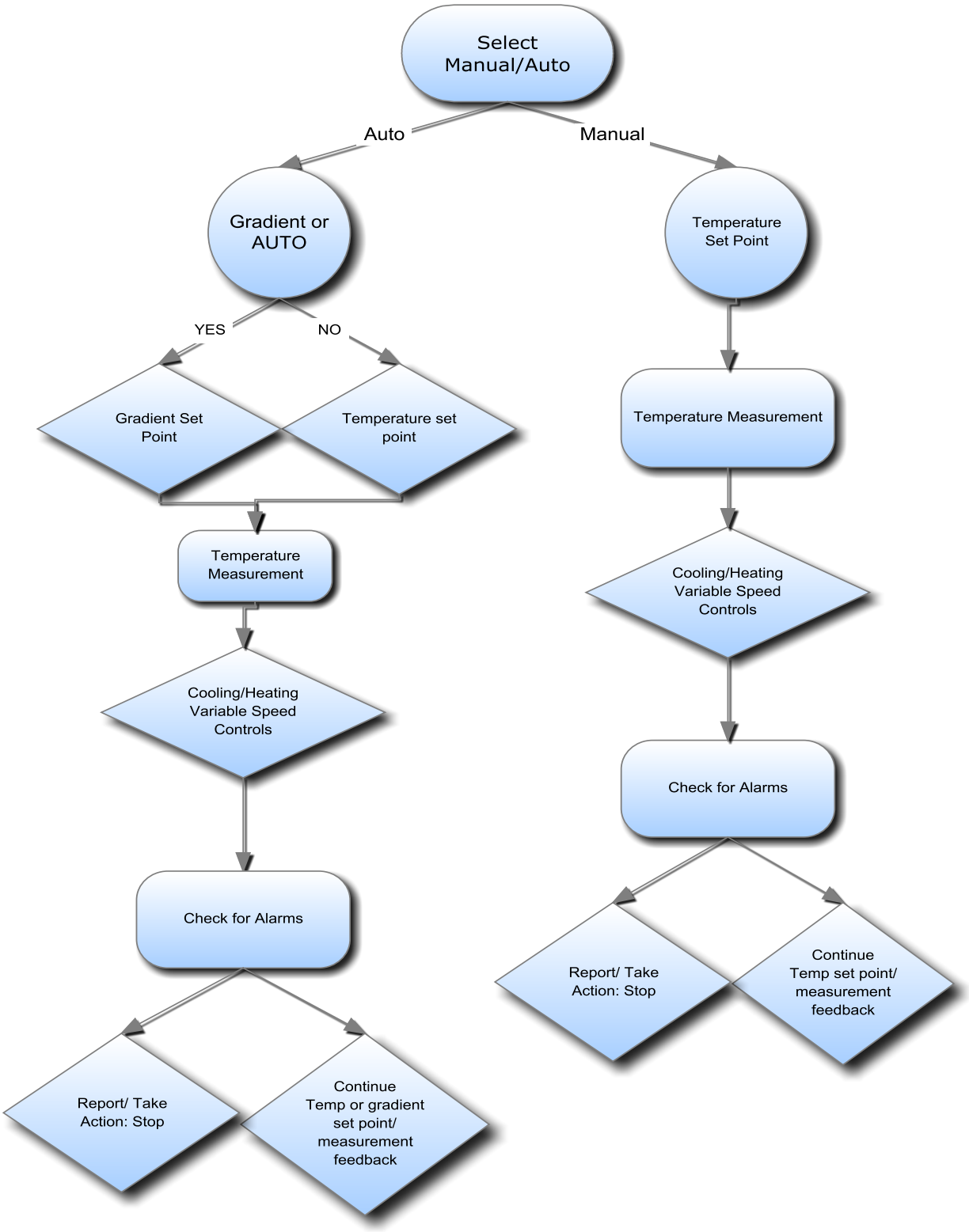

Figure 2. Simple flow chart describing the interface between patient and temperature conditioning device.

4. How are adjustments made to not allow patient to get too hot or too cold?
    - With respect to patient safety and ease of operation, the device will have several safety applications built in. To prevent the patient from being over heated or cooled, the device will have upper and lower limits of temperature, control systems, automatic shut-off when the temperature exceeds set points, and an alarm system to notify the operator of dangerous temperature situations.

5. Can the system be used by a medic or nurse and who will use this device?
    - The device will provide a user friendly interface displaying the following essential patient care data; patient core temperature, water temperature, and the system status which indicates the temperature set point and any necessary corrections to be made by the operator. The system will be designed with intuitive controls to promote ease of use with medics up to physicians. The system will have an automatic and manual control option for basic temperature management use and a more controlled use by physicians. The portability of the device will allow its use in the field, during airborne evacuation, and within a traditional hospital setting.

6. What is your business plan?
    - Working with medical device manufacturers. We are currently having discussions with Cincinnati Sub-Zero (CSZ) as a possible consultant on this project. CSZ is a company in the medical temperature management market. This is an established company with various products related to Hyper-Hypothermia systems.

7. How much will it cost?
    - Rocky Research will complete a cost estimate at the end of the current phase when the first prototype is fabricated and tested. At this time there are too many unknown factors associated with parts, blankets, and the overall fabrication of the prototype to estimate the cost of the device.

Blanket questions

1. Clarification on blanket(s) to be tested.
    - CSZ manufactures blankets for hyper-hypothermia systems. If CSZ becomes a consultant on this project then we can test their blankets on the device. If not, then we will evaluate other commercial off-the-shelf (COTS) blankets.

2. Will the blanket be sold as part of the device?

- The blanket may be sold as part of the device, but should also be available as a standalone product. Single use or multiple use blankets may be sold, depending on what would be most convenient for the military.

3. Will recommendations be made?
   - Based on patient simulation testing, recommendations will be made as to the various types of blankets to be used with the system. (ie. Pads, whole body blankets, smaller blankets placed in specific locations on the patient, head wraps, etc.). As well as preferences may be requested by military experts.

4. Will design recommendations/changes be made to manufacturer when tests show that COTS blankets are not sufficient?
   - Yes, recommendations may be made to develop and custom blankets specific to our needs.

5. What is price of recommended COTS blankets?
   - The prices for the various blankets manufactured by Cincinnati Sub-Zero are given in table 1.

Table 1: List prices for various blankets manufacture by Cincinnati Sub-Zero

	Type	Model	Size	Quantity	Cost
Convective hyper-hypothermia water blankets/wraps	**Single-Use Blanket**	Maxi-Therm	Adult	Box 5	$127.00
			Pediatric	Box 5	$90.00
			Infant	Box 5	$72.00
	Reusable Blanket	Plasti-Pad	Adult	Each	$193.00
			Pediatric	Each	$157.00
			Infant	Each	$129.00
	Reusable Mattress/Pad	Gelli-Roll	Adult	Each	$1,420.00
			Pediatric	Each	$1,180.00
			Infant	Each	$861.00
	Single-Use Wrap for brain cooling	Head Wrap	One Size	Box 10	$2,080.00
Accessories	**Connection Hose**	Compatible All Models	N/A	Each	$63.00

Temperature Sensor Questions

1. What temperature sensors/probes and placement to be used? (Correlation to core temperature)
   - Most commercially available hyper-hypothermia devices currently on the market are able to accommodate multiple temperature sensor probes. The three main temperature probes used are rectal, esophageal, and urethral Foley catheter.
   - The accuracy of a temperature probe can vary depending on the condition and injuries of the patient. Having multiple options of temperature probes is essential for measuring an accurate core body temperature.

2. Interval of temperature measurement?
   - The Blanketrol III from Cincinnati Sub-Zero is able to measure and update the temperature reading on the user display every 5 seconds. The newest version of this system can also come with data logger software which can capture data at the following user chosen rates (30 seconds, 1 minute, 5 minutes, 15 minutes, 30 minutes or 60 minutes). This capability would be built into the system being designed by Rocky Research.

3. Will the sensor be sold as part of the device?
   - The temperature sensor will likely be sold with the device, but should also be sold separately as an accessory. The temperature sensor may also be sold in disposable or reusable models.

4. What is price of recommended sensors?
   - Cincinnati Sub-Zero sells disposable and reusable temperature probes. The temperature probes are sold in units of 20 and range in price from $93.00 to $158.00. A reusable cable which interfaces with the temperature probe and hyper-hypothermia system is also sold. The cables range in price from $45.00 to $48.00. A port would be built into the system being designed by Rocky Research to interface with the temperature probe.

5. The Working Group made it clear that any device to be considered needs to be non-invasive. Would the temperature probes you suggested make this a more invasive device or are these probes already used to monitor the patient without the warming/cooling device?
   - The three main temperature probes (invasive) currently used on the market for hyper-hypothermia devices are rectal, esophageal and the foley catheter. Other non-invasive probes (skin temperature probe) may also be used to interface with the device, though they may not be as accurate in measuring core body temperature. Skin temperature probes are traditionally not as accurate as rectal, esophageal, or foley catheters

(generally inaccurate to a degree greater than 1°C), and are prone to loss of adhesion. In a trauma scenario where heating is desired (prevention of the lethal triad), an accurate core temperature reading is crucial for the function of the body temperature conditioning device. However, in situations where more advanced care is not available the skin temperature probe may be useful for basic preliminary data collection or activation of the system. Once more advanced care becomes available, invasive temperature monitoring should be the preferred method for measuring body temperature. It may be recommended that both types of temperature probes (invasive/non-invasive) be carried as basic accessories for this device.

Prototype Questions

1. Where is User Interface and what information needs to be displayed?
    - The user interface will be similar to existing normothermia systems (figure 3), and will offer simple programmable body temperature regulation. The system will have both an automatic and manual control setting to enable the operator or physician to have control over the patients care. The user interface will display the common patient care information typically found in current commercially available patient warming devices. This includes the following; patient core temperature, water temperature, and the system status which indicates the temperature set point and any necessary corrections to be made by the operator.

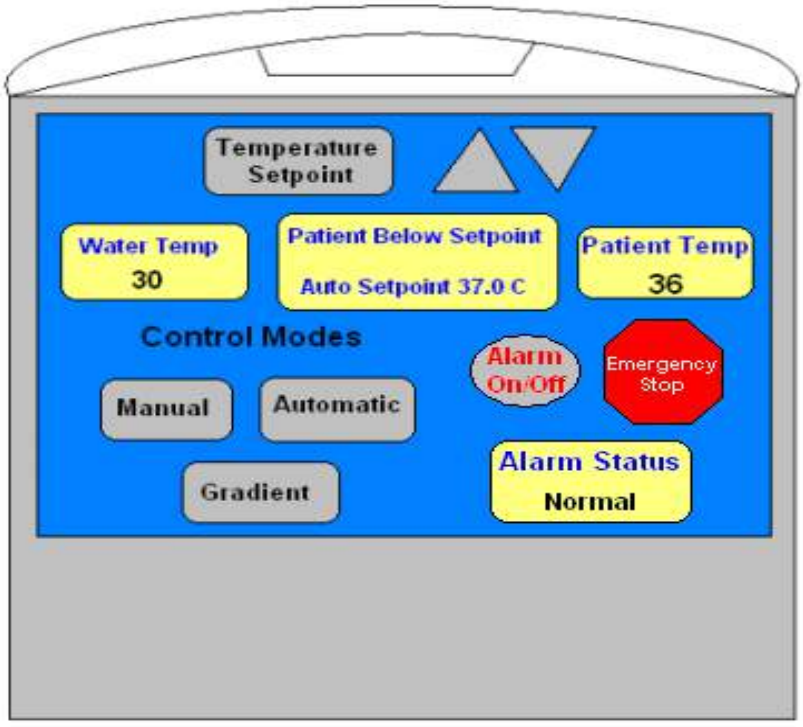

Figure 3. Example of generalized schematic of graphical user interface

2. What are safety parameters for maximum and minimum temperature?
    - Based on existing patient warming systems currently on the market, the allowable patient core temperature control range is approximately 30 – 40^{o}C. Also, the typical water temperature control range is approximately 4 – 42^{o}C. This temperature range allows for sufficient heating and cooling capacity while staying within human thermal comfort ranges and preventing the possibility of thermal burns from the device (Figure 4). Figure 4 describes the relationship between temperature of direct skin contact and exposure time to cause thermal injury. At higher temperatures, a shorter exposure time is required to cause thermal injury. Whereas at lower temperatures, a longer exposure time is required to cause thermal injury. These average temperature ranges are based on the specifications of three commercially available systems; Arctic Sun 5000, Medi-Therm III (MTA-7900), and the Blanketrol III.

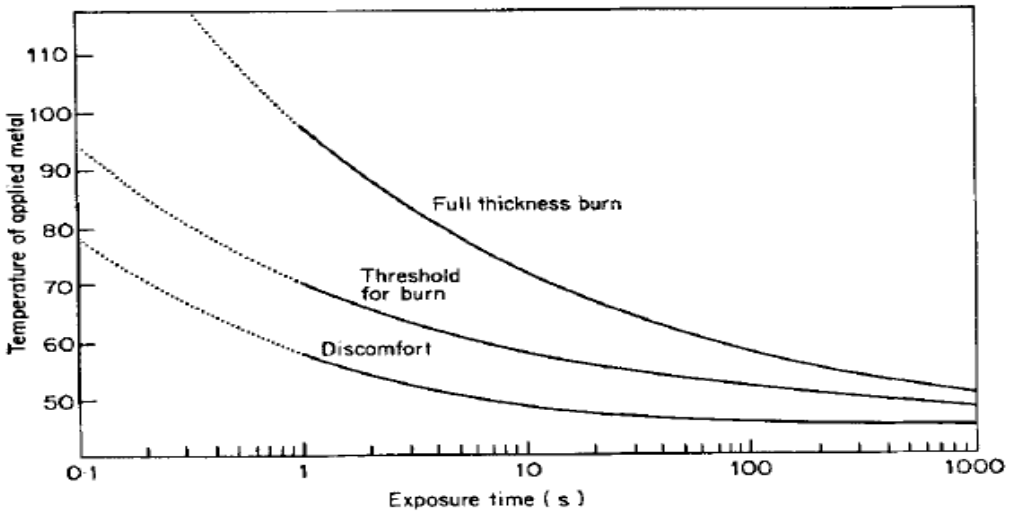

Figure 4. Relationship between temperature of direct skin contact and exposure time to cause thermal injury [1].

3. Include alarm system to avoid dangerous situations (i.e. when X number of failed attempts to adjust temperature).
    - To prevent the system from overheating or cooling the patient, the device will have upper and lower limits of temperature, control systems, automatic shut-off when the temperature exceeds set points, and an alarm system to notify the operator of dangerous temperature situations. As mentioned during the teleconference, a unique feature relevant to military applications may be an on/off switch to the system alarm. This feature would be necessary with use during military applications as the alarm

lights or sounds may give away the position of military personnel within a combat zone.

Algorithm to Control Patient Temperature Questions

1. What are your algorithms for temperature management, and what are they based on?
   - The proposed system will have automatic, manual, and a gradient temperature control options. Existing control algorithms for vapor compression systems and water temperature will be modified for patient body temperature. The gradient temperature control (GTC) algorithm is based on multipoint control of surface temperature. The GTC algorithm directly controls the average temperature of all points as well as the temperature difference between each pair of points. The algorithm also includes methods to eliminate the interference of each control output on the other control points. When temperature inputs are received, an average temperature and the temperature differences between each pair of points is calculated. Proportional integral derivative (PID) control is performed for the current value of the control points. PID control is a generic feedback control loop mechanism designed to minimize error. The PID output values are distributed to prevent them from affecting PID control performance at other points, eliminating the possibility of interference.

2. To initiate use, do you plan to allow the user to prompt rapid cooling or heating verses temperature maintenance? (Thus reducing lag time to let the system figure out what is needed).

   - There will be gradient temperature control in addition to auto and manual options

3. For rapid cooling or heating, what is the desired rate a first responder would hope to achieve with standard techniques, and what can the system do within its designed safety range for energy (heat) flux?

   - In terms of rapid heating or cooling, the thermal expansion valve (TXV) designed by Rocky Research allows for variable speed system operation of the vapor compression system over a wide range of capacities without damage to the compressor. This allows for the system to reach its maximum cooling or heating value within a short period of time. However, the overall design of the device is mainly to control patient temperature and not specifically the water temperature. Also, the system is designed primarily for temperature management and may not be suitable for rapid heating or cooling of the patient as the conditions and patients injuries may not be feasible.

4. What are safety parameters for maximum and minimum temperature and how do you plan to incorporate this in the algorithm?

    - As mentioned above, the safety parameters for temperature will be based on existing patient warming systems currently on the market; the allowable patient core temperature control range is approximately 30 – 40^{o}C. Also, the typical water temperature control range is approximately 4 – 42^{o}C. Safety parameters will be included within both the logic control and in the hardware where if one fails the redundant system ensures that there is no over/under shoot of patient temperature.

5. What are your safety parameters for maximum heat flux across the system in contact with the patient, and how do you plan to incorporate this in the algorithm?
    - The relationship between heat flux and exposure time to cause thermal injury is described in figure 5. Safety parameters for maximum heat flux between the system and patient will be based on this data. At higher heat flux densities, a shorter exposure time is required to cause thermal injury. Whereas at lower heat flux densities, a longer exposure time is required to cause thermal injury. However, this data is based on skin contact with a heat metal plate and will need to be further evaluated during the patient simulation testing.

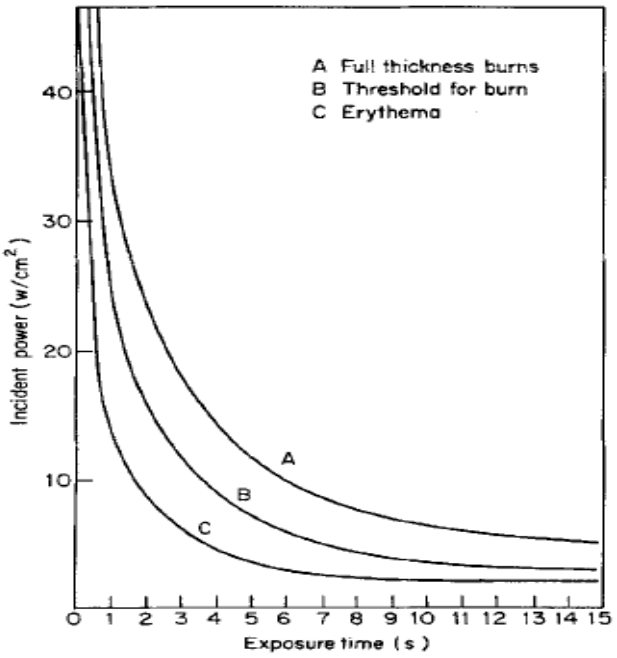

Figure 5. Relationship between heat flux and exposure time to cause thermal injury [1]

6. Will you monitor and display trends (i.e. patient has been steadily losing temperature as x degrees / minute)?

- Yes, to be determined.

7. If the system notices it cannot compensate for patients temperature changes, how will the system notify the user?
    - The user interface will include a gradient variable button/function which activates the gradient variable mode. The gradient variable mode operation is based on the temperature of the patient relative to the set point temperature. The difference between the set-point and patient core body temperature will be reported. This accounts for situations in which the system is unable to compensate for the patient's temperature changes.

References:

[1] Bull, J.P., Lawrence, J.C., Thermal conditions to produce skin burns. Fire and Materials. 3: 100-105, 1979.